National Library of Canada
Acquisitions and Bibliographic Services Branch
395 Wellington Street
Ottawa, Ontario
K1A 0N4

Bibliothèque nationale du Canada
Direction des acquisitions et des services bibliographiques
395, rue Wellington
Ottawa (Ontario)
K1A 0N4

Your file Votre référence

Our file Notre référence

NOTICE

The quality of this microform is heavily dependent upon the quality of the original thesis submitted for microfilming. Every effort has been made to ensure the highest quality of reproduction possible.

If pages are missing, contact the university which granted the degree.

Some pages may have indistinct print especially if the original pages were typed with a poor typewriter ribbon or if the university sent us an inferior photocopy.

Reproduction in full or in part of this microform is governed by the Canadian Copyright Act, R.S.C. 1970, c. C-30, and subsequent amendments.

AVIS

La qualité de cette microforme dépend grandement de la qualité de la thèse soumise au microfilmage. Nous avons tout fait pour assurer une qualité supérieure de reproduction.

S'il manque des pages, veuillez communiquer avec l'université qui a conféré le grade.

La qualité d'impression de certaines pages peut laisser à désirer, surtout si les pages originales ont été dactylographiées à l'aide d'un ruban usé ou si l'université nous a fait parvenir une photocopie de qualité inférieure.

La reproduction, même partielle, de cette microforme est soumise à la Loi canadienne sur le droit d'auteur, SRC 1970, c. C-30, et ses amendements subséquents.

Canada

UNIVERSITY OF ALBERTA

CALCIUM-INDUCED STRUCTURAL CHANGES IN THE REGULATORY DOMAIN OF TROPONIN-C BY MULTIDIMENSIONAL NMR SPECTROSCOPY

BY

STÉPHANE M. GAGNÉ

A thesis submitted to the Faculty of Graduate Studies and Research in partial fulfillment of the requirements for the degree of Master of Science.

DEPARTMENT OF BIOCHEMISTRY

Edmonton, Alberta

Fall 1994

ISBN 0-315-95031-5

Canada

Name Stephanie Gagné

Dissertation Abstracts International is arranged by broad, general subject categories. Please select the one subject which most nearly describes the content of your dissertation. Enter the corresponding four-digit code in the spaces provided.

Psychology

SUBJECT TERM

0467

SUBJECT CODE

U·M·I

Subject Categories

THE HUMANITIES AND SOCIAL SCIENCES

COMMUNICATIONS AND THE ARTS

Architecture 0729
Art History 0377
Cinema 0900
Dance 0378
Fine Arts 0357
Information Science 0723
Journalism 0391
Library Science 0399
Mass Communications 0708
Music 0413
Speech Communication 0459
Theater 0465

EDUCATION

General 0515
Administration 0514
Adult and Continuing 0516
Agricultural 0517
Art 0273
Bilingual and Multicultural 0282
Business 0688
Community College 0275
Curriculum and Instruction 0727
Early Childhood 0518
Elementary 0524
Finance 0277
Guidance and Counseling 0519
Health 0680
Higher 0745
History of 0520
Home Economics 0278
Industrial 0521
Language and Literature 0279
Mathematics 0280
Music 0522
Philosophy of 0998
Physical 0523
Psychology 0525
Reading 0535
Religious 0527
Sciences 0714
Secondary 0533
Social Sciences 0534
Sociology of 0340
Special 0529
Teacher Training 0530
Technology 0710
Tests and Measurements 0288
Vocational 0747

LANGUAGE, LITERATURE AND LINGUISTICS

Language
- General 0679
- Ancient 0289
- Linguistics 0290
- Modern 0291

Literature
- General 0401
- Classical 0294
- Comparative 0295
- Medieval 0297
- Modern 0298
- African 0316
- American 0591
- Asian 0305
- Canadian (English) 0352
- Canadian (French) 0355
- English 0593
- Germanic 0311
- Latin American 0312
- Middle Eastern 0315
- Romance 0313
- Slavic and East European 0314

PHILOSOPHY, RELIGION AND THEOLOGY

Philosophy 0422
Religion
- General 0318
- Biblical Studies 0321
- Clergy 0319
- History of 0320
- Philosophy of 0322

Theology 0469

SOCIAL SCIENCES

American Studies 0323
Anthropology
- Archaeology 0324
- Cultural 0326
- Physical 0327

Business Administration
- General 0310
- Accounting 0272
- Banking 0770
- Management 0454
- Marketing 0338

Canadian Studies 0385
Economics
- General 0501
- Agricultural 0503
- Commerce-Business 0505
- Finance 0508
- History 0509
- Labor 0510
- Theory 0511

Folklore 0358
Geography 0366
Gerontology 0351
History
- General 0578
- Ancient 0579
- Medieval 0581
- Modern 0582
- Black 0328
- African 0331
- Asia, Australia and Oceania 0332
- Canadian 0334
- European 0335
- Latin American 0336
- Middle Eastern 0333
- United States 0337

History of Science 0585
Law 0398
Political Science
- General 0615
- International Law and Relations 0616
- Public Administration 0617

Recreation 0814
Social Work 0452
Sociology
- General 0626
- Criminology and Penology 0627
- Demography 0938
- Ethnic and Racial Studies 0631
- Individual and Family Studies 0628
- Industrial and Labor Relations 0629
- Public and Social Welfare 0630
- Social Structure and Development 0700
- Theory and Methods 0344

Transportation 0709
Urban and Regional Planning 0999
Women's Studies 0453

THE SCIENCES AND ENGINEERING

BIOLOGICAL SCIENCES

Agriculture
- General 0473
- Agronomy 0285
- Animal Culture and Nutrition 0475
- Animal Pathology 0476
- Food Science and Technology 0359
- Forestry and Wildlife 0478
- Plant Culture 0479
- Plant Pathology 0480
- Plant Physiology 0817
- Range Management 0777
- Wood Technology 0746

Biology
- General 0306
- Anatomy 0287
- Biostatistics 0308
- Botany 0309
- Cell 0379
- Ecology 0329
- Entomology 0353
- Genetics 0369
- Limnology 0793
- Microbiology 0410
- Molecular 0307
- Neuroscience 0317
- Oceanography 0416
- Physiology 0433
- Radiation 0821
- Veterinary Science 0778
- Zoology 0472

Biophysics
- General 0786
- Medical 0760

EARTH SCIENCES

Biogeochemistry 0425
Geochemistry 0996
Geodesy 0370
Geology 0372
Geophysics 0373
Hydrology 0388
Mineralogy 0411
Paleobotany 0345
Paleoecology 0426
Paleontology 0418
Paleozoology 0985
Palynology 0427
Physical Geography 0368
Physical Oceanography 0415

HEALTH AND ENVIRONMENTAL SCIENCES

Environmental Sciences 0768
Health Sciences
- General 0566
- Audiology 0300
- Chemotherapy 0992
- Dentistry 0567
- Education 0350
- Hospital Management 0769
- Human Development 0758
- Immunology 0982
- Medicine and Surgery 0564
- Mental Health 0347
- Nursing 0569
- Nutrition 0570
- Obstetrics and Gynecology 0380
- Occupational Health and Therapy 0354
- Ophthalmology 0381
- Pathology 0571
- Pharmacology 0419
- Pharmacy 0572
- Physical Therapy 0382
- Public Health 0573
- Radiology 0574
- Recreation 0575
- Speech Pathology 0460
- Toxicology 0383

Home Economics 0386

PHYSICAL SCIENCES

Pure Sciences

Chemistry
- General 0485
- Agricultural 0749
- Analytical 0486
- Biochemistry 0487
- Inorganic 0488
- Nuclear 0738
- Organic 0490
- Pharmaceutical 0491
- Physical 0494
- Polymer 0495
- Radiation 0754

Mathematics 0405
Physics
- General 0605
- Acoustics 0986
- Astronomy and Astrophysics 0606
- Atmospheric Science 0608
- Atomic 0748
- Electronics and Electricity 0607
- Elementary Particles and High Energy 0798
- Fluid and Plasma 0759
- Molecular 0609
- Nuclear 0610
- Optics 0752
- Radiation 0756
- Solid State 0611

Statistics 0463

Applied Sciences

Applied Mechanics 0346
Computer Science 0984
Engineering
- General 0537
- Aerospace 0538
- Agricultural 0539
- Automotive 0540
- Biomedical 0541
- Chemical 0542
- Civil 0543
- Electronics and Electrical 0544
- Heat and Thermodynamics 0348
- Hydraulic 0545
- Industrial 0546
- Marine 0547
- Materials Science 0794
- Mechanical 0548
- Metallurgy 0743
- Mining 0551
- Nuclear 0552
- Packaging 0549
- Petroleum 0765
- Sanitary and Municipal 0554
- System Science 0790

Geotechnology 0428
Operations Research 0796
Plastics Technology 0795
Textile Technology 0994

PSYCHOLOGY

General 0621
Behavioral 0384
Clinical 0622
Developmental 0620
Experimental 0623
Industrial 0624
Personality 0625
Physiological 0989
Psychobiology 0349
Psychometrics 0632
Social 0451

UNIVERSITY OF ALBERTA

RELEASE FORM

NAME OF AUTHOR: STÉPHANE M. GAGNÉ

TITLE OF THESIS: CALCIUM- INDUCED STRUCTURAL CHANGES IN THE REGULATORY DOMAIN OF TROPONIN-C BY MULTIDIMENSIONAL NMR SPECTROSCOPY

DEGREE: MASTER OF SCIENCE

YEAR THIS DEGREE GRANTED: 1994

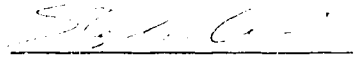

Stéphane M. Gagné

10654 84th Avenue

Edmonton, AB

T6G 2H7

October 7 1994

UNIVERSITY OF ALBERTA

FACULTY OF GRADUATE STUDIES AND RESEARCH

The undersigned certify that they have read, and recommended to the Faculty of Graduate Studies and Research for acceptance, a thesis entitled "Calcium-induced structural changes in the regulatory domain of troponin-C by multidimensional NMR spectroscopy" submitted by Stéphane M. Gagné in partial fulfillment of the requirements for the degree of Master of Science in Biochemistry.

Dr. Brian D. Sykes

Dr. Cyril M. Kay

Dr. Zygmunt Derewenda

Dr. George Kotovych

Dr. Lawrence McIntosh

Cette thèse est dédiée

à la mémoire de mon meilleur ami,

Nicolas Zajac

ABSTRACT

Multidimensional NMR spectroscopy was used to investigate the calcium-induced structural changes in the regulatory N-domain of troponin-C (1-90). The chemical shift information, along with detailed NOE analysis and $^3J_{HNH\alpha}$ coupling constants, permitted the determination and quantification of the Ca^{2+}-induced secondary structural change in the N-domain of troponin-C. For both structures five helices and two short β-strands were found, as was observed in the apo N-domain of the crystal structure of whole troponin-C [Herzberg, O. & James, M.N.G. (1988) *J. Mol. Biol.* **203**, 761-779]. The major conformational change observed is the straightening of helix-B upon Ca^{2+}-binding. The possible importance and role of this conformational change is explored. Previous circular dichroism studies on the regulatory domain of TnC showed a significant Ca^{2+}-induced increase in negative ellipticity, suggesting a significant increase in helical content upon Ca^{2+} binding. The present study shows that there is virtually no change in α-helical content associated with the transition from apo to the $2Ca^{2+}$ st[illegible]of the N-domain of TnC. Therefore the Ca^{2+}-induced increase in ellip[illegible]city observed by circular dichroism does not relate to a change in helical content, but more likely to changes in spatial orientation of helices. Preliminary tertiary structure calculations of the apo- and calcium-state of the regulatory domain of troponin-C revealed an opening of the structure triggered by the binding of calcium.

ACKNOWLEDGMENTS

I first want to thank my supervisor, Dr. Brian D. Sykes, for his guidance, his stimulating discussions, his trust, and most of all, his friendship. I am really grateful to Brian for being such a good sportsman after I 'kicked his duck' on the golf course. I must also acknowledge Brian for not sending me back to Québec once he found out I could not skate. Merci Brian.

Thanks to my two closest 'lab-mates', Carolyn M. Slupsky and Dr. Frank D. Sönnichsen, who provided constant help in so many areas. Thanks Carolyn for sharing with me all the pleasures and difficulties related to the development and applications of 3D-NMR, and for all the great scientific and non-scientific discussions. Thanks Frank for sharing with me all the pleasures and difficulties related to beer drinking, and for all the great scientific and non-scientific discussions at Avenue Pizza. I must admit that some of the most stimulating and useful scientific discussions were with Frank, at Avenue, with one or three jugs of "Traditional", while playing darts.

Thanks to Dr. Sakae Tsuda for his major contribution into the apo structure; without his work, the conformational changes presented in this thesis would be incomplete. Thanks to Monica X. Li in Dr. Larry Smillies's lab for her help in the assignment process, and for making 100's of mg of protein. Thanks to Gerry McQuaid for keeping the spectrometers in such good shape, and for all the cookies, granola bars, etc.

Thanks to Mission Control™ and its members, Leigh Willard, Tim Jellard and Robert Boyko for writing the large number of programs necessary to my research, and for all their help related to computers. A special thank goes to the cutest Mission Control™ member Leigh, my spouse, for sharing with me all the pleasures...

Thanks to all the other lab members and friends who helped me in many ways: Wendy Findlay, Gary Shaw, John Bagu, Linda Golden, Larry Calhoun, Dave Corson, Sue Smith, Krishna Rajarathnam, Key-Sun Kim, David Wishart, Collen Iwanika, Colin Bigman and Gillian Henry.

Thanks to Dan Garrett and Frank Delaglio for generously providing the very useful PIPP and NMRPIPE software.

Merci à mes parents, Bernadette Boutin et Georges Gagné, pour leur aide, leur support, et pour avoir créé tout ce qu'il y a de bon en moi. Sans eux, je serais probablement encore 'dans la rue'.

Finalement, merci à Nicolas pour son amitié et pour tout ce qu'il a fait pour moi. Sans ses encouragemnets et ses coups de pied au cul, je n'aurais jamais passé à travers le bac, et cette thèse n'aurais jamais vu le jour. Merci Nicolas.

TABLE OF CONTENTS

LIST OF TABLES

LIST OF FIGURES

CHAPTER I

INTRODUCTION

Coordinate movement is essential to life. Whether it is swimming, flying, crawling, or walking, all animals use the same basic mechanism for motor control, the contraction of muscle. Even the injection of venom by a snake involves muscle contraction. A large number of protein structural changes and protein-protein interactions are involved in the process of muscle contraction. Regulation of this process in skeletal and cardiac muscle occurs through the binding of calcium to one of these proteins, troponin-C. This thesis reports the Ca^{2+}-induced structural changes which occur in troponin-C that lead to muscle contraction.

From Muscle to Troponin-C: Organization

The organization of striated muscle

Figure I-1 shows a typical vertebrate striated muscle at successive levels of organization. Striated skeletal muscles are composed of multinucleated cylindrical fibers, or myofibers, 10 to 100 µm in diameter and up to several centimeters long. Each myofiber contains a bundle of myofibrils, each about 1 µm in diameter. A myofibril is made up of a long chain of contracting units called sarcomeres, which repeat every 2.3 µm along the fibril axis. The periodic structure of the myofibril can be clearly observed by electron microscopy (figure I-2). The electron micrograph shows two bands, the A band (dark) and the I band (light), which alternate. A sarcomere is limited by the Z-lines, located in the center of the I band. The

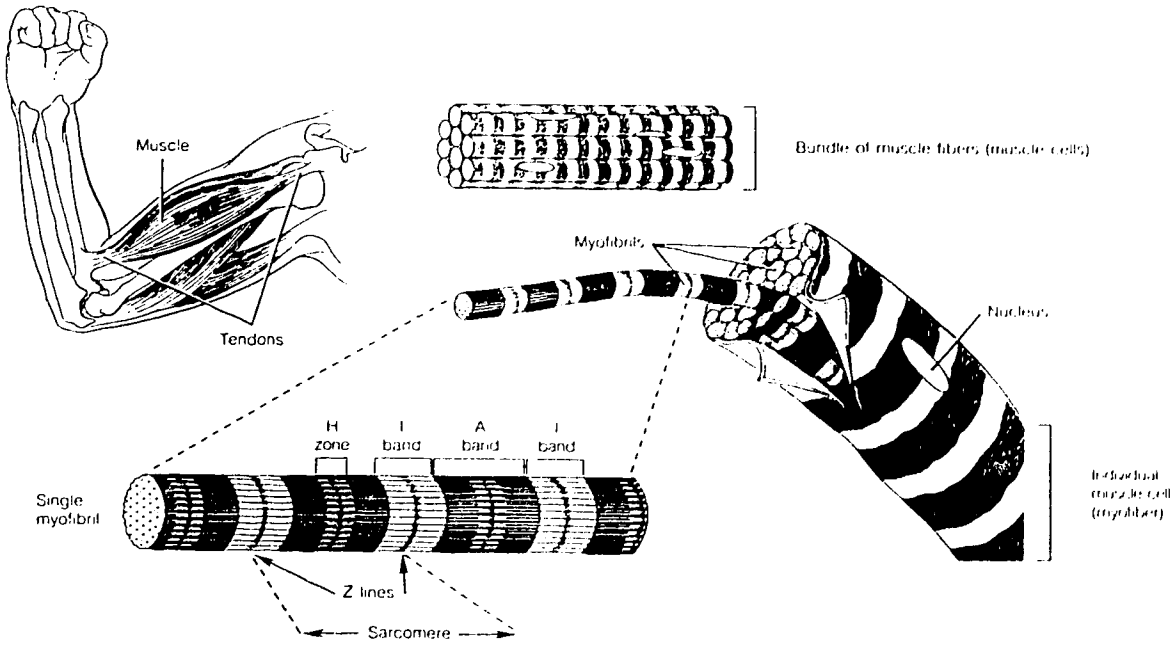

Figure I-1. Level of organization in striated muscle.

striations of the myofibrils are the result of periodic variations in concentration of two kinds of interacting filaments, the thick filament and the thin filament. Thick filaments are about 1.5 μm long and 150 Å wide and are separated by 400 Å. Thin filaments are about 1 μm long and 100 Å in diameter. In vertebrate muscle each thick filament is surrounded by six thin filaments, and each thin filament lies symmetrically among three thick filaments (figure I-2c). As a consequence of this geometry, there are twice as many thin filaments as thick filaments.

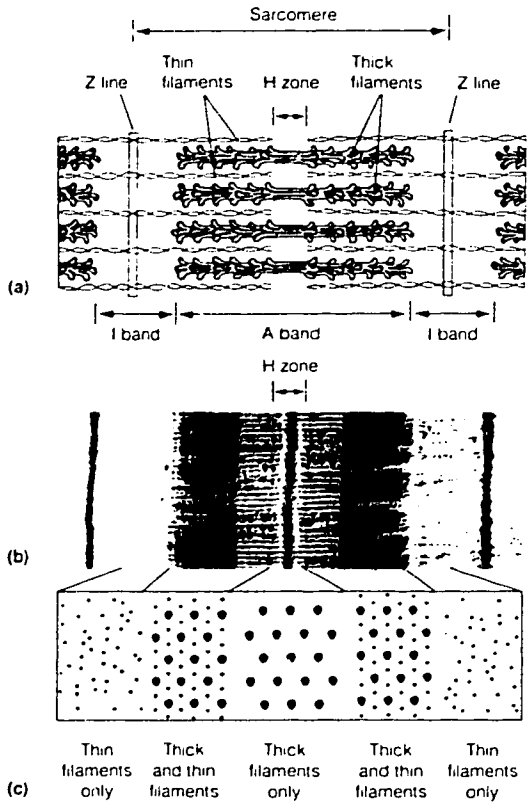

Figure I-2. Muscle structure seen at the electron microscopy level. (a) A model of the sarcomere, the repeating unit in striated muscle. The I bands, A bands, and Z lines shown in figure I-1 are identified and structural elements of the sarcomere are indicated. (b) An electron micrograph, showing the same features. (c) A schematic drawing of cross sections of a sarcomere, in the various regions shown in parts (a) and (b). Thick fibers are indicated by heavy dots, thin fibers by small dots.

The thick filament

The major constituent of the thick filament is myosin, a very large protein molecule (≈ 520 kDa) that looks like a two-headed snake (figure I-3a). Myosin is made of six polypeptide chains: two 220 kDa heavy chains and two pairs of light chains (each approximately 20 kDa). The two heavy chains associate to form a two stranded α-helical coiled coil (≈ 1300 Å long) with two globular "head" regions at one extremity. Each head is complexed with

two different light chains (often referred to as the regulatory and the essential light chains). The coiled coil accounts for the self-association of myosin and the formation of the thick filament backbone (figure I-3b). Each head is complexed with two light chains. The heads of myosin may be enzymatically cleaved by papain to isolate what are called S1 fragments, consisting of the globular regions carrying the two light chains (≈ 130 kDa). The crystal structure of myosin S1 has recently been solved [1], revealing a highly asymmetric molecule with a length of 165 Å, a width of 65 Å, and a thickness of approximately 40 Å (figure I-4).

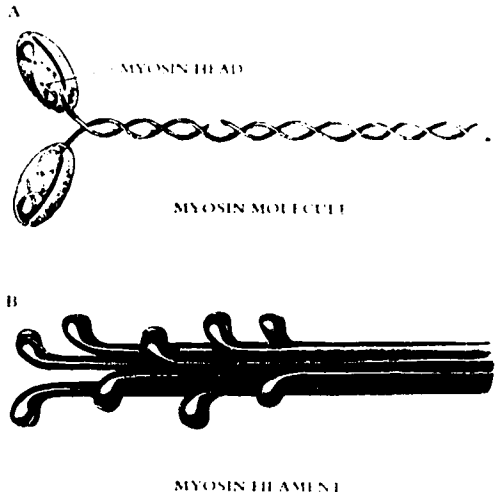

Figure I-3. The structure of myosin. (A) Each myosin molecule is a coil of two chains wrapped around one another; at the end of each chain is a globular region referred to as the "head". (B) Myosin molecules are usually combined into filaments, which are cables of myosin from which the heads protrude at regular intervals.

Figure I-4. A space filling representation of all of the atoms in the current model of myosin S1. The model is oriented such that the actin binding surface is located at the lower right-hand corner.

The thin filament

The thin filament is a more complex structure containing several proteins of which actin is the major building block. The globular monomeric form of actin (G-actin) is a protein of 385 residues arranged into four domains surrounding a deep cleft (figure I-5) [2]. Under physiological conditions, actin polymerizes to form a long, helical fiber (F-actin). The helical stacking of the globular monomers gives F-actin the appearance of two strings of beads wound around one another (figure I-6). Although actin is the main constituent of the thin filament, other proteins are essential to the contractile function of striated muscle. One of these is tropomyosin (Tm) which exists as a dimer of two polypeptide subunits (≈ 33 kDa each) that associate in a coiled-coil fashion. Electron micrographs and X-ray diffraction have localized Tm along the actin fiber. Elongated Tm polymerizes by a head-to-tail overlap of 8-11 amino acid residues, such that one Tm molecule spans seven actin monomers. At about one third of the distance from the

Figure I-5. A ribbon diagram of the 3-D structure of actin viewed roughly perpendicular to the flat face of the molecule. The molecule is thought to have a similar orientation in a filament with its long axis vertical. The right side of the molecule is thought to be exposed on the outer surface of the filament.

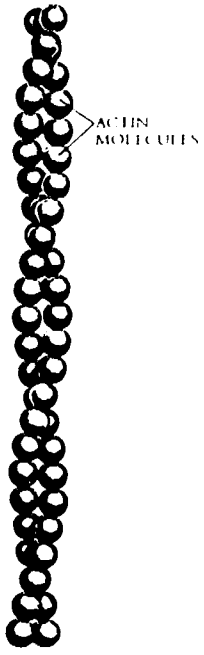

Figure I-6. An actin filament.

carboxy-terminal end of each Tm molecule resides a troponin complex. This troponin complex is formed of three subunits: troponin-T (TnT), troponin-I (TnI), and troponin-C (TnC). The proposed arrangement of actin, Tm, and the troponins in the thin filament is shown in figure I-7.

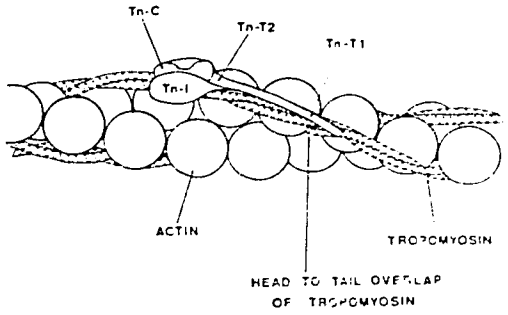

Figure I-7. Arrangement of actin, tropomyosin and troponin components in thin filaments of striated muscle.

The troponin complex

TnT is the largest of the troponin subunits and consists of 259 amino acid residues (≈ 30 kDa). TnT has direct contact with Tm, TnI and TnC, and therefore links the troponin complex to Tm. Electron micrographs have revealed the troponin complex as globular with a long rod-shaped tail identified as TnT [5]. The asymmetric TnT component, represented by its fragments TnT1 (1-158) and TnT2 (159-259), interacts with Tm both at the head-to-tail overlap (TnT1) and in a region about 13-15 nm from its

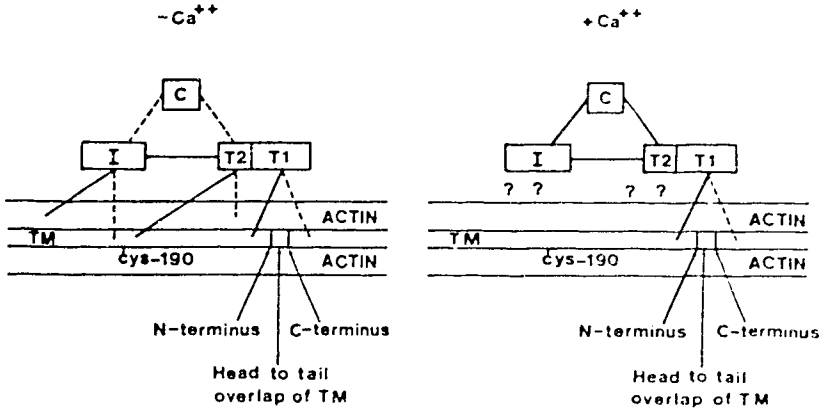

Figure I-8. Schematic representation and effects of Ca^{2+} on interactions among thin filament proteins.

C-terminal end (TnT2) (figure I-8) [3, 4]. The second troponin subunit, TnI, has a molecular weight of ≈ 21 kDa and binds to the N-terminal end of TnT2 (figure I-8) [6]. In the relaxed state, TnI also interacts with actin and probably with Tm. No tertiary structure of TnI has yet been determined. The third troponin subunit, TnC, is an acidic protein containing 150-163 residues (depending on the source). The interaction between TnC and TnT is uncertain, but some studies show that TnC may interact with the C-terminal end of TnT2 [6]. The interactions between TnC and TnI are, however, well characterized [9], and are found to be Ca^{2+}-dependant. A schematic representation of the interactions amongst thin filament proteins is shown in figure I-8.

Troponin-C

TnC (≈ 18 kDa) has four Ca^{2+}-binding sites; two high-affinity sites (III and IV) which are believed to be always occupied by either Ca^{2+} or Mg^{2+} under physiological conditions, and two low-affinity Ca^{2+}-specific sites (I and II) which regulate muscle contraction. The crystal structures of turkey skeletal TnC [7] and chicken skeletal TnC [8] reveal a 66% α-helical protein having two globular domains, each containing two calcium binding sites, connected by an extended α-helix (figure I-9). In these structures only sites III and IV in the C-terminal domain are occupied by Ca^{2+}, whereas the regulatory sites in the N-domain are in the apo state. All four Ca^{2+}-binding sites show the helix-loop-helix

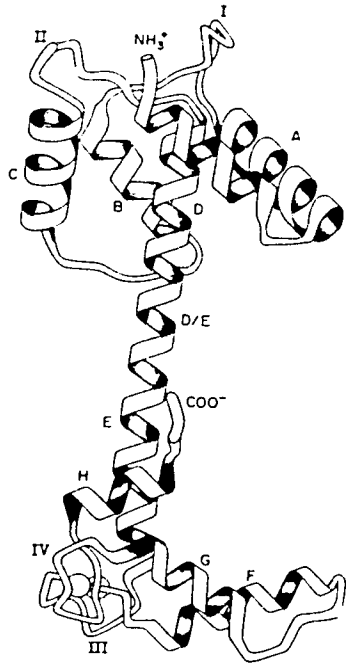

Figure I-9. Ribbon representation of the structure of turkey skeletal muscle TnC. Helices are labelled A through H; Ca^{2+}-binding sites are labelled I through IV. Sites III and IV are filled with Ca^{2+}, whereas sites I and II are apo.

motif termed the EF-hand [10]. The helix packing is, however, different in the Ca^{2+}-free regulatory N-domain compared to structures of homologous Ca^{2+}-binding proteins which are Ca^{2+}-filled [11]. A model for the structure of Ca^{2+}-filled N-domain has been proposed based on the homology between the N-domain and the C-domain [14]. The NMR solution structure of the TR_1C fragment of TnC in the apo-form [12] also shows the same structural features as is found in the N-domain of the crystal structure.

From Ca^{2+}-binding to contraction

The sliding-filament mechanism

The sliding-filament mechanism of muscle contraction postulates that the thin filament is displaced relative to the thick filament. For sliding to occur, the S1 portion of myosin attaches to a binding-site on actin to form the actomyosin complex. A conformational change then pulls it toward the center of the sarcomere (figure I-10). S1 has ATPase activity, and it is the hydrolysis of ATP by S1 that provides the free energy necessary to drive muscle contraction. A schematic representation of the proposed mechanism of force production is shown in figure I-11. For the power stroke to occur, myosin must first bind to actin, an event which is regulated by calcium.

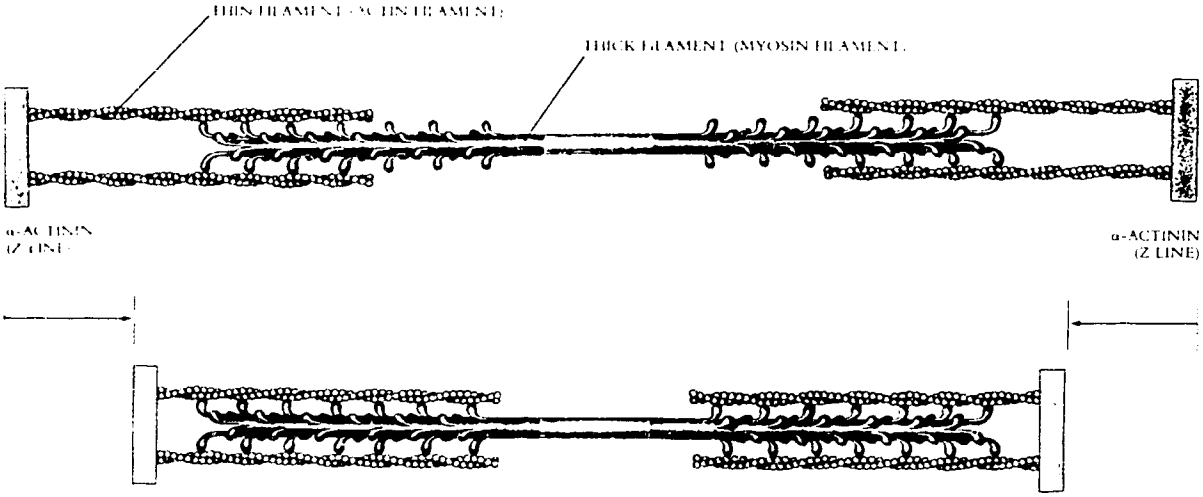

Figure I-10. The interaction of actin thin filaments and myosin thick filaments in striated muscle. The heads on the two ends of the myosin filament are oriented in opposite directions, so that as the two ends "walk" along the actin filaments in opposite direction, pulling the actin filaments and there attached α-actinin (Z-lines) toward the center of the sarcomere. The result is contraction.

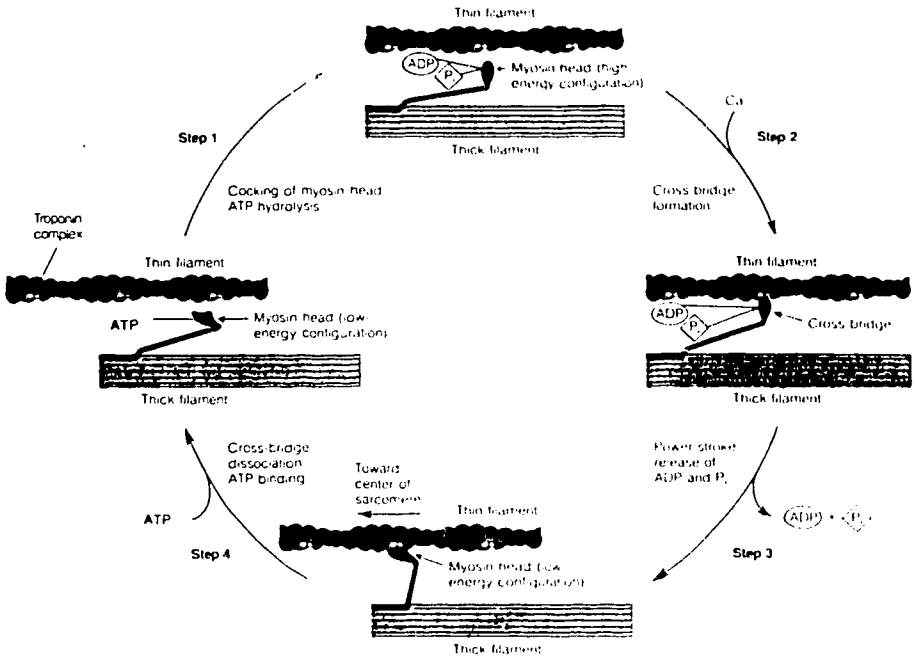

Figure I-11. The cyclic process of muscle contraction. Stages in the interaction of one myosin headpiece with a thin filament are shown.

Calcium release and binding to TnC.

In resting muscle, Ca^{2+} ions are actively pumped out of muscle fibers, concentrating the Ca^{2+} ions within the spaces of the sarcoplasmic reticulum. The concentration of free Ca^{2+} in muscle fiber in the resting state is in the neighborhood of 10^{-7} M, and the concentration of Mg^{2+} is about 10^{-3} M, so that the high-affinity sites III and IV of TnC are filled by Mg^{2+} ions, and the two low-affinity sites I and II are in the apo state. The crystal structure shown in figure I-9 is therefore related to the conformation of TnC in relaxed muscle. Upon neural stimulation, Ca^{2+} is released from the sarcoplasmic reticulum to the cytoplasm (sarcoplasm) of the muscle fiber. This Ca^{2+} influx ($[Ca^{2+}] > 10^{-6}$ M) causes the binding of two Ca^{2+} ions to the

regulatory domain of TnC, inducing a conformational change, and triggering a sequence of events that ultimately lead to muscle contraction.

The binding of Ca^{2+} induces a conformational change in TnC

While no structure for the Ca^{2+}-saturated state of TnC is known, the Ca^{2+}-induced conformational change has been studied extensively using various spectroscopic techniques including NMR, CD, fluorescence and Raman spectroscopy (reviewed in chapter II). These studies have indicated that the C-domain of TnC is mostly unstructured in the apo state, and that the binding of Ca^{2+} to site III and IV induces folding. Although previous estimates of the magnitude of the Ca^{2+}-induced changes attributable to the N-domain transition are not as clear, a recent CD study has shown significant Ca^{2+}-induced ellipticity changes in the isolated recombinant N-domain of TnC [13]. That these changes are a reflection of significant secondary structural alterations was considered a possibility. Although this conformational change has not been fully characterized, it is clear that the conformational change in TnC affects the TnC-TnI interaction.

Ca^{2+}-dependant TnC-TnI interactions

TnI (182 residues) is composed of three regions: N-domain (1-98), C-domain (120-182), and inhibitory region (99-119). The inhibitory region is the portion of TnI required to inhibit the actomyosin Mg^{2+}-ATPase (see below). Recent studies on these regions, in conjunction with TnC mutants, have shown a relationship between different TnI regions and TnC domains [9]. Binding studies have revealed that the N-terminal region of TnI interacts with the C-domain of TnC in the relaxed state, and that the inhibitory plus C-terminal region of TnI interacts with the N-domain of TnC in a Ca^{2+} dependent manner [9]. These results are summarized in figure I-12. This model suggests that TnC and TnI are always anchored

strongly in an antiparallel fashion via the N-terminal region of TnI and the C-domain of TnC. Only upon the Ca^{2+}-induced structural change in the N-domain of TnC does it interact with the C-domain of TnI.

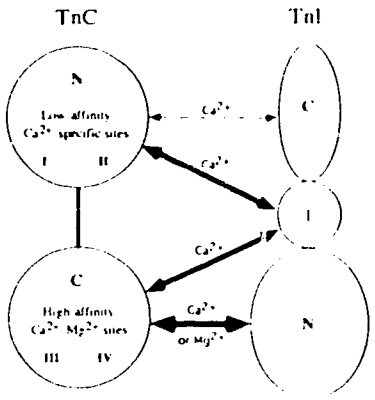

Figure I-12. Model of the TnI-TnC interaction. N and C represent the N-terminal and C-terminal domains, respectively, of TnI and TnC. I represents the inhibitory region of TnI. Some of the interactions are dependent on the presence of Ca^{2+} and occur only when sites I and II of TnC are filled during muscle activation. The Ca^{2+}-dependent interactions occur between the inhibitory region of TnI and both N- and C-terminal domains of TnC. The interactions between the N-terminal region of TnI and the C-terminal domain of TnC are Ca^{2+}/Mg^{2+}-dependent, and are believed to be present in both the relaxed and the activated state of muscle.

Release of actomyosin ATPase inhibition and power stroke

The primary role of TnI is to inhibit the formation of the actomyosin complex. When muscle is relaxed, TnI interacts with actin and physically prevents myosin from binding actin. As the N-domain of TnC binds calcium and the interaction between TnC and TnI changes, the interaction between TnI and actin weakens. The troponin-tropomyosin complex is believed to be relocated following Ca^{2+}-induced structural change in TnC, allowing the formation of the actomyosin complex (figure I-13). The power-stroke as described in figure I-10 can then occur. The various steps involved in muscle contraction are summarized in figure I-14.

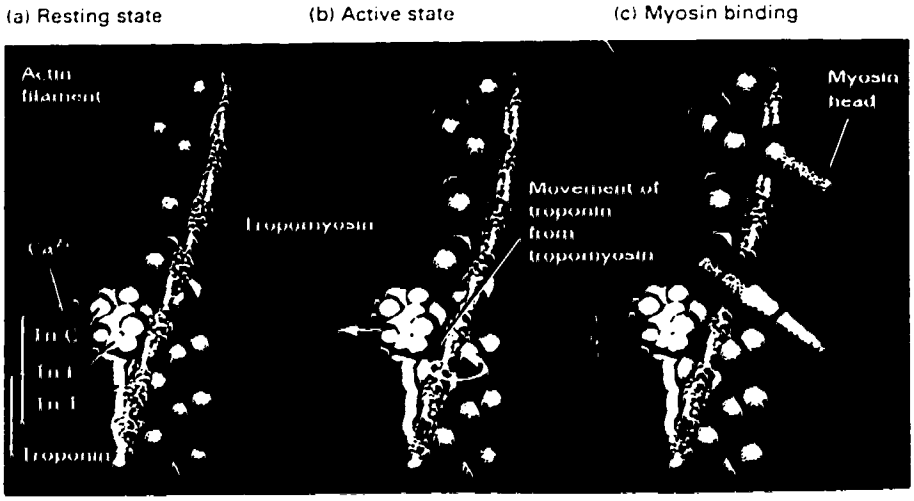

Figure I-13. Model for the regulation of contraction in striated muscle. (a) Relaxed muscle. At low Ca^{2+} concentrations (< 10^{-7} M), the configuration of actin, tropomyosin and troponin in the thin filament is such that most myosin headpieces are blocked from contact with the thin fiber. (b) Active state. At higher Ca^{2+} concentrations (> 10^{-6} M), the binding of calcium to TnC causes a rearrangement of the thin-filament fiber components so that myosin binding sites on actin are made available. (c) Myosin binds to actin and the cycle shown in figure I-11 can then occur, leading to muscle contraction.

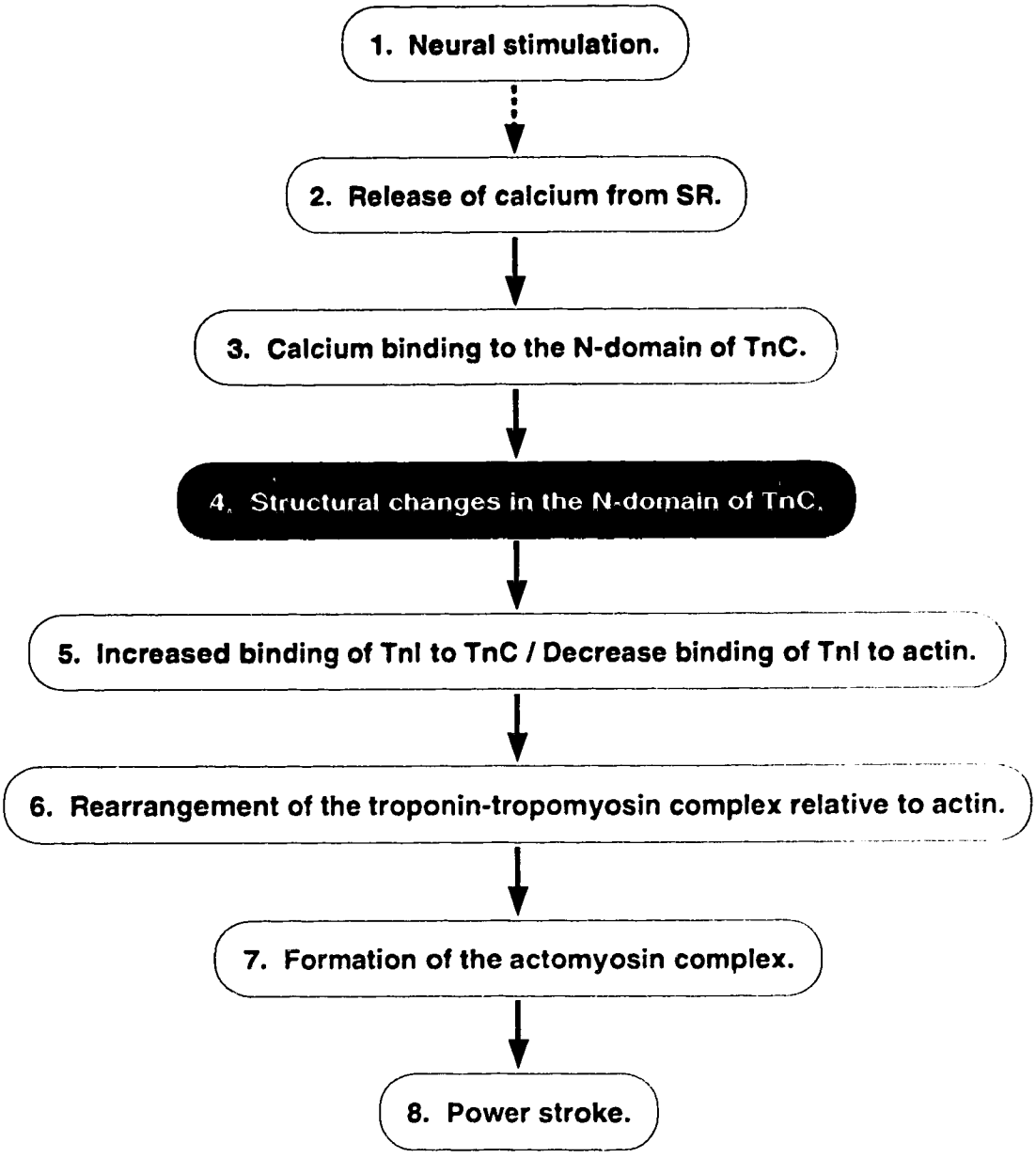

Figure I-14. Schematic represention summarizing the various steps involved in muscle contraction. The characterisation of the Ca^{2+}-induced structural changes in the regulatory domain of TnC (step 4) is the theme of this thesis.

Thesis Overview

This thesis reports the nuclear magnetic resonance (NMR) solution structure of the regulatory domain of troponin-C in the Ca^{2+}-bound state and the characterization of the Ca^{2+}-induced structural changes (step 4 in figure I-15). A large amount of knowledge about TnC has already been acquired, and some of this useful information is outlined in chapter II. Basic NMR theory necessary for the understanding of the interpretation of protein NMR data will be described in chapter III. This work is based mainly on methodologies that were developed concurrently with my research work, and chapter IV therefore describes these state-of-the-art techniques and their implementation. The first large step in the analysis of protein NMR data is the chemical shift assignment of the backbone. Chapter V first describes the strategy used to accomplish this crucial step, and presents the complete backbone assignment. This chemical shift information, along with detailed backbone NOE analysis, permitted the determination of the secondary structure of NTnC in the Ca^{2+}-state which is presented in chapter V. This chapter also offers a detailed comparison with the NMR structure of apo-NTnC, the crystal structure of TnC (where the N-domain is apo), and the $4Ca^{2+}$ TnC model. Preliminary work on the three-dimensional solution structure of Ca^{2+}-bound NTnC is briefly outlined in chapter VI. Finally, chapter VII discusses in detail the Ca^{2+}-induced structural changes in the regulatory domain of troponin-C.

References

1 Rayment, I., Rypniewski, W.R., Schmidt-Bäse, K., Smith, R., Tomchick, D.R., Benning, M.W., Winkelmann, D.A., Wesenberg, G. & Holden, H.M. (1993). *Science* **261**, 50-58.

2 Kabsch, W., Mannherz, H.G., Suck, D., Pai, E.F. & Holmes. (1990). *Nature* **347**, 37-44.

3 Mak, A.S. & Smillie, L.B. (1981). *J. Mol. Biol.* **149**, 541-550 .

4 White, S.P., Cohen, C. & Phillips Jr, G.N. (1987). *Nature* **325**, 826-828.

5 Flicker, P.F., Phillips, G.N. & Cohen, C., J. (1982). *Mol. Biol.* **162**, 495.

6 Pearlstone, J.R. & Smillie, L.B. (1978). *Can. J. Biochem.* **56**, 521.

7 Herzberg, O. & James, M. N. G. (1988). *J. Mol. Biol.* **203**, 761-779.

8 Satyshur, K.A., Pyzalska, D., Greaser, M., Rao, S.T. & Sundaralingam, M. (1994). *Acta Cryst. D* **50**, 40-49.

9 Farah, C.S., Miyamoto C.A., Ramos, C.H.I., Silva, A.C.R., Quaggio, R.B., Fujimori, K., Smillie, L.B. & Reinach, F.C. (1994). *J. Biol. Chem.* **269**, 5230-5240.

10 Kretsinger, R. H. *CRC Crit. Rev. Biochem.* **8**, 119 (1980).

11 Strynadka, N. C. J. & James, M. N. G. (1989). *Annu. Rev. Biochem.* **58**, 951-998.

12 Findlay, W.A., Sönnichsen, F.D. & Sykes, B.D. (1994). *J. Biol. Chem.* **269**, 6773-6778.

13 Li, M.X., Chandra, M., Pearlstone, J.R., Racher, K.I., Trigo-Gonzalez, G., Borgford, T., Kay, C.M. & Smillie, L.B. (1994).. *Biochemistry* **33**, 917-925.

14 Herzberg, O., Moult, J. & James, M.N.G. (1986). *J. Biol. Chem.* **261**, 2638-2644.

CHAPTER II

WHAT WE KNOW

In 1963, Ebashi discovered a new protein factor that was necessary for the Ca^{2+} sensitivity of actomyosin [1,2]. This protein system was called "native tropomyosin", but it was soon found that this system was a complex of tropomyosin and a new globular protein, which was named troponin [3]. Hartshorne and Mueller [4] were the first to observe that troponin was made of subunits. They obtained two fractions, which they named troponin A and troponin B. Troponin A, which also carried the name "EGTA sensitizing factor", was found to be required for calcium control of ATP hydrolysis by myosin [5,6]. Greaser and Gergely [7,8] later resolved troponin into the three subunits we know today and named them troponin-T, troponin-I and troponin-C, the latter corresponding to the troponin A observed previously. In 1972, Murray and Kay [15] reported for the first time that Ca^{2+} was inducing a conformational change in troponin A (troponin-C). Up to 1970, there are less then 100[§] publications related to the troponins. In the next decade, about 300 papers characterized troponin-C. Since 1980, approximately 1000 publications have reported data related to TnC. This chapter summarizes some of this data relevant to the course of my research.

[§] The number of publication is based on a search on the Medline SilverPlatter system.

Characteristics of troponin-C

The sequence

31 sequences of TnC have been determined so far, going from human skeletal muscle TnC to sea squirt smooth muscle TnC. The sequence of the protein used in the present study, chicken skeletal TnC, is listed in figure II-1. The work presented here relates to the N-terminal domain of TnC (NTnC; residue 1-90; M_w = 9977.47), and the amino acid composition of NTnC is listed in table II-1. NTnC contains exactly 50 % hydrophobic residues (hydrophobic amino acids are A, C, F, G, P, I, L, M, V, W, Y) and 50 % hydrophilic residues (hydrophilic amino acids are D, E, K, N, H, Q, R, S, T). NTnC is an acidic protein, with 23 acidic and only 7 basic amino acids.

Amino Acid	Freq (total)	Freq (percent)
A	10	11.11
C	0	0.00
D	10	11.11
E	13	14.44
F	6	6.67
G	7	7.78
H	0	0.00
I	5	5.56
K	4	4.44
L	5	5.56
M	8	8.89
N	1	1.11
P	1	1.11
Q	4	4.44
R	3	3.33
S	4	4.44
T	5	5.56
V	4	4.44
W	0	0.00
Y	0	0.00

Table II-1. Amino acid content of NTnC.

1 ASMTDQQAEA RAFLSEEMIA EFKAAFDMFD ADGGGDISTK ELGTVMRMLG
51 QNPTKEELDA IIEEVDEDGS GTIDFEEFLV MMVRQMKEDA KGKSEEELAN
101 CFRIFDKNAD GFIDIEELGE ILRATGEHVT EEDIEDLMKD SDKNNDGRID
151 FDEFLKMMEG VQ

Figure II-1. Sequence of chicken skeletal troponin-C. The first 90 residues corresponding to the domain used in this study are shown in **bold** letters.

The binding of Ca^{2+}

TnC belongs to a family of proteins that use a common motif to bind calcium, the helix-loop-helix or EF-hand motif that was first described by Kretsinger and Nockolds [9]. The spatial arrangement of a typical helix-loop-helix and the correlation with a right hand are shown in figure II-2. TnC possesses 4 of these helix-loop-helix Ca^{2+}-binding motifs. Sites III and IV have relatively high affinity for Ca^{2+} ($K_{Ca} \approx 2\times10^7$ M^{-1}) and also bind Mg^{2+} ($K_{Mg} \approx 2\times10^3$ M^{-1}). The two binding sites of the N-domain (sites I and II) are specific to Ca^{2+} and are of lower affinity. In the literature, controversial results may be found regarding the binding affinity and the cooperativity of the low affinity sites. Some groups report cooperative coupling between sites I and II, while others propose that the binding process is sequential. The determined binding affinity varies between 10^4 and 10^5. A recent detailed NMR study on NTnC has quantitatively determined the binding constants in sites I and II [10]. A Ca^{2+} titration which was monitored by 2D-{^{15}N, ^1H} HMQC experiments has revealed a stepwise binding for NTnC with affinities (K_{Ca}) of 5.3×10^5 and 5.7×10^4 M^{-1}.

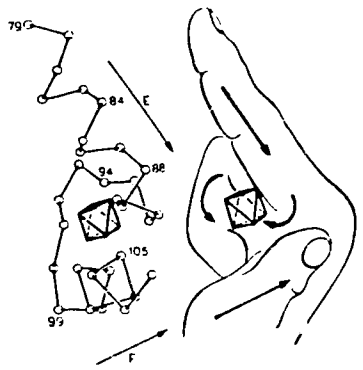

Figure II-2. A helix-loop-helix motif can be symbolized by a right hand. The first helix runs from the tip to the base of the forefinger. The flexed middle finger corresponds to the calcium binding loop. The thumb, roughly perpendicular to the forefinger, represents the second helix of the motif. This motif was first observed in the crystal structure of carp parvalbumin where one of the binding sites is formed by helix E and F, hence the term "EF-hand".

The crystal structure

The crystal structures of both chicken and turkey skeletal TnC have been solved [11, 12, 13]. A ribbon representation of the turkey skeletal crystal structure is shown in figure I-9, and a stereo view of the backbone is displayed in figure II-3. These structures reveal two globular domains, connected by a single 31-residue long central helix. Each domain contains two helix-loop helix units coupled via a short β-sheet formed by the two loops. In these crystals, Ca^{2+} is bound only in the high affinity sites, whereas sites I and II are Ca^{2+}-free. The structure of the Ca^{2+}-bound C-domain was found to be very similar to other homologous Ca^{2+}-binding

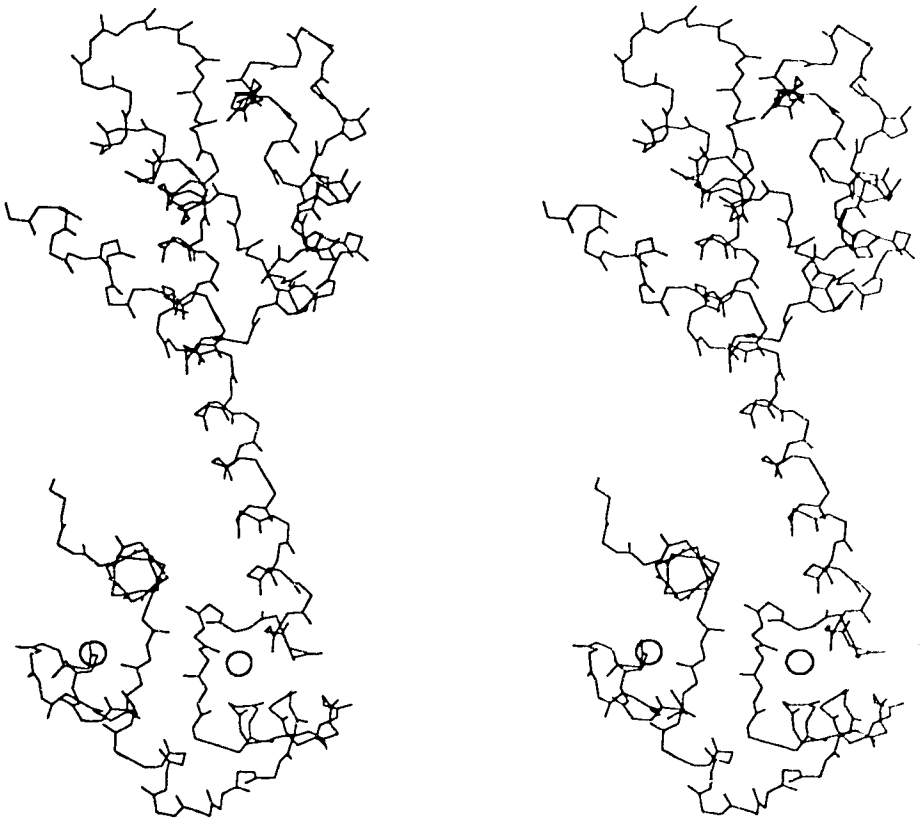

Figure II-3. Stereo view of the crystal structure of turkey skeletal troponin-C. Only the backbone N, Cα, C, O and the Ca^{2+} ions are displayed.

protein structures [14]. The apo N-domain, however, was considerably different mainly in terms of interhelix angles [14]. Table II-2 compares the interhelix angles of the N-domain of TnC with a few Ca^{2+}-bound protein structures, and clearly indicates that the A/B and C/D interhelix angles vary considerably from the usual helix-loop-helix organization.

Table II-2. Interhelix angle differences between the N-domain of TnC and other Ca2+-binding proteins. [a]

HELIX PAIR	others(range) [b]	N-domain TnC	Diff [c]
A/B or E/F	96-109	134	**32**
B/C or F/G	111-124	122	5
C/D or G/H	84-108	146	49
A/D or E/H	110-123	115	2

(a) interhelix angles obtained from ref. 14.

(b) includes TnC (C-domain only), calmodulin (2 pairs) and parvalbumin (1 pair).

(c) difference between the N-domain of TnC and the average of the four related pairs.

Ca^{2+}-induced conformational changes

Evidence of conformational changes

Evidence of the Ca^{2+}-induced conformational changes in TnC was first observed more than two decades ago in the same department as the work presented in this thesis has been done. In 1972 Murray and Kay [15], used CD spectroscopy to demonstrate that the binding of Ca^{2+} was inducing a conformational change in troponin-C (or more accurately the ancestor of troponin-C, troponin A). Over the years, proton magnetic resonance spectroscopy has been used extensively to characterize the structural changes of the two domains of TnC. These studies have shown that binding of Ca^{2+} to the high affinity sites (C-domain) induces changes in the protein fold, and that binding to the low affinity sites (N-domain) leads mainly to changes among hydrophobic side-chains [16, 17, 18, 19, 20, 21]. Laser Raman spectroscopy was also used, and revealed a large increase in α-helical content due to Ca^{2+}-binding to the C-domain sites, and none associated to the N-domain [22]. Other studies, using CD and fluorescence, reported large spectroscopic changes associated with Ca^{2+}-binding to the C-domain, and small changes when the low affinity sites were filled [23, 24, 25, 26, 27]. These studies reported a large increase of negative ellipticity when sites III and IV are filled, consistent with the NMR results. The estimates of the magnitude of the Ca^{2+}-induced far-UV CD ellipticity changes attributable to the N-domain transition were more subtle, less clearly defined, and somewhat contradictory. A recent characterization of the Ca^{2+}-induced spectroscopic changes of the recombinant NTnC clearly indicated a significant increase in the negative far UV CD ellipticity [28] (figure II-4). These data suggest a significant Ca^{2+}-induced transition involving secondary structural elements of the N domain.

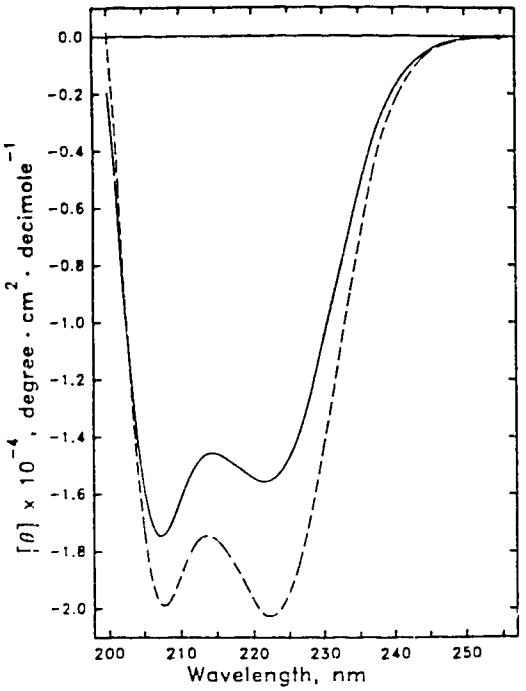

Figure II-4. Far-UV CD spectra of recombinant N-domain of TnC in the absence (—) and presence of Ca^{2+} (pCa = 3.8) (---). The binding of Ca^{2+} induces a very significant increase (~23%) in the negative values of $[\theta]_{221nm}$.

Model for the Ca^{2+}-induced structural change

By comparing the crystal structure of the apo N-domain of TnC with its homologous C-domain, Herzberg et al. proposed a model for the conformational change which occurs in the N-domain of TnC upon Ca^{2+} binding [29]. Using molecular modeling and the assumption that the Ca^{2+}-filled N-domain would adopt a conformation similar to the Ca^{2+}-filled C-domain, they deduced a tentative structure of TnC in the $4Ca^{2+}$ state. The major conformational change in their model is the movement of the B/C pair of helices away from the A/D pair, therefore exposing a hydrophobic patch (see figure II-5). This model is the only structural representation of the Ca^{2+}-saturated form of the regulatory domain of TnC.

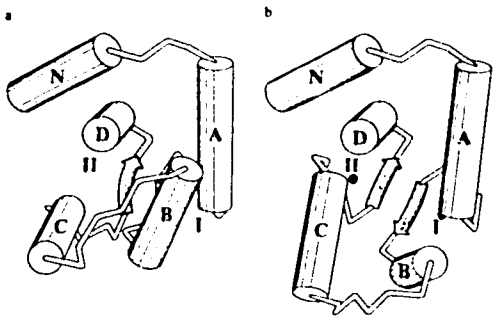

Figure II-5. Diagrammatic representation of the proposed Ca^{2+}-induced conformational change in the N-terminal domain of TnC [29]. In this model helices N, A, and D retain their relative dispositions. Helices B and C and the linker peptide move by up to 14 Å when Ca^{2+} binds. The relative dispositions of helices B and C also remain constant. (a) Ca^{2+}-free conformation of the N-terminal domain of TnC. (b) Proposed Ca^{2+}-bound conformation of this domain.

References

1 Ebashi, S. (1963). *Nature (London)* **200,** 1010.

2 Ebashi, S. & Ebashi, F. (1964). *J. Biochem. (Tokyo)* **55,** 604-613.

3 Ebashi, S. & Kodama, A. (1965). *J. Biochem. (Tokyo)* **58,** 107-108.

4 Hartshorne, D.J. & Mueller, H. (1968). *Biochem. Biophys. Res. Commun.* **31,** 647-653.

5 Schaub, M.C. & Perry, S.V. (1969).. *Biochem. J.* **115,** 993-1004.

6 Schaub, M.C., Perry, S.V. & Hackcer, W. (1972). *Biochem. J.* **126,** 237-.

7 Greaser, M.L. & Gergely, J. (1971). *J. Biol. Chem.* **246,** 4226-4233.

8 Greaser, M.L. & Gergely, J. (1973). *J. Biol. Chem.* **248,** 2125-.

9 Kretsinger, R.H. & Nockolds, C.E. (1973). *J. Biol. Chem.* **248,** 3313-3326.

10 Li, M.X., Gagné, S.M., Tsuda, S., Smillie, L.B. & Sykes, B.D. (1994). *Biochemistry,* submitted.

11 Herzberg, O. & James, M. N. G. (1988). *J. Mol. Biol.* **203,** 761-779.

12 Satyshur, K.A., Rao, S.T., Pyzalska, D., Drendel, W., Greaser, M. & Sundaralingam, M. (1988). *J. Biol. Chem.* **263,** 1628-1647.

13 Satyshur, K.A., Pyzalska, D., Greaser, M., Rao, S.T. & Sundaralingam, M. (1994). *Acta Cryst. D* **50,** 40-49.

14 Strynadka, N. C. J. & James, M. N. G. (1989). *Annu. Rev. Biochem.* **58,** 951-998.

15 Murray, A.C. & Kay, C.M. (1972) *Biochemistry* **11,** 2622-2627.

16 Levine, B.A., Mercola, D., Coffman, D. & Thornton, J.M. (1977). *J. Mol. Biol.* **115,** 743-760.

17 Seamon, K.B., Hartshorne, D.J. & Bothner-By, A.A. (1977). *Biochemistry* **16,** 4039-4046.

18 Levine, B.A., Thornton, J.M., Fernandes, R., Kelly, C.M. & Mercola, D. (1978). *Biochim. Biophys. Acta* **535,** 11-24.

19 Evans, J.S., Levine, B.A., Leavis, P.C., Gergely, J., Grabarek, Z. & Drabikowski, W. (1980). *Biochim. Biophys. Acta* **623,** 10-20.

20 Tsuda, S., Hasegawa, Y., Yoshida, M., Yagi, K. & Hikichi, K. (1988). *Biochemistry* **27**, 4120-4126.

21 Tsuda, S., Ogura, K., Hasegawa, Y., M., Yagi, K. & Hikichi, K. (1990). *Biochem.* **29**, 4951-4958.

22 Carew, E.B., Leavis, P.C., Stanley, H.E. & Gergely, J. (1980). *Biophys. J.* **30**, 351-358.

23 Nagy B. & Gergely J. (1979). *J. Biol. Chem.* **254**, 12732-12737.

24 Leavis, P.C., Rosenfeld, S.S., Gergely, J., Grabarek, Z. & Drabikowski, W. (1978). *J. Biol. Chem.* **253**, 5452-5459.

25 Leavis, P.C., Nagy, B., Lehrer, S.S., Bialkowska, H. & Gergely, J. (1980). *Arch. Biochem. Biophys.* **200**, 17-21.

26 Johnson, J.D. & Potter, J.D. (1978). *J. Biol. Chem.* **253**, 3775-3777.

27 Hincke, M.T., McCubbin, W.D. & Kay, C.M. (1978). *Can. J. Biochem.* **56**, 384-395.

28 Li, M.X., Chandra, M., Pearlstone, J.R., Racher, K.I., Trigo-Gonzalez, G., Borgford, T., Kay, C.M. & Smillie, L.B. (1994). *Biochemistry* **33**, 917-925.

29 Herzberg, O., Moult, J. & James, M.N.G. (1986). *J. Biol. Chem.* **261**, 2638-2644.

CHAPTER III

NMR FOR STRUCTURAL CHARACTERIZATION

The circumstances of the discovery of magnetic properties are veiled in the clouds of antiquity. Passages in the ancient annals of the Chinese Empire refer to a certain "south-pointing carriage" which guides men in fog or storm (~ 2637 B.C.). However, archaeological researches show that these carriages had nothing to do with the magnetic compass but were assemblies of gear wheels. 2000 years later, Thales of Miletus (640-546 B.C), the Father of Philosophy, is said to have attributed a soul to a magnet in order to explain its attractive property. More recently, the text Meng Chhi Pi Than (Dream Pool Essays) dating about A.D., 1080 written by the Chinese philosopher Shen Kua says, "Magicians rub the point of a needle with the lodestone, after which it is able to point to the south".

Although the origin of the discovery of magnetic properties is uncertain, the discovery of the nuclear magnetic resonance phenomenon is well known. It was in 1946 that Bloch at Stanford and Purcell at Harvard, working independently, were able to demonstrate that nuclei can absorb electromagnetic radiation in a strong magnetic field. The two physicists shared the 1952 Nobel prize for their work. A second Nobel prize was awarded in 1991, this time to Richard R. Ernst for his contributions to the development of the methodology of high resolution nuclear magnetic resonance (NMR) spectroscopy.

As for the safety related to long-term exposure to high magnetic fields, NMR spectroscopists can be reassured. Experiments were made in 1892 by Thomas Alva Edison and his collaborators in which they subjected themselves and one dog to very strong magnetic fields without sensing any effect.

General theory

Spins in a magnetic field

Many nuclei behave as if they were spinning charges. These are typically nuclei with odd mass (^{1}H, ^{13}C, ^{15}N, ^{31}P, etc.) and/or odd atomic number (^{2}H, ^{14}N, etc.), which possess a quantized spin angular momentum and a magnetic moment. Each nuclei with spin has a nuclear spin quantum number *I* associated with it. For a nucleus of spin quantum number *I*, there are *2I+1* allowed spin states (from *-I* to *+I*). Since the nuclei encountered in this thesis (^{1}H, ^{13}C and ^{15}N) all have a spin quantum number I=1/2, only this case will be discussed. Therefore these nuclei have two allowed spin states: -1/2 and +1/2. In the absence of a magnetic field, the two spin states have the same energy and are equally populated.

When in an applied magnetic field, however, the two spin states are not of equivalent energy. This is due to the fact that a nucleus is a charged particle, and that any moving charge generates a magnetic field of its own. In a magnetic field, all protons will have the z component of their magnetic moment either aligned to the applied magnetic field, or opposed to it (figure III-1). Hence, upon application of an external magnetic field, the

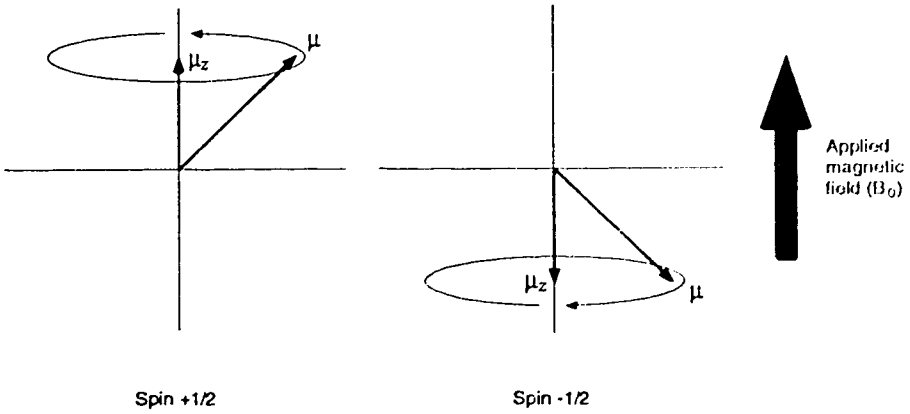

Figure III-1. The two allowed spin states for a nuleus of spin 1/2.

degenerate spin states split into two states of unequal energy (figure III-2).

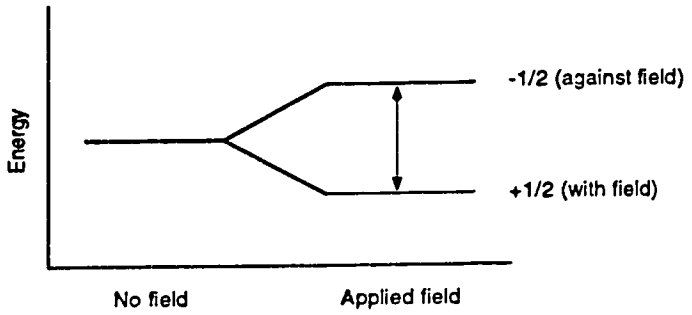

Figure III-2. The energy separation of a spin 1/2 in a magnetic field.

The NMR phenomenon occurs when nuclei absorb energy and change their spin state. The energy absorbed (ie. the energy difference between the two states) is quantized. This ΔE is proportional to the applied magnetic field $\mathbf{B}_0$ and is also dependent on the particular nuclei involved. The energy difference between two spin states is given by:

$$\Delta E = h\nu = \left(\frac{h}{2\pi}\right)\gamma \mathbf{B}_0$$

where h = Planck's constant
ν = the frequency of resonance
γ = gyromagnetic ratio, a characteristic of the paticular nucleus

Energy is absorbed by nuclei because of the fact that, in an applied magnetic field, nuclei precess about their own axis of spin with an angular frequency ω, which is called the Larmor frequency. The angular frequency, ω, is directly proportional to the applied magnetic field. For example, a proton in a 141 000 Gauss field has a frequency of precession of approximately 600 MHz. Energy can be absorbed if radiofrequency waves of this same frequency are applied. This absorption phenomenon is called resonance.

From a single spin to many spins

So far I have been talking about a single spin in a static field. However, what we actually observe is the macroscopic magnetization, or the sum of all the microscopic transitions. Therefore I will now discuss and refer to the bulk magnetization, **M**. At equilibrium in a static field **M** is perfectly aligned with the applied magnetic field, as the xy components of the individual spins cancel out (figure III-3a).

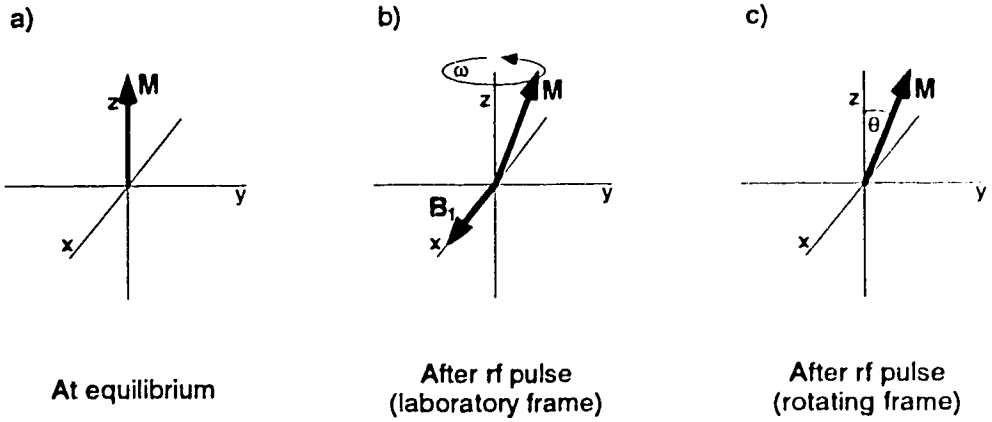

Figure III-3. Application of a pulse. a) Bulk magnetisation **M** at equilibrium in a magnetic field applied along the z axis. b) Magnetisation **M** after the application of a short pulse along the x axis, as viewed in the static laboratory frame. c) Same as b), but in a rotating frame precessing at frequency ω.

Observation of NMR phenomenon

There are three major components in any NMR experiment: pulses, delays and acquisition. Pulses refer to the application of radiofrequency (rf) waves for a certain delay (typically in the 1-100 μs range). An rf pulse usually covers the range of frequencies that are to be observed. If an rf pulse is applied for a short period of time in such a way that it produces a second magnetic field $\mathbf{B}_1$ which is perpendicular to the field $\mathbf{B}_0$, the bulk

magnetization will be pertubed and will precess at the Larmor frequency (see figure III-3b). If, instead of looking at **M** in the fixed laboratory reference frame, we look at it in a rotating frame which also precesses at the Larmor frequency, we would observe a static **M** which is tilted by θ degrees relative to the z axis. The angle θ ("flip angle") is proportional to the length of the pulse t_p and to the magnitude of $\mathbf{B}_1$.

The application of a 90° pulse on the x axis will bring the magnetization **M** on the y axis. Having a coil in the xy plane allows the recording of the oscillating current generated by the precessing magnetization. The system, however, goes back to equilibrium, with the *xy* magnetization slowly fading and the z magnetization growing. The result recorded is shown in figure III-4 and is called a free-induction decay (FID). The FID is a signal oscillating at a frequency corresponding to precession frequency of the nucleus minus a reference frequency (ω-ω_{ref}). Using a mathematical operation called Fourier transform (FT), the time domain is transformed into a frequency domain in order to obtain an NMR spectrum (figure III-4). Of course in real life, more than one proton would be observed. The FID and one-dimensional ^{1}H spectrum of NTnC are shown in figure III-5.

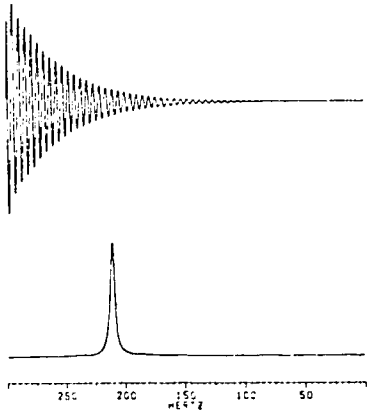

Figure III-4. The NMR observed signal is an FID (time domain) which is Fourier Transformed to produce an NMR spectrum (frequency domain).

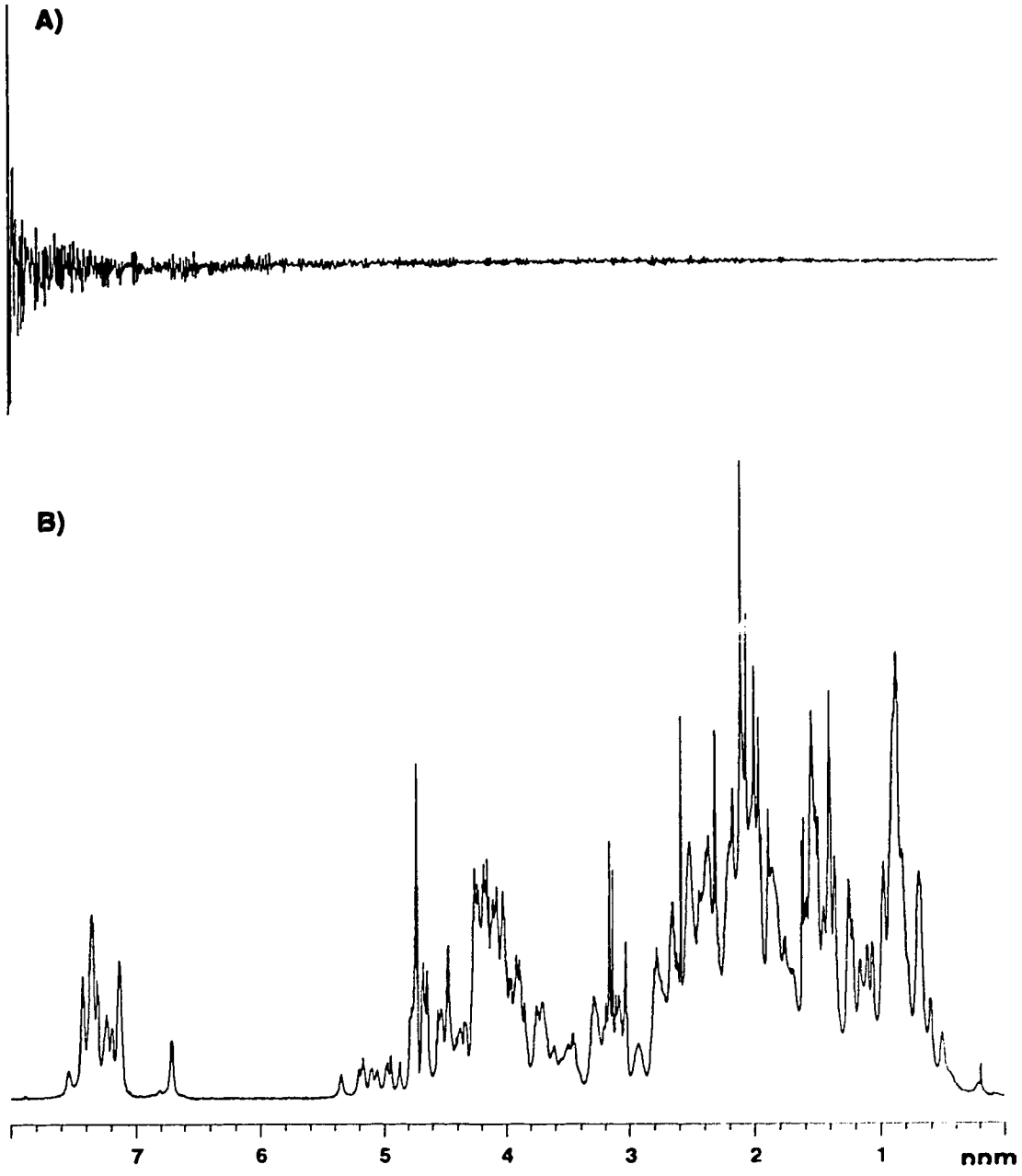

Figure III-5. Real life FID (A) and its corresponding spectrum (B) obtained after Fourier Transform. Shown here is a ^1H spectrum of NTnC complexed with Ca^{2+} acquired in D_2O. One-dimensional spectra of proteins are typically very crowded (this spectrum contains over 550 protons).

As will be seen in chapter IV, NMR experiments typically contain many pulses which are often separated by delays. The complete description of the effect of the combination of various pulses and delays will not be given in this thesis, as it would exceed the size and objectives of this thesis, which is the resolution of the solution structure of Ca^{2+}-saturated NTnC and the characterization of its Ca^{2+}-induced structural changes. I will, however, briefly discuss the two other types (ie. other than chemical shift) of NMR phenomena extensively used in this thesis: through-bond correlation and through-space correlation.

Chemical shift

Of course, NMR would be useless to chemists and biochemists if all protons (or other nuclei) would be precessing at the same frequency. In a molecule, different protons generally have different electronic environments. This is due to circulating electrons which also generate small magnetic fields of their own. A different electronic environment leads to a different effective magnetic field sensed by a given nucleus, and that nucleus will resonate at a different frequency. Therefore, protons in a 141 000 Gauss field will not all resonate at 600 MHz, but actually in the range 600 000 000 ± 6000 Hz. This shielding (or deshielding) effect is measured in Hertz and is usually reported relative to a certain reference compound. Since it is dependent on the strength of the applied field, this shift is divided by the frequency at which the spectrometer operates. The result is a field-independent measure, called the chemical shift (δ) with units of ppm (parts per million):

$$\delta\,(\text{ppm}) = \frac{\text{shift in Hz from a reference}}{\text{spectrometer frequency in MHz}}$$

Proton chemical shifts are typically found within a 15 ppm window.

Through-bond correlation

Nuclei are not antisocial and they actually do "talk" to each other. One of the communication modes, or correlations, that can be observed by NMR is a through-bond correlation called J-coupling. This correlation occurs only between nuclei that are connected by a certain number of bonds (typically 1-3 bonds). The magnitude of this coupling is referred to as the coupling constant J (in Hz), and can vary from 0 to a few hundred Hertz. The simplest through-bond correlation experiment used in this work is the 2D-{^{15}N, ^{1}H}-HMQC, a heteronuclear experiment (correlates two different kinds of nuclei). This experiment also introduces the concept of multi-dimensional NMR spectroscopy.

In the multi-dimensional experiments used in this work, chemical shifts are detected more than once, and the chemical shifts from one dimension are correlated to the chemical shifts of the other(s) dimension(s) using a mode of communication determined by the pulse sequence. In the case of the 2D-{^{15}N, ^{1}H}-HMQC, the first dimension (F1) reports ^{15}N chemical shifts, the second dimension (F2) reports ^{1}H chemical shifts, and the correlation observed is a one-bond connectivity (or one-bond coupling) between ^{1}H and ^{15}N. The pulse sequence for this experiment is shown in figure III-6. The resulting 2D spectrum is shown in figure III-7. In a protein, this experiment shows a correlation for each of the backbone amide (plus some side-chain correlations from residues that possess NH or NH_2 groups).

Through-space correlation

The most useful NMR correlation to the structural NMR spectroscopist is without any doubt the through-space correlation. This correlation, named the NOE (nuclear Overhauser effect), occurs between nuclei that are close

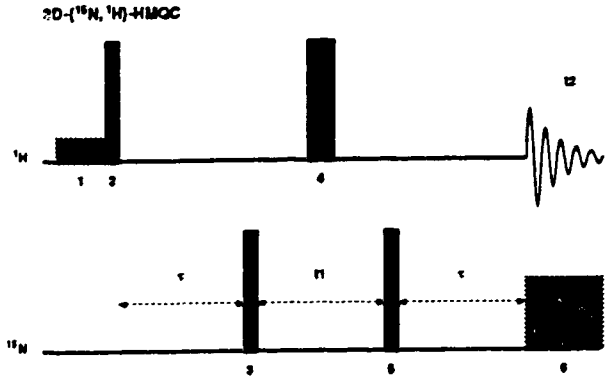

Figure III-6. Pulse sequence of the 2D-{^{15}N, ^{1}H}-HMQC experiment. Narrow and large bars indicate 90° and 180° pulses, respectively. Shaded squares represent decoupling periods. The ^{15}N chemical shifts are recorded during the evolution time t1 and ^{1}H chemical shifts are detected during the t2 evolution time. More details about this experiment is given in chapter IV.

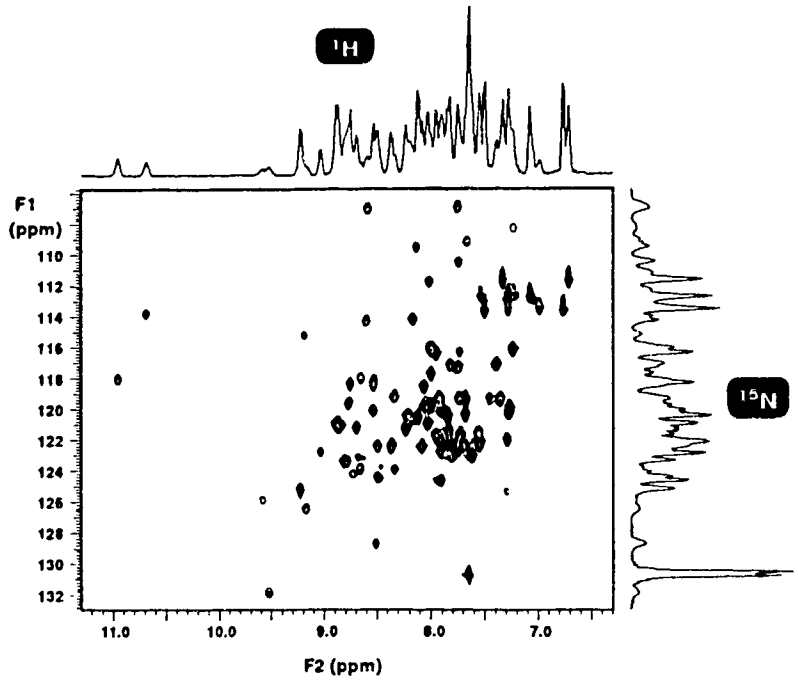

Fifure III-7. Two-dimensional {^{15}N, ^{1}H}-HMQC acquired using the pulse sequence of figure III-6. The sample is uniformly ^{15}N-labelled NTnC (Ca^{2+}-saturated). On top is a 1D projection corresponding to the 1D-spectrum of the amide protons. On the right is a 1D projection corresponding to the 1D-spectrum of the amide nitrogens. Each correlation peak therefore represents one backbone amide, or side-chain HN/HN_2 group.

in space. In simplest terms the magnitude of the NOE is proportional to $1/r^6$, where r is the distance between two nuclei.

$$\mathbf{NOE} \propto \frac{1}{r^6}$$

Due to this relationship, the NOE fades quickly with distance, and NOE's are not normally observed between protons that are more than 5 Å apart. The pulse sequence for a conventional 2D-NOESY experiment is shown in figure III-8, and the resulting spectrum is displayed in figure III-9. In the homonuclear 2D-NOESY, ^1H chemical shifts are detected in both dimensions (F1 and F2), and the magnitude of the correlations observed is inversely proportional (to the sixth power) to the distance between the protons at chemical shift F1 and the protons at chemical shift F2.

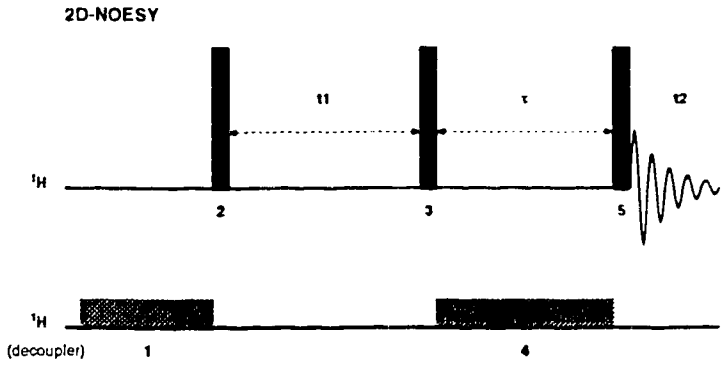

Figure III-8. Pulse sequence of the 2D-NOESY experiment. Here proton chemical shifts are recorded both during t1 and t2. The correlation measured in this experiment in the NOE between different protons. The NOE correlation develops during the mixing time (τ).

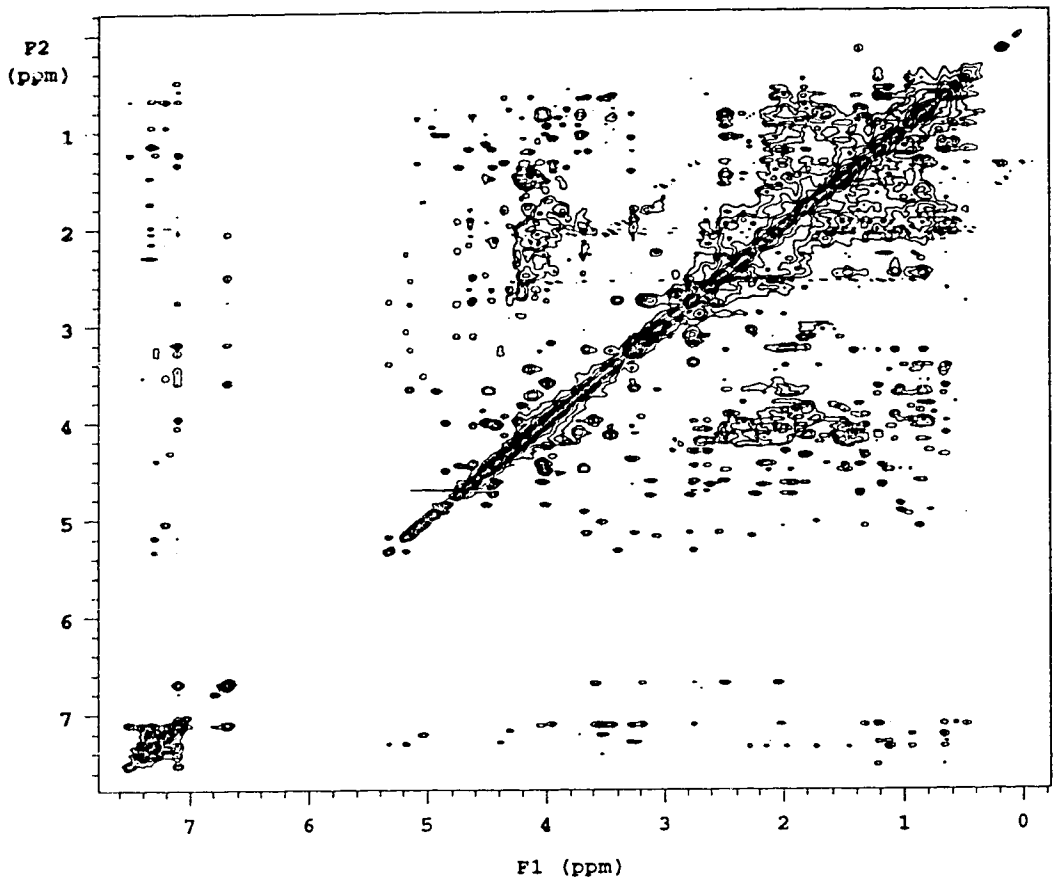

Figure III-9. Two-dimensional NOESY spectrum obtained from the pulse sequence of figure III-8. In this spectrum, both dimensions (F1 and F2) represent ^{1}H chemical shifts. The peaks observed correlate to distances between protons in F1 and F2.

From NMR spectra to solution structure

Chemical shift assignment

The first step of solving an NMR structure is the determination of all the chemical shifts of interest. This step is often the most time consuming (the complete assignment of NTnC involved about 1000 nuclei to be assigned) but also probably the most entertaining (for people who like to solve puzzles). A description of the approach I used will be given in chapters V and VI for the backbone and side-chain assignments, respectively. Through-bond correlation experiments are primarily used for the assignment, but NOE data are usually also necessary for complete assignments. The chemical shift distribution in proteins is reasonable, as can be seen in figure III-10, but chemical shift overlap is inevitable in a large proteins (see figure III-5b).

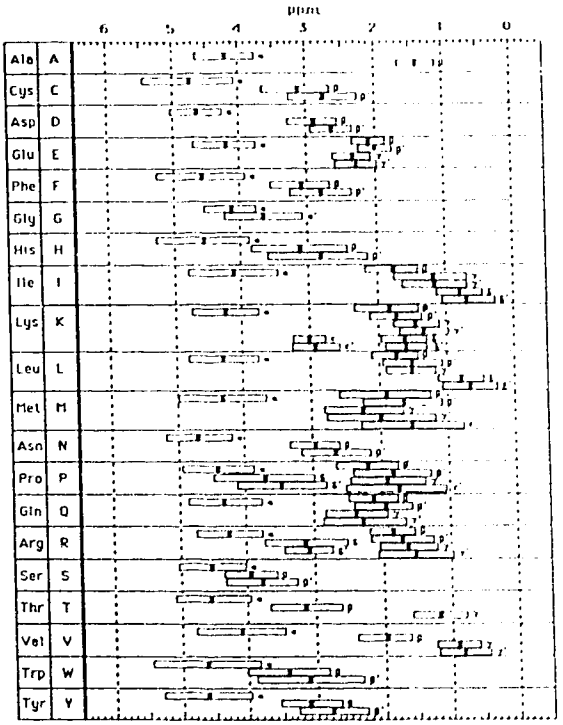

Figure III-10. Distribution of ^{1}H chemical shifts in proteins. The horizontal bars correspond to the range of chemical shifts within 1 standard deviation of the mean, and the dark portion is the actual average chemical shift. Statistics like the one illustrated in this figure are extremely useful to help assign protein NMR spectra.

Secondary structure determination

Once most of the backbone resonances and backbone NOE's are assigned, the secondary structure of a protein can be determined. This can usually be accomplished via two methods, which may be combined to give an accurate determination of the secondary structural features of a protein. The first method involves interpretation of the NOE data, and is based on the fact that different secondary structure stretches have different NOE patterns (or different interproton distances). This approach has been developed by Kurt Wüthrich [7], and is illustrated in figure III-11. The second approach, known as the chemical shift index (CSI), relies solely on the chemical shifts of the backbone nuclei, and has been optimized by Wishart et al. [4, 5, 6]. The basis of this approach is clearly illustrated in figure III-12 and III-13, showing the relationship between chemical shifts and protein secondary structure. The chemical shift statistics compiled by David Wishart [4, 5, 6] has played an important role in both the assignment and the secondary structure determination stage. More details on the secondary structure determination will be given in chapter V.

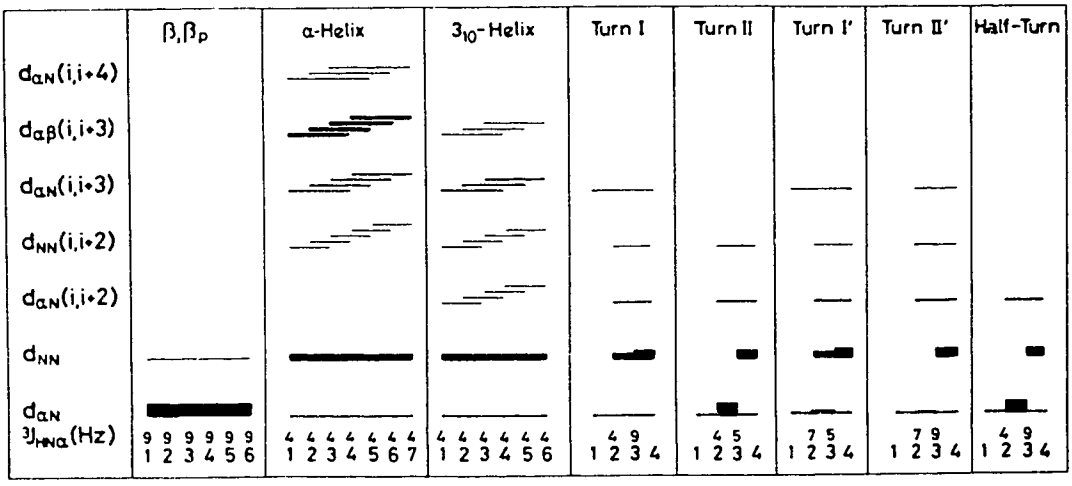

Figure III-11. Survey of expected NOE's in various secondary structures [7]. The thickness of the lines represents the NOESY cross-peak intensities.

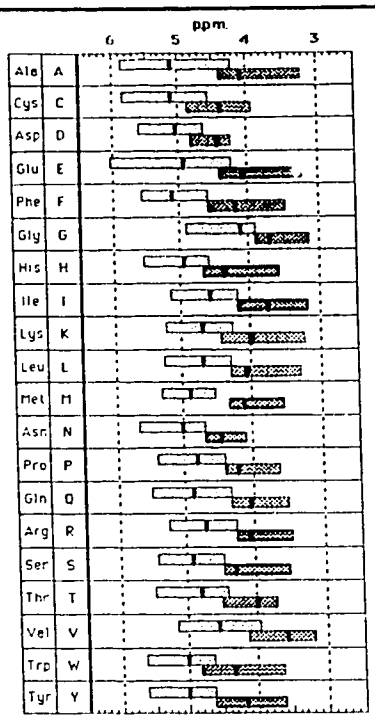

Figure III-12. Distribution of α-proton chemical shifts in helices (dark bars) and β-strands (light bars). α-proton chemical shifts can therefore be used to estimate secondary structure.

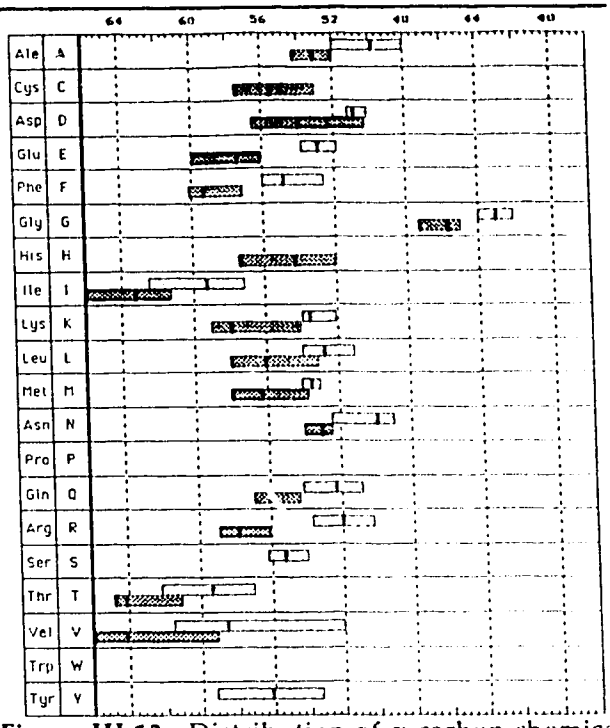

Figure III-13. Distribution of α-carbon chemical shifts in helices (dark bars) and β-strands (light bars). Similar to α-protons, α-carbon chemical shifts are useful for characterizing secondary structure.

Tertiary solution structure determination

After all the resonances in the protein have been assigned, as many NOE's as possible must be subsequently assigned. Nowadays, this step is usually done in a semi-automated way with the help of computer software. Details regarding the assignment of over 1000 NOE's will be briefly given in chapter VI. This NOE data is then transformed into distance information and fed to a structure calculation program. Typically 20-60 structures are calculated in order to cover most of the allowed conformational space that agrees with the experimental data. Figure III-14 summarizes the various steps involved in protein NMR structural studies.

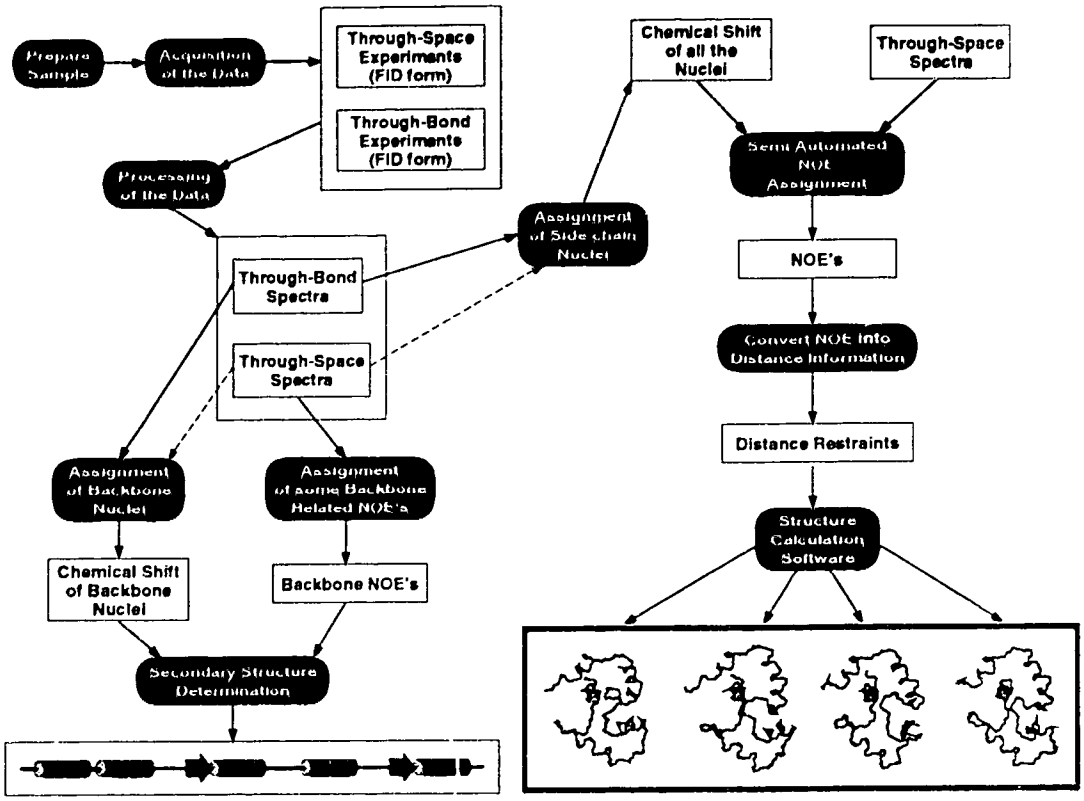

Figure III-14. Schematic diagram of the various steps involved in a typical protein structure determination by NMR. Rounded boxes/reverse text represents processes, and squared boxes/black text represent input or output from a process. Dashed arrows represent a minor contribution to the corresponding process.

References

1 Bax, A., Griffey, R.H. & Hawkins, B.L. (1983). *J. Magn. Reson.* **55**, 301-315.

2 Jeener, J., Meier, B.H., Bachmann, P. & Ernst, R.R. (1979). *J. Chem. Phys.* **71**, 4546-4553.

3 Macura, S. & Ernst, R.R. (1980). *Mol. Phys.* **41**, 95-117.

4 Wishart, D.S., Sykes, B.D. & Richards, F.M. (1991). *J. Mol. Biol.* **222**, 311-333.

5 Wishart, D.S. & Sykes, B.D. (1994a). *Methods in enzymology: nuclear magnetic resonance part C* (in press).

6 Wishart, D.S. & Sykes, B.D. (1994b). *J. Biomol NMR* **4**, 171-180.

7 Wüthrich, K. (1986). *NMR of proteins and nucleic acids.* New York: John Wiley & Sons.

CHAPTER IV

GETTING THE DATA

Two-dimensional NMR has been used in recent years as a structural tool for small proteins [1]. Since spectral overlap is proportional to the size of the protein studied, analysis of larger proteins using 2D-NMR becomes tedious and structure determination is limited to a fairly low resolution. With the development of multidimensional heteronuclear NMR (3D- and 4D-NMR) in the last few years [2], and the feasible $^{15}N/^{13}C$ labeling of proteins via cloning and expression, NMR is now a powerful structural method for proteins in the 10-20 kDa range. These 3D- and 4D-NMR techniques allow removal of most of the overlap in NMR spectra, resulting in more complete analyses and high resolution solution structures.

First Things First: Getting the Protein

NTnC preparation and ^{13}C and ^{15}N labeling

Although I was not involved in the preparation of the protein I used during my research, that protein did not fall from the sky. I believe it is essential to include the procedure behind the preparation of NTnC simply because... no protein ≡ no structure. On this note, I reiterate my acknowledgment to the people in Dr. Smillie's lab, especially to Monica X. Li who produced ~400 mg of uniformly labelled ^{15}N-NTnC and ~200 mg of uniformly double-labelled $^{15}N/^{13}C$-NTnC.

For the preparation of NTnC the polymerase chain reaction was performed by using two 30 mer oligonucleotides and pTZ18.TnC (91stop) as a template. The construction of pTZ18.TnC (91 stop) was described in Li et al. [3]. The 5′-end oligonucleotide for the polymerase chain reaction was designed to include codons corresponding to amino acid residues 1-6 of TnC (underlined) and flanked on the 5′ direction by an initiation codon (bold letters) and nucleotides of the pET3a vector [4] including the NdeI restriction enzyme site:

5′-GAGATATACATATG<u>GCGTCAATGACGGACC</u>-3′.

The 3′ end oligonucleotide includes a sequence (underlined) corresponding to amino acid residues 85-90 of the non-coding strand of the TnC gene. This is preceded in the 5′ direction by a complimentary sequence for a stop codon (bold letters) and a BamHI restriction site:

5′-AATATGGATCCTA<u>GGCGTCCTCTTTCATCT</u>-3′.

Polymerase chain reaction was performed in a Perkin Elmer thermal cycler (model 480) using Taq polymerase and conditions essentially as described by Ho et al. [5]. The amplified DNA fragment was digested with restriction enzymes NdeI and BamHI and ligated into the corresponding sites of expression vector pET3a plasmid DNA cleaved with the same enzymes [4]. The ligation mixture was transformed into competent *E.Coli*

BL21(DE3) pLys S cells and the entire region of the TnC gene sequenced to ascertain the correctness of the amplification by the Taq polymerase enzyme. The expression of NTnC was carried out in minimal medium utilizing the isopropyl β-D-thiogalactopyranoside induction protocol of Studier et al. [4]. The minimal medium consisted of M9 salts as described by Maniatis et al. [6] with $(NH_4)_2SO_4$ replacing NH_4Cl. Each one liter medium at pH 7.5 contained 6g Na_2HPO_4, 3g KH_2PO_4, 0.5g NaCl and 1g $(NH_4)_2SO_4$ to which was added 2 ml of mineral mixture (1M $MgSO_4$, 0.1mM $FeCl_3$ and 12.5mM $ZnSO_4$), 1 ml of 100 mM $CaCl_2$ and 1 ml of vitamin mixture (0.1g/100ml each of D-biotin, choline chloride, folic acid, niacinamide, D-pantothenic acid and pyridoxal chloride, 0.5g/100ml thiamine chloride, 0.01g/100ml riboflavin, all in H_2O). Glucose (3g) dissolved in 20ml H_2O was added with supplements of ampicillin and chloramphenicol to final concentrations of 100μg/ml and 25μg/ml respectively. The above additives were sterilized separately by filtration. For expression of uniformly enriched ^{15}[N] and/or ^{13}[C] NTnC, the $(NH_4)_2SO_4$ and/or glucose of the medium were replaced with ^{15}[N] $(NH_4)_2SO_4$ (99.9 atom %) and/or ^{13}[C] glucose (99.0 atom %) respectively, both purchased from Isotec Inc. Purification of NTnC followed the previously published procedure for fusion TnC [7]. During expression in *E. Coli*, the N-terminal Met, corresponding to the initiation codon, is cleaved off leaving Ala-1 as the N-terminal residue. Overall recovery of NTnC was ~100mg/liter of growth culture.

NMR sample preparation

Upon reception of the protein, I first removed the Ca^{2+} from the sample. To make the calcium-free sample (apo-NTnC), decalcification was accomplished by using G-25 gel filtration: 10mg of the sample dissolved in 1ml of 0.5M EDTA (pH=8.0) was applied to a 160ml (1.5x90cm) G-25 gel filtration column and eluted with 25mM NH_4HCO_3. The profile of the separation is shown in figure IV-1. Fractions containing protein were

pooled, lyophilized, dissolved in Ca^{2+}-free water and lyophilized again to volatilize all of the NH_4HCO_3. 10mg of apo-NTnC sample was dissolved in 0.5ml of 100mM KCl in either H_2O (H_2O:D_2O=9:1) or D_2O (99.996%), to give a final concentration of 2mM. 4.2 mM of $CaCl_2$ was added to obtain the $2Ca^{2+}$ form of NTnC. Upon addition of $CaCl_2$ the pH usually drops between pH 5 and 6, and NaOH (or NaOD) was used to adjust the pH up to 6.7. The same procedure was used for the unlabelled, the ^{15}N and the $^{15}N/^{13}C$ samples.

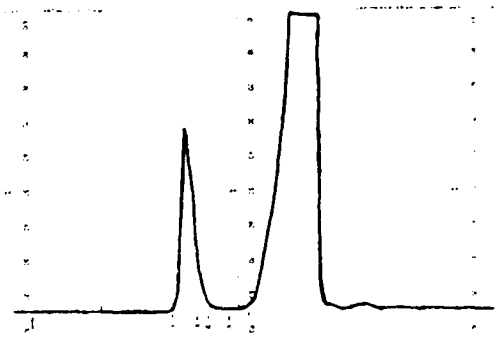

Figure IV-1. Profile of the separation on G25 column. The first peak (left) is NTnC and the second peak is EDTA.

Data Acquisition

Overview

All experiments were carried out on a Varian Unity-600 NMR spectrometer operating at a temperature of 30°C. The following experiments were used for the study of NTnC·2Ca: 2D{^{15}N-^{1}H} HMQC [8], 3D-HNCA [9], 3D-HNCO [9], 3D-HNCOCA [9], 3D-HCACO [10], 3D-^{15}N-edited NOESY (150 ms) [11], and 3D-^{15}N-edited TOCSY (70 ms) [12]. The $^{3}J_{HN\text{-}H\alpha}$ coupling constants were obtained from HMQC-J experiments [18] with the following numbers of complex points and spectral widths: (^{1}H) 1024, 8000 Hz, (^{15}N) 384, 1800 Hz . For the spectra recorded in H_2O, water suppression was achieved by presaturation (1.0-1.2 sec.).

Acquisition and processing

In all experiments, the ^{1}H acquisition dimension was centered at the water frequency (4.67 ppm) with a spectral width of 13.33 ppm (5.00 ppm in the HCACO case). The indirectly detected ^{15}N carrier position and spectral width were either 119.22 ppm and 28.01 ppm (HNCA, HNCOCA and HNCO), or 117.44 ppm and 23.03 ppm (^{15}N-edited NOESY and ^{15}N-edited TOCSY). The corresponding parameters for the ^{13}Cα were either 55.83 ppm and 30.25 ppm (HNCA, HCACO), or 56.11 and 24.18 (HNCOCA). Finally, the ^{13}CO carrier position and spectral width were either 177.11 ppm and 11.93 ppm (HNCO), or 176.34 ppm and 18.05 ppm (HCACO).

For the HCACO experiment, the number of complex points acquired was 512 in F3 (^{1}H); for all other 3D experiments, 1024 complex points were acquired in F3 (^{1}H). For the HNCA and HNCOCA experiments, there were 48 and 32 complex points acquired in F2 (^{13}Cα) and F1 (^{15}N), respectively; the time-domain was increased by 32 complex points in both F2 and F1 dimensions by means of linear prediction and, after zero-filling, the final spectra consisted of 1024 * 256 * 64 points. The number of complex points acquired for the HNCO was 64 in F2 (^{13}CO) and 32 in F1 (^{15}N); 32 additional complex points were predicted in the F1 dimension to finally generate, after

zero-filling, a 1024 * 128 * 64 point spectrum. For the HCACO, we acquired 35 complex points in F2 (^{13}CO) and 28 complex points in F1 (^{13}Cα); both F2 and F1 time-domain were subsequently extended using linear prediction to give a 512 * 128 * 64 point spectrum. In the case of the ^{15}N-edited NOESY and ^{15}N-edited TOCSY, 32 and 128 complex points were acquired in F2 (^{15}N) and F1(^{1}H), respectively; 32 complex points were added to the F2 dimension by linear prediction to obtain a final 1024 * 64 * 256 points spectrum. The HMQC-J's were processed to a final size of 2048 * 2048 points with a 90°-shifted sinebell in F2 (^{1}H) and the following filtering VNMR parameters in F1 (^{15}N) : GF=0.06 (NTnC-apo), GF=0.05 (NTnC-2Ca), LB=-8, -10, -12, -14, -16, -18, -20, -22, -24, -26, -28. The splittings at various LB's were fitted with the HMQCJFIT software [19] to obtain the $^{3}J_{HNH\alpha}$ coupling constants.

For all experiments except the HCACO, a post-acquisition solvent suppression by convolution of the time-domain data was applied prior to Fourier transform [13]. In most of the cases, a 60°-shifted squared sinebell was applied in F1 and F2, and a 90°-shifted sinebell function in F3. After Fourier transform of the F3 dimension, parts of the spectra without resonances were discarded, when possible, prior to the processing of F2 and F1, thus reducing the size of the final spectra by 50% or 75%.

Processing of the 2D and 3D data sets was accomplished using either the VNMR software (VNMR 4.1A, Varian, Palo Alto, CA) or NMRPIPE (Delaglio et al., NIDDK, NIH, MD, unpublished). When used within the VNMR software, extension of the time domain was achieved using the linear prediction algorithm *lpfft*. Automatic peak-picking of the transformed 3D spectra was achieved using the CAPP program [14]. Since CAPP is run at the noise level and every spectrum contains imperfections, a number of false peaks are usually picked. Most of those peaks were removed automatically by using the in-house program PPFILT (Willard & Gagné, PENCE, University of Alberta, unpublished). PPFILT filters the peak list of a 3D spectrum through a high signal-to-noise 2D spectrum (or another 3D spectrum). For example, the 3D-^{15}N-edited NOESY has been filtered through a 2D-^{15}N-HMQC. In the last step of the peak-picking, we used the

interactive graphic-based program PIPP [14] to visualize the output of CAPP/PPFILT and edit the peak-pick table. Both processing and peak-picking were accomplished on a Sun Sparc2 workstation. The chemical shift reference used for ^{1}H and ^{13}C is 2,2-dimethyl-2-silapentane-5-sulfonic acid (DSS). ^{15}N chemical shifts are reported relative to external acidic NH_4Cl (24.93 ppm).

Pulse sequence programming

The developement of a multitude of three- and four-dimensional experiments occured in the last few years, as my research project was going along. The three-dimensional pulse sequences used in this study were available only from the literature at the time, and I had to implement them first, along with Carolyn M. Slupsky. Pulse sequences were written in C, the programming language used by the VNMR software to control the spectrometer. The pulse sequence code I wrote will not be listed in this chapter, but can be found in appendix A. The rest of this chapter will present all the pulse sequences implemented and used. Each pulse sequence will be described by:

1) Main reference(s)
2) Correlation(s) observed by the experiment
3) Coupling constant involved in the experiment
4) Comments
5) Pulse sequence

   Note: For all pulse sequences, narrow and large pulse indicate 90° and 180° pulses, respectively. Oval pulses correspond to shifted-laminar pulse [17] Gray-filled rectangular indicate decoupling.
6) Phase cycling

   † indicates pulse shifted 90° for hypercomplex F1

   ‡ indicates pulse shifted 90° for hypercomplex F2
7) Delays
8) Spectra

2D-{^{15}N, ^{1}H}-HMQC

References: Summers, M.F., Marzilli, L.G. & Bax, A.
J. Amer. Chem. Soc. **108**, 4285-4294 (1986) [15]

Bax, A., Griffey, R.H. & Hawkins, B.L.
J. Magn. Reson. **55**, 301-315 (1983) [16]

Correlations: Correlates ^{1}HN to covalently bonded ^{15}N. One peak is found for each observable backbone amide (all amino acids except Pro). Although the backbone correlations are the most used, other peaks appear in the spectra. Gln and Asn side-chains display two additional correlations (one for each proton of the NH_2 group) which appear like a doublet. Arg side-chains can have up to five additional correlations (one for the ^{1}HNε and one for each of the 4 ^{1}HNζ); these correlations are not always observable due to exchange with the water. Lys, His and Trp can also display side-chain correlations.

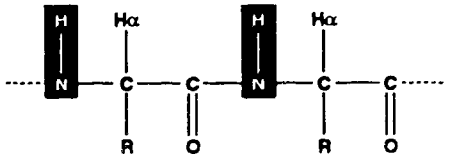

Figure IV-2: Correlations observed in 2D-{^{15}N, ^{1}H}-HMQC

Coupling constant: $^{1}J_{NH}$ ~ 95 Hz

Comments: This experiment is not used for the assignment purpose

itself. The role of the 2D-{^{15}N, ^{1}H}-HMQC is rather to provide a first idea of the spectral dispersion and to aid in choosing the ^{15}N spectral window for the 3D experiments. Folding of ^{15}N resonances, which is often desired in some 3D-experiments, can be predicted using this experiment. Therefore a 2D-{^{15}N, ^{1}H}-HMQC with a large spectral window (~ 80 ppm centered at ~ 105 ppm) should always be one of the first steps in a study involving heteronuclear multidimensional experiments. This experiment can also be used to get accurate ^{1}H and ^{15}N chemical shifts, since the resolution is usually better in this experiment versus 3D-experiments.

Pulse sequence:

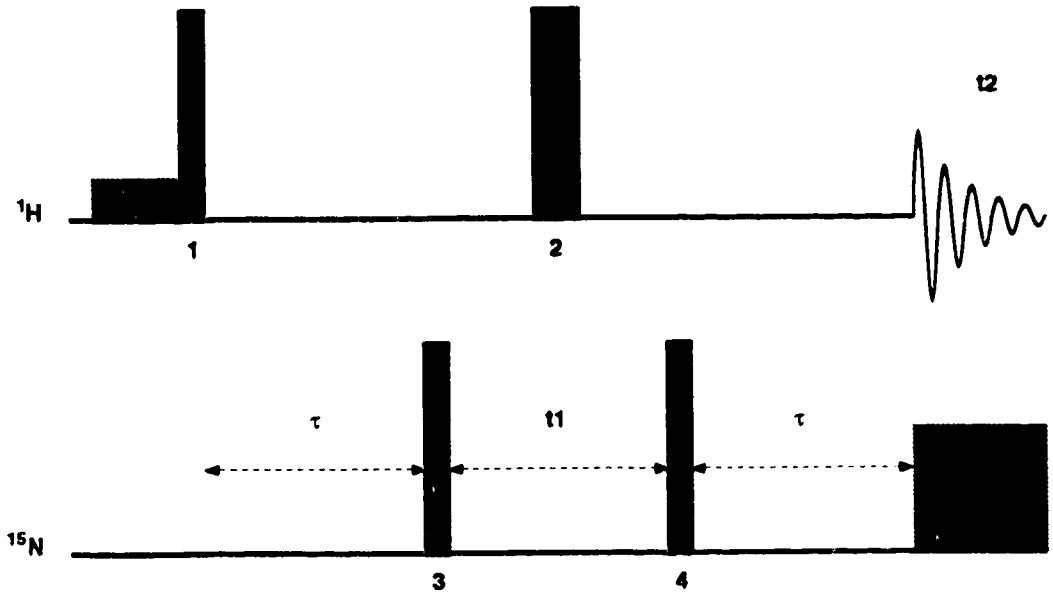

Figure IV-3: Pulse scheme of the 2D-{^{15}N, ^{1}H}-HMQC

Phase cycling:

1	x x y y
2	x x y y
$3^{\dagger}$	x -x x -x
4	x x y y
Acq	x -x y -y

Delay:

$\tau \approx 1/(2\times{}^1J_{HN})$

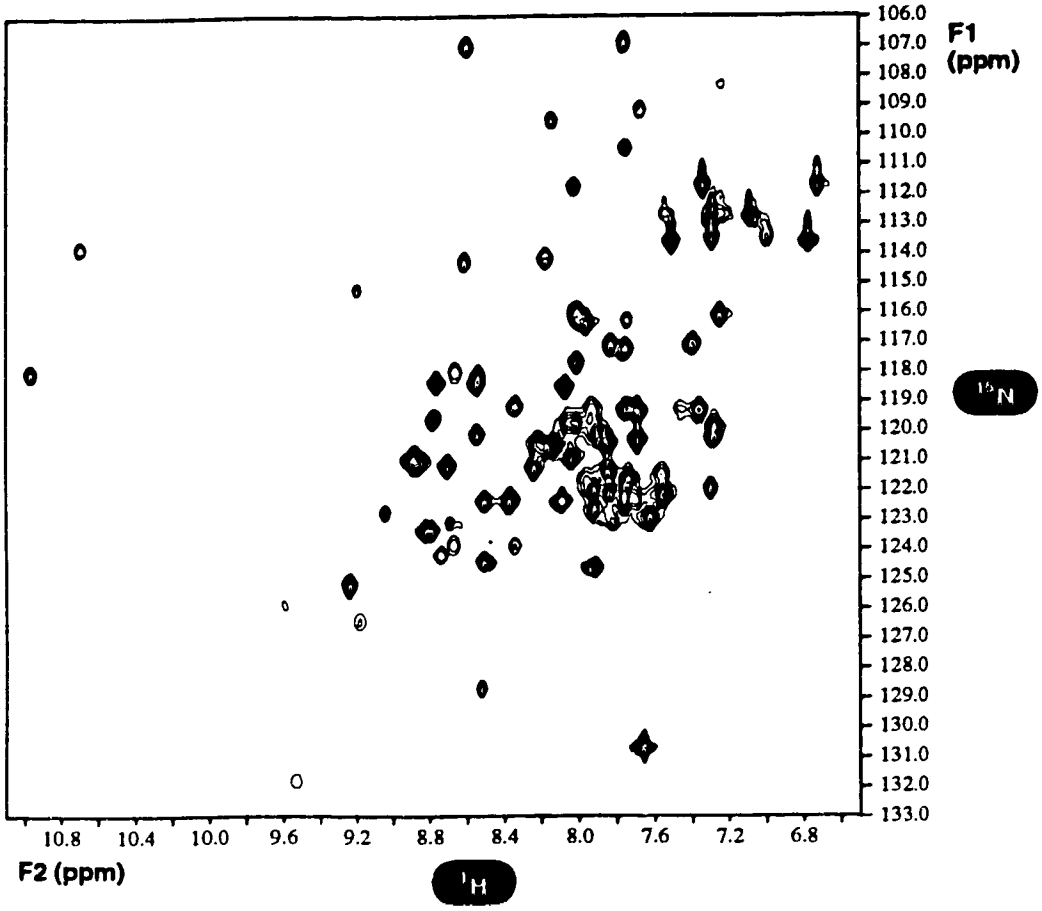

Figure IV-4. 2D-{^{15}N, ^{1}H}-HMQC spectrum of NTnC·2Ca

3D-HNCA

Reference: Grzesiek, S. & Bax, A.
J. Magn. Res. **96**, 432-440 (1992) [9]

Correlations: Correlates backbone amides with both the intra-residue $^{13}C\alpha$ and the inter-residue (i, i-1) $^{13}C\alpha$. ^{1}H, ^{15}N and $^{13}C\alpha$ resonances are observed. For each $^{1}H/^{15}N$ pair, there is a strong $^{13}C\alpha$ peak for the intra-residue correlation and a weaker $^{13}C\alpha$ peak for the inter-residue correlation.

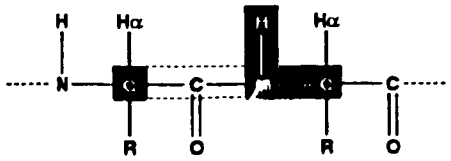

Figure IV-5: Correlations observed in 3D-HNCA

Coupling constant:		
	$^{1}J_{NH}$	~ 95 Hz
	$^{1}J_{NC\alpha}$	~ 9-13 Hz
	$^{2}J_{NC\alpha}$	~ 5-10 Hz

Comments: This experiment is used for the sequential backbone assignment through the $^{13}C\alpha$.

Pulse sequence:

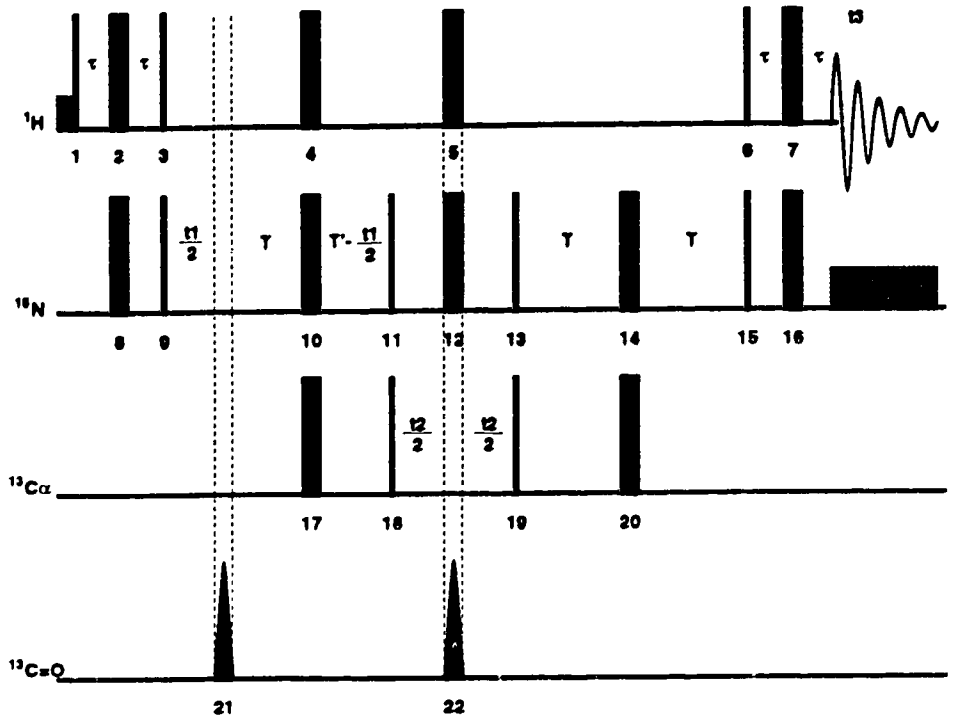

Figure IV-6: Pulse scheme of the 3D-HNCA

Phase cycling:

1	x	2 x	3 y -y
4	x	5 x	6 x
7	x	8 x -x	9† x
10	x x x x y y y y	-x -x -x -x -y -y -y -y	
11	y y y y y y y y	y y y y y y y y	
	-y -y -y -y -y -y -y -y	-y -y -y -y -y -y -y -y	
12	x	13 x	14 x
15	y	16 x	
17	x x x x x x x x	x x x x x x x x	
	-x -x -x -x -x -x -x -x	-x -x -x -x -x -x -x -x	

18‡	x x -x -x 19 x 20 x
21	x 22 x
Acq	x -x -x x -x x x -x x -x -x x -x x x -x
	-x x x -x x -x -x x -x x x -x x -x -x x

Delays:

$\tau \approx 1/(4\times{}^{1}J_{HN})$

T = 13.5 ms

T′ = T + pulse width (21)

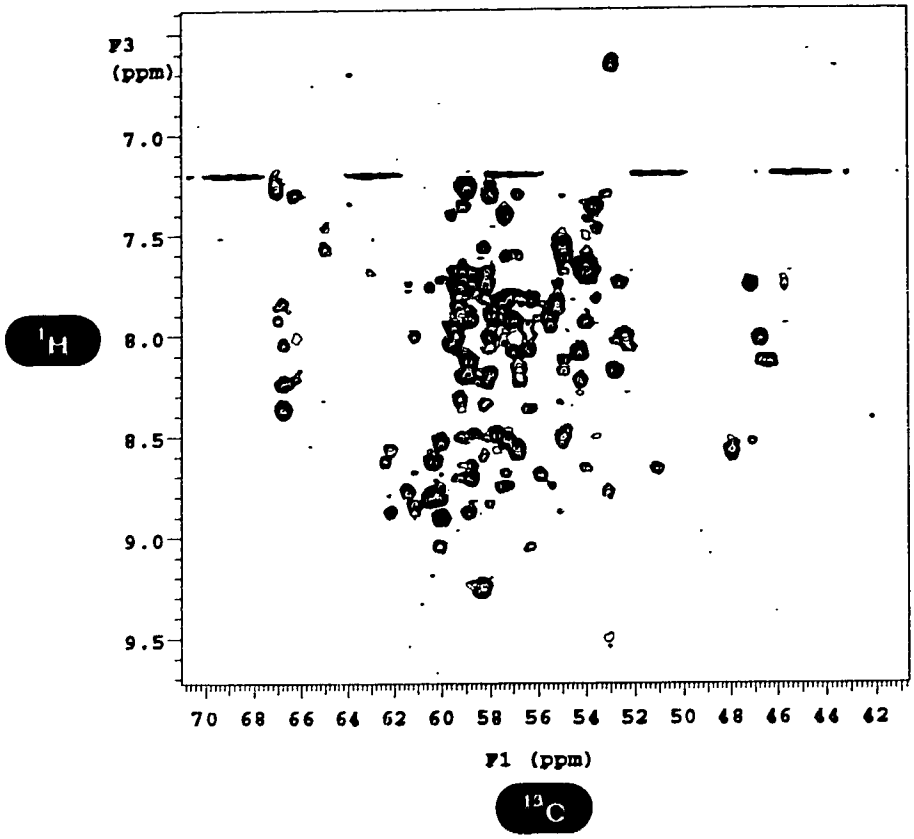

Figure IV-7. Projection of the 64 planes of the HNCA spectrum of NTnC·2Ca.

3D-HNCOCA

Reference: Grzesiek, S. & Bax, A.
J. Magn. Res. **96**, 432-440 (1992) [9]

Correlations: Correlates backbone amides with only the inter-residue (i, i-1) $^{13}C\alpha$. ^{1}H, ^{15}N and $^{13}C\alpha$ are observed. For each $^{1}H/^{15}N$ pair, there is only one strong inter-residue $^{13}C\alpha$ correlation.

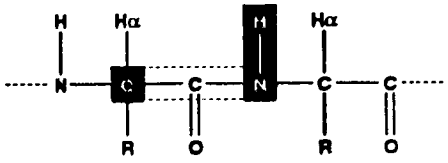

Figure IV-8: Correlations observed in 3D-HNCOCA

Coupling constant:

$^{1}J_{NH}$	~ 95 Hz
$^{1}J_{NCO}$	~ 15 Hz
$^{1}J_{C\alpha CO}$	~ 55 Hz

Comments: This experiment is used for the sequential backbone assignment through the $^{13}C\alpha$.

Pulse sequence:

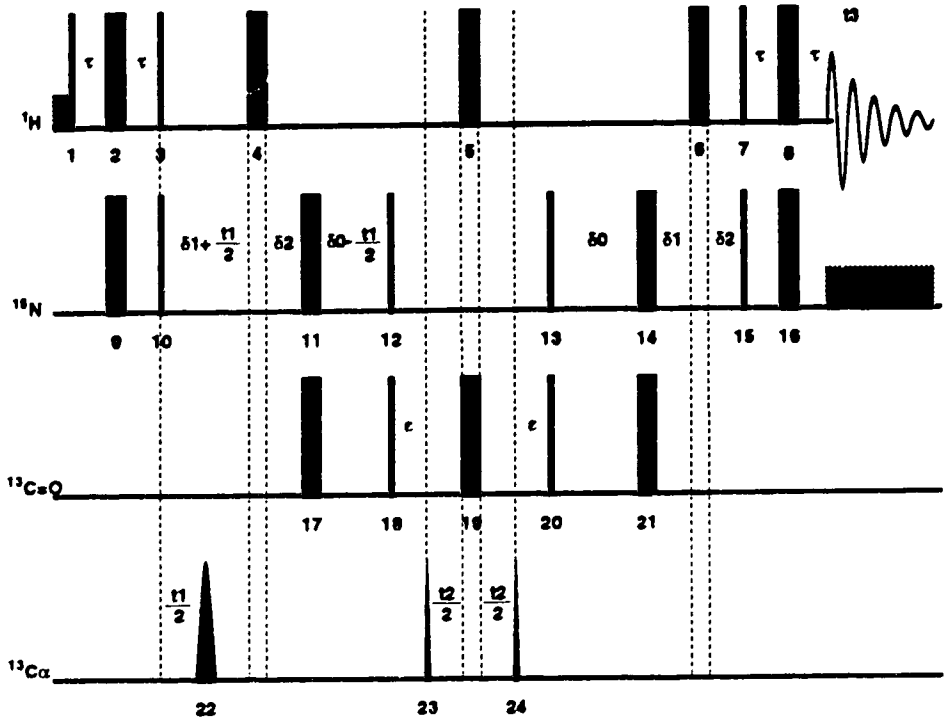

Figure IV-9: Pulse scheme of the 3D-HNCOCA

Phase cycling:

1	x	2 x	3 y -y
4	x	5 x	6 x
7	x	8 x	9 x -x
10†	x		
11	x x x x y y y y -x -x -x -x -y -y -y -y		
12	x -x	13 x	14 x
15	x	16 x	17 x
18	x	19 x	20 x
21	x	22 x	23‡ x x -x -x
24	x		
Acq	x x -x -x -x -x x x		

Delays:

$\tau \approx 1/(4 \times {}^{1}J_{HN})$

$\delta 1 = 7.25ms$

$\delta 2 = 2.75ms$

$\delta 0 = \delta 1 + \delta 2 +$ pulse width (22)

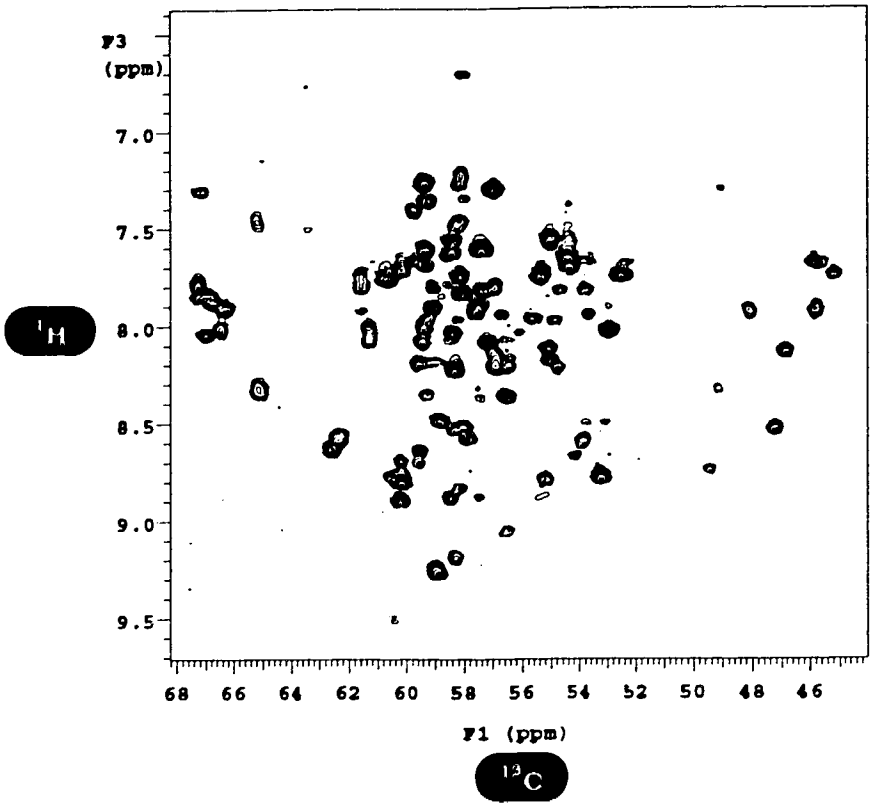

Figure IV-10. Projection of the 64 planes of the HNCOCA spectrum of NTnC·2Ca.

3D-HNCO

Reference: Grzesiek, S. & Bax, A.
J. Magn. Res. **96**, 432-440 (1992) [9]

Correlations: Correlates backbone amides with only the inter-residue (i, i-1) $^{13}C=O$. ^{1}H, ^{15}N and $^{13}C=O$ are observed. For each $^{1}H/^{15}N$ pair, there is only one strong inter-residue $^{13}C=O$ correlation.

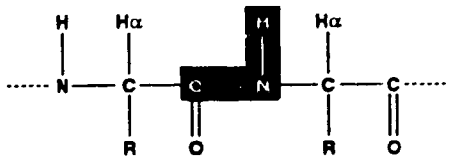

Figure IV-11: Correlations observed in 3D-HNCO

Coupling constant: $^{1}J_{NH}$ ~ 95 Hz
$^{2}J_{NCO}$ ~ 15 Hz

Comments: This experiment is used for the sequential backbone assignment through the $^{13}C=O$.

Pulse sequence:

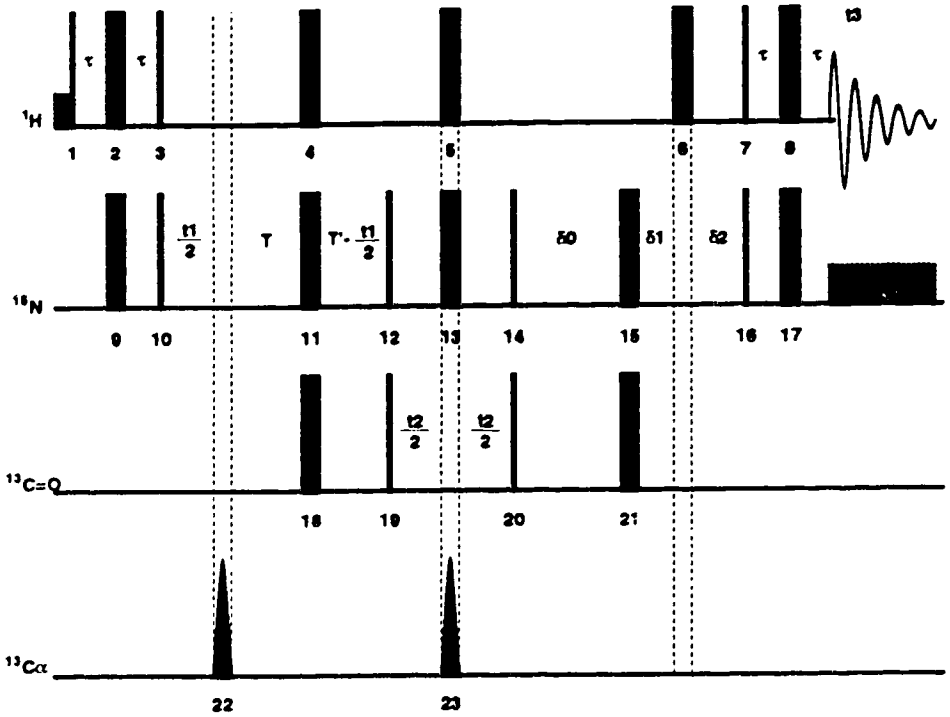

Figure IV-12: Pulse scheme of the 3D-HNCO

Phase cycling:

1	x	2 x	3 y -y
4	x	5 x	6 x
7	x	8 x	9 x -x
10†	x		
11	x x x x y y y y -x -x -x -x -y -y -y -y		
12	x -x	13 x	14 x
15	x	16 x	17 x
18	x	19‡ x x -x -x	20 x
21	x	22 x	23 x
Acq	x x -x -x -x -x x x		

Delays:

$\tau \approx 1/(4\times{}^{1}J_{HN})$

$\delta 1 = 7.25ms$

$\delta 2 = 2.75ms$

$\delta 0 = \delta 1 + \delta 2 +$ pulse width (22)

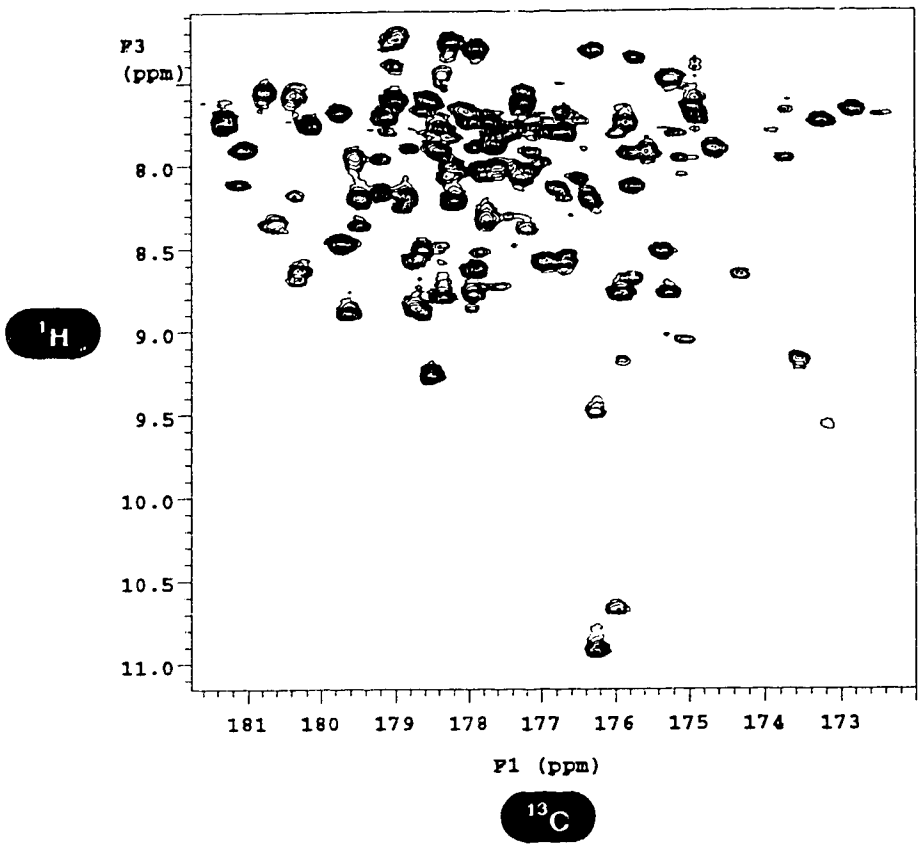

Figure IV-13. Projection of the 64 planes of the HNCO spectrum of NTnC·2Ca.

3D-HCACO

Reference: Powers, R., Gronenborn, A.M., Clore, G.M. & Bax, A. *J. Magn. Reson.* **94**, 209-213 (1991) [10]

Correlations: Correlates backbone CHα with the intra-residue $^{13}C=O$. $^{1}H\alpha$, $^{13}C\alpha$ and $^{13}C=O$ are observed. For each $^{1}H\alpha/^{13}C\alpha$ pair, there is only one strong intra-residue $^{13}C=O$ correlation.

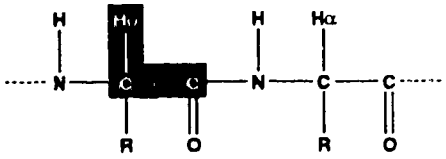

Figure IV-14: Correlations observed in 3D-HCACO

Coupling constant: $^{1}J_{CH}$ ~ 140 Hz

$^{1}J_{C\alpha CO}$ ~ 55 Hz

Comments: This experiment is used for the sequential backbone assignment through the $^{13}C=O$.

Pulse sequence:

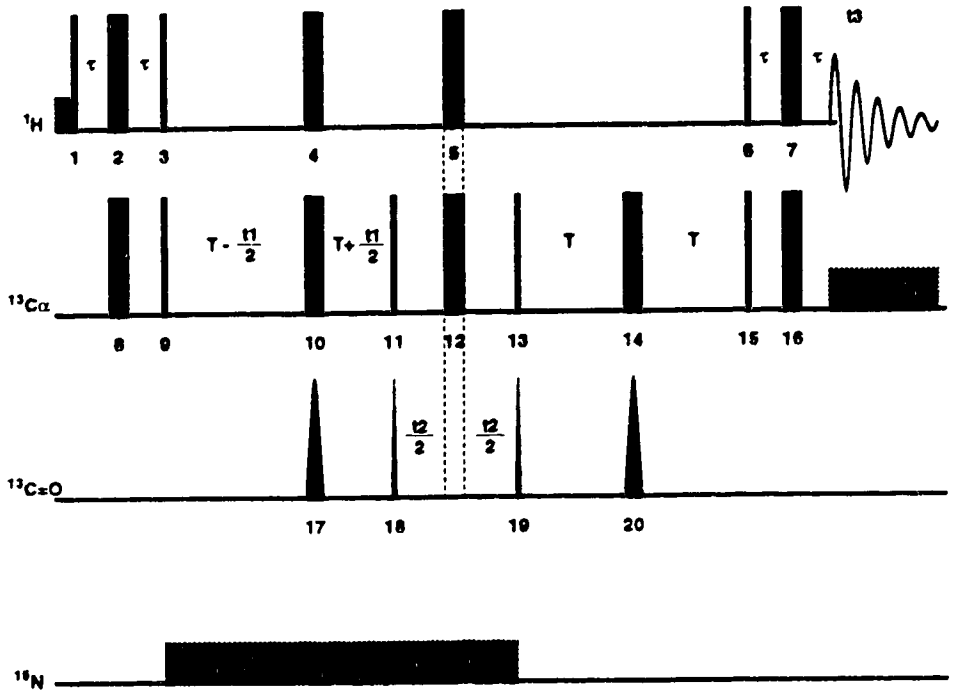

Figure IV-15: Pulse scheme of the 3D-HCACO

Phase cycling:

1	x	2 x	3 y
4	x	5 x	6 x
7	x	8 x x x x -x -x -x -x	
9†	x		
10	x x x x x x x x -x -x -x -x -x -x -x -x		
11	y y y y -y -y -y -y		
12	x x x x x x x x -x -x -x -x -x -x -x -x		
13	y	14 x	15 x
16	x	17 x	18‡ x -x
19	x x -x -x	20 x	
Acq	x -x -x x -x x x -x		

Delays:

$\tau \approx 1/(4\times{}^{1}J_{HC})$

T = 3.5 ms

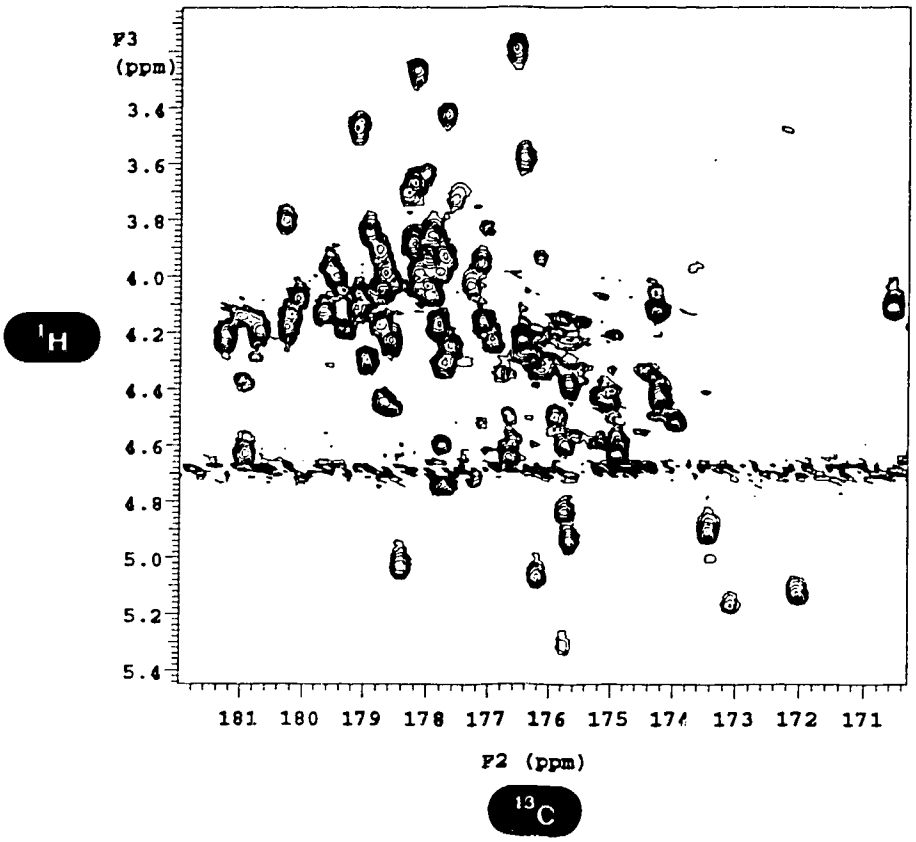

Figure IV-16. Projection of the 64 planes of the HCACO spectrum of NTnC·2Ca.

3D-^{15}N-edited-NOESYHMQC

Reference: Kay, L.E, Marion, D. & Bax, A.
J. Magn. Res. **84**, 72-84 (1989) [11]

Correlations: Produces a three-dimensional NOE spectrum where the ^{1}H-^{1}H NOESY is edited through ^{15}N chemical shifts. Therefore, only NOE's related to HN groups are observed. This experiment is simply a 2D NOESY experiment combined with a 2D-{^{15}N, ^{1}H}-HMQC experiment. In the diagram below, the ^{15}N chemical shift is observed in the F2 dimension, the protons at the origin of the arrows are observed in the F1 dimension, and protons at the end of the arrows (^{1}HN) are observed in the F3 dimension (acquisition).

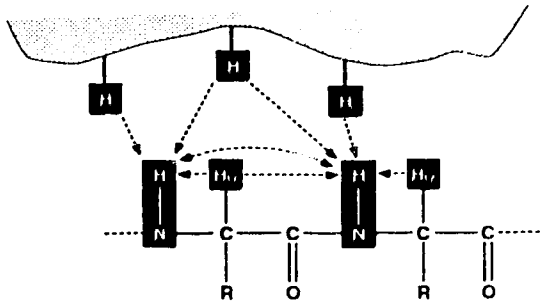

Figure IV-17: Correlations observed in 3D-^{15}N-edited NOESYHMQC

Coupling constant: $^{1}J_{NH}$ ~ 95 Hz

Comments: This experiment is used for the sequential backbone assignment, for secondary structure determination and for tertiary structure determination

Pulse sequence:

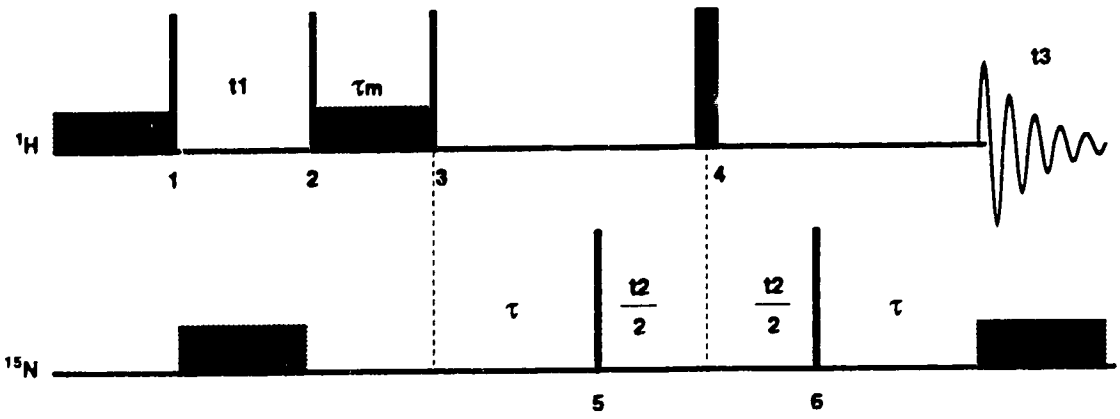

Figure IV-18: Pulse scheme of the 3D-^{15}N-edited NOESYHMQC

Phase cycling:

1†	x -x x -x y -y y -y
2	x x x x y y y y
3	x x x x y y y y
4	x x x x y y y y
5‡	x x -x -x y y -y -y
6	x x x x y y y y
Acq	x -x -x x y -y -y y

Delays:

$\tau \approx 1/(2\times{}^1J_{HN})$

τm = 150 ms (NOESY mixing time)

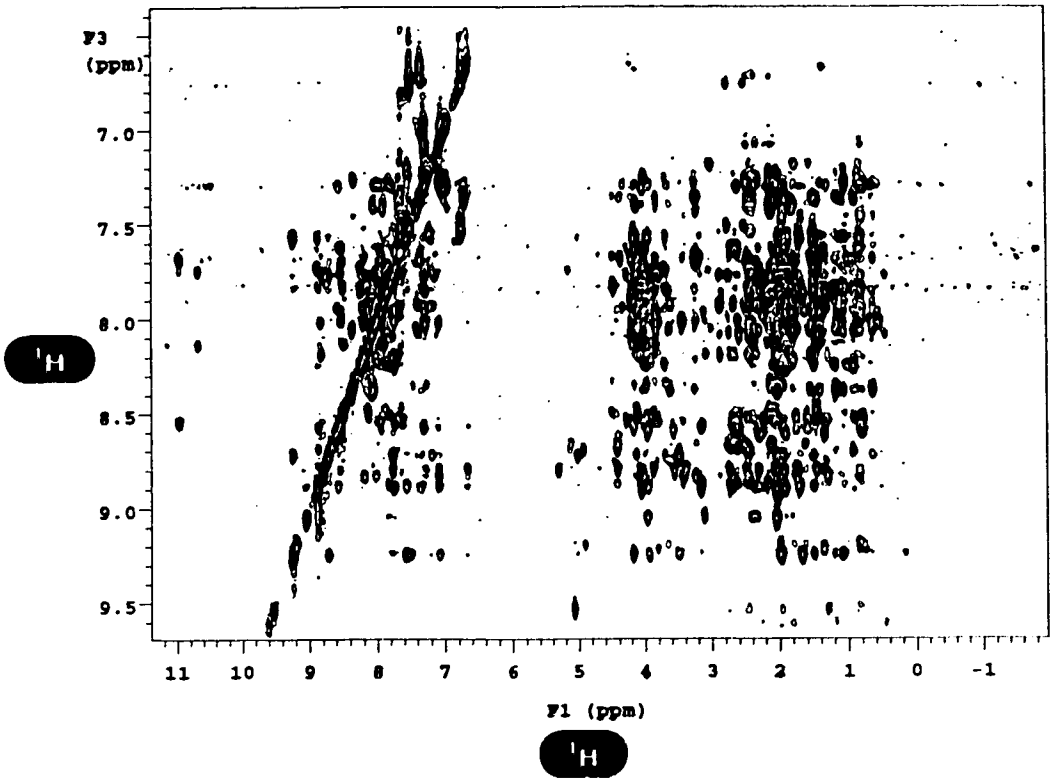

Figure IV-19. Projection of the 64 planes of the ^{15}N-edited NOESYHMQC spectrum of NTnC·2Ca.

3D-^{15}N-edited-TOCSYHMQC

Reference: Marion, D., Driscoll, P.C., Kay, L.E., Wingfield, P.T., Bax, A, Gronenborn, A.M. & Clore, G.M. *Biochemistry* **28**, 6150-6156 (1989) [12]

Correlations: Produces a three-dimensional TOCSY spectrum where the ^{1}H-^{1}H TOCSY is edited through the ^{15}N chemical shift. Therefore, only TOCSY correlations related to HN groups are observed. This experiment is simply a 2D ^{1}H-^{1}H TOCSY experiment combined with a 2D-{^{15}N, ^{1}H}-HMQC experiment. The ^{15}N chemical shift is observed in the F2 dimension, the ^{1}HN chemical shift is observed in the F3 dimension (acquisition), and all other ^{1}H's are observed in the F1 dimension .

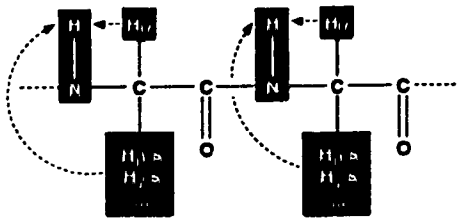

Figure IV-20: Correlations observed in 3D-^{15}N-edited TOCSYHMQC

Coupling constant: $^{1}J_{NH}$ ~ 95 Hz

Comments: This experiment is use for general assignment purpose.

Pulse sequence:

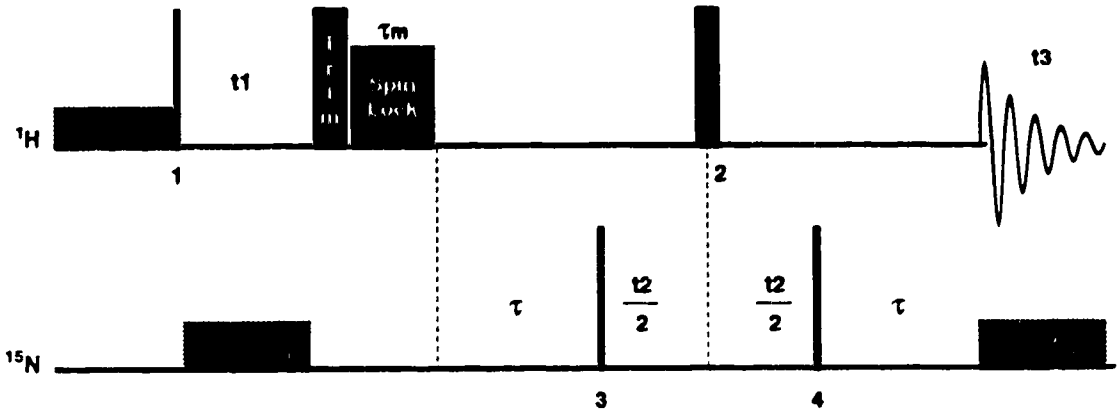

Figure IV-21: Pulse scheme of the 3D-^{15}N-edited TOCSYHMQC

Phase cycling:

$1^{\dagger}$	x x y y
2	x x y y
$3^{\ddagger}$	x -x y -y
4	x -x y -y
Acq	x x y y -x -x -y -y

Delays:

$\tau \approx 1/(2\times{}^{1}J_{HN})$

τm = 70 ms (TOCSY mixing time)

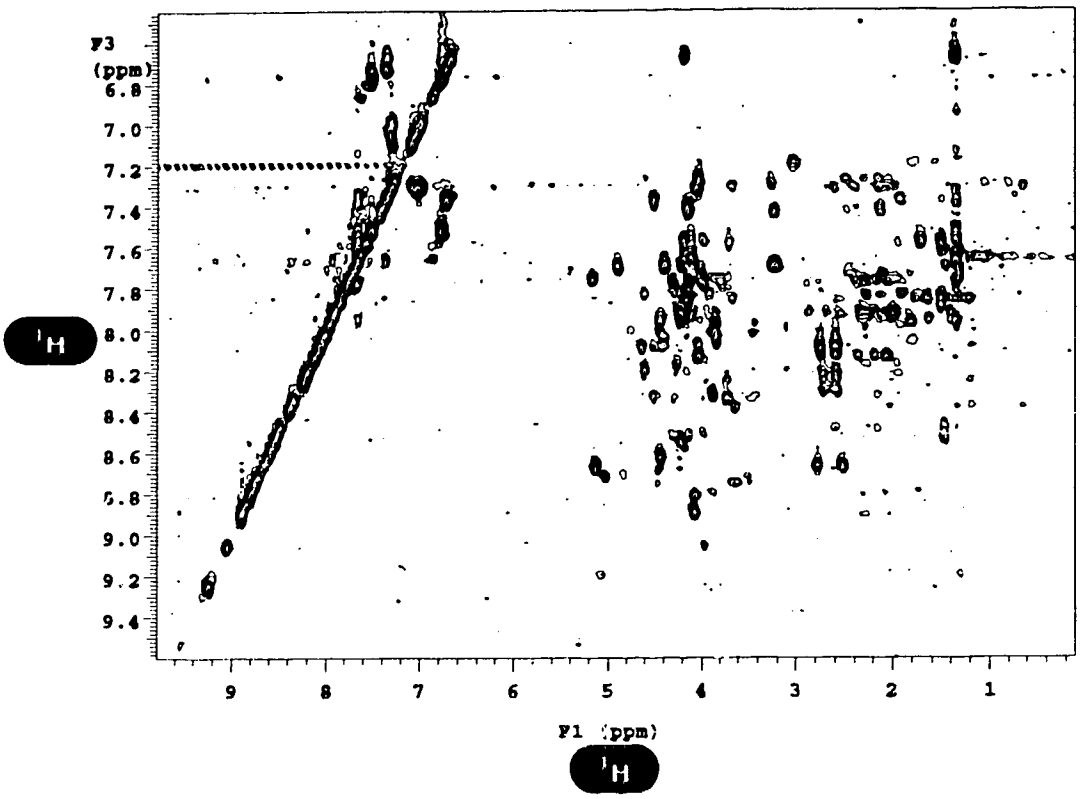

Figure IV-22. Projection of the 64 planes of the ^{15}N-edited TOCSYHMQC spectrum of NTnC·2Ca.

References

1 Wüthrich, K. (1986). *NMR of proteins and nucleic acids.* New York: John Wiley & Sons.

2 Clore, G.M. & Gronenborn, A.M. (1991). *Science* **252**, 1390-1399.

3 Li, M.X., Chandra, M., Pearlstone, J.R., Racher, K.I., Trigo-Gonzalez, G., Borgford, T., Kay, C.M. & Smillie, L.B. (1994). *Biochemistry* **33**, 917-925.

4 Studier, F. W., Rosenberg, A.H., Dunn, J. J., &Dubendorff, J. W. (1990). *Methods Enzmol.* **185**, 60-89.

5 Ho, S. N., Hunt, H. D., Horton, R. M., Pullen, J. K., & Pease, L. R. (1989). *Gene* **77**, 51-59.

6 Maniatis, T., Fritsch, E.F. & Sambrook, J. (1982). *Molecular cloning: A laboratory manual.* Cold Spring Harbor Laboratory, Cold Spring Harbor, NY.

7 Golosinska, K., Pearlstone, J. R., Borgford, T., Oikawa, K., Kay, C. M., Carpenter, M.R., Smillie, L.B. (1991). *J. Biol. Chem.* **266**, 15797-15809.

8 Bax, A., Griffey, R.H. & Hawkins, B.L. (1983). *J. Magn. Reson.* **55**, 301-315.

9 Grzesiek, S. & Bax, A. (1992). *J. Magn. Res.* **96**, 432-440.

10 Powers, R., Gronenborn, A.M., Clore, G.M. & Bax, A. (1991). *J. Magn. Reson.* **94**, 209-213.

11 Kay, L.E., Marion, D. & Bax, A. (1989). *J. Magn. Res.* **84**, 72-84.

12 Marion, D., Driscoll, P.C., Kay, L.E., Wingfield, P.T., Bax, A, Gronenborn, A.M. & Clore, G.M. (1989). *Biochemistry* **28**, 6150-6156.

13 Marion, D., Ikura, M. & Bax, A. (1989b). *J. Magn. Reson.* **84**, 425-430.

14 Garrett, D.S , Powers, R., Gronenborn, A.M. & Clore, G.M. (1991). *J. Magn. Res.* **95**, 214-220.

15 Summers, M.F., Marzilli, L.G. & Bax, A. (1986). *J. Amer. Chem. Soc.* **108**, 4285-4294.

16 Bax, A., Griffey, R.H. & Hawkins, B.L. (1983). *J. Magn. Reson.* **55**, 301-315.

17 Patt, S.L. (1992). *J. Magn. Reson.* **96**, 94-102.

18 Kay, L.E., Bax, A. (1990). *J. Magn. Reson.* **86**, 110-126.

19 Goodgame, M.M., Geer, S.M. (1993). *J. Magn. Reson.* **Series A 102**, 246-248.

CHAPTER V

BACKBONE ASSIGNMENTS AND CALCIUM-INDUCED SECONDARY STRUCTURAL CHANGES

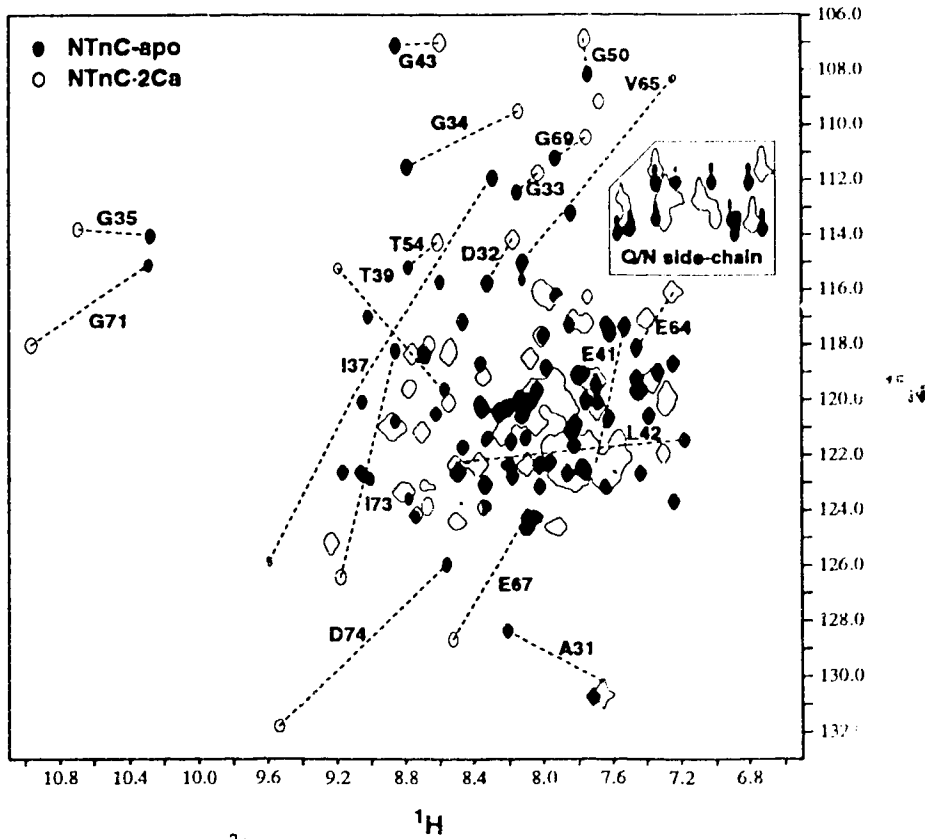

Figure V-1. Does Ca^{2+} induce any changes in NTnC? Well... a picture is worth a thou and words...

Two- and three-dimensional multinuclear NMR provide high resolution spectra with well-resolved signals from individual nuclei that can be used to determine structure and probe conformational changes in detail. The occurrence of conformational changes in the regulatory domain of TnC is clearly indicated by the chemical shift differences between the apo and 2 Ca^{2+} states of NTnC. These changes are very well pictured when comparing the 2D{^{15}N-^{1}H} HMQC spectrum of NTnC-apo and NTnC·2Ca (Fig. V-1). With the exception of the asparagine and glutamine side-chain correlations, each cross-peak in the displayed region of the 2D{^{15}N-^{1}H}-HMQC represents a backbone amide NH. NTnC contains 1 proline, and thus a maximum of 89 ^{15}N-^{1}HN backbone amide correlations may be observed; 86 and 84 backbone amides were observed and assigned for NTnC-apo and NTnC·2Ca, respectively. The missing correlations correspond to amide hydrogens that are in fast exchange with the solvent, and therefore are saturated during solvent presaturation. The very low overlap between the ^{15}N and/or ^{1}H chemical shifts of NTnC-apo and NTnC·2Ca reveals that the perturbations due to Ca^{2+} binding are propagated throughout the entire molecule. In order to properly attribute these changes to individual amino acids or regions in the protein, we first carefully assigned the backbone ^{1}HN, ^{15}N and $^{1}H\alpha$ resonances for NTnC-apo and the ^{1}HN, ^{15}N, $^{1}H\alpha$, $^{13}C\alpha$ and ^{13}CO resonances for NTnC·2Ca.

Backbone assignment

Assignment of NTnC-apo

The assignment for NTnC-apo has been done mainly by Sakae Tsuda and was based on conventional methods using 2D-COSY, 2D-TOCSY and 3D-^{15}N-edited TOCSY experiments to identify spin-systems, and 2D-NOESY and 3D-^{15}N-edited NOESY experiments to identify inter-residue connectivities along the polypeptide chain [1]. The assignment of the NTnC-apo was based in part on the assignment of the TR_1C fragment [2] and followed a similar procedure except for the fact that the ^{15}N-edited NOESY and TOCSY experiments were used to resolve some ambiguities. The complete ^{1}HN, ^{15}N and ^{1}Hα assignments for NTnC-apo are listed in table V-1.

Assignment of NTnC·2Ca

For NTnC·2Ca a different approach, which relies on heteronuclear scalar coupling, was used to obtain sequential connectivities along the protein backbone [3]. Similar approaches which also rely on various combinations of correlations between ^{1}HN, ^{15}N, ^{1}Hα, ^{13}Cα and ^{13}CO nuclei have been successfully applied for various proteins, including the homologous protein calmodulin [3, 4]. Two types of sequential assignment were used: one centered on the ^{13}Cα and another centered on the ^{13}CO. The first type of sequential assignment was accomplished by combining the strong intra-residue ^{1}HN(i)-^{15}N(i)-^{13}Cα(i) and the weaker sequential ^{1}HN(i)-^{15}N(i)-^{13}Cα(i-1) connectivities from the HNCA experiment, the sequential ^{1}HN(i)-^{15}N(i)-^{13}Cα(i-1) connectivity from the HNCOCA experiment, and the d_{NN}(i, i±1) NOE connectivities from the ^{15}N-edited NOESY experiment. The role of the four chemical shift coordinates of each d_{NN} [^{1}HN(i); ^{15}N(i); ^{15}N(i±1); ^{1}HN(i±1)], which were automatically found in

the peak list using the in-house program CHAINS (Boyko & Gagné, MRC group in Protein Structure and Function, University of Alberta, unpublished), was to confirm the Cα-based sequential assignment and to resolve some ambiguities resulting from overlapping Cα. An example of HNCA, HNCOCA and d_{NN} connectivities is shown on figure V-2a, b and e, respectively. A total of 153 connectivities were found in the HNCA (80 intra-residue and 73 sequential) and 77 sequential connectivities in the HNCOCA. The second strategy for sequential assignment, now relying on the ^{13}CO, was performed by combining the intra-residue $^{1}H\alpha(i)$-$^{13}C\alpha(i)$-$^{13}CO(i)$ connectivity from the HCACO experiment, the sequential $^{1}HN(i+1)$-$^{15}N(i+1)$-$^{13}CO(i)$ connectivity from the HNCO experiment, and the intra-residue $^{1}HN(i)$-$^{15}N(i)$-$^{1}H\alpha(i)$ from the ^{15}N-edited TOCSY experiment. An example of these connectivities is shown on figure V-2c, d and f. Overall, 89 intra-residue connectivities were found in the HCACO, and 82 sequential ones in the HNCO. In both procedures, the ^{15}N-edited TOCSY was used to identify the spin-system related to each $^{1}HN/^{15}N$ pair. Not all spin-systems could be identified in the TOCSY experiment, mainly because of the small ^{1}HN-$^{1}H\alpha$ coupling constants which are characteristic of α-helices. However, residue identification could often be helped by comparing the observed $^{1}H\alpha$, $^{13}C\alpha$ and ^{13}CO chemical shifts to their corresponding expected value [5]. Using this procedure, the near-complete ^{1}HN, ^{15}N, $^{1}H\alpha$, $^{13}C\alpha$ and ^{13}CO resonance assignments of NTnC·2Ca have been achieved and listed in Table V-2.

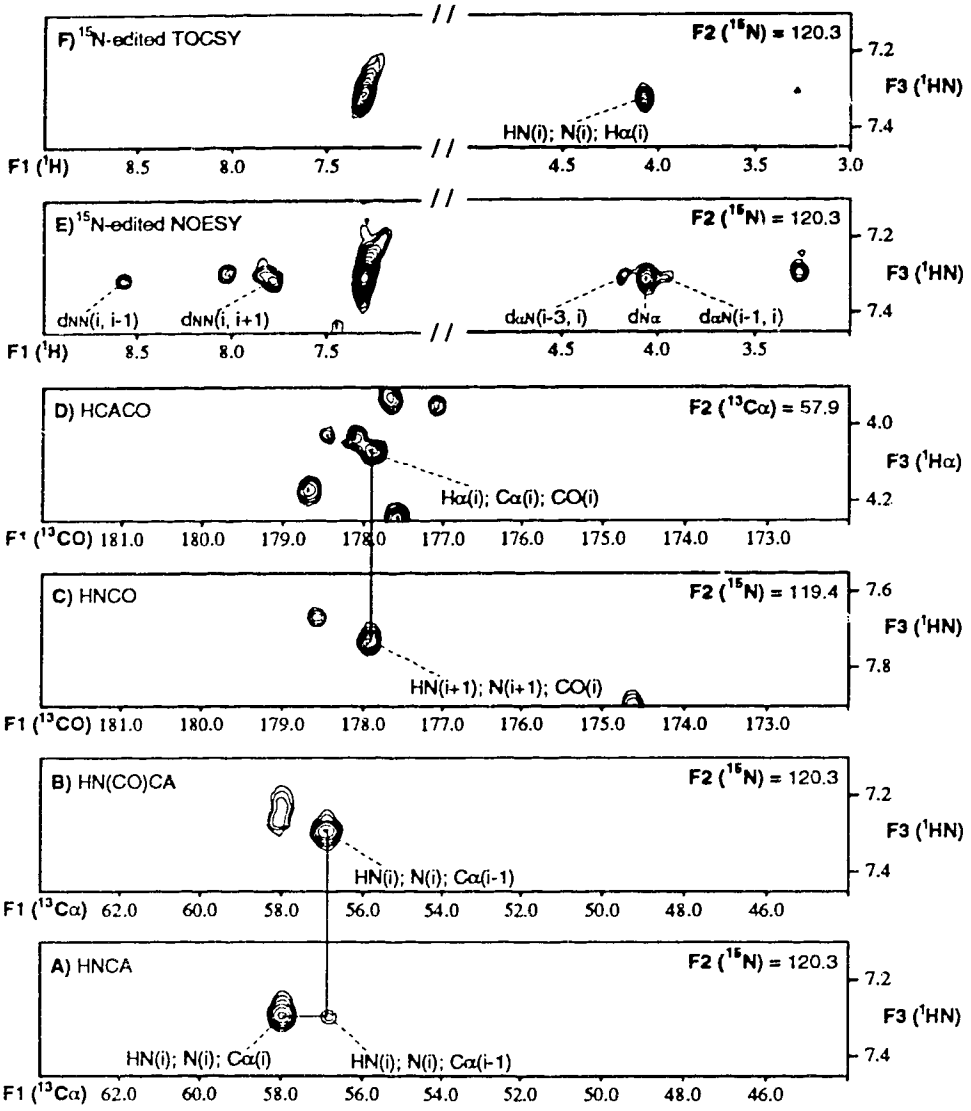

Figure V-2. Connectivities related to one residue of NTnC·2Ca, M28, in various 3D-experiments. The HNCA (A) and HNCOCA (B) experiments provide sequential information via the ^{13}Cα chemical shift. Similar sequential information can also be obtained via the ^{13}CO chemical shift by combining the HNCO (C), the HCACO (D) and the ^{15}N-edited TOCSY (F) experiments. The ^{15}N-edited NOESY (E) experiment also provide sequential information [d_{NN}, $d_{\alpha N}$(i-3, i) and $d_{\alpha N}$(i-1,i)].

Table V-1: Polypeptide Backbone ^{1}H and ^{15}N Chemical Shifts for the apo N-Domain of Chicken Troponin-C at pH6.6 and 30 °C

	^{15}N	^{1}HN	$^{1}H\alpha$		^{15}N	^{1}HN	$^{1}H\alpha$		^{15}N	^{1}HN	$^{1}H\alpha$
A1	—	—	4.12	A31	128.4	8.15	4.10	I61	122.3	7.94	3.75
S2	—	—	4.45	D32	115.8	8.33	4.72	I62	121.8	8.45	3.45
M3	—	—	4.60	G33	112.6	8.13	3.79, 4.05	E63	119.1	7.76	3.99
T4	115.7	8.12	4.22	G34	111.6	8.78	3.92, 4.16	E64	118.1	7.46	4.13
D5	121.6	8.34	4.50	G35	114.0	10.28	3.80, 4.34	V65	115.0	8.11	4.21
Q6	121.5	8.29	4.14	D36	119.1	7.81	5.58	D66	123.1	8.34	5.15
Q7	122.3	8.18	4.00	I37	111.9	8.31	4.65	E67	124.3	8.07	4.12
A8	124.3	8.05	4.13	S38	115.8	8.58	4.86	D68	117.2	8.45	4.66
E9	120.6	8.12	4.07	T39	119.6	8.58	3.76	G69	111.3	7.93	3.85, 3.91
A10	124.8	8.10	4.13	K40	121.4	8.10	4.14	S70	120.1	9.05	4.26
R11	116.4	7.93	3.90	E41	117.3	7.53	4.70	G71	115.1	10.28	3.86, 4.16
A12	120.8	7.61	4.25	L42	121.4	7.19	3.77	T72	113.3	7.88	5.43
F13	119.4	7.69	4.35	G43	107.1	8.84	3.49, 3.76	I73	118.3	8.87	4.79
L14	119.8	7.42	4.38	T44	119.8	7.45	3.76	D74	126.0	8.57	5.61
S15	117.3	7.86	4.50	V45	123.2	7.63	3.54	F75	120.1	8.36	3.50
E16	122.9	9.00	3.91	M46	118.7	8.35	3.81	E76	117.8	7.96	3.75
E17	120.8	8.87	4.05	R47	120.2	8.12	4.61	E76	120.5	8.27	3.97
M18	122.7	7.75	3.99	M48	123.2	8.01	4.23	F78	122.7	8.46	3.98
I19	120.7	8.09	3.37	L49	119.0	7.33	4.57	L79	120.2	8.11	3.42
A20	121.1	7.83	4.17	G50	108.2	7.74	3.81, 4.30	V80	118.8	7.25	3.28
E21	122.8	7.85	4.17	Q51	119.6	8.03	4.46	M81	119.9	7.75	3.91
F22	122.7	9.04	4.90	N52	118.5	8.69	5.15	M82	120.3	8.18	4.04
K23	122.7	9.17	3.75	P53	—	—	4.75	V83	121.5	8.19	3.55
A24	121.7	7.84	4.17	T54	115.1	8.79	4.35	R84	120.2	7.68	3.87
A25	120.8	7.38	4.32	K55	123.7	8.78	3.91	Q85	117.7	7.59	3.98
F26	120.3	8.35	3.66	E56	118.3	8.75	4.05	M86	118.8	7.93	4.20
D27	116.8	9.02	4.33	E57	122.4	7.79	4.01	K87	120.9	7.79	4.16
M28	119.3	7.45	3.94	L58	122.6	8.50	4.02	E88	122.3	8.10	4.26
F29	117.3	7.64	4.34	D59	120.6	8.63	4.32	D89	122.8	8.20	4.63
D30	123.7	7.24	4.87	A60	122.7	7.42	4.19	A90	130.8	7.70	4.12

Table V-2: Polypeptide Backbone ^{1}H, ^{13}C and ^{15}N Chemical Shifts for the Ca^{2+}-saturated state of the N-Domain of Chicken Troponin-C at pH6.7 and 30 °C

	^{15}N	$^{13}C\alpha$	^{13}CO	^{1}HN	$^{1}H\alpha$		^{15}N	$^{13}C\alpha$	^{13}CO	^{1}HN	$^{1}H\alpha$
A1	—	51.8	174.2	—	4.14	M46	117.7	59.4	178.3	8.01	3.91
S2	—	58.3	173.9	—	4.52	R47	120.5	58.9	181.0	8.22	4.64
M3	—	56.0	176.6	—	4.64	M48	122.8	58.8	175.6	7.94	4.22
T4	116.1	61.1	175.0	8.01	4.44	L49	—	53.6	175.9	7.19	4.34
D5	123.0	57.3	178.7	8.69	4.44	G50	106.9	45.7	174.6	7.75	3.70, 4.12
Q6	120.9	58.8	179.1	8.87	4.07	Q51	119.4	53.9	174.3	7.95	4.43
Q7	123.0	58.3	177.8	7.83	3.93	N52	118.0	51.0	172.1	8.66	5.14
A8	124.4	54.9	181.1	8.50	4.14	P53	—	62.6	177.8	—	4.74
E9	120.5	58.8	178.8	8.13	4.04	T54	114.3	60.2	175.2	8.60	4.43
A10	124.5	55.5	179.2	7.92	4.11	K55	123.3	60.0	178.3	8.79	3.88
R11	116.5	59.4	178.0	7.96	3.85	E56	118.3	60.6	180.1	8.80	4.08
A12	120.4	53.7	178.6	7.69	4.23	E57	122.6	60.4	179.5	7.77	4.00
F13	119.4	59.2	175.7	7.68	4.38	L58	121.6	58.0	178.6	7.96	4.03
L14	119.4	53.6	176.0	7.37	4.50	D59	120.1	57.2	179.0	8.54	4.30
S15	117.2	56.3	175.0	7.83	4.59	A60	123.0	54.8	180.3	7.63	4.18
E16	122.7	60.1	179.6	9.05	3.97	I61	121.5	65.0	178.3	7.57	3.71
E17	120.9	60.2	179.1	8.89	4.07	I62	119.3	65.0	177.7	7.46	3.42
M18	121.6	58.3	178.1	7.73	4.03	E63	119.1	59.3	178.2	8.35	4.00
I19	121.2	66.8	177.6	8.24	3.72	E64	116.2	58.9	179.4	7.27	4.04
A20	122.2	55.1	181.3	7.84	4.19	V65	108.3	60.8	175.4	7.26	4.59
E21	122.2	59.1	180.3	7.77	4.14	D66	—	53.5	177.3	—	4.70
F22	121.2	58.8	178.5	8.72	5.03	E67	128.7	59.2	176.9	8.53	4.23
K23	125.1	58.3	177.2	9.24	3.95	D68	116.2	52.4	177.7	8.01	4.73
A24	122.2	54.9	180.7	7.57	4.19	G69	110.4	47.1	175.3	7.75	3.81, 3.88
A25	122.0	55.0	177.9	7.57	3.98	S70	118.2	60.1	176.2	8.54	4.22
F26	121.2	62.2	176.6	8.88	3.17	G71	118.0	45.6	172.8	10.97	3.44, 4.13
D27	118.6	56.9	177.8	8.57	4.19	T72	109.3	58.1	173.5	7.68	4.92
M28	120.3	57.9	177.9	7.30	4.05	I73	126.5	60.4	176.2	9.19	5.07
F29	119.4	58.2	177.7	7.78	4.30	D74	131.9	53.1	175.9	9.53	5.32
D30	119.7	52.1	176.7	8.08	4.50	F75	119.7	61.5	176.4	8.79	3.59
A31	130.4	55.0	179.1	7.68	4.11	E76	117.3	58.8	180.3	7.77	3.80
D32	114.3	52.7	177.8	8.19	4.59	E76	120.7	57.9	178.8	8.19	4.17
G33	111.8	46.7	175.7	8.02	3.85, 3.85	F78	123.4	61.2	177.3	8.83	4.04
G34	109.6	46.3	175.9	8.14	3.98, 4.09	L79	119.8	58.0	179.1	8.02	3.47
G35	113.8	45.3	173.2	10.69	3.67, 4.47	V80	120.3	67.2	178.2	7.29	3.27
D36	116.2	52.6	173.1	7.75	5.17	M81	121.5	59.3	178.2	7.35	3.69
I37	125.9	60.1	175.7	9.61	4.94	M82	118.6	56.4	179.4	8.07	4.05
S38	124.0	55.7	175.9	8.70	4.85	V83	122.3	66.9	178.1	8.38	3.64
T39	115.1	66.9	177.0	9.22	3.82	R84	120.8	59.4	179.0	8.06	3.86
K40	122.7	59.3	179.7	7.84	4.12	Q85	117.2	57.3	177.9	7.40	4.15
E41	122.3	58.8	179.7	7.70	4.13	M86	120.1	57.9	177.6	7.92	4.25
L42	122.4	57.8	178.7	8.52	3.99	K87	120.4	57.5	177.1	7.86	4.17
G43	107.1	47.8	175.5	8.58	3.59, 3.98	E88	121.9	57.0	176.5	7.91	4.30
T44	119.7	67.2	176.3	7.94	3.94	D89	122.3	54.0	174.9	8.08	4.63
V45	122.0	66.3	177.5	7.30	3.69	A90	130.7	53.7	170.6	7.65	4.12

Secondary structure

Secondary structure determination strategy

There are three reliable secondary structure determination methods that are commonly used in NMR: one is based on the NOE connectivities characteristic of different secondary structures [1], another is based on the $^3J_{HNH\alpha}$ coupling constants [12], and the last one is based on the characteristic backbone chemical shift values of the α-helix, β-sheet and random coil residues [5, 6]. I have applied the three approaches to NTnC-apo and NTnC·2Ca, with special attention to the quantification aspects of the NOE approach.

NOE connectivities found in NOESY spectra usually contain, among others, the $d_{\alpha N}(i-1, i)$ and the $d_{N\alpha}(i, i)$. The $d_{N\alpha}(i, i)$ NOE is non-informative by itself, the intra-residue HN-Hα distance being covalently restricted to between 2.2 and 3.1Å, and being realistically found in the 2.7 to 3.1Å range for α-helices and β-sheets. For the $d_{\alpha N}(i-1, i)$ NOE, the allowed $HN_{(i)}$-$H\alpha_{(i-1)}$ distance is found in a wider range (2.2 to 3.6Å), and the magnitude of the $d_{\alpha N}(i-1, i)$ NOE could be used to differentiate between a residue found in the right-handed α-helix region (3.4Å < $HN_{(i)}$-$H\alpha_{(i-1)}$ < 3.6Å) and one in the β-sheet region (2.2Å < $HN_{(i)}$-$H\alpha_{(i-1)}$ < 3.1Å). However, the inaccuracy of this measurement (mainly due to the variation of amide exchange rate along the sequence) makes it a poor criterion for secondary structure identification. This inadequacy can be overcome by using the ratio of these two NOE's, $d_{N\alpha}/d_{\alpha N}$ (for simplicity, $d_{N\alpha}(i, i)$ NOE/$d_{\alpha N}(i-1, i)$ NOE is abbreviated to $d_{N\alpha}/d_{\alpha N}$). This ratio is larger than 1 for β-strands, and smaller than 1 for right-handed α-helices (see figure V-3). Since these two NOE's are related to the same amide HN, the $d_{N\alpha}/d_{\alpha N}$ ratio has the advantage of being independent of amide exchange and can be quantitated more safely. Note that the magnitude of this ratio relates mainly to the ψ torsion angle of residue (i-1), if only the right-handed α-helix and the

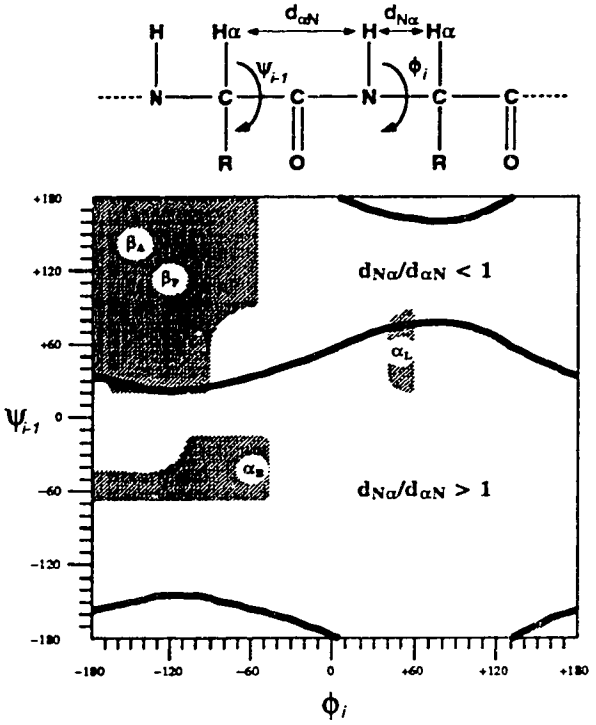

Figure V-3. ϕ/ψ map showing the relation between the $d_{N\alpha}/d_{\alpha N}$ ratio and the major secondary structure regions. The shaded areas represent the energy-favoured ϕ_i/ψ_{i-1} regions for two residues in a protein. β_A, β_P, α_R and α_L represent ideal ϕ/ψ angle for antiparallel β-sheet, parallel β-sheet, right-handed α-helix and left-handed α-helix, respectively. The thick line is the contour for $d_{N\alpha}/d_{\alpha N} = 1$ from a contour map generated by varying the ϕ_2 and ψ_1 in a dipeptide. $d_{N\alpha}/d_{\alpha N}$ represent the expected ratio between the $d_{N\alpha}(i, i)$ and $d_{\alpha N}(i-1, i)$ NOEs obtained from the measure of $[r(HN_i\text{-}H\alpha_{i-1}) / r(HN_i\text{-}H\alpha_i)]^{1/6}$, where r is the distance between two protons. A representation of the various parameters used in the ϕ/ψ map for a two residues is shown above the map. The β-sheet region is clearly characterized by a $d_{N\alpha}/d_{\alpha N} < 1$ whereas the right-handed α-helix is localized in the $d_{N\alpha}/d_{\alpha N} > 1$ region, making the $d_{N\alpha}/d_{\alpha N}$ ratio an accurate criteria for secondary structure determination.

β-sheet regions are considered. We therefore used this ratio as one of the criteria for secondary structure characterization, by measuring the ratio of the intensity of the $d_{\alpha N}(i-1, i)$ and $d_{N\alpha}(i, i)$ NOE found on the ^{15}N plane of residue (i) in the ^{15}N-edited NOESY. The second NOE criterion used is the $d_{\alpha N}(i-3, i)$ connectivity which is representative of α-helices [1]. Examples of $d_{N\alpha}$, $d_{\alpha N}$ and $d_{\alpha N}(i-3, i)$ connectivities can be found in figure V-2e. The third criterion included in the determination of the secondary structure is the chemical shift index, which is applied using the methodology described by Wishart & Sykes [5, 6]. The CSI was determined using the $^1H\alpha$ chemical shifts for NTnC-apo, and the consensus of the $^1H\alpha$, $^{13}C\alpha$ and

^{13}CO indexes without any smoothing for NTnC·2Ca. Structural information about torsion angles can also be obtained from scalar coupling constants based on Karplus equations [13]. The relation between the backbone phi angle and the $^{3}J_{HNH\alpha}$ coupling constant is available [12] and is used as the fourth criterion to defined secondary structure. $^{3}J_{HNH\alpha} < 6Hz$ was taken to indicate helices, whereas $^{3}J_{HNH\alpha} > 8$ Hz was taken to indicate β secondary structure. Unambiguous absence of splitting at high resolution enhancement (LB = -28) was interpreted as $^{3}J_{HNH\alpha} < 6Hz$.

Definition of helices can be a delicate issue, since different methods can be used [7]. Therefore it is vital to clearly stipulate the approach used before stating that an helix starts or ends at a certain residue. The information obtained from the data presented in this paper is the following: (1) the occurence of a $d_{N\alpha}/d_{\alpha N} > 1$ indicates that residue *i-1* possesses a ψ angle in the α-helical region; (2) $d_{\alpha N}$(i-3, i) NOE suggest that residue *i-3*, *i-2*, and *i-1* are in helical conformation, but does not give any information about the φ/ψ angle of residue *i*, although it may suggest that HN_i is hydrogen-bonded to either CO_{i-4} or CO_{i-3}; (3) the CSI reports predominantly information about the φ and ψ angle of its related residue, since backbone chemical shifts are closely related to the main-chain φ/ψ angle [8]; (4) the $^{3}J_{HNH\alpha}$ reports estimation of the φ angle. Ideally all four criteria should agree, but due to factors which are not related to secondary structure (NOE overlap, spin-diffusion, chemical shift affected by aromatic ring, etc.), a consensus is used instead. Therefore, helices were defined using the following rules: (1) residues were defined as helical when more than half of the available criteria (consensus of $d_{N\alpha}/d_{\alpha N}$, $d_{\alpha N}$(i-3, i), CSI, and $^{3}J_{HNH\alpha}$) were characteristic of an α-helix; (2) at least 4 consecutive helical residues were necessary to start a helix; (3) the N-terminal residue of a helix must possess a consensus of the following: a $d_{N\alpha}/d_{\alpha N} > 1$ with the next residue, a $d_{\alpha N}$(i-3, i), an α-helix CSI and a $^{3}J_{HNH\alpha} < 6Hz$; (4) the C-terminus of a helix must have a consensus of the following: a $d_{N\alpha}/d_{\alpha N} > 1$ with the next residue, a $d_{\alpha N}$(i-3, i) between residue i-2 and i+1, an α-helix

CSI, and a $^3J_{HNH\alpha} < 6$ Hz. The methodology used in this study for secondary structure determination is therefore closely related to a secondary structure definition based on ϕ/ψ angle [7]. The compilation of the $d_{N\alpha}/d_{\alpha N}$, $d_{\alpha N}(i-3, i)$, CSI and $^3J_{HNH\alpha}$,, along with the secondary structure, for NTnC-apo and NTnC·2Ca are represented in figure V-4 and V-5, respectively.

NTnC-apo; secondary structure

Five helices were found by NMR for NTnC-apo: helix N, A, B, C and D. This is the same as is found in the crystal structures of TnC. According to the criteria described above, the N-helix is well defined from T4 to F13. The tight turn linking the N-helix and the A-helix is characterized by a $d_{N\alpha}/d_{\alpha N} < 1$ observed for S15 and E16, indicating positive ψ angles for both L14 and S15. The A-helix unambiguously spans from E16 to M28. The negative CSI of F22 in the center of the A-helix might occur due to a deshielding orientation of the aromatic ring. No regular secondary structure is observed for the F29-G35 segment, whereas the next three residues are well defined as β-strand by the CSI. The ($d_{N\alpha}/d_{\alpha N} < 1$) between I37 and T39 indicate positive ψ angles between D36 and S38, and the $^3J_{HNH\alpha} > 8$Hz of D36 and I37 indicate β-stand characteristic ϕ angle for these residues.

The B-helix of NTnC-apo is less well defined by the NOE's due to some $^1H\alpha$ resonances appearing very close to the water resonance (4.70 and 4.61 for E41 and R47, respectively) and $^1H\alpha$ overlap (in particular in the L42-T44 segment). Even if some of the $d_{N\alpha}/d_{\alpha N}$ and $d_{\alpha N}(i-3, i)$ are ambiguous in the B-helix, the absence of an NOE between K40-Hα and G43-HN is unambiguous (figure V-6). This is in perfect agreement with the crystal structure, where these two protons are separated by 5.19Å. The $^3J_{HNH\alpha} > 8$Hz of E41 is also in agreement with the X-ray coordinates, where this residue had a ϕ angle of -96°. The T39-M48 stretch shows two β-sheet-like CSI; one for E41, and the other for R47. These two non-helical

chemical shifts are however consistent with the geometry of the B-helix in the crystal structure, as demonstrated by chemical shift calculations made using the crystal coordinates and the SHIFTS program (Jellard et al., PENCE, University of Alberta; Ösapay & Case, 1991). These calculations showed α-helix-like upfield shift relative to the random coil value for all ^{1}Hα in the T39-M48 segment, except for E41 due to irregular φ/ψ angles (-96°/-7°), and for K47 due to the particular orientation of the Q51 C=O bond. The rationalization related to K47Hα is based on chemical shift calculations with and without Q51CO, which demonstrated that Q51CO induces a downfield shift on K47Hα. Helix-B therefore spans from L42 to M48, but can also be viewed as spanning from T39 to M48 with a kink at residue E41.

No particular secondary structure is associated with L49-T54. The last two helices, C and D, are very well defined, spanning from K55 to E64 and F75 to K87, respectively. The second Ca^{2+}-binding loop, like the first one, possesses no distinct NOE or CSI features for the first six residues, and a β-strand for the last three residues, T72-D74. The three C-terminal residues are relatively flexible/unstructured

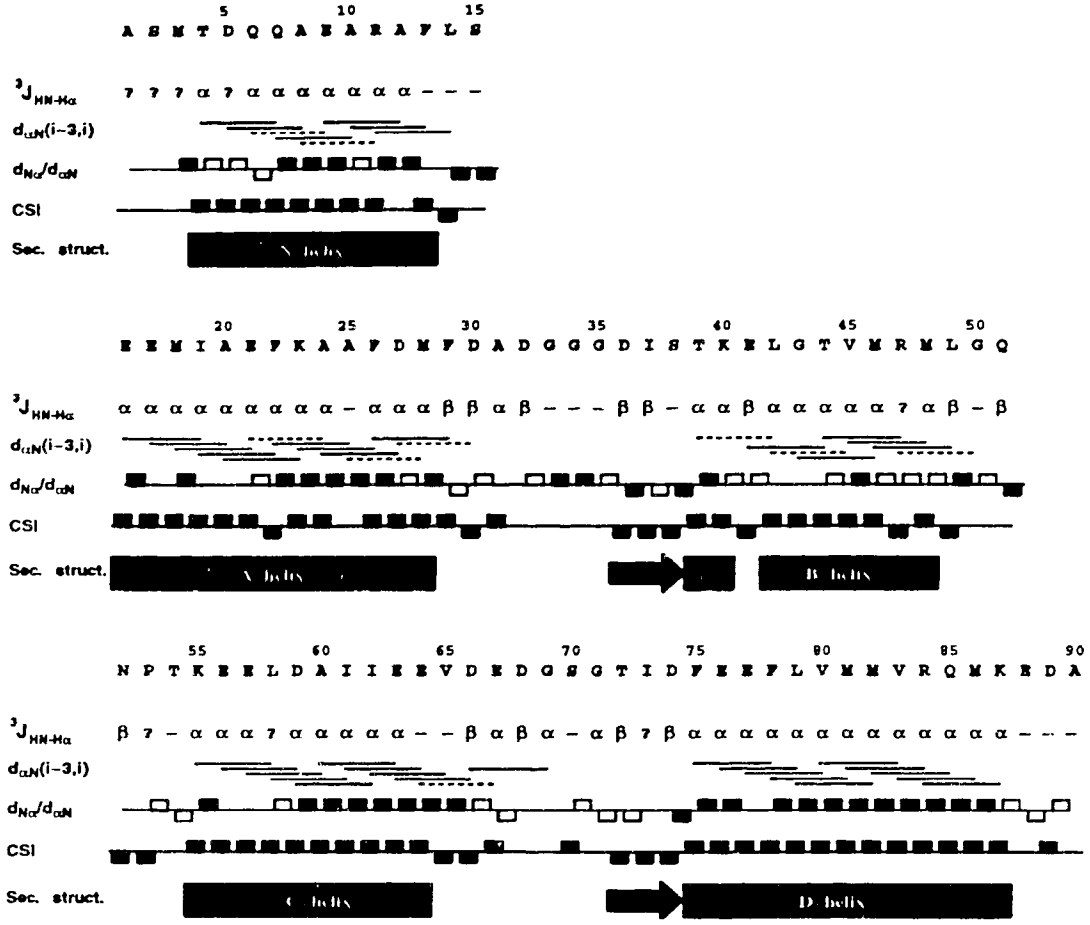

Figure V-4. Schematic representation of the secondary structure determination of NTnC-apo. $d_{\alpha N}(i-3, i)$ represents the NOE connectivity between $H\alpha_{i-3}$ and HN_i; $d_{N\alpha}/d_{\alpha N}$ represents the ratio between the $d_{N\alpha}(i, i)$ and $d_{\alpha N}$ (i-1, i) NOE intensities (upward and downward relate to $d_{N\alpha}/d_{\alpha N}$ >1 and $d_{N\alpha}/d_{\alpha N}$ <1, respectively); CSI represents the chemical shift index (Wishart & Sykes, 1994a, 1994b) for the α-protons only (upward and downward relate to α-helix and β-strand characteristic, respectively); 3JHN-Hα reports values of J < 6Hz (α), J > 8 Hz (β). Intermediate J's are represented by a dash (-), and ambiguous or unavailable J's by a question mark (?). Dotted lines and open squares indicate amguities. The compilation of the secondary structure as determined by these criteria is found on the last line of each segments; rectangles and arrows indicate helices and β-strand, respectively. The kink in the B-helix (see text) is represented by a break at residue 41.

NTnC·2Ca; secondary structure

Five helices are also found in the calcium saturated form of NTnC, with slightly different lengths for some of them in comparison to the apo form. Considering that the amide protons of the first 3 residues are not observed due to fast exchange, and that the CSI is variable for the A1-T4 segment, the first four residues are probably disordered. The N-helix is very well defined from D5 to F13. The A-helix is also well delineated from E16 to F29 using our criteria, having only one ambiguous $d_{\alpha N}(i-3, i)$. The first calcium-binding loop of NTnC does not show any regular secondary structure features from D30 to G35. The binding-loop ends with a short β-strand (D36-S38) defined by negative CSI's for D36, I37 and S38, $d_{N\alpha}/d_{\alpha N} < 1$ for I37 and S38, and $^3J_{HNH\alpha} > 8$ Hz for I37 and S38. The B-helix is the least-well defined using the $d_{N\alpha}/d_{\alpha N}$ criterion, due to overlap or very weak NOEs. However, the $d_{\alpha N}(i-3, i)$, CSI and $^3J_{HNH\alpha}$ unambiguously characterize the B-helix from T39 to R47. Unfortunately, since the ^{15}N of L49 is unassigned, the only secondary structure information available for M48 is its CSI and it $^3J_{HNH\alpha}$, which are both characteristic of helices. Helix-B is therefore assumed to extend from T39 to M48. The L49-T54 section of NTnC·2Ca shows variations for both the $d_{N\alpha}/d_{\alpha N}$ and the CSI, and is categorized as a 6 residue linker between helices B and C. The C-helix is also well characterized from K55 to E63, with some ambiguity about its C-terminus. As can be seen in the 2D{^{15}N-^1H} HMQC NMR spectrum(figure V-1), V65 is one of the weakest observable amides, leading to virtually no observable NOEs in the 3D-^{15}N-edited NOESY. In addition, the amide of D66 is unassigned or non-observable, so that only the CSI and the $^3J_{HNH\alpha}$ are available to characterize E64. The C-helix therefore ended at E64. The V65-G71 segment does not have any α-helix or β-sheet character. Finally, the second β-strand (T72-D74) and helix-D (F75-K87) are well defined by the NMR data. The C-terminal residues E88-A90 are flexible, as for the apo structure.

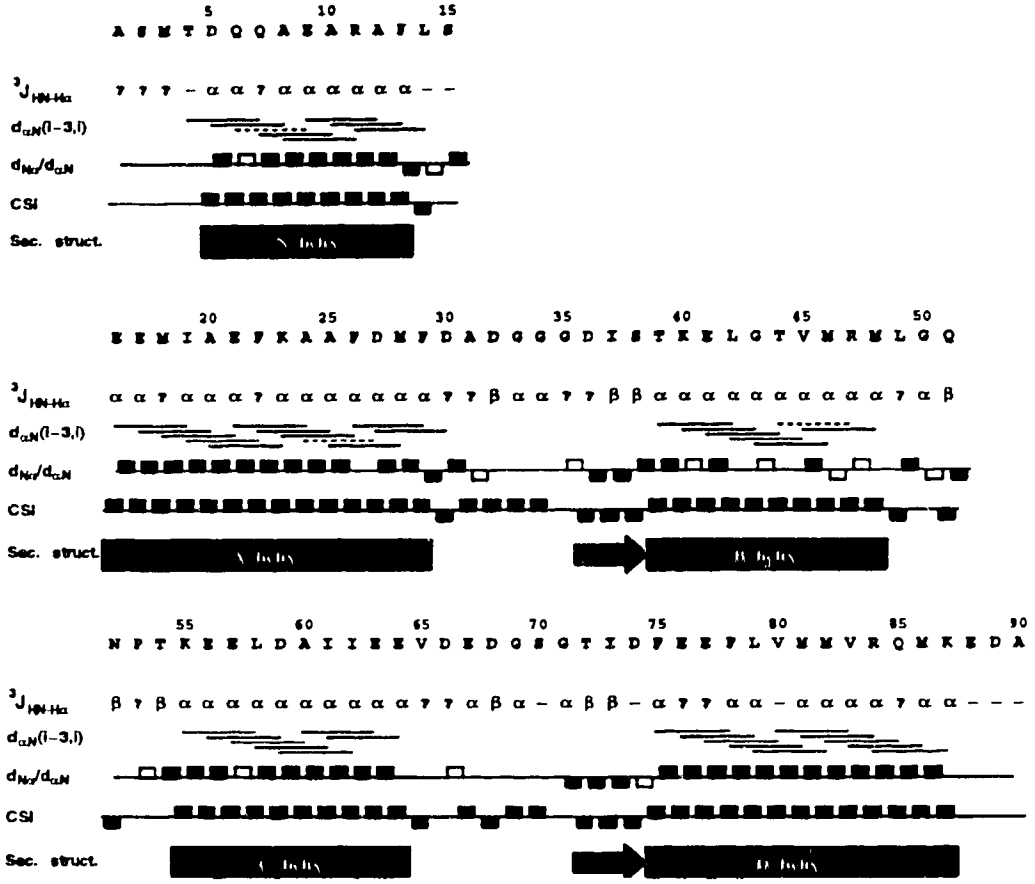

Figure V-5. Schematic representation of the secondary structure determination of NTnC·2Ca. The representation used is the same as in figure V-4, except for the CSI, which is a consensus of the $^1H\alpha$, $^{13}C\alpha$ and ^{13}CO index.

Ca^{2+}-induced conformational changes

Secondary structural change

In order to fully characterize the secondary structural changes that occur in NTnC upon calcium binding, we compared the secondary structures obtained for NTnC-apo and NTnC·2Ca from this study, the NMR secondary structure of the TR_1C fragment [2], and the crystal structure of TnC [10]. To obtain a comparison as consistent as possible for the helices, all structures were compared in terms of "NMR helices". For the X-ray structure, we extracted the $d_{N\alpha}/d_{\alpha N}$ ratio NOE, the $d_{\alpha N}(i-3, i)$ NOE and the $^3J_{HNH\alpha}$ expected from the crystal coordinates based on distance alone or on ϕ angle, and used them to define the helices with the approach described above for NTnC. The TR_1C helices were defined based on the NOE data presented by [2]. The comparison of the helices from these four structures is summarized in Table V-3. The N-helix can be considered identical for the

Table V-3: Location of α-Helices in the N-Domain of Troponin-C

	Residue Range			
α-helix	X-ray (apo) [a]	TR_1C (apo) [b]	NTnC-apo [c]	NTnC·Ca2 [c]
N	M3-F13	—	T4-F13	D5-F13
A	E16-M28	E16-D26[d]	E16-M28	E16-F29
B	T39-K40 L42-M48	L42-L49	T39-K40 L42-M48	T39-M48
C	K55-E64	K55-E64	K55-E64	K55-E64
D	F75-A90	F75-M86	F75-R87	F75-R87

[a] Herzberg & James (1988). Helix limits based on expected $^3J_{HNH\alpha}$ and NOE's from crystal coordinates.

[b] Findlay & Sykes (1993). NMR secondary structure of turkey skeletal TnC fragment (residues 12-87).

[c] Present study. Helix range based on $^3J_{HNH\alpha}$, CSI, $d_{\alpha N}(i, i+3)$ NOE and $d_{N\alpha}/d_{\alpha N}$ NOE ratio.

[d] Revision of the NOE data of TR_1C suggest that the C-termini of helix-A is M28 (see text)

x-ray, NTnC-apo and NTnC·2Ca, the only possible variance being different flexibility for the first few residues. The A-helix is invariant between the x-ray and NTnC-apo, and is one residue longer in NTnC·2Ca. Although the NOE's presented previously for TR_1C indicated D26 as being the C-terminus of helix-A, the chemical shift identities between NTnC-apo and TR_1C for the $^1H\alpha$ of residues E16-A31 ($\Delta\delta \leq 0.02$ ppm) suggests that both have identical ϕ/ψ angles. A revision of the NOE data related to helix-A of TR_1C (data not shown) showed NOE connectivities identical to the ones presented in this paper for NTnC-apo, and therefore helix-A is believed to end at M28 in all 3 apo structures and at F29 in the Ca^{2+} structure.

The B-helix in the crystal structure possesses a kink due to a deviation from ideal helical ϕ/ψ angles at E41 (ϕ=-96°, ψ=-7°). This ϕ angle is reflected in the NTnC-apo solution structure by a $^3J_{HNH\alpha} > 8$ Hz (figure 7). In terms of expected $d_{\alpha N}$(i-3, i) in the crystal structure, there should be a strong NOE for L42 (3.0 Å), a non-observable NOE for G43 (5.2 Å), and medium NOE's for the T44-G50 stretch (3.3-3.8 Å). The NTnC-apo NOESY spectrum shows an ambiguous $d_{\alpha N}$(i-3, i) for L42 and none for G43, whereas the NTnC·2Ca spectrum reveals $d_{\alpha N}$(i-3, i) for both L42 and G43 (figure V-6). Consequently, the kink at the N-terminus of helix-B is observed in the x-ray, TR_1C and NTnC-apo structures. This kink is however absent in the structure of NTnC·2Ca, as indicated by the NOE connectivities (figure V-5 and V-6) and $^3J_{HNH\alpha} < 6$Hz (figure 5 and 7).

Site II of NTnC-apo is similar to the crystal conformation, as indicated by the G69 $d_{\alpha N}$(i-3, i) NOE (fig. V-4). This NOE is the only $d_{\alpha N}$(i-3, i) expected for a non-helical region in the crystal structure (3.69 Å). The NOE spectrum of NTnC·2Ca does not exhibit this $d_{\alpha N}$(i-3, i), indicating some Ca^{2+}-induced conformational change in site II. Finally, the conformation of helix-D is not affected by Ca^{2+}-binding.

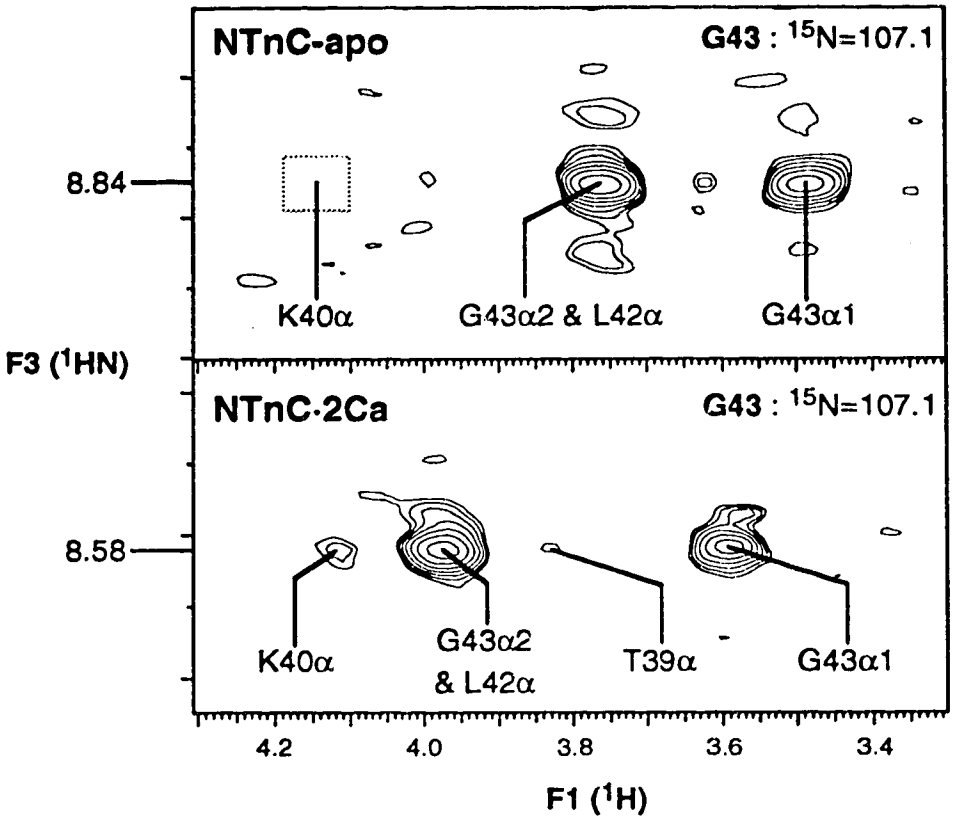

Figure V-6. Comparison of the NOE connectivities of G43's amide proton for NTnC-apo and NTnC·2Ca in their ^{15}N-edited NOESY. The 3D NOESY spectrum of NTnC·2Ca unambiguously indicates the presence of a $d_{\alpha N}$(i-3, i) between K40 and G43. This NOE is absent in the spectrum of NTnC-apo, as would be expected from the crystal structure (see text); the expected positon of this $d_{\alpha N}$(i-3, i) is indicated by a box. Note that the ^{15}N-edited NOESY spectra of NTnC-apo is plotted at the noise level. This difference in NOE connectivity between NTnC-apo and NTnC·2Ca is one of the indications that the kink of helix-B at E41 is straightened upon Ca^{2+}-binding. The observation of a very weak $d_{\alpha N}$(i-4, i) between T39 and G43 in the spectra of NTnC·2Ca also support this idea (those two protons are separated by 5.39 Å in the crystal structure of TnC).

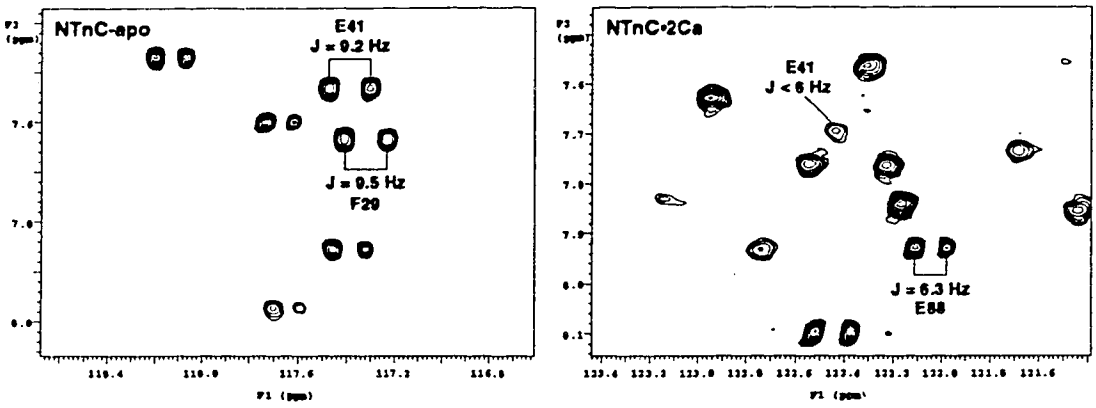

Figure V-7. Comparison of the $^3J_{HNH\alpha}$ coupling constant of E41 for NTnC-apo and NTnC·2Ca in their HMQC-J spectrum. A coupling constant of 9.2 Hz was measured for NTnC-apo using the HMQCJFIT program (see text), indicating that E41 has a β characteristic ϕ angle in the apo form of NTnC. In the spectrum of NTnC·2Ca, no splitting is observed, indicating that E41 has a $^3J_{HNH\alpha}$ < 6 Hz and that this residue has an α characteristic ϕ angle in the Ca^{2+} form of NTnC. Note the splitting observed for E88 ($^3J_{HNH\alpha}$ = 6.3 Hz) which clearly indicate that E41 has a $^3J_{HNH\alpha}$ < 6 Hz in NTnC·2Ca. Both spectrum were processed in the same way (VNMR parameters GF=0.05, LB=-28).

Chemical shift change

Since the chemical shift of a nucleus is affected by its environment, the chemical shift changes which occur in NTnC upon Ca^{2+}-binding can be interpreted in terms of structural changes. Figure V-8 compiles those changes for each residue, using a relative chemical shift change which includes $^{1}H\alpha$, ^{1}HN and ^{15}N. As expected, site I and II are the most affected by the binding of Ca^{2+} due to conformational changes and the proximate presence of two calcium ions. The most affected residue is I37 (figure V-1 and V-8), located in the middle of the first β-strand. The second β-strand chemical shifts are also strongly affected. Interestingly, the largest variation observed outside of the binding loops occurs at E41 and L42; this observation is consistent with the NOE variation observed at the beginning of the B-helix (figure V-6). On average, the B/A helix pair is strongly affected by the calcium-induced structural change, whereas the C-D pair is less perturbed. The N-helix is only weakly perturbed, as is the B-C linker.

Helical content

In order to assess the helical content of NTnC-apo and NTnC·2Ca, I used two approaches, one based upon number of residues in helical segments, and a second based upon all residues susceptible of having helical ϕ/ψ angles. I first directly count the number of residues found in helices according to the data presented in figure V-4 and V-5 for the two forms of NTnC. The NMR secondary structure of NTnC-apo shows 54-56 residues in well-defined helices, and a similar number, 55, is found for NTnC·2Ca. Even if this helical residue count is not perfectly accurate, these results do not explain the Ca^{2+}-induced ellipticity increase observed in the CD spectra of NTnC [11].

The second approach attempts to estimate the proportion of time that each residue spends with helical ϕ/ψ angles. Due to the relationships

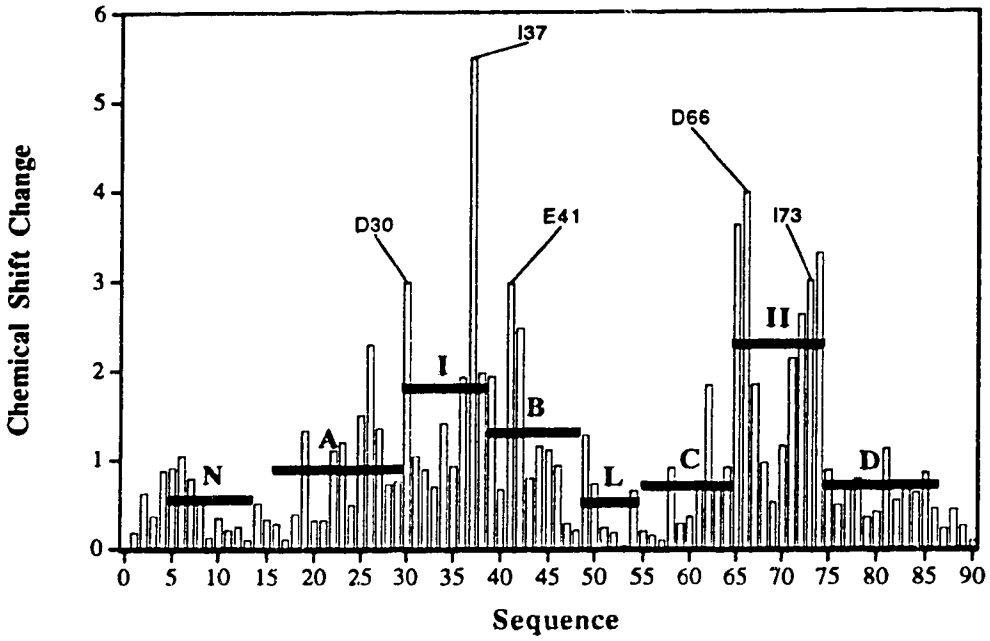

Figure V-8. Chemical shift change along the sequence of NTnC induced by the binding of calcium. The chemical shift change for each residue is obtained by averaging the normalized change of the backbone $^{1}H\alpha$, ^{1}HN and ^{15}N chemical shifts. The normalized chemical shift change for a particular nucleus of each residue is obtained by dividing the observed shift change by the average shift change for all residues. Therefore, a chemical shift change of 1 is equivalent to the average change observed for all residues. The horizontal bars indicated the average change for various segments of NTnC: N, A, B, C and D represent the five respective helices, I and II represent the binding loop in site I and II, and L represents the B-C linker. As expected, the largest changes are observed in the two Ca^{2+}-binding loops. The third largest change is found in helix-B, mainly due to E41 and L42; this observation is one of the evidences for the straightening of that helix upon Ca^{2+}-binding.

between α-proton chemical shifts and backbone dihedral angles [8], the helical content of a protein (in terms of ϕ, ψ) can also be approximated by using the chemical shift differences ($\Delta\delta$) from the random coil value [5]. In this case, every residue with an upfield shift relative to the random coil

value is accounted for, whether it is in a helix or not. By its nature, this method is quite comparable to the quantification of secondary structure made by CD. We calculated the average $\Delta\delta$'s from the random coil values for the $^1H\alpha$'s of NTnC-apo and NTnC·2Ca. 62 residues had an upfield shift characteristic of α-helical structure in NTnC-apo, with an average $\Delta\delta$ of -0.37 ppm. The NTnC·2Ca assignment revealed 63 upfield-shifted $^1H\alpha$, with an average $\Delta\delta$ of -0.36 ppm. The regular shift from random-coil chemical shift in helical residues is -0.38 ppm [5]. The crystal structure of TnC has 65 residues with ψ between -10° and -70°. The number of upfield-shifted α-protons for NTnC-apo and NTnC·2Ca is in agreement with the crystal structure, especially when considering that truncation at residue 90 in NTnC is likely to reduce helix-D by 2-3 residues compared to the whole TnC. As for the results from the residue count, the $\Delta\delta$'s do not show any increase of helical content in NTnC upon Ca^{2+}-binding.

References

1 Wüthrich, K. (1986). *NMR of proteins and nucleic acids.* New York: John Wiley & Sons.

2 Findlay, W.A. & Sykes, B.D. (1993). *Biochemistry* **32**, 3461-3467.

3 Ikura, M., Kay, L.E. & Bax, A. (1990). *Biochemistry* **29**, 4659-4667.

4 Ikura, M., Spera, S., Barbato, G., Kay, L.E., Krinks, M. & Bax, A. (1991). *Biochemistry* **30**, 9216-9228.

5 Wishart, D.S. & Sykes, B.D. (1994a). *Methods in enzymology: nuclear magnetic resonance part C* (in press).

6 Wishart, D.S. & Sykes, B.D. (1994b). *J. Biomol NMR* **4**, 171-180.

7 Richards, F.M. & Kundrot, C.E. (1988). *Prot. Struct. Funct. Genet.* **3**, 71-84.

8 Wishart, D.S., Sykes, B.D. & Richards, F.M. (1991). *J. Mol. Biol.* **222**, 311-333.

9 Ösapay, K. & Case, D.A. (1991). *J. Am. Chem. Soc.* **113**, 9436-9444.

10 Herzberg, O. & James, M. N. G. (1988). *J. Mol. Biol.* **203**, 761-779.

11 Li, M.X., Chandra, M., Pearlstone, J.R., Racher, K.I., Trigo-Gonzalez, G., Borgford, T., Kay, C.M. & Smillie, L.B. (1994). *Biochemistry* **33**, 917-925.

12 Pardi, A., Billeter, M., Wüthrich, K. (1984). *J. Mol. Biol.* **180**, 741-751.

13 Karplus, M. (1963). *J. Am. Chem. Soc.* **85**, 2870-2871.

CHAPTER VI

SIDE-CHAIN ASSIGNMENTS AND PRELIMINARY TERTIARY STRUCTURE

The previous chapter reported a detailed quantification of the calcium-induced secondary structural changes in the regulatory domain of troponin-C. This quantification clearly shows that the secondary structural features of the N-domain of TnC are not significantly affected by the binding of Ca^{2+}. Now that the secondary structure question has been answered, others must be asked. "What are the calcium-induced tertiary structural changes?". "Is the model proposed by Herzberg et al. [1] close to reality?".

This chapter presents results that answer these questions. The results involved are preliminary and need more refinement. Therefore this chapter is kept to a minimum as its outcome, the very low resolution solution structure of NTnC·2Ca, is regarded only as a "Note added in proof" to the discussion made in the next chapter.

Getting distance restraints

Side-chain assignments

The assignment of the side-chain ^{1}H and ^{13}C chemical shifts has been achieved using the following experiments: ^{15}N-edited TOCSYHMQC, ^{15}N-edited NOESYHMQC, HCCHCOSY [4], and ^{13}C-edited NOESYHMQC. The ^{15}N-edited TOCSYHMQC and the ^{15}N-edited NOESYHMQC experiments have been described in chapter IV. The ^{13}C-edited NOESYHMQC was not described in previous chapters, but is basically the same as the ^{15}N-edited NOESYHMQC, except for the fact that it is ^{13}C-edited. The HCCHCOSY [4] pulse sequence was kindly provided by Lewis E. Kay (Univ. of Toronto) and is a ^{13}C-edited through-bond 3D-experiment correlating two protons having their carbon separated by one bond. A schematic representation of the correlation expected in each of these five experiments is shown in figure VI-1 for a glutamate residue. Although all four experiments were necessary to complete the backbone assignment, the HCCHCOSY was definitely the most useful one. Examples of the two ^{13}C-edited experiments used for this assignment are shown in figure VI-2 and VI-3. Examples of some planes of the two ^{15}N-edited experiments were given in chapter V.

The side-chain assignments have been completed at approximately 90 %. The missing assignments are usually due to serious overlap. A list of the chemical shifts assigned so far for NTnC·2Ca can be found in appendix B.

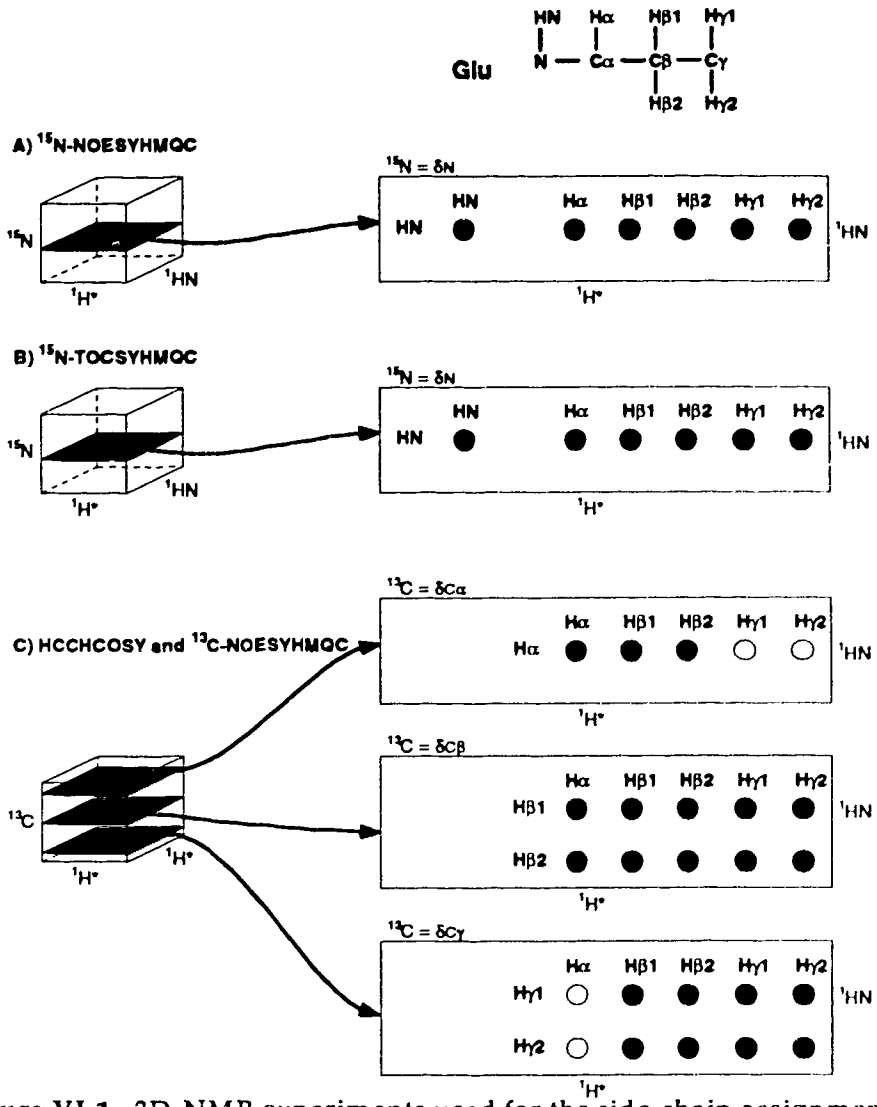

Figure VI-1. 3D-NMR experiments used for the side-chain assignments of NTnC·2Ca. **A)** ^{15}N-edited NOESYHMQC usually show NOE cross-peak between backbone amide and every other intra-residue protons (also show a number of inter-residue cross-peak). **B)** ^{15}N-edited TOCSYHMQC can show correlation between amide and all intra-residue proton, but often (especially with helical proteins) correlation with protons further than the Hβ's are not observed. **C)** HCCHCOSY and ^{13}C-edited NOESYHMQC are two ^{13}C-edited experiments. Filled peaks represent correlations expected in both experiments and opened peaks represent correlations observed only in the ^{13}C-edited NOESYHMQC. As for the ^{15}N-edited NOESY, the ^{13}C-edited NOESY also shows a number of inter-residue correlations (not shown here).

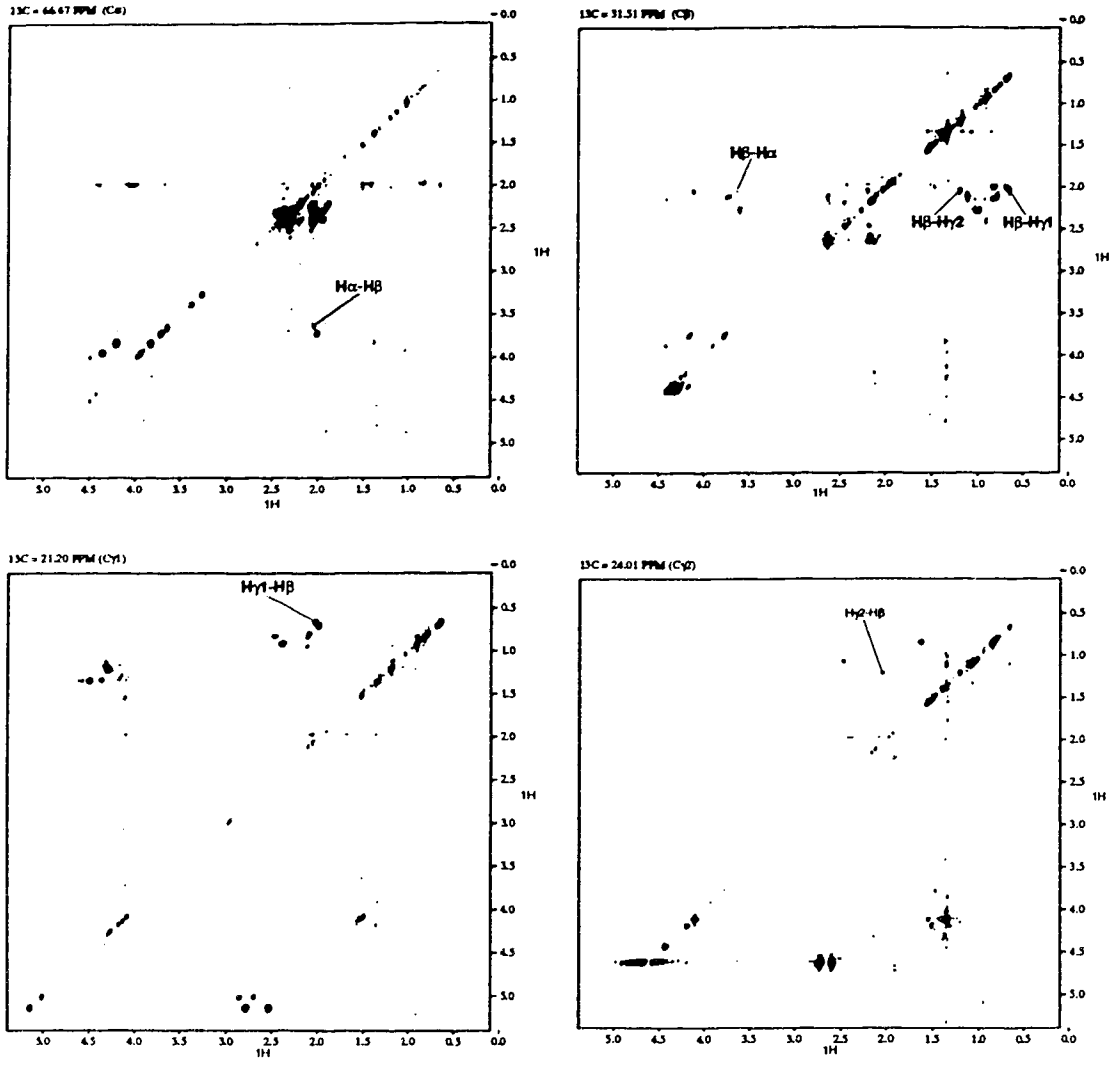

Figure VI-2. Correlations found for Val83 in the HCCHCOSY spectrum. Valine residues having four aliphatic carbons, four sets of correlations can be found on four ^{13}C planes corresponding to the ^{13}C chemical shifs of valine's Cα, Cβ, Cγ1 and Cγ2.

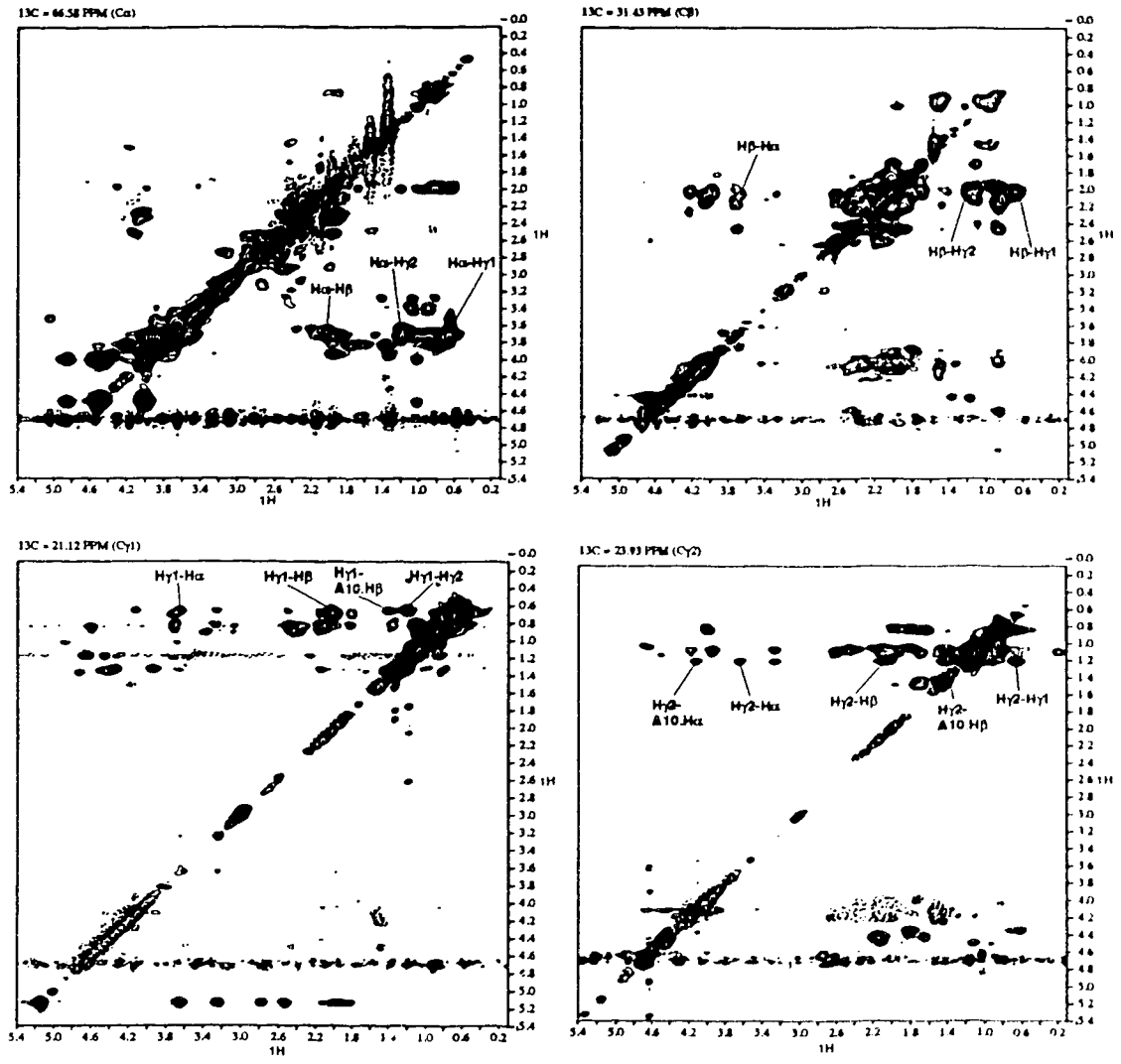

Figure VI-3. Correlations found for Val83 in the ^{13}C-edited NOESYHMQC spectrum. As for the HCCHCOSY, correlations can be found on four different planes corresponding to the Cα, Cβ, Cγ1 and Cγ2 chemical shifts. Note the few long range NOE's between a N-terminal residues (Ala10) and C-terminal residue (Val83)

NOE assignments

The assignment of the NOE's in the ^{15}N-edited NOESYHMQC and ^{13}C-edited NOESYHMQC spectra was performed with the PIPP software [2]. The PIPP program takes as input a chemical shift list, a NOESY spectra and optionally one or more pdb coordinate files. The program works as follows: 1) PIPP displays the spectra; 2) the user clicks on an NOE peak; 3) PIPP compares the chemical shift coordinates of the peak selected with the chemical shifts assignment list and selects possible assignments within a specified error range; 4) if pdb coordinates are provided, it does a second "trim" by keeping only the assignments that are in agreement within a specified distance boundary with the structure(s) provided; 5) from the assignments proposed, the user can then manually choose an assignment. The specified chemical shift error range was ±0.04 ppm for ^{1}H and ±0.75 ppm for ^{13}C and ^{15}N. Two sets of coordinates were provided to the program: one was the crystal structure coordinates and the other the model coordinates[1]. The distance cutoff was set to 12 Å, small enough to discard a few unrealistic assignment possibilities, but large enough not to bias the NOE assignments. Any assignment that was ambiguous was left unassigned. Using this approach, over 1000 NOE's were assigned.

NOE calibration

Calibration of NOE is often a tricky issue, and it is at its worse when it comes to three-dimensional NOE spectra. Immediately after the assignment stage, it was obvious that a single c[illegible]bration for all the NOE's was inappropriate. This is due to factors like different ^{13}C relaxation rate or different amide exchange rate among various residues.

To solve this problem, I applied the ideas I developped for the secondary structure characterization to the calibration of NOE's. As was explained in chapter V, the distances (or dihedral angles) related to $d_{N\alpha}$ and

$d_{\alpha N}$ NOE's can be determined fairly accurately using the $d_{N\alpha}/d_{\alpha N}$ ratio. Therefore the $d_{\alpha N}$ NOE's were calibrated by comparison to the $d_{N\alpha}$ NOE. Additionaly, the $d_{\alpha N}(i, i+3)$ were calibrated by comparison to both the $d_{N\alpha}$ and the $d_{\alpha N}$ NOE's. Note that these three NOE's are all related to the same amide and therefore appear on the same ^{15}N plane. The actual calibration used for these NOE's is summarized in the little "nawk" scripts listed at the beginning of appendix C. Note that only those NOE's are calibrated, and all the others are set to an upper limit of 5 Å. The final list of all the NOE's used for structure calibration, along with their lower and upper distance limits, is found in appendix C.

Tertiary structure

Structure calculation

Using the DGII program (Biosym Technologies) and the restraints listed in appendix C, 64 structures were calculated. The parameters used for the calculations are listed at the end of appendix C.

Structure families

It was obvious after just a few structure calculations that all the structures would not converge the same way. Therefore families of structures were defined in the following way:

1) Calculation of the pair-wise RMSD for the 64 structure (RMSD of backbone N, Cα and CO for residues 4-87 only). Structure #15 has the largest number (15) a pair-wise RMSD < 2.0 Å.
2) Superimposition of the 15 structures to structure #15 and then average these 16 structures to generate an average structure (AVG_1). The average RMSD of the 16 structures to AVG_1 is 1.45±0.17 Å.
3) Superimpose all 64 structures to AVG_1. 24 structures are found to have RMSD < 2.0 Å.
4) Average the 24 structures (AVG_2). The average RMSD of the 24 structures to AVG_2 is 1.55±0.22 Å.
5) Superimpose 64 structures to AVG_2. 25 structures are found to have RMSD < 2.0 Å.
6) Average the 25 structures (AVG_3). The average RMSD of the 25 structures to AVG_3 is 1.56±0.23 Å.
7) Superimpose 64 structures to AVG_3. Still 25 structures are found to have RMSD < 2.0 Å. 28 structures have RMSD < 2.5 Å.
8) Average the 28 structures (AVG_4). The average RMSD of the 28

structures to AVG_4 is 1.62±0.26 Å.

9) Superimpose 64 structures to AVG_4. 29 structures are found to have RMSD < 2.5 Å. There is no additional structures if RMSD cutoff is increased to 3.0 Å.

10) Average of the 29 structures (AVG_5). The average RMSD of the 29 structures to AVG_5 is 1.67±0.29 Å.

These 29 structures are considered as being part of the same family of structures. Using the same cyclic approach, the left structures were classified in 5 additional famillies. The characteristic of those 6 families of structures are summarized in Table VI-1.

Table VI-1. Characteristic of the family of structures.

Family	Error Function†	NOE Violations/residue (> 0.1 Å)
#1 (29)	0.106	1.5
#2 (11)	0.221	7.0
#3 (5)	0.148	3.4
#4 (3)	0.175	4.3
#5 (3)	0.246	8.7
others (13)	0.308	10.4

† The error function is a function which measures the total violations of the constraints by the coordinates.

Since family #1 is the most populated, the one with the lowest energy and the one with the less violations, it is considered as being the "good structure". Therefore only this family will be considered, and it is refered to as the tertiary structure of NTnC·2Ca.

Structure characteristic

The superimposition of 29 DGII structures of NTnC·2Ca with their average are shown in Figure VI-4 along with some structure statistics. Although the resolution of the NMR structure is very low at the present stage, the global fold of the protein can be characterized. The relative orientation of the helices in this solution structure of NTnC·2Ca are quite different from the crystal structure and more similar to the proposed model. Although the present NMR structure of NTnC·2Ca shows obvious differences with the model, it is still too early to make any statements. The solution structure of NTnC-apo has also been recently solved by NMR (Sakae Tsuda et al., personal communication) and it is clear that the structure of the regulatory domain of TnC is opening upon Ca^{2+}-binding, as was predicted by Herzberg et al. [1] (figure VI-5).

Figure VI-4. (page 111) Solution NMR structure of the regulatory domain of TnC. 29 structures generated with DGII are superimposed to their average structure. The two Ca^{2+} ions were added and positioned by comparison with the coordinates of the C-domain of TnC in the crystal structure of $2Ca^{2+}$ TnC [3]. The RMSD graph (top right) indicate that the two Ca^{2+}-binding loops, the B-C linker and the C-terminal part of NTnC are poorly defined. The number of NOE violations is small, as shown in the bar graph at the bottom right. Only two violations greater then 0.25 Å can be found in 29 structures.

Figure VI-5. (page 112) Superimposition of the apo and Ca^{2+}-saturated average NMR structure of the N-domain of TnC. The superimposition clearly shows the opening of the regulatory domain upon Ca^{2+}-binding. The opening is very similar to the model proposed by Herzberg, Moult & James [1]. Although there is some differences, the NMR structures need to be refined before conclusions may be made.

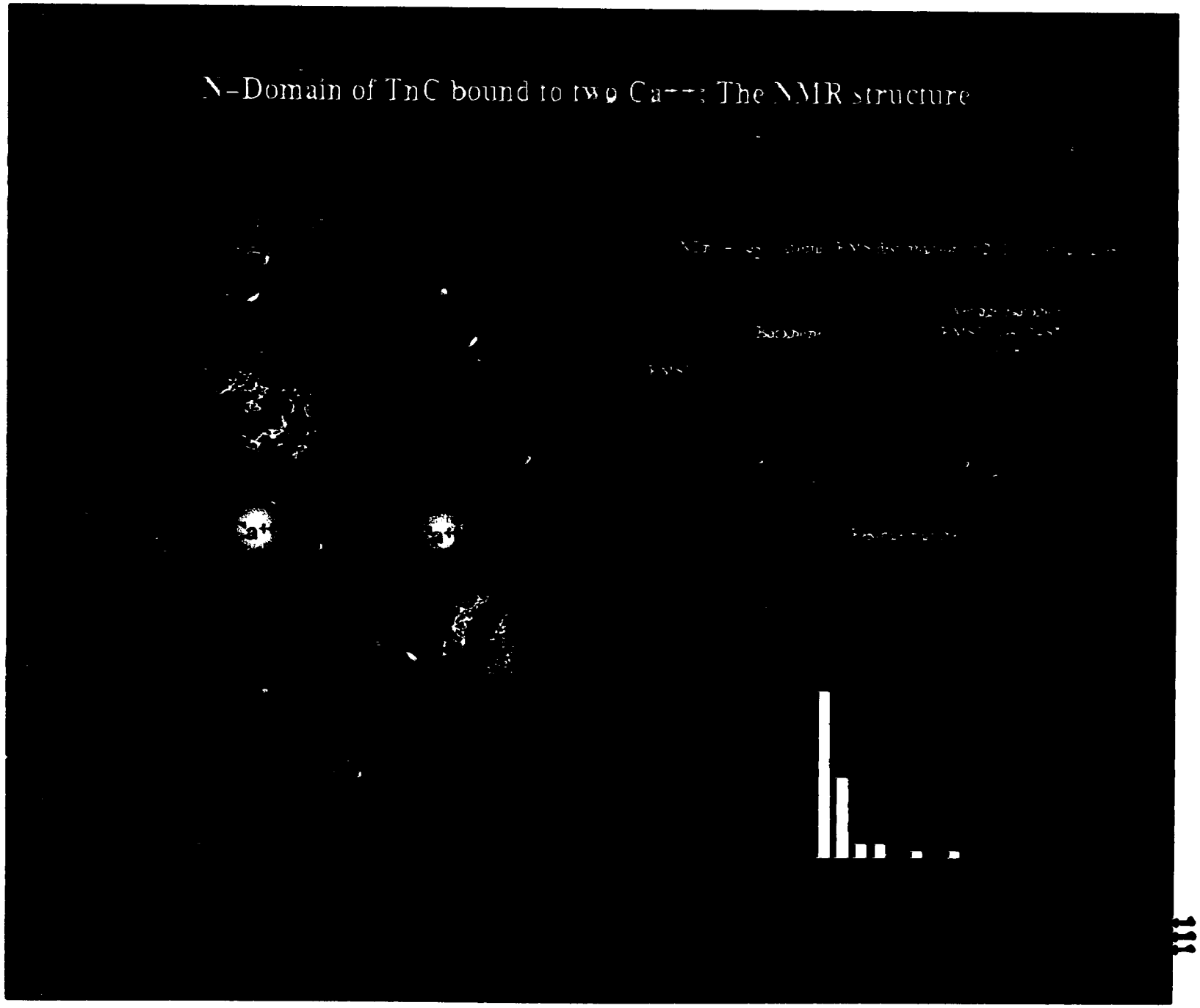
N-Domain of TnC bound to two Ca++: The NMR structure

Calcium- induced structural change of N-Domain of TnC

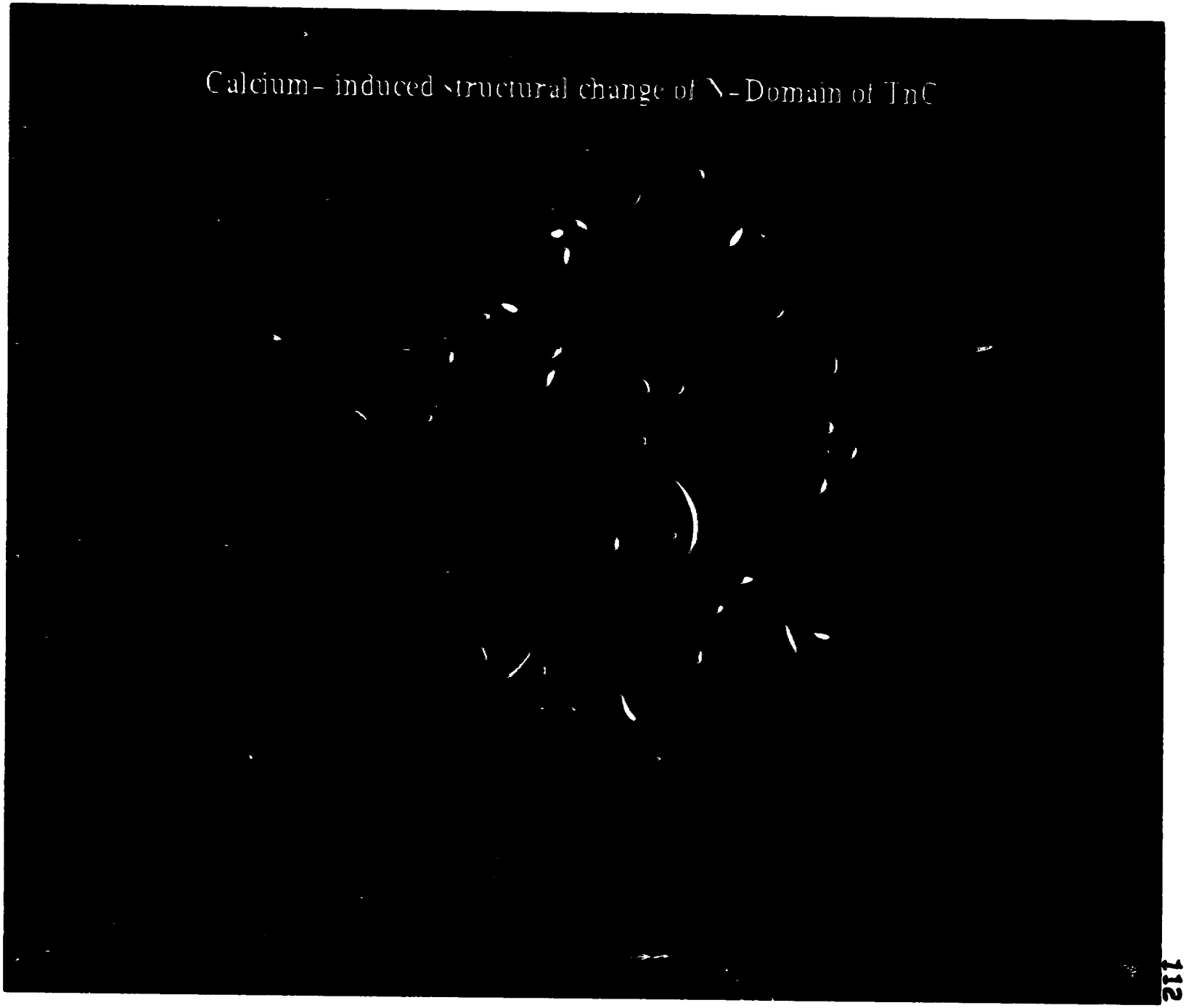

References

1 Herzberg, O., Moult, J. & James, M.N.G. (1986). *J. Biol. Chem.* **261**, 2638-2644.

2 Garrett, D.S., Powers, R., Gronenborn, A.M. & Clore, G.M. (1991). *J. Magn. Res.* **95**, 214-220.

3 Herzberg, O. & James, M. N. G. (1988). *J. Mol. Biol.* **203**, 761-779.

4 Ikura, M., Kay, L.E. & Bax, A. (1991). *J. Biomol. NMR* **1**, 299-304.

CHAPTER VII

DISCUSSION

It is well recognized that muscle contraction is triggered by a Ca^{2+}-induced structural change in the regulatory domain of TnC (see review by Grabarek et al. [1]). The results presented in this paper indicate that the secondary structural features of NTnC are not strongly affected by the binding of calcium. For both NTnC-apo and NTnC·2Ca, an N-terminal helix and two helix-loop-helix motifs joined by a short β-sheet are observed in solution. When compared to the crystal structure of turkey TnC where the N-domain is found in the apo form [2], the NMR solution data of NTnC-apo shows only similarities. Even the kink observed by x-ray crystallography at residue 41 of helix-B is observed in solution, as supported by the absence of the G43 $d_{\alpha N}$(i-3, i) the non-helical $^1H\alpha$ chemical shift of E41.

The secondary structure of NTnC·2Ca, as determined by NMR, is very similar to NTnC-apo (figure V-4 and V-5). The binding of calcium to NTnC does not induce any noticeable differences in terms of secondary structure for three of the five helices. Helix-C and helix-B appear to be shortened by one residue at their C-termini in NTnC·2Ca. Although some ambiguity is related to these observations, the length and relative position of helix-B and helix-C in NTnC·2Ca are exactly the same as observed in the NMR secondary structure of homologous Ca^{2+}-binding protein calmodulin [3]. Helix-A and -D were also found at the same position in calmodulin as in NTnC·2Ca, even though calmodulin lacks the N-helix.

The geometry of the B-helix is affected. The kink at residue 41 is removed upon calcium binding, leading to a regular helix from T39 to M48. These changes result in an increase of symmetry between the two binding

sites upon addition of calcium. This is in agreement with the model proposed by Herzberg et al. [4] and many helix-loop-helix protein structures which were solved in the Ca^{2+}-saturated state either by X-ray crystallography [5, 6] or NMR [7, 8]. Since the conformational changes occurring in the two Ca^{2+}-binding loops are not presented here in detail and must await the refinement of the tertiary structure of NTnC·2Ca, the straightening of helix-B is the major Ca^{2+}-induced structural change we can assess at this time. This change is localized at E41, a position which corresponds to the third most conserved residue in calcium-binding sites of proteins having the helix-loop-helix motif [9]. This invariant glutamate has both oxygen atoms of its carboxylate group coordinating the Ca^{2+} ion in a bidentate manner [5]. The E41 ϕ/ψ dihedral angles in the crystal structure of TnC are -96°/-7°, whereas the average angles for that position in 11 loops that have Ca^{2+} bound (from 5 different Ca^{2+}-binding proteins) are -66°/-41° [5]. The E41 ϕ/ψ transition from -96°/-7° to -66°/-41° can, by itself, account for most of the Ca^{2+}-induced reorientation of the B- and C-helix described by the Herzberg model [4] and observed by NMR in the preliminary structure presented in chapter VI. The consequence of this dihedral change is pictured in figure VII-1, where the removal of the kink in the B-helix of the crystal structure not only puts this helix in an orientation similar to the model, but also reorients the C-helix, giving a helical arrangement which is consistent with the model and other Ca^{2+}-binding protein structures solved in the Ca^{2+} form.

Figure VII-1. (page 116) Schematic representation of the Ca^{2+}-induced straightening of helix-B, and its possible impact on the tertiary fold of NTnC. (I) the Ca^{2+}-free crystal structure (Herzberg & James, 1988); (II) the predicted Ca^{2+}-saturated structure (Herzberg et al., 1986); (III) same as (I) with helix-B straightened by changing the ϕ/ψ backbone angle of E41 from -96/-7 to -66/-41. As can be seen by comparing (II) and (III) the straightening of helix-B, which is the predominant Ca^{2+}-induced secondary structure change observed by NMR in NTnC, could account for most of the opening of NTnC upon Ca^{2+}-binding.

Crystal structure of TnC
N-domain in apo state
Proposed model for
Ca++-saturated structure
Crystal structure of TnC with
modified

An important outcome of the present study is the conclusion that there is virtually no change in α-helical content in the transition from apo to the $2Ca^{2+}$ state of the N-domain of TnC. Although previous estimates of the magnitude of the Ca^{2+}-induced far UV CD ellipticity changes attributable to the N-domain transition have been somewhat contradictory [10, 11, 12, 13], a recent study [14] on isolated NTnC has shown clearly a very significant increase (~23%) in the negative values of $[\theta]_{221nm}$. This Ca^{2+}-induced ellipticity change must now be attributed to features other than an increase in helical content. Among several possible structural factors affecting the relationship between helical content and ellipticity [15], that attributable to helix-helix interaction seems the most plausible for NTnC. As cited in this review, both experimental and theoretical studies suggest a decrease in the CD intensity of ~10% for two antiparallel helices separated by 7-10 Å compared to a single α-helix. In the Ca^{2+}-induced opening of the structure NTnC [4, chapter VI], the B and C helices move as a unit relative to the N, A and D helices. As a result, the orientations of helix-B and helix-C to those of A and D change from nearly antiparallel to roughly perpendicular. In other words the helix packing in the apo form of NTnC would produce a smaller ellipticity signal than expected assuming only contributions from the secondary structure. Other contributions could include the removal of the kink at residue 41 of helix-B [16], Ca^{2+}-induced aggregation and the effects of alterations in the environment of clustered Phe side-chains [15]. However, these are likely to be of lesser significance than contributions arising from reorientation of helices. In any case the present study shows that it is the Ca^{2+}-induced tertiary structural changes, not the secondary structural ones, that are responsible for the CD ellipticity change in the N-domain of troponin-C.

References

1 Grabarek, Z., Tao, T. & Gergely, J. (1992). *J. Muscle Res. Cell Motil.* **13**, 383-393.

2 Herzberg, O. & James, M. N. G. (1988). *J. Mol. Biol.* **203**, 761-779.

3 Ikura, M., Spera, S., Barbato, G., Kay, L.E., Krinks, M. & Bax, A. (1991). *Biochemistry* **30**, 9216-9228.

4 Herzberg, O., Moult, J. & James, M.N.G. (1986). *J. Biol. Chem.* **261**, 2638-2644.

5 Strynadka, N. C. J. & James, M. N. G. (1989). *Annu. Rev. Biochem.* **58**, 951-998.

6 McPhalen, C.A., Strynadka, N.C.J. & James, M.N.G. (1991). *Adv. Prot. Chem.* **42**, 77-144.

7 Ikura, M., Clore, G.M., Gronenborn, A.M., Zhu, G., Klee, C.B. & Bax, A. (1992). *Science* **256**, 632-638.

8 Akke, M., Drakenberg, T. & Chazin, W.J. (1992). *Biochemistry* **31**, 1011-1020.

9 Marsden, B.J., Shaw, G.S. & Sykes, B.D. (1990). *Biochem. Cell. Biol.* **68**, 587-601.

10 Hincke, M.T., McCubbin, W.D. & Kay, C.M. (1978). *Can. J. Biochem.* **56**, 384-395

11 Johnson, J.D. & Potter, J.D. (1978). *J. Biol. Chem.* **253**, 3775-3777.

12 Leavis, P.C., Rosenfeld, S.S., Gergely, J., Grabarek, Z. & Drabikowski, W. (1978). *J. Biol. Chem.* **253**, 5452-5459.

13 Nagy B. & Gergely J. (1979). *J. Biol. Chem.* **254**, 12732-12737.

14 Li, M.X., Chandra, M., Pearlstone, J.R., Racher, K.I., Trigo-Gonzalez, G., Borgford, T., Kay, C.M. & Smillie, L.B. (1994). *Biochemistry* **33**, 917-925.

15 Manning, M.C. (1989). *J. Pharm. Biomed. Analysis* **7**, 1103-1119.

16 Chen, Y.H., Yang, T.Y. & Chan, K.M. (1974). *Biochemistry* **13**, 3350-3359.

CONCLUDING REMARKS

I believe the results presented in this thesis bring the understanding of muscle contraction at the molecular level one step forward. The characterization of the secondary structure brings clarification into the understanding of the CD changes observed in previous studies. This should not be regarded as an attempt to diminish the CD studies, but as data that could be used to enhance the understanding of special cases like this one in CD spectroscopy.

Although the solution structure of the Ca^{2+}-saturated regulatory domain of TnC still needs to mature, it clearly demonstrates for the first time that the Herzberg-Moult-James model is a good model. The assignments and the preliminary structure presented here are setting up the stage for the refinement of the NMR structure which will deliver the details of the Ca^{2+}-induced structural changes in the regulatory domain of TnC.

Although the complete characterization of the Ca^{2+}-induced structural changes in TnC is fascinating, probably more exciting is the fact that the results obtained during my graduate studies provide the essential tools for the structural characterization of NTnC complex with fragments of TnI, a study which will bring understanding in the next step of muscle contraction.

APPENDIX A

PULSE SEQUENCES CODE

1. HNCA

```
/* hnca_ct_sl.c  -  HNCA 3D experiment by Kay et al.; uses a
                    frequency-shifted pulse on the CO spins; has
                    RF duality.  This experiment does constant time
                       in the N15 dimension and optional spinlock purge
                       pulses for suppression of H2O.

   Parameters:

      sspul = 'y':  selects for Trim(x)-Trim(y) sequence at the start
                    of the pulse sequence
      f1180 = 'n':  standard t1 timing
              'y':  modified t1 timing for t1(1) = half the dwell time
      f2180 = 'n':  standard t2 timing
              'y':  modified t2 timing for t2(1) = half the dwell time
              'n':  normal experiment
       fad1 = 'y':  TPPI axial-peak displacement along t1
              'n':  standard phasecycle
       fad2 = 'y':  TPPI axial-peak displacement along t2 (3D experiment)
              'n':  standard phasecycle
    satmode = 'y':  H1 presaturation during relaxtion delay
     satfrq = frequency of 1H presaturation for all periods
     satdly = saturation time during the relaxation period
     satpwr = saturation power for all periods of presaturation with xmtr
         hs = 'yn':  homospoil pulse (hst) during the d1 relaxation delay
    spinlck = flag to check if spin lock purge pulses are to be used
    sltime1 = spin lock time in ms of first spin lock period
    sltime2 = spin lock time in ms of second spin lock period
              (should be different than sltime1).
      slpwr = spin lock power level.
       tpwr = power level for 1H transmitter pulses
         pw = 90 degree xmtr pulse length for protons (the observed nucleus)
        dof = should be set to Ca frequency
    pwcalvl = power level for Ca decoupler pulses
       pwca = 90 degree decoupler pulse length for Ca at ' wcalvl'
    pwcolvl = power level for C0 decoupler pulses
       pwco = 90 degree decoupler pulse length for C0 at 'pwcolvl'
      co180 = C=O shaped pulse
       hard = hard shaped pulse
   pwn15lvl = power level for N15 decoupler pulses
      pwn15 = 90 degree decoupler pulse length for N15
      dpwr2 = power level for N15 broadband decoupling
      inept = inept delay in sequence (NH scalar coupling)
      const = constant-time delay
         dm = 'nnnnn':  no broadband decoupling of N15 during acquisition
              'nnnny':  broadband heteronuclear decoupling of N15
                        during acquisition
        dm2 = 'n':  no broadband decoupling of C13 during acquisition

     phase = 1,2:  hypercomplex experiment with F1 quadrature (complex F1-FT)
    phase2 = 1,2:  hypercomplex experiment with F2 quadrature (complex F2-FT)

     modified from hncoca_ct.c(S.Gagne)  07/04/92

     modified to include constant-time in F2 (S.Gagne) 07/04/92
        ref.: Grzesiez and Bax, J. Mag. Reson., 96, 432-440 (1992).

     modified to include spin lock purge pulses (C. Slupsky), Feb, 1993

*/
```

```
#include <standard.h>
#include <math.h>

#define MIN_DELAY    0.2e-6        /* shortest executable delay */


static int      phs1[2] = {0,2},
                phs2[2] = {1,3},
                phs3[1] = {0},
               phs4[16] = {0,0,0,0,1,1,1,1,2,2,2,2,3,3,3,3},
               phs5[32] = {0,0,0,0,0,0,0,0,0,0,0,0,0,0,0,0,
                           2,2,2,2,2,2,2,2,2,2,2,2,2,2,2,2},
               phs6[32] = {1,1,1,1,1,1,1,1,1,1,1,1,1,1,1,1,
                           3,3,3,3,3,3,3,3,3,3,3,3,3,3,3,3},
                phs7[4] = {0,0,2,2},
                phs8[1] = {1},
                rec[32] = {0,2,2,0,2,0,0,2,0,2,2,0,2,0,0,2,
                           2,0,0,2,0,2,2,0,2,0,0,2,0,2,2,0};

static double d2_init = 0.0,
              d3_init = 0.0;


pulsesequence()
{
/* VARIABLE DECLARATION */
   char satmode[MAXSTR],
             co180[MAXSTR],
             hard[MAXSTR],
             sspul[MAXSTR],
        spinlck[MAXSTR],
             fad1[MAXSTR],
             fad2[MAXSTR],
             f1180[MAXSTR],
             f2180[MAXSTR];

   int  phase,
             phase2,
             satmove,
             t1_counter,
             t2_counter,
             c13dev = DODEV,
             n15dev = DO2DEV;

 double ss,
             t1evol,
             t2evol_1,
             t2evol_2,
             sw1,
             sw2,
             ni2,
             pwcalvl,
             pwca,
             pwcolvl,
             pwco,
             pwn15lvl,
             pwn15,
             satfrq,
             satdly,
             satpwr,
        sltime1,
        sltime2,
        slpwr,
             inept,
             const;

/* Load variables */
   satfrq = getval("satfrq");
   satdly = getval("satdly");
   satpwr = getval("satpwr");
   sltime1 = getval("sltime1");
   sltime2 = getval("sltime2");
   slpwr = getval("slpwr");
   pwcalvl = getval("pwcalvl");
   pwca = getval("pwca");
   pwcolvl = getval("pwcolvl");
   pwco = getval("pwco");
   pwn15lvl = getval("pwn15lvl");
```

```
    pwn15 = getval("pwn15");
    inept = getval("inept");
    const = getval("const");
    ss = getval("ss");
    sw1 = getval("sw1");
    sw2 = getval("sw2");
    ni2 = getval("ni2");
    phase = (int) (getval("phase") + 0.5);
    phase2 = (int) (getval("phase2") + 0.5);

    getstr("sspul", sspul);
    getstr("co180", co180);
    getstr("hard", hard);
    getstr("fad1", fad1);
    getstr("fad2", fad2);
    getstr("satmode", satmode);
    getstr("f1180", f1180);
    getstr("f2180", f2180);
    getstr("spinlck", spinlck);


/* Load phase cycles */
    settable(t1, 2, phs1);
    settable(t2, 2, phs2);
    settable(t3, 1, phs3);
    settable(t4, 16, phs4);
    settable(t5, 32, phs5);
    settable(t6, 32, phs6);
    settable(t7, 4, phs7);
    settable(t8, 1, phs8);
    settable(t9, 32, rec);


/* Check conditions */
    satmove = ( fabs(tof - satfrq) >= 0.1 );

    if ( (dm2[A] == 'y') || (dm2[B] == 'y') || (dm2[C] == 'y')
              || (dm2[D] == 'y') )
    {
       text_error("'dm2' must be to 'nnnnn' or 'nnnny' for N15 decoupling\n");
       abort(1);
    }

    if ( (dm[A] == 'y') || (dm[B] == 'y') || (dm[C] == 'y')
              || (dm[D] == 'y') || (dm[E] == 'y') )
    {
       text_error("'dm' must be to 'n' for C13\n");
       abort(1);
    }

    if ( (const) <= (((ni2/sw2)/2)+0.0002) )
    {  text_error("'const' must be larger then '(ni2/sw2)/2'");
       abort(1);
    }


/* Determine steady-state mode */
    if (ss < 0)
    {
       ss *= (-1);
       initval(ss, ssval);
       initval(ss, ssctr);
    }


/* Add in States-Haberkorn element */
    if (phase2 == 2)          /* N15 t1 element */
       tsadd(t3, 1, 4);

    if (phase == 2)           /* C13 t2 element */
       tsadd(t7, 1, 4);


/* Add in FAD */
    if (fad2[A] == 'y')               /* for N15 */
    {
       if (ix == 1)
         d3_init = d3;
```

```
      t2_counter = (int) ( (d3 - d3_init)*sw2 + 0.5 );
      if (t2_counter % 2)
      {
         tsadd(t3, 2, 4);   /* first N15 90-degree pulse      */
         tsadd(t9, 2, 4);   /* receiver phase cycle           */
      }
   }

   if (fad1[A] == 'y')              /* for C13 */
   {
      if (ix == 1)
        d2_init = d2;

      t1_counter = (int) ( (d2 - d2_init)*sw1 + 0.5 );
      if (t1_counter % 2)
      {
         tsadd(t7, 2, 4);        /* first C13a 90-degree pulse   */
         tsadd(t9, 2, 4);        /* receiver phase cycle         */
      }
   }


/* BEGIN ACTUAL PULSE SEQUENCE CODE */
   status(A);
      rlpower(tpwr, TODEV);        /*  H1 hard-pulse power level     */
      rlpower(pwn15lvl, n15dev);   /*  N15 hard-pulse power level    */
      rlpower(pwcolvl, c13dev);    /*  CO 180 power                  */

      if (sspul[A] == 'y')
      {
         rgpulse(200*pw, zero, rof1, 0.0);
         rgpulse(200*pw, one, 0.0, rof2);
      }
      hsdelay(d1);

/* selective saturation period */
      if (satmode[A] == 'y')
      {
         if (satmove)
            offset(satfrq, TODEV);

         rlpower(satpwr, TODEV);
         rgpulse(satdly, zero, 4.0e-5, 0.2e-6);
         if (satmove)
            offset(tof, TODEV);

         rlpower(tpwr, TODEV);
         delay(1.0e-5);
      }


/* Pulse train */
   status(B);
      rcvroff();

         txphase(zero);          /* 1H phase */
      dec2phase(t1);         /* N15 phase */
      decphase(zero);                /* C13 phase */
      rgpulse(pw, zero, 0.0, 0.0);
      delay(inept);

      sim3pulse(2*pw,0.0, 2*pwn15, zero, zero, t1, 0.0, 0.0);
      dec2phase(t3);         /* N15 phase */
      if (spinlck[0] == 'y')
      {
         rlpower(slpwr, TODEV);
         delay(inept-POWER_DELAY);
         xmtron();
         delay(sltime1);
         xmtroff();
         rlpower(tpwr,TODEV);
      }
      else
      {
         delay(inept);
      }
      txphase(t2);                   /* H1 phase  */
```

```
      sim3pulse(pw, 0.0, pwn15, t2, zero, t3, 0.0, 0.0);
      txphase(zero);
      dec2phase(t4);

      t1evol = d3;   /* N15 is governed by ni2 and sw2 */
      if (f2180[0] == 'y')
         t1evol += 0.5/sw2;

      if (t1evol < MIN_DELAY)
         t1evol = 0.0;

      delay(t1evol/2);
      decshaped_pulse(co180, 2*pwco, zero, 0.0, 0.0);


   status(C);
      decphase(t5);
      rlpower(pwcalvl,c13dev);
      delay(const - POWER_DELAY);
      sim3pulse(2*pw, 2*pwca, 2*pwn15, zero, t5, t4, 0.0, 0.0);
      decphase(t7);
      dec2phase(t6);
      delay(const + 2*pwco - (t1evol/2) );
      sim3pulse(0.0, pwca, pwn15, zero, t7, t6, 0.0, 0.0);

      rlpower(pwcolvl, c13dev);
      decphase(zero);
      dec2phase(zero);

      t2evol_1 = d2/2;      /* C13 is governed by ni and sw1 */
      t2evol_2 = d2/2;      /* C13 is governed by ni and sw1 */
      if (f1180[0] == 'y')
         {
         t2evol_1 += 0.25/sw1;
         t2evol_2 += 0.25/sw1;
         }
         if ( (t2evol_1 > MIN_DELAY) || (t2evol_2 > MIN_DELAY) )
         {
         t2evol_1 -= pwca/2 + pwco + POWER_DELAY + WFG_START_DELAY;
         t2evol_2 -= pwca/2 + pwco + POWER_DELAY + WFG_STOP_DELAY;

         if (t2evol_1 < MIN_DELAY)
            t2evol_1 = 0.0;
         if (t2evol_2 < MIN_DELAY)
            t2evol_2 = 0.0;
       }

      delay(t2evol_1);

      sim3shaped_pulse(hard, co180, hard, 2*pw, 2*pwco, 2*pwn15, zero, zero, zero,
0.0, 0.0);

      rlpower(pwcalvl, c13dev);
      delay(t2evol_2);

      sim3pulse(0.0, pwca, pwn15, zero, zero, zero, 0.0, 0.0);
      delay(const);
      sim3pulse(0.0, 2*pwca, 2*pwn15, zero, zero, zero, 0.0, 0.0);
      dec2phase(t8);
      delay(const);


   status(D);

      sim3pulse(pw, 0.0, pwn15, zero, zero, t8, 0.0, 0.0);
      dec2phase(zero);
      delay(inept);
      sim3pulse(2*pw, 0.0, 2*pwn15, zero, zero, zero, 0.0, 0.0);
      if (spinlck[0] == 'y')
      {
         rlpower(slpwr, TODEV);
         delay(inept-POWER_DELAY);
         xmtron();
         delay(sltime2);
         xmtroff();
         rlpower(tpwr,TODEV);
      }
```

```
      else
      {
         delay(inept);
      }

      rcvron();

      rlpower(dpwr2, DO2DEV);


   status(E);
      setreceiver(t9);
}
```

2. HNCOCA.

```
/* hncoca_ct.c   -  HN(CO)CA 3D experiment by Kay et al.; uses a
                    frequency-shifted pulse on the Ca spins; has
                    RF duality

          no proton decoupling is used(as opposed to hncoca.c)
          constant-time experiment in f2

   Parameters:

      sspul = 'y':  selects for Trim(x)-Trim(y) sequence at the start
                    of the pulse sequence
      f1180 = 'n':  standard t1 timing
              'y':  modified t1 timing for t1(1) = half the dwell time
      f2180 = 'n':  standard t2 timing
              'y':  modified t2 timing for t2(1) = half the dwell time
              'n':  normal experiment
       fad1 = 'y':  TPPI axial-peak displacement along t1
              'n':  standard phasecycle
       fad2 = 'y':  TPPI axial-peak displacement along t2 (3D experiment)
              'n':  standard phasecycle
    satmode = 'y':  H1 presaturation during relaxtion delay
     satfrq = frequency of 1H presaturation for all periods
     satdly = saturation time during the relaxation period
     satpwr = saturation power for all periods of presaturation with xmtr
         hs = 'yn':  homospoil pulse (hst) during the d1 relaxation delay
       tpwr = power level for 1H transmitter pulses
         pw = 90 degree xmtr pulse length for protons (the observed nucleus)
        dof = should be set to C0 frequency
   pwcalvl = power level for Ca decoupler pulses
      pwca = 90 degree decoupler pulse length for Ca at 'pwcalvl'
    cashape = frequency-shifted pulse for Ca excitation
  pwca2lvl = power level for Ca 180 decoupler pulses
     pwca2 = 180 degree decoupler pulse length for Ca at 'pwcalvl'
  cashape2 = frequency-shifted pulse for Ca 180 excitation
   pwco1vl = power level for C0 decoupler pulses
      pwco = 90 degree decoupler pulse length for C0 at 'pwco1vl'
  pwco21vl = power level for shorter C0 pulse
     pwco2 = 90 degree decoupler pulse length for C0 at 'pwco21vl'
  pwn151vl = power level for N15 decoupler pulses
     pwn15 = 90 degree decoupler pulse length for N15
     dpwr2 = power level for N15 broadband decoupling
     inept = inept delay in sequence (NH scalar coupling; ~2.4 ms)
      tau1 = first delay in sequence (~8.3 ms)
      tau2 = second delay in sequence (~3.0 ms)
      tau3 = third delay in sequence (~5.5 ms
       dm2 = 'nnnnn':  no broadband decoupling of N15 during acquisition
             'nnnny':  broadband heteronuclear decoupling of N15
                       during acquisition
        dm = 'n':  no broadband decoupling of C13 during acquisition

     phase = 1,2:  hypercomplex experiment with F1 quadrature (complex F1-FT)
    phase2 = 1,2:  hypercomplex experiment with F2 quadrature (complex F2-FT)

   modified from hncoca1FSP.c(S.Farmer,Varian)  1/27/92

 modified from hncocaxx.c to include constant-time in F2 (S.Gagne) 07/01/92
      ref.: Grzesiez and Bax, J. Magn. Reson., 96, 432-440 (1992).

NOTE :
------

SHAPED PULSE : carrier on C=0 and shaped pulse on Ca

*/


#include <standard.h>
#include <math.h>

#define MIN_DELAY    0.2e-6        /* shortest executable delay */

static int     phs1[4] = {0,0,2,2},
```

```
                phs2[2] = {0,2},
                phs3[8] = {0,0,0,0,2,2,2,2},
               phs5[16] = {0,0,0,0,0,0,0,0,2,2,2,2,2,2,2,2},
                rec[16] = {0,2,2,0,2,0,0,2,2,0,0,2,0,2,2,0};

static double d2_init = 0.0,
              d3_init = 0.0;


pulsesequence()
{
/* VARIABLE DECLARATION */
   char          satmode[MAXSTR],
                 sspul[MAXSTR],
                 fad1[MAXSTR],
                 fad2[MAXSTR],
                 f1180[MAXSTR],
                 f2180[MAXSTR],
                 cashape[MAXSTR],
                 cashape2[MAXSTR];
   int             phase,
                 phase2,
                 satmove,
                 t1_counter,
                 t2_counter,
                 c13dev = DODEV,
                 n15dev = DO2DEV;
   double          ss,
                 t1evol,
                 t2evol_1,
                 t2evol_2,
                 sw1,
                 sw2,
                 ni2,
      pwcalvl,
      pwca,
      pwca2lvl,
      pwca2,
      pwcolvl,
      pwco,
      pwco2lvl,
      pwco2,
      pwn15lvl,
      pwn15,
      satfrq,
      satdly,
      satpwr,
                 inept,
                 tau2,
                 tau1,
                 tau3;


/* Load variables */
   satfrq = getval("satfrq");
   satdly = getval("satdly");
   satpwr = getval("satpwr");
   pwcalvl = getval("pwcalvl");
   pwca = getval("pwca");
   pwca2lvl = getval("pwca2lvl");
   pwca2 = getval("pwca2");
   pwcolvl = getval("pwcolvl");
   pwco = getval("pwco");
   pwco2lvl = getval("pwco2lvl");
   pwco2 = getval("pwco2");
   pwn15lvl = getval("pwn15lvl");
   pwn15 = getval("pwn15");
   inept = getval("inept");
   tau2 = getval("tau2");
   tau1 = getval("tau1");
   tau3 = getval("tau3");
   ss = getval("ss");
   sw1 = getval("sw1");
   sw2 = getval("sw2");
   ni2 = getval("ni2");
   phase = (int) (getval("phase") + 0.5);
   phase2 = (int) (getval("phase2") + 0.5);
```

```
   getstr("cashape", cashape);
   getstr("cashape2", cashape2);
   getstr("sspul", sspul);
   getstr("fad1", fad1);
   getstr("fad2", fad2);
   getstr("satmode", satmode);
   getstr("f1180", f1180);
   getstr("f2180", f2180);


/* Load phase cycles */
   settable(t1, 4, phs1);
   settable(t2, 2, phs2);
   settable(t3, 8, phs3);
   settable(t4, 16, rec);
   settable(t5, 16, phs5);


/* Check conditions */
   satmove = ( fabs(tof - satfrq) >= 0.1 );

   if ( (dm2[A] == 'y') || (dm2[B] == 'y') || (dm2[C] == 'y')
            || (dm2[D] == 'y') )
   {
      text_error("'dm2' must be to 'nnnnn' or 'nnnny' for N15 decoupling\n");
      abort(1);
   }

   if ( (dm[A] == 'y') || (dm[B] == 'y') || (dm[C] == 'y')
            || (dm[D] == 'y') || (dm[E] == 'y') )
   {
      text_error("'dm' must be to 'n' for C13\n");
      abort(1);
   }

   if ( (tau2+tau1) <= ((ni2/sw2)/2) )
   {  text_error("'tau2+tau1' must be larger then '(ni2/sw2)/2'");
      abort(1);
   }


/* Determine steady-state mode */
   if (ss < 0)
   {
      ss *= (-1);
      initval(ss, ssval);
      initval(ss, ssctr);
   }


/* Add in States-Haberkorn element */
   if (phase2 == 2)          /* N15 t1 element */
      tsadd(t2, 1, 4);

   if (phase == 2)           /* C13 t2 element */
      tsadd(t3, 1, 4);


/* Add in FAD */
   if (fad2[A] == 'y')             /* for N15 */
   {
      if (ix == 1)
        d3_init = d3;

      t2_counter = (int) ( (d3 - d3_init)*sw2 + 0.5 );
      if (t2_counter % 2)
      {
         tsadd(t2, 2, 4);  /* first N15 90-degree pulse       */
         tsadd(t4, 2, 4);  /* receiver phase cycle            */
      }
   }

   if (fad1[A] == 'y')             /* for C13 */
   {
      if (ix == 1)
        d2_init = d2;

      t1_counter = (int) ( (d2 - d2_init)*sw1 + 0.5 );
```

```
      if (t1_counter % 2)
      {
         tsadd(t3, 2, 4);        /* first C13a 90-degree pulse    */
         tsadd(t4, 2, 4);        /* receiver phase cycle          */
      }
   }


/* BEGIN ACTUAL PULSE SEQUENCE CODE */
   status(A);
      rlpower(tpwr, TODEV);        /*  H1 hard-pulse power level     */
      rlpower(pwn15lvl, n15dev);   /*  N15 hard-pulse power level    */
      rlpower(pwca2lvl, c13dev);   /*  Ca 180 power                  */

      if (sspul[A] == 'y')
      {
         rgpulse(200*pw, zero, rof1, 0.0);
         rgpulse(200*pw, one, 0.0, rof2);
      }
         hsdelay(d1);

/* selective saturation period */
      if (satmode[A] == 'y')
      {
         if (satmove)
            offset(satfrq, TODEV);

         rlpower(satpwr, TODEV);
         rgpulse(satdly, zero, 4.0e-5, 0.2e-6);
         if (satmove)
            offset(tof, TODEV);

         rlpower(tpwr, TODEV);
         delay(1.0e-5);
      }


/* Pulse train */
   status(B);
      rcvroff();

      rgpulse(pw, zero, rof1, 0.0);
      dec2phase(t1);          /* N15 phase */
      decphase(zero);                 /* C13 phase */
      delay(inept);

      sim3pulse(2*pw,0.0, 2*pwn15, zero,zero, t1, 0.0, 0.0);
      txphase(t1);                    /* H1 phase  */
      dec2phase(t2);          /* N15 phase */
      delay(inept);

      getelem(t1, ct, v14);
      add(one, v14, v14);

      sim3pulse(pw,0.0, pwn15, v14,zero, t2, 0.0, 0.0);
      txphase(zero);
      dec2phase(zero);

      t1evol = d3;   /* N15 is governed by ni2 and sw2 */
      if (f2180[0] == 'y')
         t1evol += 0.5/sw2;

      if (t1evol > MIN_DELAY)
      {
         t1evol -= pwn15 + pwca2 + 2*WFG_START_DELAY;
         if (t1evol < MIN_DELAY)
            t1evol = 0.0;
      }

      delay(t1evol/2);
      decshaped_pulse(cashape2,pwca2,zero,0.0,0.0);
      delay(tau1 - pwca2/2 - WFG_STOP_DELAY - pw);
      rgpulse(2*pw, zero, 0.0, 0.0);


   status(C);
      delay(tau2/2 - pw);
      rlpower(pwc0lvl,c13dev);
```

```
      delay( (tau2/2) - POWER_DELAY - pwco );
      sim3pulse(0.0, 2*pwco,2*pwn15, zero, zero,zero,0.0,0.0);
      delay(tau2 + tau1 - pwco - pwco/2 - (t1evol/2) - pwn15/2 - pwca2/2 -
            WFG_START_DELAY);
      sim3pulse(0.0,pwco,pwn15, zero, zero,zero, 0.0, 0.0);

      delay(tau3/2 - pwco/2);
      rlpower(pwcalvl, c13dev);
      decphase(t3);
      delay( (tau3/2) - POWER_DELAY - WFG_START_DELAY - pwca/2);
      decshaped_pulse(cashape, pwca, t3, 0.0, 0.0);

      t2evol_1 = t2evol_2 = d2/2; /* C13 is governed by ni and sw */
      if (f1180[0] == 'y')
      {
         t2evol_1 += 0.25/sw1;
         t2evol_2 += 0.25/sw1;
      }

      if ( (t2evol_1 > MIN_DELAY) || (t2evol_2 > MIN_DELAY) )
      {
         t2evol_1 -= pwca/2 + pwco2 + POWER_DELAY + WFG_STOP_DELAY;
         t2evol_2 -= pwca/2 + pwco2 + POWER_DELAY + WFG_START_DELAY;

         if (t2evol_1 < MIN_DELAY)
            t2evol_1 = 0.0;
         if (t2evol_2 < MIN_DELAY)
            t2evol_2 = 0.0;
      }

      decphase(zero);
      rlpower(pwco2lvl, c13dev);
      delay(t2evol_1);

      simpulse(2*pw, 2*pwco2, zero, zero, 0.0, 0.0);

      rlpower(pwcalvl, c13dev);
      delay(t2evol_2);

      decshaped_pulse(cashape, pwca, zero, 0.0, 0.0);
      delay( (tau3/2) - WFG_STOP_DELAY - pwca/2 );
      rlpower(pwcolvl, c13dev);
      delay( (tau3/2) - POWER_DELAY - pwco/2 );


   status(D);
      sim3pulse(0.0,pwco,pwn15,zero,zero, t5, 0.0, 0.0);
      delay(tau1 + tau2 - pwco/2 - pwco );
      sim3pulse(0.0,2*pwco,2*pwn15,zero, zero, zero, 0.0, 0.0);
      delay(tau1 - pwco - pw);

      rgpulse(2*pw, zero, 0.0, 0.0);
      delay(tau2 - pw - pwn15/2);
      sim3pulse(pw,0.0, pwn15, zero,zero, zero, 0.0, 0.0);
      delay(inept);
      sim3pulse(2*pw,0.0, 2*pwn15, zero, zero,zero, 0.0, 0.0);

      rlpower( ((n15dev == DODEV) ? dpwr : dpwr2), n15dev);
      rlpower( ((c13dev == DODEV) ? dpwr : dpwr2), c13dev);
      delay(rof2);
      rcvron();
      delay(inept - rof2 - 2*POWER_DELAY);


   status(E);
      setreceiver(t4);
}
```

3. HNCO.

```
/* hnco_ct.c     - HNCO 3D experiment with constant-time evolution in F1 (15N)
                 - 13C carrier (dec #1) on C=O and shifted pulse on Ca
                 - ref.: Grzesiez and Bax, J. Magn. Reson., 96, 432-440 (1992).
                 - programmed by S.M. Gagne (6 July 1992)
                 - last revised (13 August 1992)

   Parameters:

      sspul = 'y':  selects for Trim(x)-Trim(y) sequence at the start
                    of the pulse sequence
      f1180 = 'n':  standard t1 timing
              'y':  modified t1 timing for t1(1) = half the dwell time
      f2180 = 'n':  standard t2 timing
              'y':  modified t2 timing for t2(1) = half the dwell time
              'n':  normal experiment
       fad1 = 'y':  TPPI axial-peak displacement along t1
              'n':  standard phasecycle
       fad2 = 'y':  TPPI axial-peak displacement along t2 (3D experiment)
              'n':  standard phasecycle
    satmode = 'y':  H1 presaturation during relaxtion delay
     satfrq = frequency of 1H presaturation for all periods
     satdly = saturation time during the relaxation period
     satpwr = saturation power for all periods of presaturation with xmtr
         hs = 'yn':  homospoil pulse (hst) during the d1 relaxation delay
       tpwr = power level for 1H transmitter pulses
         pw = 90 degree xmtr pulse length for protons (the observed nucleus)
       hard = hard shape-pulse for 1H and 15N
        dof = should be set to C0 frequency
    pwcalvl = power level for Ca decoupler pulses
    pwca180 = 180 degree decoupler pulse length for Ca at 'pwcalvl'
    cashape = frequency-shifted pulse for 180 degree Ca excitation
              (see cashape note below)
    pwcolvl = power level for C0 decoupler pulses
       pwco = 90 degree decoupler pulse length for C0 at 'pwcolvl'
   pwn15lvl = power level for N15 decoupler pulses
      pwn15 = 90 degree decoupler pulse length for N15
      dpwr2 = power level for N15 broadband decoupling
      inept = inept delay in sequence (1/4*NH scalar coupling) (about 2.45ms)
       tau2 = second delay in sequence ( about 3ms )
       tau1 = first delay in sequence ( about 10ms )
        dm2 = 'nnnnn':  no broadband decoupling of N15 during acquisition
              'nnnny':  broadband heteronuclear decoupling of N15
                        during acquisition
         dm = 'n':  no broadband decoupling of C13 during acquisition
         nt = multiple of 16

      phase = 1,2:  hypercomplex experiment with F1 quadrature (complex F1-FT)
     phase2 = 1,2:  hypercomplex experiment with F2 quadrature (complex F2-FT)


-------------------------------------------------------------------------------
NOTES:

cashape :  the first null of the 180 Ca shifted pulse should correspond to
           the frequency of the C=O carrier (dof)

constant time :     the constant-time evolution period is equal to 2*(tau1+tau2)
            and should be set to an odd multiple of 1/(2JNH) (~26 ms)

Sensitivity : this experiment is more sensitive then the HNCA or
              HN(CO)CA ; less transients are necessary for the HNCO.

Suggestions from SMG :
      inept, tau1, tau2 optimization : Start with the default values then
             optimize on the first increment (ni=ni2=phase=phase2=1) in
             order to maximize the intensity of the signal. Optimize first
             inept,then tau2 and finally tau1.

-------------------------------------------------------------------------------

*/
```

```
#include <standard.h>
#include <math.h>

#define MIN_DELAY    0.2e-6        /* shortest executable delay */
#define SIM3SH_START_DELAY 30.2e-6
#define SIM3SH_STOP_DELAY 12.2e-6


static int     phs1[2] = {0,2},
               phs2[2] = {1,3},
               phs3[1] = {0},
               phs4[16]= {0,0,0,0,1,1,1,1,2,2,2,2,3,3,3,3},
              phs5[4] = {0,0,2,2},
              phs6[2] = {0,2},
               rec[8] = {0,0,2,2,2,2,0,0};

static double d2_init = 0.0,
              d3_init = 0.0;


pulsesequence()
{
/* VARIABLE DECLARATION */
   char          satmode[MAXSTR],
              sspul[MAXSTR],
              fad1[MAXSTR],
              fad2[MAXSTR],
              f1180[MAXSTR],
              f2180[MAXSTR],
              hard[MAXSTR],
              cashape[MAXSTR];
   int          phase,
              phase2,
              satmove,
              t1_counter,
              t2_counter,
              c13dev = DODEV,
              n15dev = DO2DEV;
   double       ss,
              t1evol,
              t2evol_1,
              t2evol_2,
              sw1,
              sw2,
              ni2,
      pwca1v1,
      pwca180,
      pwco1v1,
      pwco,
      pwn151v1,
      pwn15,
      satfrq,
      satdly,
      satpwr,
              inept,
              tau2,
              tau1;


/* Load variables */
   satfrq = getval("satfrq");
   satdly = getval("satdly");
   satpwr = getval("satpwr");
   pwca1v1 = getval("pwca1v1");
   pwca180 = getval("pwca180");
   pwco1v1 = getval("pwco1v1");
   pwco = getval("pwco");
   pwn151v1 = getval("pwn151v1");
   pwn15 = getval("pwn15");
   inept = getval("inept");
   tau2 = getval("tau2");
   tau1 = getval("tau1");
   ss = getval("ss");
   sw1 = getval("sw1");
   sw2 = getval("sw2");
   ni2 = getval("ni2");
   phase = (int) (getval("phase") + 0.5);
   phase2 = (int) (getval("phase2") + 0.5);
```

```
   getstr("cashape", cashape);
   getstr("hard", hard);
   getstr("sspul", sspul);
   getstr("fad1", fad1);
   getstr("fad2", fad2);
   getstr("satmode", satmode);
   getstr("f1180", f1180);
   getstr("f2180", f2180);


/* Load phase cycles */
   settable(t1, 2, phs1);
   settable(t2, 2, phs2);
   settable(t3, 1, phs3);
   settable(t4, 16, phs4);
   settable(t5, 4, phs5);
   settable(t6, 2, phs6);
   settable(t7, 8, rec);


/* Check conditions */
   satmove = ( fabs(tof - satfrq) >= 0.1 );

   if ( (dm2[A] == 'y') || (dm2[B] == 'y') || (dm2[C] == 'y')
            || (dm2[D] == 'y') )
   {
      text_error("'dm2' must be to 'nnnnn' or 'nnnny' for N15 decoupling\n");
      abort(1);
   }

   if ( (dm[A] == 'y') || (dm[B] == 'y') || (dm[C] == 'y')
            || (dm[D] == 'y') || (dm[E] == 'y') )
   {
      text_error("'dm' must be to 'n' for C13\n");
      abort(1);
   }

   if ( (tau2+tau1) <= ((ni2/sw2)/2) )
   {  text_error("'tau2+tau1' must be larger then '(ni2/sw2)/2'");
      abort(1);
   }


/* Determine steady-state mode */
   if (ss < 0)
   {
      ss *= (-1);
      initval(ss, ssval);
      initval(ss, ssctr);
   }


/* Add in States-Haberkorn element */
   if (phase2 == 2)          /* N15 t1 element */
      tsadd(t3, 1, 4);

   if (phase == 2)           /* C13 t2 element */
      tsadd(t5, 1, 4);


/* Add in FAD */
   if (fad2[A] == 'y')             /* for N15 */
   {
      if (ix == 1)
        d3_init = d3;

      t2_counter = (int) ( (d3 - d3_init)*sw2 + 0.5 );
      if (t2_counter % 2)
      {
         tsadd(t3, 2, 4);   /* first N15 90-degree pulse       */
         tsadd(t7, 2, 4);   /* receiver phase cycle            */
      }
   }

   if (fad1[A] == 'y')             /* for C13 */
   {
      if (ix == 1)
```

```
        d2_init = d2;

      t1_counter = (int) ( (d2 - d2_init)*sw1 + 0.5 );
      if (t1_counter % 2)
      {
         tsadd(t5, 2, 4);        /* first C13a 90-degree pulse    */
         tsadd(t7, 2, 4);        /* receiver phase cycle          */
      }
   }


/* BEGIN ACTUAL PULSE SEQUENCE CODE */
   status(A);
      rlpower(tpwr, TODEV);        /*  H1 hard-pulse power level     */
      rlpower(pwn15lvl, n15dev);   /*  N15 hard-pulse power level    */
      rlpower(pwcalvl, c13dev);    /*  Ca 180 power                  */

      if (sspul[A] == 'y')
      {
         rgpulse(200*pw, zero, rof1, 0.0);
         rgpulse(200*pw, one, 0.0, rof2);
      }
         hsdelay(d1);

/* selective saturation period */
      if (satmode[A] == 'y')
      {
         if (satmove)
            offset(satfrq, TODEV);

         rlpower(satpwr, TODEV);
         rgpulse(satdly, zero, 4.0e-5, 0.2e-6);
         if (satmove)
            offset(tof, TODEV);

         rlpower(tpwr, TODEV);
         delay(1.0e-5);
      }


/* Pulse train */
   status(B);
      rcvroff();

      rgpulse(pw, zero, rof1, 0.0);
      dec2phase(t1);          /* N15 phase */
      decphase(zero);               /* C13 phase */
      delay(inept);

      sim3pulse(2*pw,0.0, 2*pwn15, zero,zero, t1, 0.0, 0.0);
      txphase(t2);                  /* H1 phase  */
      dec2phase(t3);          /* N15 phase */
      delay(inept);

      sim3pulse(pw,0.0, pwn15, t2,zero, t3, 0.0, 0.0);
      txphase(zero);
      dec2phase(t4);

      t1evol = d3;   /* N15 is governed by ni2 and sw2 */
      if (f2180[0] == 'y')
         t1evol += 0.5/sw2;

      if (t1evol > MIN_DELAY)
      {
         t1evol -= pwn15 + pwca180 + 2*WFG_START_DELAY ;
         if (t1evol < MIN_DELAY)
            t1evol = 0.0;
      }

      delay(t1evol/2);
      decshaped_pulse(cashape,pwca180,zero,0.0,0.0);


   status(C);
      delay( (tau1 + tau2)/2 - pwca180/2 - WFG_STOP_DELAY);
      rlpower(pwc01vl,c13dev);
      delay( (tau1 + tau2)/2 - POWER_DELAY );
      sim3pulse(2*pw, 2*pwc0, 2*pwn15, zero, zero, t4,0.0,0.0);
```

```
            decphase(t5);
            dec2phase(t6);
      delay(tau1 + tau2 - (t1evol/2 + pwn15/2 + pwca180/2 + WFG_START_DELAY -
            pwco/2) );
            sim3pulse(0.0,pwco,pwn15, zero, t5, t6, 0.0, 0.0);

      rlpower(pwcalvl, c13dev);
      decphase(zero);
            dec2phase(zero);

      t2evol_1 = t2evol_2 = d2/2; /* C13 is governed by ni and sw */
      if (f1180[0] == 'y')
      {
         t2evol_1 += 0.25/sw1;
         t2evol_2 += 0.25/sw1;
      }

      if ( (t2evol_1 > MIN_DELAY) || (t2evol_2 > MIN_DELAY) )
      {
         t2evol_1 -= pwco/2 + pwca180/2 + POWER_DELAY + SIM3SH_START_DELAY;
         t2evol_2 -= pwco/2 + pwca180/2 + POWER_DELAY + SIM3SH_STOP_DELAY;

         if (t2evol_1 < MIN_DELAY)
            t2evol_1 = 0.0;
         if (t2evol_2 < MIN_DELAY)
            t2evol_2 = 0.0;
      }

      delay(t2evol_1);

      sim3shaped_pulse(hard,cashape,hard,2*pw, pwca180, 2*pwn15, zero, zero,
            zero,0.0, 0.0);

      rlpower(pwcolvl, c13dev);
      delay(t2evol_2);


   status(D);
      sim3pulse(0.0,pwco,pwn15,zero,zero, zero, 0.0, 0.0);
      delay(tau1 + tau2 - pwco/2);
      sim3pulse(0.0,2*pwco,2*pwn15,zero, zero, zero, 0.0, 0.0);
      delay(tau1 - pw);

      rgpulse(2*pw, zero, 0.0, 0.0);
      delay(tau2 - pw -pwn15/2);
      sim3pulse(pw,0.0, pwn15, zero,zero, zero, 0.0, 0.0);
      delay(inept);
      sim3pulse(2*pw,0.0, 2*pwn15, zero, zero,zero, 0.0, 0.0);

      rlpower( ((n15dev == DODEV) ? dpwr : dpwr2), n15dev);
      rlpower( ((c13dev == DODEV) ? dpwr : dpwr2), c13dev);
      delay(rof2);
      rcvron();
      delay(inept - rof2 - 2*POWER_DELAY);


   status(E);
      setreceiver(t7);
}
```

4. HCACO.

```
/* hcaco_ct.c    - HCACO 3D experiment with constant-time evolution in F1 (Ca)
                 - 13C carrier (dec #1) on Ca and shifted pulse on C=O
                 - ref.: 1. R. Powers, A.M. Gronenborn, G.M. Clore, and A. Bax,
                           J. Magn. Reson., 94, 209-213 (1991).
                         2. L.E. Kay, M. Ikura, R. Tschudin, and A. Bax,
                           J. Magn. Res., 89, 496-514.
                 - written for spectrometer with only three channel, so used
                   consecutive Ca/C=O instead of simultaneous ones.
                 - programmed by S.M. Gagne (24 August 1992)
                 - last revised by S.M. Gagne (28 september 1992)

   Parameters:

      sspul = 'y':  selects for Trim(x)-Trim(y) sequence at the start
                    of the pulse sequence
      f1180 = 'n':  standard t1 timing
              'y':  modified t1 timing for t1(1) = half the dwell time
      f2180 = 'n':  standard t2 timing
              'y':  modified t2 timing for t2(1) = half the dwell time
              'n':  normal experiment
       fad1 = 'y':  TPPI axial-peak displacement along t1
              'n':  standard phasecycle
       fad2 = 'y':  TPPI axial-peak displacement along t2 (3D experiment)
              'n':  standard phasecycle
    satmode = 'y':  H1 presaturation during relaxtion delay
     satfrq = frequency of 1H presaturation for all periods
     satdly = saturation time during the relaxation period (see NOTES below)
     satpwr = saturation power for all periods of presaturation with xmtr
              (see NOTES below)
         hs = 'yn':  homospoil pulse (hst) during the d1 relaxation delay
       tpwr = power level for 1H transmitter pulses
         pw = 90 degree xmtr pulse length for protons (the observed nucleus)
       hard = hard shape-pulse for 1H
        dof = should be set to Ca frequency
    pwcalvl = power level for Ca decoupler pulses
       pwca = 90 degree decoupler pulse length for Ca at 'pwcalvl'
     co180 = C=O 180 frequency-shifted pulse (see NOTES below)
      co90 = C=O 90 frequency-shifted pulse (see NOTES below)

      dpwr2 = power level for N15 broadband decoupling
      inept = inept delay in sequence (1/4*NH scalar coupling) (about 2.45ms)
     constT = half of the constant-time duration (see NOTES below)
        dm2 = 'nnnnn':  no broadband decoupling of N15
              'nnynn':  broadband heteronuclear decoupling of N15
                        during t1/t2 evolution period
         dm = 'nnnnn':  no broadband decoupling of C13 during acquisition
              'nnnny':  broadband heteronuclear decoupling of C13
                        during acquisition
         nt = multiple of 16

      phase = 1,2:  hypercomplex experiment with F1 quadrature (complex F1-FT)
     phase2 = 1,2:  hypercomplex experiment with F2 quadrature (complex F2-FT)


------------------------------------------------------------------------------
NOTES:

co180,co90 :  the first null of the CO shifted pulse should correspond to
              the frequency of the Ca carrier (dof).  If the frequency
              shift is set to 18181.8 Hz (for a pwco90=55us), a sw2 (C=O) of
              1818.18 will have the proper number of folding and usually
              covers all the backbone C=O.

constant time :      the constant-time evolution period is equal to 2*(constT).
               Resolution in the t1 dimension is limited by the fact that
                 the t1 acquisition period is restricted to the constant-time
                 duration (2*constT). As a reasonable compromise between high
                 sensitivity and acceptable resolution, a constant-time
                 duration of 7ms is used (constT=3.5ms). 7ms also correspond
                 to ~1/(JHaCa), so that the Ca spin will be antiphase with
                 respect to the Ha at the end of the time 2*constT.

water suppression : since the HCACO is done in D2O, no water suppression
                    or very low satpwr can be used with this experiment.
```

```
d1/satdly : d1 (or satdly if water suppression is used) can be shorter
            than usual, because of the relatively short Ha T1 (~0.7s). A
            relaxation delay of about 0.8s can usually be used without any
            problem.

Sensitivity : this experiment is a lot more sensitive then the HNCA or
              HN(CO)CA.  Less transients are necessary and since the spectral
              width in C=O is usually small, less increment in F2 (ni) are
              necessary.

-------------------------------------------------------------------------------

*/


#include <standard.h>
#include <math.h>

#define MIN_DELAY    0.2e-6        /* shortest executable delay */
#define SIMSH_START_DELAY 20.2e-6
#define SIMSH_STOP_DELAY 8.2e-6


static int
               phs1[8] = {0,0,0,0,2,2,2,2},
               phs2[1] = {0},
               phs3[16]= {0,0,0,0,0,0,0,0,2,2,2,2,2,2,2,2},
               phs4[8] = {1,1,1,1,3,3,3,3},
               phs5[2] = {0,2},
               phs6[4] = {0,0,2,2},
                rec[8] = {0,2,2,0,2,0,0,2};

static double
              d2_init = 0.0,
              d3_init = 0.0;


pulsesequence()
{
/* VARIABLE DECLARATION */
   char
              satmode[MAXSTR],
              sspul[MAXSTR],
              fad1[MAXSTR],
              fad2[MAXSTR],
              f1180[MAXSTR],
              f2180[MAXSTR],
              co180[MAXSTR],
              co90[MAXSTR];
   int
              phase,
              phase2,
              satmove,
              t1_counter,
              t2_counter,
              c13dev = DODEV,
              n15dev = DO2DEV;
   double
              ss,
              t1evol,
              t2evol_1,
              t2evol_2,
              sw1,
              sw2,
              ni,
              pwcalvl,
              pwca,
              satfrq,
              satdly,
              satpwr,
              inept,
              constT;


/* Load variables */
   satfrq = getval("satfrq");
```

```
   satdly = getval("satdly");
   satpwr = getval("satpwr");
   pwcalvl = getval("pwcalvl");
   pwca = getval("pwca");
   inept = getval("inept");
   constT = getval("constT");
   ss = getval("ss");
   sw1 = getval("sw1");
   sw2 = getval("sw2");
   ni = getval("ni");
   phase = (int) (getval("phase") + 0.5);
   phase2 = (int) (getval("phase2") + 0.5);

   getstr("co180", co180);
   getstr("co90", co90);
   getstr("sspul", sspul);
   getstr("fad1", fad1);
   getstr("fad2", fad2);
   getstr("satmode", satmode);
   getstr("f1180", f1180);
   getstr("f2180", f2180);


/* Load phase cycles */
   settable(t1, 8, phs1);
   settable(t2, 1, phs2);
   settable(t3, 16, phs3);
   settable(t4, 8, phs4);
   settable(t5, 2, phs5);
   settable(t6, 4, phs6);
   settable(t7, 8, rec);


/* Check conditions */
   satmove = ( fabs(tof - satfrq) >= 0.1 );

   if ( (dm2[A] == 'y') || (dm2[B] == 'y') || (dm2[D] == 'y')
            || (dm2[E] == 'y') )
   {
      text_error("'dm2' must be to 'nnnnn' or 'nnynn' for N15 decoupling\n");
      abort(1);
   }

   if ( (dm[A] == 'y') || (dm[B] == 'y') || (dm[C] == 'y')
            || (dm[D] == 'y') )
   {
      text_error("'dm' must be to 'nnnnn' or 'nnnny' for C13\n");
      abort(1);
   }

   if ( (constT) <= (.0001 + (ni/sw1)/2) )
   {  text_error("'constT' must be larger then '(ni/sw1)/2'");
      abort(1);
   }


/* Determine steady-state mode */
   if (ss < 0)
   {
      ss *= (-1);
      initval(ss, ssval);
      initval(ss, ssctr);
   }


/* Add in States-Haberkorn element */

   if (phase == 2)          /* Ca t1 element */
      tsadd(t2, 1, 4);

   if (phase2 == 2)         /* C=O t2 element */
      tsadd(t5, 1, 4);


/* Add in FAD */
   if (fad1[A] == 'y')             /* for Ca */
   {
      if (ix == 1)
```

```
        d2_init = d2;

      t1_counter = (int) ( (d2 - d2_init)*sw1 + 0.5 );
      if (t1_counter % 2)
      {
         tsadd(t2, 2, 4);  /* first Ca 90-degree pulse       */
         tsadd(t7, 2, 4);  /* receiver phase cycle           */
      }
   }

   if (fad2[A] == 'y')            /* for C=O */
   {
      if (ix == 1)
        d3_init = d3;

      t2_counter = (int) ( (d3 - d3_init)*sw2 + 0.5 );
      if (t2_counter % 2)
      {
         tsadd(t5, 2, 4);       /* first C=O 90-degree pulse   */
         tsadd(t7, 2, 4);       /* receiver phase cycle         */
      }
   }


/* BEGIN ACTUAL PULSE SEQUENCE CODE */
   status(A);
      rlpower(tpwr, TODEV);          /*   H1 hard-pulse power level    */
      rlpower(dpwr2, n15dev);        /*   N15 decoupling power level   */
      rlpower(pwcalvl, c13dev);      /*   Ca power level               */

      if (sspul[A] == 'y')
      {
         rgpulse(200*pw, zero, rof1, 0.0);
         rgpulse(200*pw, one, 0.0, rof2);
      }
         hsdelay(d1);

/* selective saturation period */
      if (satmode[A] == 'y')
      {
         if (satmove)
            offset(satfrq, TODEV);

         rlpower(satpwr, TODEV);
         rgpulse(satdly, zero, 4.0e-5, 0.2e-6);
         if (satmove)
            offset(tof, TODEV);

         rlpower(tpwr, TODEV);
         delay(1.0e-5);
      }


/* Pulse train */
   status(B);
      rcvroff();

      rgpulse(pw, zero, rof1, 0.0);
      decphase(t1);              /* Ca phase  */
      delay(inept);

      simpulse(2*pw,2*pwca, zero,t1, 0.0, 0.0);
      txphase(one);              /* H1 phase  */
      decphase(t2);
      delay(inept);

      simpulse(pw,pwca, one,t2, 0.0,0.0);
      txphase(zero);
      decphase(t3);

      t1evol = d2;                /* Ca is governed by n1 and sw */
      if (f1180[0] == 'y')
         t1evol += 0.5/sw1;


   status(C);
      delay(constT - t1evol/2  - WFG_START_DELAY);
      simpulse(2*pw,2*pwca, zero,t3, 0.0, 0.0);
```

```
      decphase(zero);
      decshaped_pulse(co180, 2*pwca, zero, 0.0,0.0);
      decphase(t4);
      delay(constT + t1evol/2 - WFG_STOP_DELAY - WFG_START_DELAY);
      decrgpulse(pwca, t4, 0.0,0.0);
      decphase(t5);
      decshaped_pulse(co90, pwca, t5, 0.0,0.0);
      decphase(t3);

      t2evol_1 = t2evol_2 = d3/2; /* C=O is governed by ni2 and sw2 */
      if (f1180[0] == 'y')
      {
         t2evol_1 += 0.25/sw2;
         t2evol_2 += 0.25/sw2;
      }

      if ((t2evol_1 > MIN_DELAY) || (t2evol_2 > MIN_DELAY))
      {
         t2evol_1 -= pwca/2 + pwca + WFG_STOP_DELAY ;
         t2evol_2 -= pwca/2 + pwca + WFG_START_DELAY ;

         if (t2evol_1 < MIN_DELAY)
            t2evol_1 = 0.0;
         if (t2evol_2 < MIN_DELAY)
            t2evol_2 = 0.0;
      }

      delay(t2evol_1);

      simpulse(2*pw,2*pwca, zero,t3, 0.0,0.0);
      decphase(t6);
      delay(t2evol_2);

   status(D);
      decshaped_pulse(co90,pwca, t6, 0.0,0.0);
      decphase(one);
      decrgpulse(pwca, one, 0.0,0.0);
      delay(constT - WFG_STOP_DELAY - WFG_START_DELAY);
      decphase(zero);
      decshaped_pulse(co180,2*pwca, zero, 0.0,0.0);
      decrgpulse(2*pwca, zero, 0.0,0.0);
      delay(constT -  WFG_STOP_DELAY);
      simpulse(pw,pwca, zero,zero, 0.0,0.0);
      delay(inept);
      simpulse(2*pw,2*pwca, zero,zero, 0.0,0.0);

      rlpower( ((n15dev == DODEV) ? dpwr : dpwr2), n15dev);
      rlpower( ((c13dev == DODEV) ? dpwr : dpwr2), c13dev);
      delay(rof2);
      rcvron();
      delay(inept - rof2 - 2*POWER_DELAY);


   status(E);
      setreceiver(t7);
}
```

5. ^{15}N-edited NOESY HMQC.

```
/* nosyhmqc3rf3d -  NOESY-HMQC 3D sequence
                - written in hypercomplex phase sensitive mode only
       uses the 2nd decoupler for the X pulses

  Sequence:

  NOESY-HMQC:

  status :    A-|-B|----C-----|-----------D-----------------|-E--
     1H  :    90-t1-90-mix-90-1/2J-         180         -1/2J- Acq (t3)
      X  :       BB                 90-t2/2-    -t2/2-90        BB
 phtable :    t1     t3      t3       t2        t3       t3       t4 or t5

  Parameters:

       d2 = First evolution time
       d3 = Second evolution time
      mix = NOESY mixing time.
   pwx2lvl = power level for X pulses
   pwx2    = 90 degree X pulse
   jxh     = X-H coupling constant
   dpwr2   = power level for X decoupling
   tpwr    = power level for H pulses
   pw      = 90 degree H pulse
    phase =   1,2: gives HYPERCOMPLEX (t1) acquisition;
    ni    = number of t1 increments
    phase2=   1,2: gives HYPERCOMPLEX (t2) acquisition;
    ni2   = number of t2 increments
   satflg  = flag to do xmtr presaturation at satfrq and satpwr
             during relaxation (satdly) and mixing (mix) periods
   satfrq  = saturation frequency for xmtr presaturation
   satpwr  = saturation power for xmtr presaturation
   satdly  = saturation period follows D1
   sspul = 'y': selects for saturation sequence at start of pulse sequence
   nosyflg= 'n': turns off NOESY part of the sequence
   hmqcflg= 'n': turns off HMQC part of the sequence

  Plane processing:

     array = phase2,phase

        np x ni  :  wft2d('ni',#i,1,0,0,0,0,0,0,0,0,0,-1,0,0,0,0,0)
        np x ni2 : wft2d('ni2',#i,1,0,0,0,0,0,0,0,0,0,0,-1,0,0,0)

     array = phase,phase2

        np xni   :  wft2d('ni',#i,1,0,0,0,0,0,0,0,0,0,0,0,-1,0,0,0)
        np x ni2 : wft2d('ni2',#i,1,0,0,0,0,0,0,0,0,0,0,-1,0,0,0,0,0)

  phase table:

        t1 = 0 2 0 2 1 3 1 3  - first proton pulse
        t2 = 0 0 2 2 1 1 3 3  - first carbon pulse
        t3 = 0 0 0 0 1 1 1 1  - all other pulses
        t4 = 0 2 2 0 1 3 3 1  - receiver
        t5 = 0 2 0 2 1 3 1 3  - receiver if hmqcflg='n'

             Feb 07 1991     (vvk)
    revised: March 01, 1991 (vvk)  June 14, 1991(gg)
                            Sept 29, 1991 (bds/cms) to correct satflg[C] */


#include <standard.h>

pulsesequence()
{
   double          satpwr,
                   satdly,
                   satfrq,
                   mix,
                   jxh,
                   pwx2lvl,
                   pwx2,
```

```
                tau;
   int          phase2,
                phase;
   char         sspul[MAXSTR],
                satflg[MAXSTR],
                nosyflg[MAXSTR],
                hmqcflg[MAXSTR];

/* LOAD VARIABLES */
   satdly = getval('satdly');
   satfrq = getval('satfrq');
   satpwr = getval('satpwr');
   mix = getval('mix');
   pwx2lvl = getval('pwx2lvl');
   pwx2 = getval('pwx2');
   jxh = getval('jxh');
   tau = 1/(2.0*jxh);
   phase = (int) (getval('phase') + 0.5);
   phase2 = (int) (getval('phase2') + 0.5);
   getstr('sspul', sspul);
   getstr('satflg',satflg);
   getstr('nosyflg',nosyflg);
   getstr('hmqcflg',hmqcflg);


   initval(pwx2lvl,v6);
   initval(dpwr2,v7);
   initval(tpwr,v8);
   initval(satpwr,v9);


/* CHECK CONDITIONS */


/* DETERMINE STEADY-STATE MODE */


/* STEADY-STATE PHASECYCLING

/* PHASECYCLE */

   loadtable('nosyhmqc3d');     /* t1 = 0 2 0 2 1 3 1 3
                                   t2 = 0 0 2 2 1 1 3 3
                                   t3 = 0 0 0 0 1 1 1 1
                                   t4 = 0 2 2 0 1 3 3 1
                                   t5 = 0 2 0 2 1 3 1 3      */

   getelem(t1,ct,v1);
   getelem(t2,ct,v2);

   if (hmqcflg[A] == 'n')
    getelem(t5,ct,oph);
   else
    getelem(t4,ct,oph);

   initval(2.0*(double)(((int)(d2*getval('sw1')+0.5)%2)),v13);
   initval(2.0*(double)(((int)(d3*getval('sw2')+0.5)%2)),v14);

     if (phase == 2)
        incr(v1);
     if (phase2 == 2)
        incr(v2);
     add(v1,v13,v1);
     add(v2,v14,v2);

   add(oph,v13,oph);
   add(oph,v14,oph);


/* BEGIN THE ACTUAL PULSE SEQUENCE */
   status(A);                /* relaxation status */
   power(v8,TODEV);
   power(v7,DO2DEV);
   dec2phase(zero);
   if (sspul[A] == 'y')
   {
      rgpulse(pw*200, zero, rof1,rof2);
```

```
      rgpulse(pw*200, one, rof1,rof2);
   }
   else
      hsdelay(d1);

   if (satflg[A] == 'y')
     {
        if (satfrq != tof)
         offset(satfrq,TODEV);
        power(v9,TODEV);
        rgpulse(satdly,zero,rof1,rof1);
        power(v8,TODEV);
        if (satfrq != tof)
          offset(tof,TODEV);
        delay(40.0e-6);
     }
   else
     delay(satdly);

     if (nosyflg[A] != 'n')
      {
       rgpulse(pw, v1, rof1, 1.0e-6);

   status(B);
         if (d2>0)
          delay(d2 - rof1 - 1.0e-6 - (4*pw/3.1416));
         else delay(d2);

    status(C);
       rgpulse(pw, t3, rof1, 1.0e-6);
       if (satflg[C] == 'y')
        {
          if (satfrq != tof)
           offset(satfrq,TODEV);
          power(v9,TODEV);
          rgpulse(mix,zero,2.0e-6,rof1);
          power(v8,TODEV);
          if (satfrq != tof)
           offset(tof,TODEV);
          delay(40.0e-6);
        }
        else
         hsdelay(mix);
     status(D);
         power(v6,DO2DEV);
        rgpulse(pw, t3, rof1, 0.0);
       }
      else
       rgpulse(pw, v1, rof1, 0.0);


      if (hmqcflg[A] != 'n')
       {
        rcvroff();
        delay(tau - 0.5*pw - 0.5*pwx2 - rof1);
        txphase(t3);
        dec2rgpulse(pwx2,v2,rof1,0.0);
         dec2phase(t3);
         delay(d3/2.0);
        rgpulse(2.0*pw, t3, 0.0, 0.0);
         dec2phase(t3);
         delay(d3/2.0);
        dec2rgpulse(pwx2,t3,0.0,rof1);
        rcvron();
        delay(tau - 4.2e-6 - 0.5*pwx2 - rof1);
       }
      power(v7,DO2DEV);
      delay(rof2);

    status(E);                                    /* acquisition status */
}
```

6. ^{15}N-edited TOCSY HMQC.

```
/* tocsyhmqc3d3rf -  TOCSY-HMQC 3D sequence
                  - written in hypercomplex phase sensitive mode only
                  - uses the 2nd decoupler for the X pulses
                  - modified from nosyhmqc3d3rf by smg/bds Feb. 20 1992
                  - last revised Feb. 24 1992 by smg
  Sequence:

  TOCSY-HMQC:

  status :     A-|--B--|---C----|--------------D--------------|----E----
     1H  :       -90-t1-spinlock-1/2J-         180         -1/2J- Acq (t3)
      X  :         BB     BB           90-t2/2-    -t2/2-90          BB
 phtable :        t1       t5          t2        t3       t3          t4

  Parameters:

         d2 = First evolution time (TOCSY)
         d3 = Second evolution time (HMQC)
     pwx2lvl = power level for X pulses
        pwx2 = 90 degree X pulse
         jxh = X-H coupling constant
       dpwr2 = power level for X decoupling
        tpwr = power level for H pulses
          pw = 90 degree H pulse at power tpwr
       phase = 1,2: gives HYPERCOMPLEX (t1) acquisition;
          ni = number of t1 increments
      phase2 = 1,2: gives HYPERCOMPLEX (t2) acquisition;
         ni2 = number of t2 increments
      satflg = flag to do xmtr presaturation at satfrq and satpwr
               during relaxation (satdly)
      satfrq = saturation frequency for xmtr presaturation
      satpwr = saturation power for xmtr presaturation
      satdly = saturation period follows D1
       p1lvl = power level for spinlock
          p1 = 90 degree H pulse for mlev17
         mix = TOCSY mixing time
        trim = trim pulse preceeding mlev17
          hs = 'yn': homospoil pulse (hst) during the d1 relaxation delay
    wdwfctr = multiplication "window" factor of p1


  Plane processing:

     array = phase2,phase

        np x ni  :  wft2d('ni',#i,1,0,0,0,0,0,0,0,0,0,-1,0,0,0,0,0)
        np x ni2 : wft2d('ni2',#i,1,0,0,0,0,0,0,0,0,0,0,-1,0,0,0)

     array = phase,phase2

        np xni   :  wft2d('ni',#i,1,0,0,0,0,0,0,0,0,0,0,0,-1,0,0,0)
        np x ni2 : wft2d('ni2',#i,1,0,0,0,0,0,0,0,0,0,0,-1,0,0,0,0)

  phase table:

        t1 = 0 0 1 1           - first proton pulse
        t2 = 0 2 1 3           - first nitrogen pulse
        t3 = 0 0 1 1           - 180 and second nitrogen pulse
        t4 = 0 2 1 3           - receiver
        t5 = 0 0 1 1 2 2 3 3   - spinlock

                 modified by smg/bds 20 Feb 92 */

#include <standard.h>

mleva()
{
   double wdwfctr,window;
   wdwfctr=getval("wdwfctr");
   window = (wdwfctr*p1);
   rgpulse(p1,v3,0.0,window);
   rgpulse(2*p1,v4,0.0,window);
   rgpulse(p1,v3,0.0,0.0);
}
```

```
mlevb()
{
   double wdwfctr,window;
   wdwfctr=getval('wdwfctr');
   window = (wdwfctr*p1);
   rgpulse(p1,v5,0.0,window);
   rgpulse(2*p1,v12,0.0,window);
   rgpulse(p1,v5,0.0,0.0);
}


pulsesequence()
{
   double          satpwr,
                   satdly,
                   satfrq,
                   mix,
                   jxh,
                   pwx2lvl,
                   pwx2,
                   cycles,
                   trim,
                   wdwfctr,
                   window,
                   p1lvl,
                   tau;
       int        phase,
                   phase2;
       char       satflg[MAXSTR];

/* LOAD VARIABLES */
   satdly  = getval('satdly');
   satfrq  = getval('satfrq');
   satpwr  = getval('satpwr');
   p1lvl   = getval('p1lvl');
   mix     = getval('mix');
   trim    = getval('trim');
   wdwfctr = getval('wdwfctr');
   window  = (wdwfctr*p1);
   pwx2lvl = getval('pwx2lvl');
   pwx2    = getval('pwx2');
   jxh     = getval('jxh');
   tau     = 1/(2.0*jxh);
   phase   = (int) (getval('phase') + 0.5);
   phase2  = (int) (getval('phase2') + 0.5);
   getstr('satflg',satflg);


   initval(pwx2lvl,v6);
   initval(dpwr2,v7);
   initval(tpwr,v8);
   initval(satpwr,v9);
   initval(p1lvl,v10);


/* CHECK CONDITIONS */
   if ((p1lvl-tpwr) >=0)
       {
         printf('tpwr is for H hard pulse. \ n');
          abort(1);
       }

/* DETERMINE STEADY-STATE MODE */


/* STEADY-STATE PHASECYCLING

/* PHASECYCLE */

   loadtable('toxyhmqc3d');     /* t1 = 0 0 1 1
                                   t2 = 0 2 1 3
                                   t3 = 0 0 1 1
                                   t4 = 0 2 1 3
                                   t5 = 0 0 1 1 2 2 3 3
                                */
```

```
    getelem(t1,ct,v1);
    getelem(t2,ct,v2);
    getelem(t4,ct,oph);
    getelem(t5,ct,v3);

    initval(2.0*(double)(((int)(d2*getval("sw1")+0.5)%2)),v13);
    initval(2.0*(double)(((int)(d3*getval("sw2")+0.5)%2)),v14);

    if (phase == 2)
         incr(v1);
    if (phase2 == 2)
         incr(v2);

    add(v1,v13,v1);
    add(v2,v14,v2);

    add(one,v3,v4);
    add(one,v4,v5);
    add(one,v5,v12);

    add(oph,v13,oph);
    add(oph,v14,oph);


/* BEGIN THE ACTUAL PULSE SEQUENCE */
   status(A);                                  /* preparation period */
    power(v8,TODEV);
    power(v7,DO2DEV);
    dec2phase(zero);
    hsdelay(d1);

    if (satflg[A] == 'y')
    {
       if (satfrq != tof)
         offset(satfrq,TODEV);
       power(v9,TODEV);
       rgpulse(satdly,zero,rof1,rof1);
       power(v8,TODEV);
       if (satfrq != tof)
         offset(tof,TODEV);
       delay(40.0e-6);
    }
    else
      delay(satdly);

  status(B);                                   /* t1 evolution period */
    rgpulse(pw, v1, rof1, 1.0e-6);
    power(v10,TODEV);
    rcvroff();

    txphase(v4);
    if (d2>0)
      delay(d2 - 1.0e-6 -5.0e-6 -(2*pw/3.1416));
    else delay(d2);

  status(C);                                   /* TOCSY mixing period */
    /* calculate and initialize loop counter */

       cycles = (mix-trim)/(64.66*p1+32*window);
       cycles=2.0*(double)(int)(cycles/2.0);
       initval(cycles,v11);
       if (cycles > 1.0)
        {
          rgpulse(trim,v4,5.0e-6,0.0);
         starthardloop(v11);
               mleva(); mlevb(); mlevb(); mleva();
               mlevb(); mlevb(); mleva(); mleva();
               mlevb(); mleva(); mleva(); mlevb();
               mleva(); mleva(); mlevb(); mlevb();
               rgpulse(0.66*p1,v4,0.0,0.0);
         endhardloop();
        }

  status(D);                                  /* HMQC and t2 evolution period */
    power(v8,TODEV);
    power(v6,DO2DEV);
    rcvroff();
```

```
    delay(tau - 0.5*pwx2 - rof1);
    txphase(t3);
    dec2rgpulse(pwx2,v2,rof1,0.0);
    dec2phase(t3);
    delay(d3/2.0);
    rgpulse(2.0*pw, t3, 0.0, 0.0);
    dec2phase(t3);
    delay(d3/2.0);
    dec2rgpulse(pwx2,t3,0.0,rof1);
    rcvron();
    delay(tau - 4.2e-6 - 0.5*pwx2 - rof1);
    power(v7,DO2DEV);
    delay(rof2);

  status(E);                          /* acquisition status */
}
```

7. ^{13}C-edited NOESY HMQC.

```
/* nosyhmqc3d -  NOESY-HMQC 3D sequence
                 Will do standard HMQC, standard NOESY, or NOESY-HMQC 3D
                 - written in hypercomplex phase sensitive mode only


  Sequence:

  NOESY-HMQC:
  status :    A-|-B|----C-----|-------D----------------------|-E----
     1H  :    90-t1-90-mix-90-1/2J-         180         -1/2J- Acq (t3)
      X  :       BB                 90-t2/2-    -t2/2-90        BB
   phase :    t1     t3      t3       t2        t3       t3       t4 or t5

  Parameters:

        d2 = First evolution time
        d3 = Second evolution time
       mix = NOESY mixing time.
    pwxlvl = power level for X pulses
    pwx    = 90 degree X pulse
    jxh    = X-H coupling constant
    dpwr   = power level for X decoupling
    tpwr   = power level for H pulses
    pw     = 90 degree H pulse
     phase =   1,2: gives HYPERCOMPLEX (t1) acquisition;
     ni    = number of t1 increments
     phase2=   1,2: gives HYPERCOMPLEX (t2) acquisition;
     ni2   = number of t2 increments

    satflg  = flag to do xtmr presaturation at satfrq and satpwr
              during relaxation(satdly) and mixing(mix) periods [ynyn]
    satfrq  = saturation frequency for xmtr presaturation
    satpwr  = saturation power for xmtr presaturation
    satdly  = saturation period follows d1
    sspul = 'y': selects for HS-90-HS sequence at start of pulse sequence
    nosyflg= 'n': turns off NOESY part of the sequence (std HMQC with the current
                                                        phase cycling)
    hmqcflg= 'n': turns off HMQC part of the sequence (std NOESY with only 2-step
                                                       phase cycling)
plane processing:

      array = phase2,phase

        np x ni  :   wft2d('ni',#i,1,0,0,0,0,0,0,0,0,0,0,-1,0,0,0,0,0)
        np x ni2 :  wft2d('ni2',#i,1,0,0,0,0,0,0,0,0,0,0,0,-1,0,0,0)

 array = phase, phase2

      np x ni  :  wft2d('ni',#i,1,0,0,0,0,0,0,0,0,0,0,0,-1,0,0,0)
   np x ni2 : wft2d('ni2',#i,1,0,0,0,0,0,0,0,0,0,0,-1,0,0,0,0,0)

 phase table:

        t1 = 0 2 0 2 1 3 1 3    - first H pulse
        t2 = 0 0 2 2 1 1 3 3    - first X pulse
        t3 = 0 0 0 0 1 1 1 1    - all other pulses
        t4 = 0 2 2 0 1 3 3 1    - receiver
        t5 = 0 2 0 2 1 3 1 3    - receiver if hmqcflg ='n'

             Feb 07 1991    (vvk)
   revised:  March 01, 1991 (vvk) typed in bds 4 April 91

      revised: November 05, 1992 by S. Gagne ( change status C to
             mixing time only)

      revised: May 02, 1993 by S. Gagne  :   change HMQC part to be
             like 2D hmqc (so now uses decon/decoff... during HMQC
             portion).  See 13C excitation profile in 'Pulse Sequence
             Notes' p. 7-8.


             */
```

```
#include <standard.h>

pulsesequence()
{
   double          satpwr,
                   satdly,
                   satfrq,
                   mix,
                   jxh,
                   pwxlvl,
                   pwx,
                   tau;
   int             phase2,
                   phase;
   char            sspul[MAXSTR],
                   satflg[MAXSTR],
                   nosyflg[MAXSTR],
                   hmqcflg[MAXSTR];

/* LOAD VARIABLES */
   satdly = getval("satdly");
   satfrq = getval("satfrq");
   satpwr = getval("satpwr");
   mix = getval("mix");
   pwxlvl = getval("pwxlvl");
   pwx = getval("pwx");
   jxh = getval("jxh");
   tau = 1/(2.0*jxh);
   phase = (int) (getval("phase") + 0.5);
   phase2 = (int) (getval("phase2") + 0.5);
   getstr("sspul", sspul);
   getstr("satflg",satflg);
   getstr("nosyflg",nosyflg);
   getstr("hmqcflg",hmqcflg);


   initval(pwxlvl,v6);
   initval(dpwr,v7);
   initval(tpwr,v8);
   initval(satpwr,v9);


/* CHECK CONDITIONS */


/* DETERMINE STEADY-STATE MODE */


/* STEADY-STATE PHASECYCLING

/* PHASECYCLE */

   loadtable("nosyhmqc3d");

   getelem(t1,ct,v1);
   getelem(t2,ct,v2);

   if (hmqcflg[A] == 'n')
    getelem(t5,ct,oph);
   else
    getelem(t4,ct,oph);

   initval(2.0*(double)(((int)(d2*getval("sw1")+0.5)%2)),v13);
   initval(2.0*(double)(((int)(d3*getval("sw2")+0.5)%2)),v14);

     if (phase == 2)
        incr(v1);
     if (phase2 == 2)
        incr(v2);
     add(v1,v13,v1);
     add(v2,v14,v2);

   add(oph,v13,oph);
   add(oph,v14,oph);


/* BEGIN THE ACTUAL PULSE SEQUENCE */
```

```
status(A);                  /* relaxation status */
power(v8,TODEV);
power(v7,DODEV);
decphase(zero);
if (sspul[A] == 'y')
{
   hsdelay(hst + 0.001);
   rgpulse(pw, zero, rof1,rof2);
   hsdelay(hst+d1);
}
else
   hsdelay(d1);

if (satflg[A] == 'y')
  {
     if (satfrq != tof)
      offset(satfrq,TODEV);
     power(v9,TODEV);
     rgpulse(satdly,zero,rof1,rof1);
     power(v8,TODEV);
     if (satfrq != tof)
       offset(tof,TODEV);
     delay(40.0e-6);
  }
else
  delay(satdly);

  if (nosyflg[A] != 'n')
   {
    rgpulse(pw, v1, rof1, 1.0e-6);

status(B);
      if (d2>0)
       delay(d2 - rof1 - 1.0e-6 - (4*pw/3.1416));
      else delay(d2);


 status(C);
    rgpulse(pw, t3, rof1, 1.0e-6);
    if (satflg[C] == 'y')
     {
       if (satfrq != tof)
        offset(satfrq,TODEV);
       power(v9,TODEV);
       rgpulse(mix,zero,2.0e-6,rof1);
       power(v8,TODEV);
       if (satfrq != tof)
        offset(tof,TODEV);
       delay(40.0e-6);
      }
     else
      hsdelay(mix);
   status(D);
      power(v6,DODEV);
     rgpulse(pw, t3, rof1, 0.0);
    }
   else
    rgpulse(pw, v1, rof1, 0.0);


   if (hmqcflg[A] != 'n')
  {
     rcvroff();
     txphase(t3);
          decphase(v2);
    delay(tau - 0.5*pw - 0.5*pwx - rof1);
   if (d3 <= 2*pw)           /* allows 1H 180 to occur during */
   {                  /* t1 evolution period */
     delay(rof1);
     if (pwx >= (pw - 0.5e-6))
     {
        decon();
        delay(pwx - (2*pw - d3)/2);
        xmtron();
        delay(pw - d3/2);
        decoff();
        decphase(t3);
        delay(d3);
```

```
            decon();
            delay(pw - d3/2);
            xmtroff();
            delay(pwx - (2*pw - d3)/2);
            decoff();
         }
         else
         {
            xmtron();
            delay((2*pw - d3)/2 - pwx);
            decon();
            delay(pwx);
            decoff();
            decphase(t3);
            delay(d3);
            decon();
            delay(pwx);
            decoff();
            delay((2*pw - d3)/2 - pwx);
            xmtroff();
         }
      }
      else
      {

        decrgpulse(pwx,v2,rof1,0.0);
         delay(d3/2.0 - pw + 0.5e-6);
         decphase(t3);
        rgpulse(2.0*pw, t3, 0.0, 0.0);
         delay(d3/2.0 - pw + 0.5e-6);
        decrgpulse(pwx,t3,0.0,0.0);
         }
        rcvron();
              delay(rof2);
       power(v7,DODEV);
        delay(tau - 4.2e-6 - 0.5*pwx - rof2);
      }

   status(E);                                    /* acquisition status */
}
```

APPENDIX B

ASSIGNMENTS

```
1 ALA
CA              51.760
HA               4.140
CB              19.300
HB#              1.560
C              174.200
; 0.0
2 SER
CA              58.310
HA               4.520
CB              63.800
HB#              3.880
C              173.900
; 0.0
3 MET
#N
#HN
CA              55.950
HA               4.640
#CB
#HB1
#HB2
#CG
#HG1
#HG2
CE              16.600
HE#              2.070
C              176.600
; 0.0
4 THR
N              116.090
HN               8.013
CA              61.085
HA               4.43·
CB              70.400
HB               4.652
CG2             21.310
HG2#             1.176
C              175.000
; 0.0
5 ASP
N              123.048
HN               8.689
CA              57.323
HA               4.443
CB              40.195
HB1              2.627
HB2              2.733
CG             179.800
C              178.700
; 0.0
6 GLN
N              120.857
HN               8.869
CA              58.810
HA               4.066
CB              30.575
HB1              2.050
HB2              2.166
CG              35.403
HG1              2.345
HG2              2.500
CD             180.300
NE2            112.861
HE21             7.088
HE22             7.292
C              179.100
; 0.0
7 GLN
N              123.005
HN               7.830
CA              58.260
HA               3.927
#CB
HB1              2.080
HB2              2.170
CG              33.600
HG#              2.420
CD             180.300
NE2            112.676
HE21             7.238
HE22             7.552
C              177.800
; 0.0
8 ALA
N              124.412
HN               8.502
CA              54.890
HA               4.137
CB              17.930
HB#              1.480
C              181.100
; 0.0
9 GLU
N              120.466
HN               8.130
CA              58.800
HA               4.043
CB              29.800
HB#              2.070
#CG
HG1              2.190
HG2              2.380
CD             180.000
C              178.800
; 0.0
10 ALA
N              124.523
HN               7.918
CA              55.467
HA               4.112
CB              18.007
HB#              1.405
C              179.200
; 0.0
11 ARG
N              116.476
HN               7.965
CA              59.390
HA               3.850
CB              29.980
HB#              1.820
CG              26.370
HG1              1.660
```

```
HG2              1.720
CD              43.100
HD#              3.240
#NE
#HE
#NH1
#HH11
#HH12
#NH2
#HH21
#HH22
C              178.000
; 0.0
12 ALA
N              120.407
HN               7.687
CA              53.670
HA               4.230
CB              18.500
HB#              1.460
C              178.600
; 0.0
13 PHE
N              119.369
HN               7.685
CA              59.243
HA               4.383
CB              41.017
HB1              3.225
HB2              3.280
#CD#
#HD#             7.270
HD1              7.270
HD2              7.270
#CE#
#HE#             7.380
HE1              7.380
HE2              7.380
#CZ
#HZ
C              175.700
; 0.0
14 LEU
N              119.357
HN               7.366
CA              53.588
HA               4.498
CB              44.700
HB1              1.508
HB2              1.932
CG              26.490
HG               2.106
CD1             28.310
HD1#             0.925
CD2             24.542
HD2#             1.126
C              176.000
; 0.0
15 SER
N              117.230
HN               7.832
CA              56.340
HA               4.586
CB              65.378
HB1              4.036
HB2              4.424
C              175.000
; 0.0
16 GLU
N              122.712
HN               9.048
CA              60.087
HA               3.973
CB              29.200
HB1              2.035
HB2              2.070
CG              36.780
HG1              2.353
HG2              2.413
CD             183.700
C              179.600
; 0.0
17 GLU
N              120.911
HN               8.887
CA              60.227
HA               4.072
CB              28.833
HB1              1.942
HB2              2.047
CG              36.700
HG1              2.295
HG2              2.370
CD             184.400
C              179.100
; 0.0
18 MET
N              121.593
HN               7.730
CA              58.345
HA               4.034
CB              33.162
HB1              1.852
HB2              2.113
CG              32.673
HG1              2.413
HG2              2.468
CE              17.340
HE#              2.030
C              178.100
; 0.0
19 ILE
N              121.192
HN               8.243
CA              66.778
HA               3.717
CB              37.744
HB               1.994
CG1             29.100
HG11             1.045
HG12             1.700
CD1             13.400
HD1#             0.920
CG2             17.453
HG2#             1.206
C              177.600
; 0.0
20 ALA
N              122.221
HN               7.842
CA              55.120
HA               4.193
CB              17.700
HB#              1.510
C              181.300
; 0.0
21 GLU
N              122.218
HN               7.769
CA              59.150
HA               4.140
CB              29.200
HB1              1.965
HB2              2.050
CG              36.100
HG1              2.180
HG2              2.410
CD             183.700
C              180.300
; 0.0
22 PHE
N              121.178
HN               8.720
CA              58.800
HA               5.027
CB              37.660
```

```
HB#              3.510
#CD#
#HD#               7.200
HD1              7.190
HD2              7.190
#CE#
#HE#               7.340
HE1              7.340
HE2              7.340
#CZ
#HZ
C              178.500
; 0.0
23 LYS
N              125.141
HN               9.240
CA              58.280
HA               3.953
CB              31.315
HB#              1.992
CG              24.130
HG#              1.091
CD              26.754
HD1              0.185
HD2              1.371
CE              42.003
HE#              2.605
C              177.200
; 0.0
24 ALA
N              122.246
HN               7.570
CA              54.910
HA               4.190
CB              17.700
HB#              1.505
C              180.700
; 0.0
25 ALA
N              122.034
HN               7.572
CA              55.050
HA               3.980
CB              18.422
HB#              1.724
C              177.900
; 0.0
26 PHE
N              121.157
HN               8.882
CA              62.218
HA               3.170
CB              39.600
HB#              2.740
#CD#
#HD#               6.680
HD1              6.680
HD2              6.680
#CE1
#HE#               7.100
HE1              7.100
HE2              7.100
#CZ
#HZ
C              176.600
; 0.0
27 ASP
N              118.589
HN               8.571
CA              56.900
HA               4.186
CB              40.005
HB1              2.613
HB2              2.670
CG             179.800
C              177.800
; 0.0
28 MET
N              120.330
HN               7.305
CA              57.880
HA               4.055
CB              32.007
HB1              2.058
HB2              2.158
CG              33.030
HG1              2.408
HG2              2.625
CE              17.527
HE#              1.962
C              177.900
; 0.0
29 PHE
N              119.395
HN               7.777
CA              58.213
HA               4.304
CB              38.930
HB1              2.768
HB2              2.897
#CD#
#HD#               7.160
HD1              7.170
HD2              7.170
#CE#
#HE#
#CZ
#HZ
C              177.700
; 0.0
30 ASP
N              119.737
HN               8.084
CA              52.053
HA               4.504
CB              38.748
HB1              1.462
HB2              2.469
CG             178.800
C              176.700
; 0.0
31 ALA
N              130.390
HN               7.682
CA              54.985
HA               4.110
CB              19.330
HB#              1.534
C              179.100
; 0.0
32 ASP
N              114.340
HN               8.193
CA              52.727
HA               4.592
CB              40.000
HB1              2.732
HB2              3.110
CG             181.800
C              177.800
; 0.0
33 GLY
N              111.810
HN               8.020
CA              46.700
HA#              3.850
C              175.700
; 0.0
34 GLY
N              109.600
HN               8.137
CA              46.300
HA1              3.980
HA2              4.090
C              175.900
; 0.0
```

```
35 GLY
N              113.800
HN               10.685
CA               45.255
HA1               3.673
HA2               4.475
C               173.200
; 0.0
36 ASP
N              116.198
HN               7.750
CA              52.568
HA               5.175
CB              41.385
HB1              3.053
HB2              2.262
CG             179.400
C              173.100
; 0.0
37 ILE
N              125.902
HN               9.613
CA              60.082
HA               4.942
CB              39.935
HB               1.821
CG1             26.997
HG1#             1.200
CD1             14.739
HD1#             0.475
CG2             17.555
HG2#             0.941
C              175.700
; 0.0
38 SER
N              124.028
HN               8.696
CA              55.672
HA               4.848
CB              66.547
HB1              3.990
HB2              4.490
C              175.900
; 0.0
39 THR
N              115.113
HN               9.216
CA              66.900
HA               3.822
CB              68.243
HB               4.200
CG2             23.170
HG2#             1.370
C              177.000
; 0.0
40 LYS
N              122.682
HN               7.840
CA              59.257
HA               4.120
CB              32.630
HB1              1.775
HB2              1.923
CG              24.743
HG1              1.407
HG2              1.500
CD              29.235
HD#              1.683
CE              42.013
HE#              2.995
C              179.700
; 0.0
41 GLU
N              122.287
HN               7.698
CA              58.795
HA               4.130
#CB
#HB1
#HB2
CG              35.800
HG#              2.473
CD             180.000
C              179.700
; 0.0
42 LEU
N              122.373
HN               8.519
CA              57.820
HA               3.990
CB              42.894
HB1              1.607
HB2              1.762
CG              26.525
HG               1.630
CD1             25.520
HD1#             0.821
CD2             24.130
HD2#             0.840
C              178.700
; 0.0
43 GLY
N              107.127
HN               8.584
CA              47.795
HA1              3.592
HA2              3.975
C              175.500
; 0.0
44 THR
N              119.744
HN               7.942
CA              67.195
HA               3.935
CB              69.040
HB               4.351
CG2             21.675
HG2#             1.323
C              176.300
; 0.0
45 VAL
N              121.999
HN               7.298
CA              66.310
HA               3.687
CB              31.360
HB               1.993
CG1             22.200
HG1#             0.815
CG2             21.200
HG2#             0.673
C              177.500
; 0.0
46 MET
N              117.661
HN               8.006
CA              59.364
HA               3.910
CB              32.070
HB1              1.818
HB2              2.068
CG              33.881
HG1              2.435
HG2              2.636
CE              17.527
HE#              1.932
C              178.800
; 0.0
47 ARG
N              120.507
HN               8.218
CA              58.900
HA               4.643
CB              30.100
HB1              1.930
HB2              1.990
```

```
CG              28.497
HG1              1.810
HG2              1.910
CD              43.200
HD#              3.246
NE              86.000
HE               7.430
#NH1
#HH11
#HH12
#NH2
#HH21
#HH22
C              181.000
; 0.0
48 MET
N              122.785
HN               7.940
CA              58.803
HA               4.221
CB              32.636
HB1              2.324
HB2              2.538
CG              32.986
HG1              2.702
HG2              2.935
CE              17.515
HE#              2.152
C              175.600
; 0.0
49 LEU
#N
HN               7.190
CA              53.585
HA               4.342
#CB
HB#              1.800
#CG
HG               1.800
CD1             22.340
HD1#             0.628
CD2             26.025
HD2#             0.727
C              176.900
; 0.0
50 GLY
N              106.865
HN               7.750
CA              45.657
HA1              3.704
HA2              4.115
C              174.600
; 0.0
51 GLN
N              119.405
HN               7.953
CA              53.850
HA               4.426
CB              30.593
HB1              1.646
HB2              2.130
CG              33.612
HG1              2.125
HG2              2.193
CD             180.000
NE2            113.610
HE21             7.000
HE22             7.300
C              174.300
; 0.0
52 ASN
N              118.036
HN               8.661
CA              50.952
HA               5.136
CB              39.240
HB1              2.530
HB2              2.779
CG             178.100
ND2            113.622
HD21             6.770
HD22             7.520
C              172.100
; 0.0
53 PRO
#N
CA              62.553
HA               4.744
CB              32.058
HB1              1.930
HB2              2.231
#CG
HG#              1.990
CD              49.925
HD1              3.240
HD2              3.649
C              177.800
; 0.0
54 THR
N              114.323
HN               8.600
CA              60.233
HA               4.428
CB              71.525
HB               4.730
CG2             21.860
HG2#             1.355
C              175.200
; 0.0
55 LYS
N              123.340
HN               8.790
CA              60.020
HA               3.885
CB              32.390
HB1              1.770
HB2              1.980
CG              24.773
HG#              1.483
CD              28.895
HD1              1.650
HD2              1.730
CE              42.343
HE#              3.039
C              178.300
; 0.0
56 GLU
N              118.344
HN               8.800
CA              60.597
HA               4.082
#CB
HB1              1.940
HB2              2.075
CG              37.537
HG1              2.310
HG2              2.505
CD             184.600
C              180.100
; 0.0
57 GLU
N              122.582
HN               7.771
CA              60.370
HA               4.005
#CB
#HB1
#HB2
#CG
HG#              2.310
CD             180.000
C              179.500
; 0.0
58 LEU
N              121.589
HN               7.957
```

```
CA              58.000
HA               4.025
#CB
HB#              2.080
CG              26.650
HG               1.795
CD1             23.602
HD1#             0.791
CD2             25.560
HD2#             0.846
C              178.600
; 0.0
59 ASP
N              120.110
HN               8.538
CA              57.250
HA               4.300
CB              40.098
HB1              2.628
HB2              2.708
CG             178.900
C              179.000
; 0.0
60 ALA
N              122.952
HN               7.630
CA              54.810
HA               4.179
CB              17.700
HB#              1.503
C              180.300
; 0.0
61 ILE
N              121.509
HN               7.574
CA              64.995
HA               3.706
CB              38.213
HB               1.970
CG1             28.924
HG11             1.049
HG12             1.891
CD1             13.730
HD1#             0.863
CG2             17.058
HG2#             0.830
C              178.300
; 0.0
62 ILE
N              119.304
HN               7.457
CA              64.982
HA               3.424
CB              37.588
HB               1.980
CG1             29.221
HG11             1.012
HG12             1.688
CD1             12.516
HD1#             0.768
CG2             16.278
HG2#             0.644
C              177.700
; 0.0
63 GLU
N              119.108
HN               8.347
CA              59.255
HA               3.995
CB              29.673
HB1              2.055
HB2              2.145
#CG
#HG1
#HG2
CD             180.000
C              178.200
; 0.0
64 GLU
N              116.159
HN               7.268
CA              58.850
HA               4.035
#CB
HB1              2.050
HB2              2.160
CG              37.200
HG1              2.320
HG2              2.510
CD             184.600
C              179.400
; 0.0
65 VAL
N              108.262
HN               7.260
CA              60.760
HA               4.595
CB              33.025
HB               2.468
CG1             18.960
HG1#             0.884
CG2             21.740
HG2#             0.850
C              175.400
HG#              0.860
; 0.0
66 ASP
#N
#HN
CA              53.510
HA               4.700
CB              42.300
HB1              2.600
HB2              2.750
CG             180.000
C              177.300
; 0.0
67 GLU
N              128.700
HN               8.530
CA              59.210
HA               4.230
#CB
HB1              2.030
HB2              2.250
#CG
HG1              2.250
HG2              2.370
CD             180.000
C              176.900
; 0.0
68 ASP
N              116.200
HN               8.005
CA              52.375
HA               4.734
CB              40.488
HB1              2.758
HB2              3.111
CG             180.000
C              177.700
; 0.0
69 GLY
N              110.413
HN               7.755
CA              47.100
HA1              3.805
HA2              3.875
C              175.300
; 0.0
70 SER
N              118.246
HN               8.543
CA              60.080
HA               4.220
CB              64.893
```

```
HB1          3.996
HB2          4.220
C          176.200
; 0.0
71 GLY
N          118.030
HN          10.970
CA          45.555
HA1          3.440
HA2          4.126
C          172.800
; 0.0
72 THR
N          109.260
HN           7.685
CA          58.110
HA           4.915
CB          73.680
HB           3.674
CG2         22.140
HG2#         1.023
C          173.500
; 0.0
73 ILE
N          126.510
HN           9.188
CA          60.427
HA           5.069
CB          40.585
HB           2.007
CG1         27.485
HG11         0.883
HG12         1.639
CD1         13.630
HD1#         0.850
CG2         18.006
HG2#         1.318
C          176.200
; 0.0
74 ASP
N          131.870
HN           9.532
CA          53.058
HA           5.319
CB          41.458
HB1          2.753
HB2          3.382
CG         178.700
C          175.900
; 0.0
75 PHE
N          119.711
HN           8.790
CA          61.483
HA           3.593
CB          38.610
HB1          2.058
HB2          2.500
#CD1
#HD#         6.680
HD1          6.680
HD2          6.680
#CE1
#HE#         7.090
HE1          7.090
HE2          7.090
#CZ
#HZ
C          176.400
; 0.0
76 GLU
N          117.316
HN           7.771
CA          58.795
HA           3.803
CB          27.980
HB1          1.905
HB2          1.995
CG          36.270
HG#          2.330
CD         180.000
C          180.300
; 0.0
77 GLU
N          120.723
HN           8.193
CA          57.930
HA           4.168
#CB
HB#          1.990
#CG
HG1          2.340
HG2          2.470
CD         180.000
C          178.800
; 0.0
78 PHE
N          123.381
HN           8.830
CA          61.167
HA           4.037
CB          40.087
HB1          3.268
HB2          3.430
#CD#
#HD#         7.100
HD1          7.100
HD2          7.100
#CE1
#HE#         7.270
HE1          7.280
HE2          7.280
#CZ
#HZ
C          177.300
; 0.0
79 LEU
N          119.767
HN           8.018
CA          57.960
HA           3.466
#CB
HB1          0.880
HB2          1.840
CG          25.100
HG           1.100
CD1         25.994
HD1#         0.565
CD2         23.507
HD2#         0.660
C          179.100
; 0.0
80 VAL
N          120.323
HN           7.289
CA          67.236
HA           3.267
CB          31.155
HB           2.462
CG1         21.385
HG1#         0.827
CG2         24.047
HG2#         1.066
C          178.200
; 0.0
81 MET
N          121.474
HN           7.848
CA          59.255
HA           3.692
CB          33.420
HB1          1.962
HB2          2.160
CG          31.723
HG1          2.180
HG2          2.456
```

```
CE                17.070
HE#                1.856
C                178.200
; 0.0
82 MET
N                118.572
HN                 8.070
CA                56.395
HA                 4.050
CB                31.718
HB1                0.919
HB2                1.450
CG                32.983
HG1                1.077
HG2                1.560
#CE
#HE#
C                179.400
; 0.0
83 VAL
N                122.284
HN                 8.377
CA                66.887
HA                 3.643
CB                31.518
HB                 2.041
CG1               21.324
HG1#               0.651
CG2               24.248
HG2#               1.203
C                178.100
; 0.0
84 ARG
N                120.848
HN                 8.060
CA                59.360
HA                 3.860
CB                30.120
HB#                1.865
CG                27.460
HG1                1.586
HG2                1.790
CD                43.698
HD#                3.074
NE                85.700
HE                 7.190
#NH1
#HH11
#HH12
#NH2
#HH21
#HH22
C                179.000
; 0.0
85 GLN
N                117.195
HN                 7.400
CA                57.330
HA                 4.153
#CB
#HB1
HB2                2.140
CG                33.500
HG1                2.390
HG2                2.470
CD               179.500
NE2              111.890
HE21               6.725
HE22               7.370
C                177.900
; 0.0
86 MET
N                120.148
HI                 7.924
CA                57.918
HA                 4.247
CB                33.944
HB1                2.197
HB2                2.365
CG                32.478
HG1                2.687
HG2                2.870
CE                17.090
HE#                2.277
C                177.600
; 0.0
87 LYS
N                120.418
HN                 7.856
CA                57.457
HA                 4.165
CB                33.062
HB1                1.663
HB2                1.783
CG                25.132
HG1                1.216
HG2                1.343
#CD
#HD1
#HD2
#CE
#HE1
#HE2
C                177.100
; 0.0
88 GLU
N                121.903
HN                 7.907
CA                56.960
HA                 4.300
CB                29.200
HB1                2.005
HB2                2.080
CG                36.600
HG1                2.280
HG2                2.340
CD               180.000
C                176.500
; 0.0
89 ASP
N                122.306
HN                 8.079
CA                54.035
HA                 4.630
CB                41.267
HB1                2.598
HB2                2.740
CG               180.600
C                174.900
; 0.0
90 ALA
N                130.700
HN                 7.646
CA                53.730
HA                 4.117
CB                20.270
HB#                1.345
C                170.600
; 0.0
```

APPENDIX C

NOE AND STRUCTURE CALCULATION PARAMETERS

1. NOE calibration

This is a "nawk" program that take as input a file with the following format:

```
  THR   4 HN     THR   4   HA    3380
 ASP-   5 HN    ASP-   5   HA   16000
  GLN   6 HN    ASP-   5   HA    7010
```

nawk program :

```
grep -v "GLY" $1 \
|nawk '{
diff=$2-$5
if (diff==0) {
      dna[$2]=1
      dna_N[$2]="1:"$1"_"$2":"$3
      dna_A[$2]="1:"$4"_"$5":"$6
      dna_I[$2]=$7
      }
if (diff==1) {
     dan[$2]=1
     dan_N[$2]="1:"$1"_"$2":"$3
     dan_A[$2]="1:"$4"_"$5":"$6
     dan_I[$2]=$7
     }
if (diff==3) {
     dan3[$2]=1
     dan3_N[$2]="1:"$1"_"$2":"$3
     dan3_A[$2]="1:"$4"_"$5":"$6
     dan3_I[$2]=$7
     }
}
END{
#################################################################
#          CASE              Dna_rstrnt       Dan_rstrnt
#       =========            ==========       ==========
#
#          no Dna/Dan        (L0, U0)         (L1, U1)
#          Dna only          (L0, U0)         (L1, U1)
#          Dan only          (L0, U0)         (L1, U1)
#          Dna >> Dan        (2.6, U0)        (U0, U1)
```

```
#           Dna > Dan        (2.6, U0)        (2.9, U1)
#           Dna << Dan       (2.7, U0)        (L1, 2.7)
#           Dna < Dan        (2.7, U0)        (L1, 2.9)
#           Dna ~ Dan        (2.6, U0)        (2.3, U1)
#
#############################################################
# note :   >>    :     ratio > 1.5
#                >     :     1.5 > ratio > 1.2
#                ~     :     0.833 < ratio < 1.2


for (i=1; i<=90; i++) {
if ((dna[i]==1)&&(dan[i]==1)){
      pr_dna(dna_N[i],dna_A[i],dan_A[i],dna_I[i],dan_I[i])
      }
if ((dna[i]==1)&&(dan[i]==0)) pr(dna_N[i],dna_A[i],1.8,5.0,dna_I[i])
if ((dna[i]==0)&&(dan[i]==1)) pr(dan_N[i],dan_A[i],1.8,5.0,dan_I[i])

if (dan3[i]==1) {
      if ((dna[i]==1)&&(dan[i]==1)) {

prdan3_11(dan3_N[i],dan3_A[i],dna_I[i],dan_I[i],dan3_I[i])
            }
     if ((dna[i]==1)&&(dan[i]==0)) {
         prdan3_10(dan3_N[i],dan3_A[i],dna_I[i],dan3_I[i])
         }
     if ((dna[i]==0)&&(dan[i]==1)) {
         prdan3_01(dan3_N[i],dan3_A[i],dan_I[i],dan3_I[i])
         }
      if ((dna[i]==0)&&(dan[i]==0)) {
            pr(dan3_N[i],dan3_A[i],1.8,5.0,dan3_I[i])
            }
      }
}
}

func prdan3_11 (HN,HA,dna,dan,dan3) {
      if ((dan3/dna) > 1.2) {pr(HN,HA,1.8,3.1,dan3) ; return}
      if ((dna/dan3) > 1.2) {
            if ((dan/dan3) > 1.2) {pr(HN,HA,2.8,5.0,dan3) ; return}
            if ((dan3/dan) > 1.2) {pr(HN,HA,2.8,3.6,dan3) ; return}
            pr(HN,HA,2.8,4.3,dan3)
            return
            }
      if ((dan/dan3) > 1.2) {pr(HN,HA,2.2,4.1,dan3) ; return}
      if ((dan3/dan) > 1.2) {pr(HN,HA,2.2,3.6,dan3) ; return}
      pr(HN,HA,2.2,4.3,dan3)
      return
      }

function prdan3_10(HN,HA,dna,dan3) {
     if ((dan3/dna) > 1.2) {pr(HN,HA,1.8,3.1,dan3) ; return}
      if ((dna/dan3) > 1.2) {pr(HN,HA,2.8,5.0,dan3) ; return}
      pr(HN,HA,2.8,4.1,dan3)
     return
     }

function prdan3_01(HN,HA,dan,dan3) {
     if ((dan3/dan) > 1.2) {pr(HN,HA,1.8,3.6,dan3) ; return}
     if ((dan/dan3) > 1.2) {pr(HN,HA,2.8,5.0,dan3) ; return}
     pr(HN,HA,1.9,4.3,dan3)
     return
```

```
    }

function pr_dna(HN,HA0,HA1,dna,dan){
      if (dna > dan) {
            if ((dna/dan)>1.5) {
                  pr(HN,HA0,2.6,3.1,dna)
                  pr(HN,HA1,3.1,3.6,dan)
                  return
                  }
         if ((dna/dan)>1.2) {
                  pr(HN,HA0,2.6,3.1,dna)
                  pr(HN,HA1,2.9,3.6,dan)
                  return
                  }
            }
    if (dan > dna) {
        if ((dan/dna)>1.5) {
            pr(HN,HA0,2.7,3.1,dna)
            pr(HN,HA1,2.1,2.7,dan)
            return
            }
        if ((dan/dna)>1.2) {
            pr(HN,HA0,2.7,3.1,dna)
            pr(HN,HA1,2.1,2.9,dan)
            return
            }
        }
      pr(HN,HA0,2.6,3.1,dna)
      pr(HN,HA1,2.3,3.6,dan)
      return
      }

function pr(HN,HA,LO,UP,NOE) {
      printf "%-15s%-14s%6.1f%6.1f%8.1f   10 10 1000
%7d\n",HN,HA,LO,UP,UP,NOE
      return
}'
grep "GLY" $1 \
|nawk '{
dna_N="1:"$1"_"$2":"$3
dna_A="1:"$4"_"$5":"$6
printf "%-15s%-15s   1.8     5.0        5.0   10 10 1000
%7d\n",dna_N,dna_A,$7}'
```

NOE restraints

This is the Biosym DGII restraint file used to calculate the preliminary structure of NTnC·2Ca :

```
!BIOSYM restraint 1
!
#remote_prochiral_center
1:VAL_83:HG2*    1:VAL_83:HG1*    1:VAL_83:CG2    1:VAL_83:CG1    1:VAL_83:CB
1:LEU_79:HD2*    1:LEU_79:HD1*    1:LEU_79:CD2    1:LEU_79:CD1    1:LEU_79:CG
1:VAL_65:HG1*    1:VAL_65:HG2*    1:VAL_65:CG1    1:VAL_65:CG2    1:VAL_65:CB
1:VAL_80:HG2*    1:VAL_80:HG1*    1:VAL_80:CG2    1:VAL_80:CG1    1:VAL_80:CB
1:VAL_45:HG2*    1:VAL_45:HG1*    1:VAL_45:CG2    1:VAL_45:CG1    1:VAL_45:CB
1:LEU_14:HD1*    1:LEU_14:HD2*    1:LEU_14:CD1    1:LEU_14:CD2    1:LEU_14:CG
1:LEU_58:HD1*    1:LEU_58:HD2*    1:LEU_58:CD1    1:LEU_58:CD2    1:LEU_58:CG
1:LEU_42:HD1*    1:LEU_42:HD2*    1:LEU_42:CD1    1:LEU_42:CD2    1:LEU_42:CG
1:LEU_49:HD2*    1:LEU_49:HD1*    1:LEU_49:CD2    1:LEU_49:CD1    1:LEU_49:CG
!
#chiral
1:ALAN_1:CA          S
1:SER_2:CA           S
1:MET_3:CA           S
1:THR_4:CA           S
1:THR_4:CB           R
1:ASP-_5:CA          S
1:GLN_6:CA           S
1:GLN_7:CA           S
1:ALA_8:CA           S
1:GLU-_9:CA          S
1:ALA_10:CA          S
1:ARG+_11:CA         S
1:ALA_12:CA          S
1:PHE_13:CA          S
1:LEU_14:CA          S
1:SER_15:CA          S
1:GLU-_16:CA         S
1:GLU-_17:CA         S
1:MET_18:CA          S
1:ILE_19:CA          S
1:ILE_19:CB          S
1:ALA_20:CA          S
1:GLU-_21:CA         S
1:PHE_22:CA          S
1:LYS+_23:CA         S
1:ALA_24:CA          S
1:ALA_25:CA          S
1:PHE_26:CA          S
1:ASP-_27:CA         S
1:MET_28:CA          S
1:PHE_29:CA          S
1:ASP-_30:CA         S
1:ALA_31:CA          S
1:ASP-_32:CA         S
1:ASP-_36:CA         S
1:ILE_37:CA          S
1:ILE_37:CB          S
1:SER_38:CA          S
1:THR_39:CA          S
1:THR_39:CB          R
1:LYS+_40:CA         S
1:GLU-_41:CA         S
1:LEU_42:CA          S
1:THR_44:CA          S
1:THR_44:CB          R
1:VAL_45:CA          S
1:MET_46:CA          S
1:ARG+_47:CA         S
1:MET_48:CA          S
1:LEU_49:CA          S
1:GLN_51:CA          S
1:ASN_52:CA          S
```

```
1:PRO_53:CA          S
1:THR_54:CA          S
1:THR_54:CB          R
1:LYS+_55:CA         S
1:GLU-_56:CA         S
1:GLU-_57:CA         S
1:LEU_58:CA          S
1:ASP-_59:CA         S
1:ALA_60:CA          S
1:ILE_61:CA          S
1:ILE_61:CB          S
1:ILE_62:CA          S
1:ILE_62:CB          S
1:GLU-_63:CA         S
1:GLU-_64:CA         S
1:VAL_65:CA          S
1:ASP-_66:CA         S
1:GLU-_67:CA         S
1:ASP-_68:CA         S
1:SER_70:CA          S
1:THR_72:CA          S
1:THR_72:CB          R
1:ILE_73:CA          S
1:ILE_73:CB          S
1:ASP-_74:CA         S
1:PHE_75:CA          S
1:GLU-_76:CA         S
1:GLU-_77:CA         S
1:PHE_78:CA          S
1:LEU_79:CA          S
1:VAL_80:CA          S
1:MET_81:CA          S
1:MET_82:CA          S
1:VAL_83:CA          S
1:ARG+_84:CA         S
1:GLN_85:CA          S
1:MET_86:CA          S
1:LYS+_87:CA         S
1:GLU-_88:CA         S
1:ASP-_89:CA         S
1:ALAC_90:CA         S
!
#NOE_distance
1:ILE_62:HD1*      1:ILE_62:HG11      1.800  6.500  5.000 10.00 10.00 1000.000  0.00
1:ILE_62:HD1*      1:THR_39:HG2*      1.800  8.000  5.000 10.00 10.00 1000.000  0.00
1:ILE_62:HD1*      1:ILE_62:HA        1.800  6.500  5.000 10.00 10.00 1000.000  0.00
1:ILE_62:HD1*      1:THR_39:HA        1.800  6.500  5.000 10.00 10.00 1000.000  0.00
1:ILE_62:HD1*      1:THR_39:HB        1.800  6.500  5.000 10.00 10.00 1000.000  0.00
1:ILE_62:HD1*      1:ASP-_59:HA       1.800  6.500  5.000 10.00 10.00 1000.000  0.00
1:ILE_62:HD1*      1:THR_72:HA        1.800  6.500  5.000 10.00 10.00 1000.000  0.00
1:LYS+_55:HE*      1:LYS+_55:HA       1.800  6.000  5.000 10.00 10.00 1000.000  0.00
1:LYS+_23:HE*      1:LYS+_23:HG*      1.800  7.000  5.000 10.00 10.00 1000.000  0.00
1:LYS+_23:HE*      1:LYS+_23:HB*      1.800  7.000  5.000 10.00 10.00 1000.000  0.00
1:ASP-_89:HB2      1:ASP-_89:HB1      1.800  5.000  5.000 10.00 10.00 1000.000  0.00
1:ASP-_89:HB2      1:ASP-_89:HA       1.800  5.000  5.000 10.00 10.00 1000.000  0.00
1:ASP-_74:HB2      1:ASP-_74:HB1      1.800  5.000  5.000 10.00 10.00 1000.000  0.00
1:ASP-_74:HB2      1:ASP-_74:HA       1.800  5.000  5.000 10.00 10.00 1000.000  0.00
1:ASP-_74:HB1      1:ASP-_74:HA       1.800  5.000  5.000 10.00 10.00 1000.000  0.00
1:ASP-_36:HB2      1:ASP-_36:HA       1.800  5.000  5.000 10.00 10.00 1000.000  0.00
1:ASP-_36:HB1      1:ASP-_36:HA       1.800  5.000  5.000 10.00 10.00 1000.000  0.00
1:ASP-_36:HB2      1:ASP-_36:HB1      1.800  5.000  5.000 10.00 10.00 1000.000  0.00
1:ASP-_89:HB1      1:ASP-_89:HA       1.800  5.000  5.000 10.00 10.00 1000.000  0.00
1:PHE_13:HB1       1:VAL_83:HG2*      1.800  6.500  5.000 10.00 10.00 1000.000  0.00
1:PHE_13:HB1       1:PHE_13:HA        1.800  5.000  5.000 10.00 10.00 1000.000  0.00
1:PHE_13:HB2       1:PHE_13:HA        1.800  5.000  5.000 10.00 10.00 1000.000  0.00
1:ILE_73:HB        1:ILE_73:HG2*      1.800  6.500  5.000 10.00 10.00 1000.000  0.00
1:ILE_73:HB        1:ILE_73:HG12      1.800  5.000  5.000 10.00 10.00 1000.000  0.00
1:ASP-_68:HB2      1:ASP-_68:HB1      1.800  5.000  5.000 10.00 10.00 1000.000  0.00
1:ASP-_68:HB1      1:ASP-_68:HA       1.800  5.000  5.000 10.00 10.00 1000.000  0.00
1:ASP-_68:HB2      1:ASP-_68:HA       1.800  5.000  5.000 10.00 10.00 1000.000  0.00
1:PHE_78:HB2       1:ILE_73:HG2*      1.800  6.500  5.000 10.00 10.00 1000.000  0.00
1:PHE_78:HB1       1:ILE_73:HG2*      1.800  6.500  5.000 10.00 10.00 1000.000  0.00
1:PHE_78:HB2       1:PHE_78:HA        1.800  5.000  5.000 10.00 10.00 1000.000  0.00
1:PHE_78:HB1       1:PHE_78:HA        1.800  5.000  5.000 10.00 10.00 1000.000  0.00
1:PHE_78:HB2       1:PHE_78:HB1       1.800  5.000  5.000 10.00 10.00 1000.000  0.00
1:ASP-_59:HB1      1:GLU-_56:HA       1.800  5.000  5.000 10.00 10.00 1000.000  0.00
1:ASP-_59:HB2      1:GLU-_56:HA       1.800  5.000  5.000 10.00 10.00 1000.000  0.00
1:ASP-_59:HB2      1:ASP-_59:HA       1.800  5.000  5.000 10.00 10.00 1000.000  0.00
```

1:ASP-_59:HB1	1:ASP-_59:HA	1.800	5.000	5.000	10.00	10.00	1000.000	0.00
1:ILE_37:HB	1:ILE_37:HD1*	1.800	6.500	5.000	10.00	10.00	1000.000	0.00
1:ILE_37:HB	1:ILE_37:HG2*	1.800	6.500	5.000	10.00	10.00	1000.000	0.00
1:ILE_37:HB	1:ILE_73:HG2*	1.800	6.500	5.000	10.00	10.00	1000.000	0.00
1:ILE_37:HB	1:ILE_73:HB	1.800	5.000	5.000	10.00	10.00	1000.000	0.00
1:ASP-_32:HB2	1:ASP-_32:HB1	1.800	5.000	5.000	10.00	10.00	1000.000	0.00
1:ASP-_32:HB2	1:ASP-_32:HA	1.800	5.000	5.000	10.00	10.00	1000.000	0.00
1:ASP-_32:HB1	1:ASP-_32:HA	1.800	5.000	5.000	10.00	10.00	1000.000	0.00
1:ASP-_27:HB2	1:ASP-_27:HA	1.800	5.000	5.000	10.00	10.00	1000.000	0.00
1:ASP-_27:HB1	1:ASP-_27:HA	1.800	5.000	5.000	10.00	10.00	1000.000	0.00
1:ASP-_5:HB2	1:ASP-_5:HA	1.800	5.000	5.000	10.00	10.00	1000.000	0.00
1:ASN_52:HB2	1:ASN_52:HB1	1.800	5.000	5.000	10.00	10.00	1000.000	0.00
1:ASN_52:HB1	1:PRO_53:HD2	1.800	5.000	5.000	10.00	10.00	1000.000	0.00
1:ASN_52:HB2	1:ASN_52:HA	1.800	5.000	5.000	10.00	10.00	1000.000	0.00
1:ASN_52:HB1	1:ASN_52:HA	1.800	5.000	5.000	10.00	10.00	1000.000	0.00
1:PHE_29:HB2	1:ILE_37:HD1*	1.800	6.500	5.000	10.00	10.00	1000.000	0.00
1:PHE_29:HB1	1:ILE_37:HD1*	1.800	6.500	5.000	10.00	10.00	1000.000	0.00
1:PHE_75:HB1	1:PHE_75:HB2	1.800	5.000	5.000	10.00	10.00	1000.000	0.00
1:PHE_29:HB2	1:PHE_29:HA	1.800	5.000	5.000	10.00	10.00	1000.000	0.00
1:PHE_29:HB1	1:PHE_29:HA	1.800	5.000	5.000	10.00	10.00	1000.000	0.00
1:ASP-_30:HB1	1:ASP-_30:HB2	1.800	5.000	5.000	10.00	10.00	1000.000	0.00
1:ASP-_30:HB2	1:ASP-_30:HA	1.800	5.000	5.000	10.00	10.00	1000.000	0.00
1:ASP-_30:HB1	1:ASP-_30:HA	1.800	5.000	5.000	10.00	10.00	1000.000	0.00
1:ASP-_30:HB1	1:ASP-_27:HA	1.800	5.000	5.000	10.00	10.00	1000.000	0.00
1:ASP-_30:HB2	1:ASP-_27:HA	1.800	5.000	5.000	10.00	10.00	1000.000	0.00
1:ILE_61:HB	1:ILE_62:HA	1.800	5.000	5.000	10.00	10.00	1000.000	0.00
1:ILE_61:HB	1:ILE_61:HG11	1.800	5.000	5.000	10.00	10.00	1000.000	0.00
1:ILE_61:HB	1:ILE_61:HA	1.800	5.000	5.000	10.00	10.00	1000.000	0.00
1:ILE_62:HB	1:ILE_62:HD1*	1.800	6.500	5.000	10.00	10.00	1000.000	0.00
1:ILE_62:HB	1:ILE_62:HG2*	1.800	6.500	5.000	10.00	10.00	1000.000	0.00
1:ILE_62:HB	1:ASP-_59:HA	1.800	5.000	5.000	10.00	10.00	1000.000	0.00
1:PHE_22:HB*	1:LEU_79:HD2*	1.800	7.500	5.000	10.00	10.00	1000.000	0.00
1:PHE_22:HB*	1:ILE_19:HA	1.800	6.000	5.000	10.00	10.00	1000.000	0.00
1:PHE_22:HB*	1:PHE_22:HA	1.800	6.000	5.000	10.00	10.00	1000.000	0.00
1:ILE_19:HB	1:ILE_19:HD1*	1.800	6.500	5.000	10.00	10.00	1000.000	0.00
1:ILE_19:HB	1:ILE_19:HG2*	1.800	6.500	5.000	10.00	10.00	1000.000	0.00
1:ILE_19:HB	1:ILE_19:HG12	1.800	5.000	5.000	10.00	10.00	1000.000	0.00
1:ILE_19:HB	1:ILE_19:HA	1.800	5.000	5.000	10.00	10.00	1000.000	0.00
1:ILE_19:HB	1:GLU-_16:HA	1.800	5.000	5.000	10.00	10.00	1000.000	0.00
1:ILE_62:HB	1:ILE_62:HG12	1.800	5.000	5.000	10.00	10.00	1000.000	0.00
1:ILE_62:HB	1:ILE_62:HA	1.800	5.000	5.000	10.00	10.00	1000.000	0.00
1:GLU-_56:HG2	1:GLU-_56:HB2	1.800	5.000	5.000	10.00	10.00	1000.000	0.00
1:GLU-_56:HG2	1:GLU-_56:HB1	1.800	5.000	5.000	10.00	10.00	1000.000	0.00
1:GLU-_76:HG*	1:GLU-_76:HA	1.800	6.000	5.000	10.00	10.00	1000.000	0.00
1:GLN_6:HG2	1:GLN_6:HB2	1.800	5.000	5.000	10.00	10.00	1000.000	0.00
1:GLN_6:HG1	1:GLN_6:HB2	1.800	5.000	5.000	10.00	10.00	1000.000	0.00
1:GLN_6:HG2	1:GLN_6:HG1	1.800	5.000	5.000	10.00	10.00	1000.000	0.00
1:MET_86:HB1	1:MET_86:HG1	1.800	5.000	5.000	10.00	10.00	1000.000	0.00
1:MET_86:HB2	1:MET_86:HG2	1.800	5.000	5.000	10.00	10.00	1000.000	0.00
1:MET_86:HB1	1:MET_86:HG2	1.800	5.000	5.000	10.00	10.00	1000.000	0.00
1:MET_86:HB2	1:VAL_83:HA	1.800	5.000	5.000	10.00	10.00	1000.000	0.00
1:MET_86:HB1	1:VAL_83:HA	1.800	5.000	5.000	10.00	10.00	1000.000	0.00
1:MET_86:HB1	1:MET_86:HA	1.800	5.000	5.000	10.00	10.00	1000.000	0.00
1:MET_46:HG2	1:MET_46:HB2	1.800	5.000	5.000	10.00	10.00	1000.000	0.00
1:MET_46:HG1	1:MET_46:HE*	1.800	6.500	5.000	10.00	10.00	1000.000	0.00
1:MET_46:HG2	1:MET_46:HE*	1.800	6.500	5.000	10.00	10.00	1000.000	0.00
1:MET_46:HG1	1:MET_46:HG2	1.800	5.000	5.000	10.00	10.00	1000.000	0.00
1:MET_46:HG1	1:MET_46:HA	1.800	5.000	5.000	10.00	10.00	1000.000	0.00
1:MET_81:HB1	1:MET_81:HA	1.800	5.000	5.000	10.00	10.00	1000.000	0.00
1:GLN_51:HG2	1:GLN_51:HB1	1.800	5.000	5.000	10.00	10.00	1000.000	0.00
1:GLN_51:HG1	1:GLN_51:HB1	1.800	5.000	5.000	10.00	10.00	1000.000	0.00
1:GLN_51:HG2	1:GLY_50:HA1	1.800	5.000	5.000	10.00	10.00	1000.000	0.00
1:GLN_51:HG2	1:GLN_51:HA	1.800	5.000	5.000	10.00	10.00	1000.000	0.00
1:GLN_51:HG1	1:GLN_51:HA	1.800	5.000	5.000	10.00	10.00	1000.000	0.00
1:LYS+_87:HB2	1:LYS+_87:HG2	1.800	5.000	5.000	10.00	10.00	1000.000	0.00
1:LYS+_87:HB1	1:LYS+_87:HG2	1.800	5.000	5.000	10.00	10.00	1000.000	0.00
1:MET_82:HG1	1:MET_82:HA	1.800	5.000	5.000	10.00	10.00	1000.000	0.00
1:MET_82:HG2	1:MET_82:HB1	1.800	5.000	5.000	10.00	10.00	1000.000	0.00
1:MET_82:HG1	1:MET_82:HB1	1.800	5.000	5.000	10.00	10.00	1000.000	0.00
1:MET_82:HG2	1:MET_82:HG1	1.800	5.000	5.000	10.00	10.00	1000.000	0.00
1:VAL_65:HB	1:VAL_65:HG1*	1.800	6.500	5.000	10.00	10.00	1000.000	0.00
1:VAL_65:HB	1:VAL_65:HA	1.800	5.000	5.000	10.00	10.00	1000.000	0.00
1:MET_48:HG1	1:MET_48:HB2	1.800	5.000	5.000	10.00	10.00	1000.000	0.00
1:MET_48:HG2	1:MET_48:HE*	1.800	6.500	5.000	10.00	10.00	1000.000	0.00
1:MET_48:HG1	1:MET_48:HE*	1.800	6.500	5.000	10.00	10.00	1000.000	0.00
1:MET_48:HG2	1:MET_48:HG1	1.800	5.000	5.000	10.00	10.00	1000.000	0.00
1:MET_48:HG2	1:MET_48:HA	1.800	5.000	5.000	10.00	10.00	1000.000	0.00
1:MET_48:HG1	1:MET_48:HA	1.800	5.000	5.000	10.00	10.00	1000.000	0.00

1:MET_28:HG1	1:MET_28:HA	1.800	5.000	5.000	10.00	10.00	1000.000	0.00
1:MET_18:HB2	1:MET_18:HB1	1.800	5.000	5.000	10.00	10.00	1000.000	0.00
1:MET_18:HB2	1:MET_18:HG1	1.800	5.000	5.000	10.00	10.00	1000.000	0.00
1:MET_18:HB1	1:MET_18:HG1	1.800	5.000	5.000	10.00	10.00	1000.000	0.00
1:MET_18:HB1	1:MET_18:HA	1.800	5.000	5.000	10.00	10.00	1000.000	0.00
1:MET_18:HB2	1:MET_18:HA	1.800	5.000	5.000	10.00	10.00	1000.000	0.00
1:MET_86:HG2	1:MET_86:HG1	1.800	5.000	5.000	10.00	10.00	1000.000	0.00
1:MET_86:HG2	1:MET_86:HA	1.800	5.000	5.000	10.00	10.00	1000.000	0.00
1:LYS+_55:HB2	1:LYS+_55:HG*	1.800	6.000	5.000	10.00	10.00	1000.000	0.00
1:LYS+_55:HB2	1:LYS+_55:HA	1.800	5.000	5.000	10.00	10.00	1000.000	0.00
1:LYS+_55:HB1	1:LYS+_55:HA	1.800	5.000	5.000	10.00	10.00	1000.000	0.00
1:MET_48:HB1	1:MET_48:HG1	1.800	5.000	5.000	10.00	10.00	1000.000	0.00
1:MET_48:HB1	1:MET_48:HG2	1.800	5.000	5.000	10.00	10.00	1000.000	0.00
1:MET_48:HB2	1:MET_48:HG2	1.800	5.000	5.000	10.00	10.00	1000.000	0.00
1:MET_48:HB2	1:MET_48:HA	1.800	5.000	5.000	10.00	10.00	1000.000	0.00
1:MET_48:HB1	1:MET_48:HA	1.800	5.000	5.000	10.00	10.00	1000.000	0.00
1:LYS+_40:HB2	1:LYS+_40:HG2	1.800	5.000	5.000	10.00	10.00	1000.000	0.00
1:LYS+_40:HB2	1:LYS+_40:HA	1.800	5.000	5.000	10.00	10.00	1000.000	0.00
1:LYS+_40:HB1	1:LYS+_40:HA	1.800	5.000	5.000	10.00	10.00	1000.000	0.00
1:MET_18:HG2	1:MET_18:HB1	1.800	5.000	5.000	10.00	10.00	1000.000	0.00
1:MET_18:HG2	1:MET_18:HB2	1.800	5.000	5.000	10.00	10.00	1000.000	0.00
1:MET_18:HG2	1:MET_18:HA	1.800	5.000	5.000	10.00	10.00	1000.000	0.00
1:MET_18:HG1	1:MET_18:HA	1.800	5.000	5.000	10.00	10.00	1000.000	0.00
1:MET_28:HB2	1:MET_28:HG2	1.800	5.000	5.000	10.00	10.00	1000.000	0.00
1:MET_28:HB2	1:MET_28:HA	1.800	5.000	5.000	10.00	10.00	1000.000	0.00
1:MET_28:HB1	1:MET_28:HA	1.800	5.000	5.000	10.00	10.00	1000.000	0.00
1:PRO_53:HB2	1:PRO_53:HD1	1.800	5.000	5.000	10.00	10.00	1000.000	0.00
1:PRO_53:HB2	1:PRO_53:HD2	1.800	5.000	5.000	10.00	10.00	1000.000	0.00
1:PRO_53:HB1	1:PRO_53:HD2	1.800	5.000	5.000	10.00	10.00	1000.000	0.00
1:PRO_53:HB2	1:PRO_53:HA	1.800	5.000	5.000	10.00	10.00	1000.000	0.00
1:PRO_53:HB1	1:PRO_53:HA	1.800	5.000	5.000	10.00	10.00	1000.000	0.00
1:MET_46:HB1	1:MET_46:HA	1.800	5.000	5.000	10.00	10.00	1000.000	0.00
1:MET_46:HB2	1:MET_46:HA	1.800	5.000	5.000	10.00	10.00	1000.000	0.00
1:MET_46:HB2	1:MET_46:HG1	1.800	5.000	5.000	10.00	10.00	1000.000	0.00
1:MET_46:HB1	1:MET_46:HG2	1.800	5.000	5.000	10.00	10.00	1000.000	0.00
1:MET_46:HB1	1:MET_46:HG1	1.800	5.000	5.000	10.00	10.00	1000.000	0.00
1:VAL_83:HB	1:VAL_83:HG1*	1.800	6.500	5.000	10.00	10.00	1000.000	0.00
1:VAL_83:HB	1:VAL_83:HG2*	1.800	6.500	5.000	10.00	10.00	1000.000	0.00
1:VAL_83:HB	1:ALA_10:HB*	1.800	6.500	5.000	10.00	10.00	1000.000	0.00
1:MET_82:HB2	1:MET_82:HG1	1.800	5.000	5.000	10.00	10.00	1000.000	0.00
1:MET_82:HB2	1:MET_82:HB1	1.800	5.000	5.000	10.00	10.00	1000.000	0.00
1:MET_81:HG1	1:MET_81:HG2	1.800	5.000	5.000	10.00	10.00	1000.000	0.00
1:MET_81:HG1	1:MET_81:HE*	1.800	6.500	5.000	10.00	10.00	1000.000	0.00
1:MET_81:HG2	1:MET_81:HE*	1.800	6.500	5.000	10.00	10.00	1000.000	0.00
1:MET_81:HG2	1:MET_81:HB1	1.800	5.000	5.000	10.00	10.00	1000.000	0.00
1:MET_81:HG1	1:MET_81:HA	1.800	5.000	5.000	10.00	10.00	1000.000	0.00
1:MET_81:HG2	1:MET_81:HA	1.800	5.000	5.000	10.00	10.00	1000.000	0.00
1:VAL_80:HB	1:VAL_80:HG2*	1.800	6.500	5.000	10.00	10.00	1000.000	0.00
1:VAL_80:HB	1:VAL_80:HG1*	1.800	6.500	5.000	10.00	10.00	1000.000	0.00
1:VAL_45:HB	1:VAL_45:HG2*	1.800	6.500	5.000	10.00	10.00	1000.000	0.00
1:VAL_45:HB	1:VAL_45:HG1*	1.800	6.500	5.000	10.00	10.00	1000.000	0.00
1:LYS+_23:HB*	1:LYS+_23:HA	1.800	6.000	5.000	10.00	10.00	1000.000	0.00
1:LYS+_23:HB*	1:ILE_19:HA	1.800	6.000	5.000	10.00	10.00	1000.000	0.00
1:GLN_51:HB2	1:GLN_51:HB1	1.800	5.000	5.000	10.00	10.00	1000.000	0.00
1:GLN_51:HB2	1:GLY_50:HA1	1.800	5.000	5.000	10.00	10.00	1000.000	0.00
1:GLN_51:HB2	1:GLN_51:HA	1.800	5.000	5.000	10.00	10.00	1000.000	0.00
1:GLN_51:HB1	1:GLN_51:HA	1.800	5.000	5.000	10.00	10.00	1000.000	0.00
1:GLN_6:HB1	1:GLN_6:HA	1.800	5.000	5.000	10.00	10.00	1000.000	0.00
1:GLN_6:HB2	1:GLN_6:HA	1.800	5.000	5.000	10.00	10.00	1000.000	0.00
1:ARG+_84:HB*	1:ARG+_84:HD*	1.800	7.000	5.000	10.00	10.00	1000.000	0.00
1:ARG+_47:HB*	1:ARG+_47:HD*	1.800	7.000	5.000	10.00	10.00	1000.000	0.00
1:ARG+_47:HB*	1:ARG+_47:HA	1.800	6.000	5.000	10.00	10.00	1000.000	0.00
1:GLU-_63:HB1	1:ALA_60:HB*	1.800	6.500	5.000	10.00	10.00	1000.000	0.00
1:GLU-_63:HB2	1:ALA_60:HB*	1.800	6.500	5.000	10.00	10.00	1000.000	0.00
1:GLU-_63:HB1	1:GLU-_63:HA	1.800	5.000	5.000	10.00	10.00	1000.000	0.00
1:GLU-_63:HB2	1:ALA_60:HA	1.800	5.000	5.000	10.00	10.00	1000.000	0.00
1:GLU-_63:HB1	1:ALA_60:HA	1.800	5.000	5.000	10.00	10.00	1000.000	0.00
1:GLU-_63:HB2	1:GLU-_63:HA	1.800	5.000	5.000	10.00	10.00	1000.000	0.00
1:ILE_62:HG12	1:ILE_62:HD1*	1.800	6.500	5.000	10.00	10.00	1000.000	0.00
1:ILE_62:HG12	1:ILE_62:HG2*	1.800	6.500	5.000	10.00	10.00	1000.000	0.00
1:ILE_62:HG11	1:ILE_62:HG2*	1.800	6.500	5.000	10.00	10.00	1000.000	0.00
1:ILE_62:HG11	1:ILE_62:HG12	1.800	5.000	5.000	10.00	10.00	1000.000	0.00
1:ILE_62:HG11	1:ILE_62:HA	1.800	5.000	5.000	10.00	10.00	1000.000	0.00
1:ILE_62:HG12	1:ILE_62:HA	1.800	5.000	5.000	10.00	10.00	1000.000	0.00
1:LYS+_40:HD*	1:LYS+_40:HE*	1.800	7.000	5.000	10.00	10.00	1000.000	0.00
1:LYS+_40:HD*	1:LYS+_40:HA	1.800	6.000	5.000	10.00	10.00	1000.000	0.00
1:ILE_61:HG11	1:ILE_61:HG12	1.800	5.000	5.000	10.00	10.00	1000.000	0.00
1:ILE_61:HG12	1:ILE_61:HD1*	1.800	6.500	5.000	10.00	10.00	1000.000	0.00

1:ILE_61:HG11	1:ILE_61:HA	1.800	5.000	5.000	10.00	10.00	1000.000	0.00
1:ILE_61:HG12	1:ILE_61:HA	1.800	5.000	5.000	10.00	10.00	1000.000	0.00
1:LYS+_55:HD1	1:LYS+_55:HE*	1.800	6.000	5.000	10.00	10.00	1000.000	0.00
1:LYS+_55:HD2	1:LYS+_55:HE*	1.800	6.000	5.000	10.00	10.00	1000.000	0.00
1:GLU-_17:HB1	1:GLU-_17:HG1	1.800	5.000	5.000	10.00	10.00	1000.000	0.00
1:ARG+_47:HG1	1:ARG+_47:HD*	1.800	6.000	5.000	10.00	10.00	1000.000	0.00
1:ARG+_47:HG2	1:ARG+_47:HD*	1.800	6.000	5.000	10.00	10.00	1000.000	0.00
1:ARG+_47:HG1	1:ARG+_47:HA	1.800	5.000	5.000	10.00	10.00	1000.000	0.00
1:ARG+_47:HG2	1:ARG+_47:HA	1.800	5.000	5.000	10.00	10.00	1000.000	0.00
1:LEU_14:HD1*	1:LEU_14:HD2*	1.800	8.000	5.000	10.00	10.00	1000.000	0.00
1:LEU_14:HD1*	1:ALA_10:HB*	1.800	8.000	5.000	10.00	10.00	1000.000	0.00
1:LEU_14:HD1*	1:ARG+_11:HA	1.800	6.500	5.000	10.00	10.00	1000.000	0.00
1:LEU_14:HD1*	1:LEU_14:HA	1.800	6.500	5.000	10.00	10.00	1000.000	0.00
1:GLU-_76:HB1	1:GLU-_76:HA	1.800	5.000	5.000	10.00	10.00	1000.000	0.00
1:GLU-_76:HB2	1:GLU-_76:HA	1.800	5.000	5.000	10.00	10.00	1000.000	0.00
1:ILE_73:HG11	1:ILE_73:HG2*	1.800	6.500	5.000	10.00	10.00	1000.000	0.00
1:ARG+_84:HG2	1:ARG+_84:HG1	1.800	5.000	5.000	10.00	10.00	1000.000	0.00
1:ARG+_84:HG2	1:ARG+_84:HD*	1.800	6.000	5.000	10.00	10.00	1000.000	0.00
1:ARG+_84:HG2	1:ARG+_84:HA	1.800	5.000	5.000	10.00	10.00	1000.000	0.00
1:ARG+_84:HG1	1:ARG+_84:HA	1.800	5.000	5.000	10.00	10.00	1000.000	0.00
1:ILE_73:HG11	1:ILE_73:HG12	1.800	5.000	5.000	10.00	10.00	1000.000	0.00
1:ILE_73:HG12	1:ILE_73:HG2*	1.800	6.500	5.000	10.00	10.00	1000.000	0.00
1:ILE_73:HG11	1:ILE_73:HA	1.800	5.000	5.000	10.00	10.00	1000.000	0.00
1:LYS+_23:HD2	1:LYS+_23:HG*	1.800	6.000	5.000	10.00	10.00	1000.000	0.00
1:LYS+_23:HD1	1:LYS+_23:HG*	1.800	6.000	5.000	10.00	10.00	1000.000	0.00
1:LYS+_23:HD1	1:LYS+_23:HE*	1.800	6.000	5.000	10.00	10.00	1000.000	0.00
1:LYS+_23:HD2	1:LYS+_23:HA	1.800	5.000	5.000	10.00	10.00	1000.000	0.00
1:LEU_58:HG	1:PRO_53:HB2	1.800	5.000	5.000	10.00	10.00	1000.000	0.00
1:LEU_58:HG	1:LEU_58:HB*	1.800	6.000	5.000	10.00	10.00	1000.000	0.00
1:ILE_37:HG1*	1:ILE_37:HD1*	1.800	7.500	5.000	10.00	10.00	1000.000	0.00
1:ILE_37:HG1*	1:ILE_37:HG2*	1.800	7.500	5.000	10.00	10.00	1000.000	0.00
1:ILE_37:HG1*	1:ILE_37:HB	1.800	6.000	5.000	10.00	10.00	1000.000	0.00
1:ILE_37:HG1*	1:ILE_37:HA	1.800	6.000	5.000	10.00	10.00	1000.000	0.00
1:LYS+_23:HD1	1:LYS+_23:HD2	1.800	5.000	5.000	10.00	10.00	1000.000	0.00
1:LYS+_23:HD2	1:LYS+_23:HE*	1.800	6.000	5.000	10.00	10.00	1000.000	0.00
1:LEU_58:HG	1:LEU_58:HD1*	1.800	6.500	5.000	10.00	10.00	1000.000	0.00
1:LEU_58:HG	1:LEU_58:HD2*	1.800	6.500	5.000	10.00	10.00	1000.000	0.00
1:LEU_58:HG	1:LYS+_55:HA	1.800	5.000	5.000	10.00	10.00	1000.000	0.00
1:LEU_58:HG	1:LEU_58:HA	1.800	5.000	5.000	10.00	10.00	1000.000	0.00
1:LEU_42:HG	1:LEU_42:HD1*	1.800	6.500	5.000	10.00	10.00	1000.000	0.00
1:LEU_42:HG	1:LEU_42:HA	1.800	5.000	5.000	10.00	10.00	1000.000	0.00
1:LEU_14:HG	1:LEU_14:HD2*	1.800	6.500	5.000	10.00	10.00	1000.000	0.00
1:LEU_14:HG	1:LEU_14:HD1*	1.800	6.500	5.000	10.00	10.00	1000.000	0.00
1:LEU_79:HD1*	1:LEU_79:HG	1.800	6.500	5.000	10.00	10.00	1000.000	0.00
1:LEU_79:HD1*	1:ALA_10:HB*	1.800	8.000	5.000	10.00	10.00	1000.000	0.00
1:LEU_79:HD1*	1:LEU_79:HB2	1.800	6.500	5.000	10.00	10.00	1000.000	0.00
1:LEU_79:HD1*	1:LEU_79:HA	1.800	6.500	5.000	10.00	10.00	1000.000	0.00
1:LEU_49:HD2*	1:MET_46:HA	1.800	6.500	5.000	10.00	10.00	1000.000	0.00
1:LEU_49:HD2*	1:MET_46:HG2	1.800	6.500	5.000	10.00	10.00	1000.000	0.00
1:LEU_49:HD2*	1:MET_46:HG1	1.800	6.500	5.000	10.00	10.00	1000.000	0.00
1:LEU_58:HD2*	1:LEU_58:HA	1.800	6.500	5.000	10.00	10.00	1000.000	0.00
1:LEU_42:HD1*	1:LEU_42:HA	1.800	6.500	5.000	10.00	10.00	1000.000	0.00
1:LYS+_87:HG2	1:LYS+_87:HG1	1.800	5.000	5.000	10.00	10.00	1000.000	0.00
1:LYS+_87:HG1	1:LYS+_87:HB1	1.800	5.000	5.000	10.00	10.00	1000.000	0.00
1:LYS+_87:HG1	1:LYS+_87:HB2	1.800	5.000	5.000	10.00	10.00	1000.000	0.00
1:LYS+_87:HG1	1:LYS+_87:HA	1.800	5.000	5.000	10.00	10.00	1000.000	0.00
1:LYS+_87:HG2	1:LYS+_87:HA	1.800	5.000	5.000	10.00	10.00	1000.000	0.00
1:LYS+_55:HG*	1:LYS+_55:HE*	1.800	7.000	5.000	10.00	10.00	1000.000	0.00
1:LYS+_55:HG*	1:LYS+_55:HA	1.800	6.000	5.000	10.00	10.00	1000.000	0.00
1:LYS+_55:HG*	1:LYS+_55:HD1	1.800	6.000	5.000	10.00	10.00	1000.000	0.00
1:LYS+_40:HG1	1:LYS+_40:HD*	1.800	6.000	5.000	10.00	10.00	1000.000	0.00
1:LYS+_40:HG1	1:LYS+_40:HB2	1.800	5.000	5.000	10.00	10.00	1000.000	0.00
1:LYS+_40:HG2	1:LYS+_40:HE*	1.800	6.000	5.000	10.00	10.00	1000.000	0.00
1:LYS+_40:HG1	1:LYS+_40:HE*	1.800	6.000	5.000	10.00	10.00	1000.000	0.00
1:LYS+_40:HG2	1:LYS+_40:HA	1.800	5.000	5.000	10.00	10.00	1000.000	0.00
1:LYS+_40:HG1	1:LYS+_40:HA	1.800	5.000	5.000	10.00	10.00	1000.000	0.00
1:LEU_14:HD2*	1:LEU_14:HB2	1.800	6.500	5.000	10.00	10.00	1000.000	0.00
1:LEU_14:HD2*	1:MET_86:HE*	1.800	8.000	5.000	10.00	10.00	1000.000	0.00
1:VAL_83:HG2*	1:VAL_83:HG1*	1.800	8.000	5.000	10.00	10.00	1000.000	0.00
1:VAL_83:HG2*	1:VAL_83:HA	1.800	6.500	5.000	10.00	10.00	1000.000	0.00
1:VAL_80:HG2*	1:VAL_80:HG1*	1.800	8.000	5.000	10.00	10.00	1000.000	0.00
1:VAL_80:HG2*	1:GLU-_77:HA	1.800	6.500	5.000	10.00	10.00	1000.000	0.00
1:LEU_42:HD2*	1:LEU_42:HB2	1.800	6.500	5.000	10.00	10.00	1000.000	0.00
1:LEU_42:HD2*	1:LEU_42:HA	1.800	6.500	5.000	10.00	10.00	1000.000	0.00
1:VAL_83:HG2*	1:ALA_10:HB*	1.800	8.000	5.000	10.00	10.00	1000.000	0.00
1:VAL_80:HG2*	1:ALA_10:HB*	1.800	8.000	5.000	10.00	10.00	1000.000	0.00
1:LEU_79:HD2*	1:LEU_79:HG	1.800	6.500	5.000	10.00	10.00	1000.000	0.00
1:LEU_79:HD2*	1:LEU_79:HB2	1.800	6.500	5.000	10.00	10.00	1000.000	0.00

1:LEU_58:HD1*	1:PRO_53:HB2	1.800	6.500	5.000	10.00	10.00	1000.000	0.00
1:LEU_58:HD1*	1:LEU_58:HA	1.800	6.500	5.000	10.00	10.00	1000.000	0.00
1:LEU_58:HD1*	1:GLY_43:HA1	1.800	6.500	5.000	10.00	10.00	1000.000	0.00
1:THR_39:HG2*	1:ILE_62:HG2*	1.800	8.000	5.000	10.00	10.00	1000.000	0.00
1:THR_39:HG2*	1:ASP-_59:HA	1.800	6.500	5.000	10.00	10.00	1000.000	0.00
1:THR_72:HG2*	1:GLY_71:HA2	1.800	6.500	5.000	10.00	10.00	1000.000	0.00
1:LEU_49:HD1*	1:LEU_49:HA	1.800	6.500	5.000	10.00	10.00	1000.000	0.00
1:VAL_65:HG2*	1:VAL_65:HA	1.800	6.500	5.000	10.00	10.00	1000.000	0.00
1:THR_44:HG2*	1:LEU_58:HD1*	1.800	8.000	5.000	10.00	10.00	1000.000	0.00
1:THR_44:HG2*	1:MET_48:HE*	1.800	8.000	5.000	10.00	10.00	1000.000	0.00
1:VAL_80:HG1*	1:ARG+_84:HD*	1.800	7.500	5.000	10.00	10.00	1000.000	0.00
1:ALAC_90:HB*	1:ALAC_90:HA	1.800	6.500	5.000	10.00	10.00	1000.000	0.00
1:VAL_65:HG1*	1:ILE_73:HG2*	1.800	8.000	5.000	10.00	10.00	1000.000	0.00
1:VAL_65:HG2*	1:VAL_65:HB	1.800	6.500	5.000	10.00	10.00	1000.000	0.00
1:ALA_25:HB*	1:MET_48:HE*	1.800	8.000	5.000	10.00	10.00	1000.000	0.00
1:ALA_25:HB*	1:ALA_24:HB*	1.800	8.000	5.000	10.00	10.00	1000.000	0.00
1:ALA_25:HB*	1:PHE_22:HA	1.800	6.500	5.000	10.00	10.00	1000.000	0.00
1:ALA_10:HB*	1:VAL_83:HG1*	1.800	8.000	5.000	10.00	10.00	1000.000	0.00
1:ALA_10:HB*	1:GLN_7:HA	1.800	6.500	5.000	10.00	10.00	1000.000	0.00
1:MET_48:HE*	1:VAL_45:HG1*	1.800	8.000	5.000	10.00	10.00	1000.000	0.00
1:MET_48:HE*	1:VAL_45:HG2*	1.800	8.000	5.000	10.00	10.00	1000.000	0.00
1:MET_48:HE*	1:VAL_45:HA	1.800	6.500	5.000	10.00	10.00	1000.000	0.00
1:MET_48:HE*	1:MET_48:HA	1.800	6.500	5.000	10.00	10.00	1000.000	0.00
1:MET_46:HE*	1:MET_46:HA	1.800	6.500	5.000	10.00	10.00	1000.000	0.00
1:MET_28:HE*	1:MET_28:HG1	1.800	6.500	5.000	10.00	10.00	1000.000	0.00
1:MET_28:HE*	1:MET_28:HG2	1.800	6.500	5.000	10.00	10.00	1000.000	0.00
1:MET_28:HE*	1:MET_28:HA	1.800	6.500	5.000	10.00	10.00	1000.000	0.00
1:ILE_19:HG2*	1:LEU_79:HD1*	1.800	8.000	5.000	10.00	10.00	1000.000	0.00
1:ILE_19:HG2*	1:PHE_22:HB*	1.800	7.500	5.000	10.00	10.00	1000.000	0.00
1:MET_18:HE*	1:LEU_14:HD2*	1.800	8.000	5.000	10.00	10.00	1000.000	0.00
1:MET_86:HE*	1:MET_86:HG1	1.800	6.500	5.000	10.00	10.00	1000.000	0.00
1:MET_86:HE*	1:MET_86:HG2	1.800	6.500	5.000	10.00	10.00	1000.000	0.00
1:MET_86:HE*	1:VAL_83:HA	1.800	6.500	5.000	10.00	10.00	1000.000	0.00
1:MET_86:HE*	1:MET_86:HA	1.800	6.500	5.000	10.00	10.00	1000.000	0.00
1:MET_81:HE*	1:ILE_73:HG2*	1.800	8.000	5.000	10.00	10.00	1000.000	0.00
1:MET_81:HE*	1:MET_81:HA	1.800	6.500	5.000	10.00	10.00	1000.000	0.00
1:ILE_61:HG2*	1:ILE_61:HG11	1.800	6.500	5.000	10.00	10.00	1000.000	0.00
1:ILE_61:HG2*	1:ILE_61:HG12	1.800	6.500	5.000	10.00	10.00	1000.000	0.00
1:ILE_61:HG2*	1:ILE_61:HB	1.800	6.500	5.000	10.00	10.00	1000.000	0.00
1:ILE_61:HG2*	1:ILE_61:HA	1.800	6.500	5.000	10.00	10.00	1000.000	0.00
1:MET_3:HE*	1:ASP-_68:HB2	1.800	6.500	5.000	10.00	10.00	1000.000	0.00
1:ILE_62:HG2*	1:GLU-_63:HA	1.800	6.500	5.000	10.00	10.00	1000.000	0.00
1:ILE_62:HG2*	1:ILE_62:HD1*	1.800	8.000	5.000	10.00	10.00	1000.000	0.00
1:ILE_62:HG2*	1:ASP-_66:HB2	1.800	6.500	5.000	10.00	10.00	1000.000	0.00
1:ILE_62:HG2*	1:THR_72:HA	1.800	6.500	5.000	10.00	10.00	1000.000	0.00
1:LEU_14:HB1	1:LEU_14:HD2*	1.800	6.500	5.000	10.00	10.00	1000.000	0.00
1:GLY_35:HA2	1:GLY_35:HA1	1.800	5.000	5.000	10.00	10.00	1000.000	0.00
1:ILE_37:HD1*	1:ILE_73:HD1*	1.800	8.000	5.000	10.00	10.00	1000.000	0.00
1:ILE_37:HD1*	1:ILE_37:HG2*	1.800	8.000	5.000	10.00	10.00	1000.000	0.00
1:ILE_37:HD1*	1:ILE_73:HG2*	1.800	8.000	5.000	10.00	10.00	1000.000	0.00
1:ILE_37:HD1*	1:ILE_73:HB	1.800	6.500	5.000	10.00	10.00	1000.000	0.00
1:ILE_37:HD1*	1:ILE_37:HA	1.800	6.500	5.000	10.00	10.00	1000.000	0.00
1:ILE_73:HD1*	1:ILE_73:HG2*	1.800	8.000	5.000	10.00	10.00	1000.000	0.00
1:ILE_73:HD1*	1:ILE_73:HG12	1.800	6.500	5.000	10.00	10.00	1000.000	0.00
1:ILE_73:HD1*	1:ILE_73:HA	1.800	6.500	5.000	10.00	10.00	1000.000	0.00
1:ILE_61:HD1*	1:ILE_61:HG11	1.800	6.500	5.000	10.00	10.00	1000.000	0.00
1:ILE_61:HD1*	1:ILE_61:HA	1.800	6.500	5.000	10.00	10.00	1000.000	0.00
1:ARG+_47:HD*	1:ARG+_47:HA	1.800	6.000	5.000	10.00	10.00	1000.000	0.00
1:ILE_19:HD1*	1:ILE_19:HG2*	1.800	8.000	5.000	10.00	10.00	1000.000	0.00
1:ILE_19:HD1*	1:ILE_19:HA	1.800	6.500	5.000	10.00	10.00	1000.000	0.00
1:LEU_42:HB1	1:LEU_42:HB2	1.800	5.000	5.000	10.00	10.00	1000.000	0.00
1:LEU_42:HB2	1:LEU_42:HD1*	1.800	6.500	5.000	10.00	10.00	1000.000	0.00
1:LEU_42:HB1	1:LEU_42:HD1*	1.800	6.500	5.000	10.00	10.00	1000.000	0.00
1:LEU_42:HB2	1:THR_39:HA	1.800	5.000	5.000	10.00	10.00	1000.000	0.00
1:LEU_42:HB1	1:LEU_42:HA	1.800	5.000	5.000	10.00	10.00	1000.000	0.00
1:LEU_42:HB2	1:LEU_42:HA	1.800	5.000	5.000	10.00	10.00	1000.000	0.00
1:THR_54:HB	1:THR_54:HG2*	1.800	6.500	5.000	10.00	10.00	1000.000	0.00
1:THR_54:HB	1:THR_54:HA	1.800	5.000	5.000	10.00	10.00	1000.000	0.00
1:THR_4:HB	1:THR_4:HA	1.800	5.000	5.000	10.00	10.00	1000.000	0.00
1:THR_4:HB	1:THR_4:HG2*	1.800	6.500	5.000	10.00	10.00	1000.000	0.00
1:THR_44:HB	1:VAL_45:HG1*	1.800	6.500	5.000	10.00	10.00	1000.000	0.00
1:THR_44:HB	1:THR_44:HG2*	1.800	6.500	5.000	10.00	10.00	1000.000	0.00
1:THR_44:HB	1:GLU-_41:HA	1.800	5.000	5.000	10.00	10.00	1000.000	0.00
1:THR_44:HB	1:THR_44:HA	1.800	5.000	5.000	10.00	10.00	1000.000	0.00
1:THR_39:HB	1:LEU_42:HD1*	1.800	6.500	5.000	10.00	10.00	1000.000	0.00
1:THR_39:HB	1:THR_39:HG2*	1.800	6.500	5.000	10.00	10.00	1000.000	0.00
1:VAL_80:HA	1:VAL_80:HG1*	1.800	6.500	5.000	10.00	10.00	1000.000	0.00
1:VAL_80:HA	1:VAL_80:HG2*	1.800	6.500	5.000	10.00	10.00	1000.000	0.00

1:VAL_80:HA	1:VAL_83:HG2*	1.800	6.500	5.000	10.00	10.00	1000.000	0.00
1:VAL_80:HA	1:VAL_80:HB	1.800	5.000	5.000	10.00	10.00	1000.000	0.00
1:THR_44:HA	1:THR_44:HG2*	1.800	6.500	5.000	10.00	10.00	1000.000	0.00
1:THR_44:HA	1:ARG+_47:HD*	1.800	6.000	5.000	10.00	10.00	1000.000	0.00
1:THR_44:HA	1:VAL_45:HA	1.800	5.000	5.000	10.00	10.00	1000.000	0.00
1:VAL_80:HA	1:ALA_10:HB*	1.800	6.500	5.000	10.00	10.00	1000.000	0.00
1:VAL_83:HA	1:VAL_83:HG1*	1.800	6.500	5.000	10.00	10.00	1000.000	0.00
1:VAL_83:HA	1:VAL_83:HB	1.800	5.000	5.000	10.00	10.00	1000.000	0.00
1:THR_39:HA	1:THR_39:HG2*	1.800	6.500	5.000	10.00	10.00	1000.000	0.00
1:THR_39:HA	1:LEU_42:HB1	1.800	5.000	5.000	10.00	10.00	1000.000	0.00
1:THR_39:HA	1:THR_39:HB	1.800	5.000	5.000	10.00	10.00	1000.000	0.00
1:SER_38:HB1	1:THR_72:HG2*	1.800	6.500	5.000	10.00	10.00	1000.000	0.00
1:SER_38:HB2	1:THR_72:HG2*	1.800	6.500	5.000	10.00	10.00	1000.000	0.00
1:ILE_19:HA	1:LEU_79:HD2*	1.800	6.500	5.000	10.00	10.00	1000.000	0.00
1:ILE_19:HA	1:ILE_19:HG11	1.800	5.000	5.000	10.00	10.00	1000.000	0.00
1:ILE_19:HA	1:ILE_19:HG2*	1.800	6.500	5.000	10.00	10.00	1000.000	0.00
1:ILE_19:HA	1:MET_18:HB1	1.800	5.000	5.000	10.00	10.00	1000.000	0.00
1:VAL_45:HA	1:VAL_45:HB	1.800	5.000	5.000	10.00	10.00	1000.000	0.00
1:SER_38:HB1	1:SER_38:HA	1.800	5.000	5.000	10.00	10.00	1000.000	0.00
1:SER_38:HB2	1:SER_38:HA	1.800	5.000	5.000	10.00	10.00	1000.000	0.00
1:SER_38:HB2	1:SER_38:HB1	1.800	5.000	5.000	10.00	10.00	1000.000	0.00
1:SER_15:HB1	1:SER_15:HB2	1.800	5.000	5.000	10.00	10.00	1000.000	0.00
1:SER_70:HB1	1:THR_72:HB	1.800	5.000	5.000	10.00	10.00	1000.000	0.00
1:SER_70:HB2	1:SER_70:HB1	1.800	5.000	5.000	10.00	10.00	1000.000	0.00
1:ILE_62:HA	1:ILE_62:HG2*	1.800	6.500	5.000	10.00	10.00	1000.000	0.00
1:ILE_62:HA	1:GLU-_63:HA	1.800	5.000	5.000	10.00	10.00	1000.000	0.00
1:ILE_61:HA	1:ILE_62:HA	1.800	5.000	5.000	10.00	10.00	1000.000	0.00
1:ILE_61:HA	1:ALA_60:HA	1.800	5.000	5.000	10.00	10.00	1000.000	0.00
1:PHE_26:HA	1:ILE_37:HD1*	1.800	6.500	5.000	10.00	10.00	1000.000	0.00
1:PHE_26:HA	1:ALA_25:HB*	1.800	6.500	5.000	10.00	10.00	1000.000	0.00
1:PHE_26:HA	1:PHE_26:HB*	1.800	6.000	5.000	10.00	10.00	1000.000	0.00
1:PHE_26:HA	1:PHE_29:HB2	1.800	5.000	5.000	10.00	10.00	1000.000	0.00
1:PHE_75:HA	1:PHE_78:HB2	1.800	5.000	5.000	10.00	10.00	1000.000	0.00
1:PHE_75:HA	1:PHE_78:HB1	1.800	5.000	5.000	10.00	10.00	1000.000	0.00
1:PHE_75:HA	1:PHE_75:HB2	1.800	5.000	5.000	10.00	10.00	1000.000	0.00
1:PHE_75:HA	1:PHE_75:HB1	1.800	5.000	5.000	10.00	10.00	1000.000	0.00
1:PHE_78:HA	1:ILE_73:HG2*	1.800	6.500	5.000	10.00	10.00	1000.000	0.00
1:THR_4:HA	1:THR_4:HG2*	1.800	6.500	5.000	10.00	10.00	1000.000	0.00
1:ILE_73:HA	1:ILE_73:HG12	1.800	5.000	5.000	10.00	10.00	1000.000	0.00
1:VAL_65:HA	1:VAL_65:HG1*	1.800	6.500	5.000	10.00	10.00	1000.000	0.00
1:GLU-_56:HA	1:GLU-_56:HG1	1.800	5.000	5.000	10.00	10.00	1000.000	0.00
1:GLU-_56:HA	1:GLU-_56:HG2	1.800	5.000	5.000	10.00	10.00	1000.000	0.00
1:ILE_73:HA	1:ILE_73:HG2*	1.800	6.500	5.000	10.00	10.00	1000.000	0.00
1:ILE_73:HA	1:ILE_73:HB	1.800	5.000	5.000	10.00	10.00	1000.000	0.00
1:SER_70:HA	1:SER_70:HB1	1.800	5.000	5.000	10.00	10.00	1000.000	0.00
1:THR_54:HA	1:THR_54:HG2*	1.800	6.500	5.000	10.00	10.00	1000.000	0.00
1:ILE_37:HA	1:ILE_37:HG2*	1.800	6.500	5.000	10.00	10.00	1000.000	0.00
1:ILE_37:HA	1:ILE_37:HB	1.800	5.000	5.000	10.00	10.00	1000.000	0.00
1:GLU-_17:HA	1:GLU-_17:HB2	1.800	5.000	5.000	10.00	10.00	1000.000	0.00
1:GLU-_17:HA	1:GLU-_17:HB1	1.800	5.000	5.000	10.00	10.00	1000.000	0.00
1:GLU-_17:HA	1:GLU-_17:HG1	1.800	5.000	5.000	10.00	10.00	1000.000	0.00
1:GLU-_16:HA	1:ILE_19:HD1*	1.800	6.500	5.000	10.00	10.00	1000.000	0.00
1:GLU-_16:HA	1:ILE_19:HG2*	1.800	6.500	5.000	10.00	10.00	1000.000	0.00
1:GLU-_16:HA	1:GLU-_16:HB1	1.800	5.000	5.000	10.00	10.00	1000.000	0.00
1:GLU-_16:HA	1:GLU-_16:HB2	1.800	5.000	5.000	10.00	10.00	1000.000	0.00
1:GLU-_16:HA	1:GLU-_16:HG2	1.800	5.000	5.000	10.00	10.00	1000.000	0.00
1:GLU-_16:HA	1:GLU-_16:HG1	1.800	5.000	5.000	10.00	10.00	1000.000	0.00
1:LYS+_55:HA	1:THR_54:HA	1.800	5.000	5.000	10.00	10.00	1000.000	0.00
1:ARG+_84:HA	1:ARG+_84:HD*	1.800	6.000	5.000	10.00	10.00	1000.000	0.00
1:MET_81:HA	1:ARG+_84:HG1	1.800	5.000	5.000	10.00	10.00	1000.000	0.00
1:GLU-_67:HA	1:ASP-_68:HA	1.800	5.000	5.000	10.00	10.00	1000.000	0.00
1:GLU-_63:HA	1:ASP-_66:HB2	1.800	5.000	5.000	10.00	10.00	1000.000	0.00
1:MET_46:HA	1:MET_46:HG2	1.800	5.000	5.000	10.00	10.00	1000.000	0.00
1:MET_46:HA	1:ARG+_47:HA	1.800	5.000	5.000	10.00	10.00	1000.000	0.00
1:LYS+_40:HA	1:THR_39:HA	1.800	5.000	5.000	10.00	10.00	1000.000	0.00
1:GLU-_21:HA	1:PHE_22:HA	1.800	5.000	5.000	10.00	10.00	1000.000	0.00
1:PHE_13:HA	1:LEU_14:HA	1.800	5.000	5.000	10.00	10.00	1000.000	0.00
1:GLU-_76:HA	1:LEU_79:HD1*	1.800	6.500	5.000	10.00	10.00	1000.000	0.00
1:GLU-_41:HA	1:GLU-_41:HG*	1.800	6.000	5.000	10.00	10.00	1000.000	0.00
1:PHE_22:HA	1:LEU_79:HD2*	1.800	6.500	5.000	10.00	10.00	1000.000	0.00
1:LYS+_23:HA	1:LYS+_23:HD1	1.800	5.000	5.000	10.00	10.00	1000.000	0.00
1:THR_72:HA	1:ILE_73:HG2*	1.800	6.500	5.000	10.00	10.00	1000.000	0.00
1:PHE_29:HA	1:MET_28:HA	1.800	5.000	5.000	10.00	10.00	1000.000	0.00
1:MET_18:HA	1:ILE_19:HA	1.800	5.000	5.000	10.00	10.00	1000.000	0.00
1:GLN_7:HA	1:GLN_7:HG*	1.800	6.000	5.000	10.00	10.00	1000.000	0.00
1:GLN_7:HA	1:VAL_80:HG2*	1.800	6.500	5.000	10.00	10.00	1000.000	0.00
1:SER_2:HA	1:SER_2:HB*	1.800	6.000	5.000	10.00	10.00	1000.000	0.00
1:MET_86:HA	1:MET_86:HG1	1.800	5.000	5.000	10.00	10.00	1000.000	0.00

1:MET_86:HA	1:MET_86:HB2	1.800	5.000	5.000	10.00	10.00	1000.000	0.00
1:LEU_79:HA	1:LEU_79:HD2*	1.800	6.500	5.000	10.00	10.00	1000.000	0.00
1:LEU_79:HA	1:LEU_79:HG	1.800	5.000	5.000	10.00	10.00	1000.000	0.00
1:LEU_79:HA	1:LEU_79:HB2	1.800	5.000	5.000	10.00	10.00	1000.000	0.00
1:THR_72:HA	1:THR_72:HG2*	1.800	6.500	5.000	10.00	10.00	1000.000	0.00
1:THR_72:HA	1:THR_72:HB	1.800	5.000	5.000	10.00	10.00	1000.000	0.00
1:MET_28:HA	1:MET_28:HG2	1.800	5.000	5.000	10.00	10.00	1000.000	0.00
1:LYS+_87:HA	1:LYS+_87:HB1	1.800	5.000	5.000	10.00	10.00	1000.000	0.00
1:LYS+_87:HA	1:LYS+_87:HB2	1.800	5.000	5.000	10.00	10.00	1000.000	0.00
1:GLN_85:HA	1:ARG+_84:HA	1.800	5.000	5.000	10.00	10.00	1000.000	0.00
1:ASP-_5:HA	1:ALA_8:HB*	1.800	6.500	5.000	10.00	10.00	1000.000	0.00
1:ASP-_5:HA	1:ASP-_5:HB1	1.800	5.000	5.000	10.00	10.00	1000.000	0.00
1:ASP-_59:HA	1:ILE_62:HG2*	1.800	6.500	5.000	10.00	10.00	1000.000	0.00
1:MET_82:HA	1:MET_82:HG2	1.800	5.000	5.000	10.00	10.00	1000.000	0.00
1:MET_82:HA	1:MET_82:HB1	1.800	5.000	5.000	10.00	10.00	1000.000	0.00
1:MET_82:HA	1:MET_82:HB2	1.800	5.000	5.000	10.00	10.00	1000.000	0.00
1:SER_15:HA	1:SER_15:HB1	1.800	5.000	5.000	10.00	10.00	1000.000	0.00
1:SER_15:HA	1:SER_15:HB2	1.800	5.000	5.000	10.00	10.00	1000.000	0.00
1:SER_38:HA	1:THR_72:HG2*	1.800	6.500	5.000	10.00	10.00	1000.000	0.00
1:SER_38:HA	1:THR_72:HB	1.800	5.000	5.000	10.00	10.00	1000.000	0.00
1:ALA_10:HA	1:VAL_83:HG1*	1.800	6.500	5.000	10.00	10.00	1000.000	0.00
1:ALA_10:HA	1:VAL_83:HG2*	1.800	6.500	5.000	10.00	10.00	1000.000	0.00
1:ALA_10:HA	1:ALA_10:HB*	1.800	6.500	5.000	10.00	10.00	1000.000	0.00
1:ALA_31:HA	1:ALA_31:HB*	1.800	6.500	5.000	10.00	10.00	1000.000	0.00
1:ALA_31:HA	1:ASP-_32:HA	1.800	5.000	5.000	10.00	10.00	1000.000	0.00
1:ALA_25:HA	1:ALA_25:HB*	1.800	6.500	5.000	10.00	10.00	1000.000	0.00
1:ALAC_90:HA	1:ASP-_89:HA	1.800	5.000	5.000	10.00	10.00	1000.000	0.00
1:LEU_49:HA	1:LEU_49:HD2*	1.800	6.500	5.000	10.00	10.00	1000.000	0.00
1:LEU_14:HA	1:LEU_14:HD2*	1.800	6.500	5.000	10.00	10.00	1000.000	0.00
1:LEU_14:HA	1:LEU_14:HB2	1.800	5.000	5.000	10.00	10.00	1000.000	0.00
1:ALA_12:HA	1:ALA_12:HB*	1.800	6.500	5.000	10.00	10.00	1000.000	0.00
1:ASP-_74:HA	1:ASP-_36:HB1	1.800	5.000	5.000	10.00	10.00	1000.000	0.00
1:ASP-_74:HA	1:ASP-_36:HA	1.800	5.000	5.000	10.00	10.00	1000.000	0.00
1:ASP-_36:HA	1:ASP-_74:HB1	1.800	5.000	5.000	10.00	10.00	1000.000	0.00
1:ASP-_36:HA	1:ASP-_74:HB2	1.800	5.000	5.000	10.00	10.00	1000.000	0.00
1:ASP-_32:HA	1:ALA_31:HB*	1.800	6.500	5.000	10.00	10.00	1000.000	0.00
1:ASP-_30:HA	1:ILE_37:HD1*	1.800	6.500	5.000	10.00	10.00	1000.000	0.00
1:ALAN_1:HA	1:ALAN_1:HB*	1.800	6.500	5.000	10.00	10.00	1000.000	0.00
1:ASN_52:HA	1:PRO_53:HB2	1.800	5.000	5.000	10.00	10.00	1000.000	0.00
1:PRO_53:HD1	1:PRO_53:HG*	1.800	6.000	5.000	10.00	10.00	1000.000	0.00
1:PRO_53:HD2	1:PRO_53:HG*	1.800	6.000	5.000	10.00	10.00	1000.000	0.00
1:PRO_53:HD1	1:PRO_53:HD2	1.800	5.000	5.000	10.00	10.00	1000.000	0.00
1:PRO_53:HD2	1:PRO_53:HA	1.800	5.000	5.000	10.00	10.00	1000.000	0.00
1:PRO_53:HD1	1:PRO_53:HA	1.800	5.000	5.000	10.00	10.00	1000.000	0.00
1:PRO_53:HD2	1:ASN_52:HA	1.800	5.000	5.000	10.00	10.00	1000.000	0.00
1:PRO_53:HD1	1:ASN_52:HA	1.800	5.000	5.000	10.00	10.00	1000.000	0.00
1:GLY_43:HA2	1:LEU_58:HD2*	1.800	6.500	5.000	10.00	10.00	1000.000	0.00
1:GLY_43:HA2	1:GLY_43:HA1	1.800	5.000	5.000	10.00	10.00	1000.000	0.00
1:GLY_43:HA1	1:LEU_58:HD2*	1.800	6.500	5.000	10.00	10.00	1000.000	0.00
1:GLY_71:HA2	1:ILE_62:HG2*	1.800	6.500	5.000	10.00	10.00	1000.000	0.00
1:GLY_71:HA1	1:ILE_62:HG2*	1.800	6.500	5.000	10.00	10.00	1000.000	0.00
1:GLY_71:HA2	1:GLY_71:HA1	1.800	5.000	5.000	10.00	10.00	1000.000	0.00
1:GLY_50:HA2	1:GLY_50:HA1	1.800	5.000	5.000	10.00	10.00	1000.000	0.00
1:LEU_14:HB1	1:LEU_14:HA	1.800	5.000	5.000	10.00	10.00	1000.000	0.00
1:LEU_14:HB1	1:LEU_14:HD1*	1.800	6.500	5.000	10.00	10.00	1000.000	0.00
1:LEU_14:HB2	1:LEU_14:HD1*	1.800	6.500	5.000	10.00	10.00	1000.000	0.00
1:LEU_14:HB2	1:LEU_14:HB1	1.800	5.000	5.000	10.00	10.00	1000.000	0.00
1:LEU_14:HB1	1:LEU_14:HG	1.800	5.000	5.000	10.00	10.00	1000.000	0.00
1:ARG+_84:HD*	1:ARG+_84:HG1	1.800	6.000	5.000	10.00	10.00	1000.000	0.00
1:ARG+_84:HD*	1:MET_81:HA	1.800	6.000	5.000	10.00	10.00	1000.000	0.00
1:THR_72:HB	1:ASP-_36:HB2	1.800	5.000	5.000	10.00	10.00	1000.000	0.00
1:THR_72:HB	1:ASP-_36:HB1	1.800	5.000	5.000	10.00	10.00	1000.000	0.00
1:THR_72:HB	1:GLY_71:HA2	1.800	5.000	5.000	10.00	10.00	1000.000	0.00
1:THR_72:HB	1:ASP-_36:HA	1.800	5.000	5.000	10.00	10.00	1000.000	0.00
1:THR_72:HB	1:THR_72:HG2*	1.800	6.500	5.000	10.00	10.00	1000.000	0.00
1:ARG+_47:HD*	1:ASN_52:HA	1.800	6.000	5.000	10.00	10.00	1000.000	0.00
1:ILE_73:HN	1:THR_72:HG2*	1.800	6.500	5.000	10.00	10.00	1000.000	0.00
1:ILE_73:HN	1:ILE_73:HG12	1.800	5.000	5.000	10.00	10.00	1000.000	0.00
1:ILE_73:HN	1:ILE_73:HB	1.800	5.000	5.000	10.00	10.00	1000.000	0.00
1:ILE_73:HN	1:THR_72:HB	1.800	5.000	5.000	10.00	10.00	1000.000	0.00
1:ILE_37:HN	1:ILE_37:HD1*	1.800	6.500	5.000	10.00	10.00	1000.000	0.00
1:ILE_37:HN	1:ILE_37:HG1*	1.800	6.000	5.000	10.00	10.00	1000.000	0.00
1:ILE_37:HN	1:ILE_37:HB	1.800	5.000	5.000	10.00	10.00	1000.000	0.00
1:ILE_37:HN	1:ASP-_36:HB2	1.800	5.000	5.000	10.00	10.00	1000.000	0.00
1:LYS+_23:HN	1:LYS+_23:HD1	1.800	5.000	5.000	10.00	10.00	1000.000	0.00
1:LYS+_23:HN	1:LYS+_23:HG*	1.800	6.000	5.000	10.00	10.00	1000.000	0.00
1:LYS+_23:HN	1:LYS+_23:HD2	1.800	5.000	5.000	10.00	10.00	1000.000	0.00
1:LYS+_23:HN	1:LYS+_23:HB*	1.800	6.000	5.000	10.00	10.00	1000.000	0.00

1:LYS+_23:HN	1:PHE_22:HB*	1.800	6.000	5.000	10.00	10.00	1000.000	0.00
1:LYS+_23:HN	1:PHE_22:HN	1.800	5.000	5.000	10.00	10.00	1000.000	0.00
1:ALA_10:HN	1:VAL_80:HG2*	1.800	6.500	5.000	10.00	10.00	1000.000	0.00
1:ALA_10:HN	1:ALA_10:HB*	1.800	6.500	5.000	10.00	10.00	1000.000	0.00
1:ALA_10:HN	1:GLU-_9:HN	1.800	5.000	5.000	10.00	10.00	1000.000	0.00
1:ALA_8:HN	1:VAL_80:HG2*	1.800	6.500	5.000	10.00	10.00	1000.000	0.00
1:ALA_8:HN	1:ALA_8:HB*	1.800	6.500	5.000	10.00	10.00	1000.000	0.00
1:ALA_8:HN	1:GLN_7:HB1	1.800	5.000	5.000	10.00	10.00	1000.000	0.00
1:ALA_8:HN	1:GLN_7:HB2	1.800	5.000	5.000	10.00	10.00	1000.000	0.00
1:ALA_8:HN	1:ASP-_5:HB1	1.800	5.000	5.000	10.00	10.00	1000.000	0.00
1:ALA_8:HN	1:GLN_7:HN	1.800	5.000	5.000	10.00	10.00	1000.000	0.00
1:ALA_8:HN	1:GLU-_9:HN	1.800	5.000	5.000	10.00	10.00	1000.000	0.00
1:SER_38:HN	1:SER_38:HB1	1.800	5.000	5.000	10.00	10.00	1000.000	0.00
1:SER_38:HN	1:ILE_37:HD1*	1.800	6.500	5.000	10.00	10.00	1000.000	0.00
1:SER_38:HN	1:ILE_37:HG2*	1.800	6.500	5.000	10.00	10.00	1000.000	0.00
1:SER_38:HN	1:GLU-_41:HN	1.800	5.000	5.000	10.00	10.00	1000.000	0.00
1:SER_38:HN	1:LEU_42:HN	1.800	5.000	5.000	10.00	10.00	1000.000	0.00
1:PHE_78:HN	1:ILE_73:HG2*	1.800	6.500	5.000	10.00	10.00	1000.000	0.00
1:PHE_78:HN	1:PHE_78:HB1	1.800	5.000	5.000	10.00	10.00	1000.000	0.00
1:PHE_78:HN	1:PHE_78:HB2	1.800	5.000	5.000	10.00	10.00	1000.000	0.00
1:PHE_78:HN	1:PHE_78:HE*	1.800	7.000	5.000	10.00	10.00	1000.000	0.00
1:PHE_78:HN	1:LEU_79:HN	1.800	5.000	5.000	10.00	10.00	1000.000	0.00
1:PHE_78:HN	1:GLU-_77:HN	1.800	5.000	5.000	10.00	10.00	1000.000	0.00
1:LYS+_55:HN	1:THR_54:HG2*	1.800	6.500	5.000	10.00	10.00	1000.000	0.00
1:LYS+_55:HN	1:LYS+_55:HG*	1.800	6.000	5.000	10.00	10.00	1000.000	0.00
1:LYS+_55:HN	1:LYS+_55:HD1	1.800	5.000	5.000	10.00	10.00	1000.000	0.00
1:LYS+_55:HN	1:LYS+_55:HB1	1.800	5.000	5.000	10.00	10.00	1000.000	0.00
1:LYS+_55:HN	1:LYS+_55:HB2	1.800	5.000	5.000	10.00	10.00	1000.000	0.00
1:ALA_60:HN	1:ALA_60:HB*	1.800	6.500	5.000	10.00	10.00	1000.000	0.00
1:ALA_60:HN	1:ASP-_59:HB1	1.800	5.000	5.000	10.00	10.00	1000.000	0.00
1:ALA_60:HN	1:ASP-_59:HB2	1.800	5.000	5.000	10.00	10.00	1000.000	0.00
1:ALA_60:HN	1:ILE_61:HA	1.800	5.000	5.000	10.00	10.00	1000.000	0.00
1:ALA_60:HN	1:ILE_62:HN	1.800	5.000	5.000	10.00	10.00	1000.000	0.00
1:ALA_60:HN	1:LEU_58:HN	1.800	5.000	5.000	10.00	10.00	1000.000	0.00
1:ALA_60:HN	1:GLU-_63:HN	1.800	5.000	5.000	10.00	10.00	1000.000	0.00
1:ALA_60:HN	1:ASP-_59:HN	1.800	5.000	5.000	10.00	10.00	1000.000	0.00
1:MET_48:HN	1:THR_44:HG2*	1.800	6.500	5.000	10.00	10.00	1000.000	0.00
1:MET_48:HN	1:MET_48:HE*	1.800	6.500	5.000	10.00	10.00	1000.000	0.00
1:MET_48:HN	1:MET_48:HB1	1.800	5.000	5.000	10.00	10.00	1000.000	0.00
1:GLN_7:HN	1:VAL_80:HG2*	1.800	6.500	5.000	10.00	10.00	1000.000	0.00
1:GLN_7:HN	1:GLN_7:HG*	1.800	6.000	5.000	10.00	10.00	1000.000	0.00
1:GLN_7:HN	1:GLN_6:HN	1.800	5.000	5.000	10.00	10.00	1000.000	0.00
1:ASP-_5:HN	1:THR_4:HG2*	1.800	6.500	5.000	10.00	10.00	1000.000	0.00
1:ASP-_5:HN	1:ASP-_5:HB1	1.800	5.000	5.000	10.00	10.00	1000.000	0.00
1:ASP-_5:HN	1:ASP-_5:HB2	1.800	5.000	5.000	10.00	10.00	1000.000	0.00
1:ASP-_5:HN	1:GLN_6:HN	1.800	5.000	5.000	10.00	10.00	1000.000	0.00
1:GLU-_57:HN	1:GLU-_57:HG*	1.800	6.000	5.000	10.00	10.00	1000.000	0.00
1:GLU-_57:HN	1:GLU-_56:HG2	1.800	5.000	5.000	10.00	10.00	1000.000	0.00
1:GLU-_57:HN	1:LYS+_55:HA	1.800	5.000	5.000	10.00	10.00	1000.000	0.00
1:GLU-_57:HN	1:ASP-_59:HN	1.800	5.000	5.000	10.00	10.00	1000.000	0.00
1:GLU-_57:HN	1:THR_54:HN	1.800	5.000	5.000	10.00	10.00	1000.000	0.00
1:GLU-_57:HN	1:GLU-_56:HN	1.800	5.000	5.000	10.00	10.00	1000.000	0.00
1:GLU-_57:HN	1:LEU_58:HN	1.800	5.000	5.000	10.00	10.00	1000.000	0.00
1:MET_48:HN	1:LEU_49:HD1*	1.800	6.500	5.000	10.00	10.00	1000.000	0.00
1:MET_48:HN	1:MET_48:HB2	1.800	5.000	5.000	10.00	10.00	1000.000	0.00
1:MET_48:HN	1:MET_48:HG1	1.800	5.000	5.000	10.00	10.00	1000.000	0.00
1:MET_48:HN	1:MET_48:HG2	1.800	5.000	5.000	10.00	10.00	1000.000	0.00
1:MET_48:HN	1:LEU_49:HN	1.800	5.000	5.000	10.00	10.00	1000.000	0.00
1:MET_48:HN	1:ARG+_47:HN	1.800	5.000	5.000	10.00	10.00	1000.000	0.00
1:LYS+_40:HN	1:LYS+_40:HG1	1.800	5.000	5.000	10.00	10.00	1000.000	0.00
1:LYS+_40:HN	1:LYS+_40:HB1	1.800	5.000	5.000	10.00	10.00	1000.000	0.00
1:LYS+_40:HN	1:LYS+_40:HB2	1.800	5.000	5.000	10.00	10.00	1000.000	0.00
1:LYS+_40:HN	1:THR_39:HN	1.800	5.000	5.000	10.00	10.00	1000.000	0.00
1:GLU-_16:HN	1:ILE_19:HD1*	1.800	6.500	5.000	10.00	10.00	1000.000	0.00
1:GLU-_16:HN	1:GLU-_16:HB1	1.800	5.000	5.000	10.00	10.00	1000.000	0.00
1:GLU-_16:HN	1:GLU-_16:HB2	1.800	5.000	5.000	10.00	10.00	1000.000	0.00
1:GLU-_16:HN	1:GLU-_16:HG1	1.800	5.000	5.000	10.00	10.00	1000.000	0.00
1:GLU-_16:HN	1:GLU-_16:HG2	1.800	5.000	5.000	10.00	10.00	1000.000	0.00
1:GLU-_16:HN	1:SER_15:HB2	1.800	5.000	5.000	10.00	10.00	1000.000	0.00
1:GLU-_16:HN	1:SER_15:HN	1.800	5.000	5.000	10.00	10.00	1000.000	0.00
1:GLU-_16:HN	1:GLU-_17:HN	1.800	5.000	5.000	10.00	10.00	1000.000	0.00
1:ALA_20:HN	1:GLU-_16:HA	1.800	5.000	5.000	10.00	10.00	1000.000	0.00
1:ASP-_89:HN	1:ALAC_90:HB*	1.800	6.500	5.000	10.00	10.00	1000.000	0.00
1:ASP-_89:HN	1:GLU-_88:HB2	1.800	5.000	5.000	10.00	10.00	1000.000	0.00
1:ASP-_89:HN	1:GLU-_88:HB1	1.800	5.000	5.000	10.00	10.00	1000.000	0.00
1:ASP-_89:HN	1:ASP-_89:HB2	1.800	5.000	5.000	10.00	10.00	1000.000	0.00
1:ASP-_89:HN	1:ASP-_89:HB1	1.800	5.000	5.000	10.00	10.00	1000.000	0.00
1:ASP-_89:HN	1:ALAC_90:HN	1.800	5.000	5.000	10.00	10.00	1000.000	0.00

1:ASP-_89:HN	1:GLU-_88:HN	1.800	5.000	5.000	10.00	10.00	1000.000	0.00
1:VAL_83:HN	1:MET_82:HB1	1.800	5.000	5.000	10.00	10.00	1000.000	0.00
1:VAL_83:HN	1:MET_82:HG1	1.800	5.000	5.000	10.00	10.00	1000.000	0.00
1:VAL_83:HN	1:MET_82:HB2	1.800	5.000	5.000	10.00	10.00	1000.000	0.00
1:VAL_83:HN	1:MET_82:HG2	1.800	5.000	5.000	10.00	10.00	1000.000	0.00
1:VAL_83:HN	1:VAL_83:HG1*	1.800	6.500	5.000	10.00	10.00	1000.000	0.00
1:VAL_83:HN	1:VAL_83:HG2*	1.800	6.500	5.000	10.00	10.00	1000.000	0.00
1:VAL_83:HN	1:VAL_83:HB	1.800	5.000	5.000	10.00	10.00	1000.000	0.00
1:LEU_42:HN	1:ILE_37:HD1*	1.800	6.500	5.000	10.00	10.00	1000.000	0.00
1:LEU_42:HN	1:LEU_42:HD1*	1.800	6.500	5.000	10.00	10.00	1000.000	0.00
1:LEU_42:HN	1:ILE_37:HG2*	1.800	6.500	5.000	10.00	10.00	1000.000	0.00
1:LEU_42:HN	1:LEU_42:HB1	1.800	5.000	5.000	10.00	10.00	1000.000	0.00
1:LEU_42:HN	1:LEU_42:HB2	1.800	5.000	5.000	10.00	10.00	1000.000	0.00
1:LEU_42:HN	1:GLU-_41:HG*	1.800	6.000	5.000	10.00	10.00	1000.000	0.00
1:LEU_42:HN	1:GLU-_41:HN	1.800	5.000	5.000	10.00	10.00	1000.000	0.00
1:GLU-_41:HN	1:ILE_37:HG2*	1.800	6.500	5.000	10.00	10.00	1000.000	0.00
1:GLU-_41:HN	1:LYS+_40:HG2	1.800	5.000	5.000	10.00	10.00	1000.000	0.00
1:GLU-_41:HN	1:LYS+_40:HB1	1.800	5.000	5.000	10.00	10.00	1000.000	0.00
1:GLU-_41:HN	1:LYS+_40:HB2	1.800	5.000	5.000	10.00	10.00	1000.000	0.00
1:GLU-_41:HN	1:GLU-_41:HG*	1.800	6.000	5.000	10.00	10.00	1000.000	0.00
1:ALA_24:HN	1:LYS+_23:HG*	1.800	6.000	5.000	10.00	10.00	1000.000	0.00
1:ALA_24:HN	1:LYS+_23:HB*	1.800	6.000	5.000	10.00	10.00	1000.000	0.00
1:ALA_24:HN	1:ALA_24:HB*	1.800	6.500	5.000	10.00	10.00	1000.000	0.00
1:ALA_25:HN	1:ALA_25:HB*	1.800	6.500	5.000	10.00	10.00	1000.000	0.00
1:ALA_24:HN	1:LYS+_23:HN	1.800	5.000	5.000	10.00	10.00	1000.000	0.00
1:GLU-_21:HN	1:ILE_19:HG11	1.800	5.000	5.000	10.00	10.00	1000.000	0.00
1:GLU-_21:HN	1:GLU-_21:HB1	1.800	5.000	5.000	10.00	10.00	1000.000	0.00
1:GLU-_21:HN	1:GLU-_21:HB2	1.800	5.000	5.000	10.00	10.00	1000.000	0.00
1:GLU-_21:HN	1:GLU-_21:HG1	1.800	5.000	5.000	10.00	10.00	1000.000	0.00
1:GLU-_21:HN	1:LYS+_23:HN	1.800	5.000	5.000	10.00	10.00	1000.000	0.00
1:GLU-_21:HN	1:PHE_22:HN	1.800	5.000	5.000	10.00	10.00	1000.000	0.00
1:ALA_20:HN	1:ILE_19:HG11	1.800	5.000	5.000	10.00	10.00	1000.000	0.00
1:ALA_20:HN	1:ILE_19:HG2*	1.800	6.500	5.000	10.00	10.00	1000.000	0.00
1:ALA_20:HN	1:ALA_20:HB*	1.800	6.500	5.000	10.00	10.00	1000.000	0.00
1:ALA_20:HN	1:ILE_19:HB	1.800	5.000	5.000	10.00	10.00	1000.000	0.00
1:ALA_20:HN	1:GLU-_21:HG1	1.800	5.000	5.000	10.00	10.00	1000.000	0.00
1:ALA_20:HN	1:ILE_19:HN	1.800	5.000	5.000	10.00	10.00	1000.000	0.00
1:GLU-_88:HN	1:LYS+_87:HB1	1.800	5.000	5.000	10.00	10.00	1000.000	0.00
1:GLU-_88:HN	1:LYS+_87:HB2	1.800	5.000	5.000	10.00	10.00	1000.000	0.00
1:GLU-_88:HN	1:GLU-_88:HB2	1.800	5.000	5.000	10.00	10.00	1000.000	0.00
1:GLU-_88:HN	1:GLU-_88:HB1	1.800	5.000	5.000	10.00	10.00	1000.000	0.00
1:GLU-_88:HN	1:GLU-_88:HG1	1.800	5.000	5.000	10.00	10.00	1000.000	0.00
1:GLU-_88:HN	1:GLU-_88:HG2	1.800	5.000	5.000	10.00	10.00	1000.000	0.00
1:VAL_45:HN	1:VAL_45:HG2*	1.800	6.500	5.000	10.00	10.00	1000.000	0.00
1:VAL_45:HN	1:VAL_45:HG1*	1.800	6.500	5.000	10.00	10.00	1000.000	0.00
1:VAL_45:HN	1:THR_44:HG2*	1.800	6.500	5.000	10.00	10.00	1000.000	0.00
1:VAL_45:HN	1:VAL_45:HB	1.800	5.000	5.000	10.00	10.00	1000.000	0.00
1:VAL_45:HN	1:THR_44:HB	1.800	5.000	5.000	10.00	10.00	1000.000	0.00
1:VAL_45:HN	1:THR_44:HN	1.800	5.000	5.000	10.00	10.00	1000.000	0.00
1:VAL_45:HN	1:MET_46:HN	1.800	5.000	5.000	10.00	10.00	1000.000	0.00
1:ALA_25:HN	1:PHE_26:HN	1.800	5.000	5.000	10.00	10.00	1000.000	0.00
1:MET_81:HN	1:GLU-_77:HA	1.800	5.000	5.000	10.00	10.00	1000.000	0.00
1:MET_81:HN	1:LEU_79:HD1*	1.800	6.500	5.000	10.00	10.00	1000.000	0.00
1:MET_81:HN	1:VAL_80:HG2*	1.800	6.500	5.000	10.00	10.00	1000.000	0.00
1:MET_81:HN	1:MET_81:HB1	1.800	5.000	5.000	10.00	10.00	1000.000	0.00
1:MET_81:HN	1:VAL_80:HN	1.800	5.000	5.000	10.00	10.00	1000.000	0.00
1:MET_81:HN	1:MET_82:HN	1.800	5.000	5.000	10.00	10.00	1000.000	0.00
1:MET_81:HN	1:VAL_83:HN	1.800	5.000	5.000	10.00	10.00	1000.000	0.00
1:ILE_61:HN	1:ILE_61:HG11	1.800	5.000	5.000	10.00	10.00	1000.000	0.00
1:ILE_61:HN	1:ALA_60:HB*	1.800	6.500	5.000	10.00	10.00	1000.000	0.00
1:ILE_61:HN	1:ILE_61:HG12	1.800	5.000	5.000	10.00	10.00	1000.000	0.00
1:ILE_61:HN	1:ILE_61:HB	1.800	5.000	5.000	10.00	10.00	1000.000	0.00
1:ILE_61:HN	1:ILE_62:HN	1.800	5.000	5.000	10.00	10.00	1000.000	0.00
1:LEU_58:HN	1:THR_54:HG2*	1.800	6.500	5.000	10.00	10.00	1000.000	0.00
1:LEU_58:HN	1:LEU_58:HG	1.800	5.000	5.000	10.00	10.00	1000.000	0.00
1:LEU_58:HN	1:LEU_58:HB*	1.800	6.000	5.000	10.00	10.00	1000.000	0.00
1:LEU_58:HN	1:ASP-_59:HN	1.800	5.000	5.000	10.00	10.00	1000.000	0.00
1:MET_18:HN	1:MET_18:HB1	1.800	5.000	5.000	10.00	10.00	1000.000	0.00
1:MET_18:HN	1:GLU-_17:HG1	1.800	5.000	5.000	10.00	10.00	1000.000	0.00
1:MET_18:HN	1:MET_18:HG1	1.800	5.000	5.000	10.00	10.00	1000.000	0.00
1:MET_18:HN	1:MET_18:HG2	1.800	5.000	5.000	10.00	10.00	1000.000	0.00
1:MET_18:HN	1:ILE_19:HN	1.800	5.000	5.000	10.00	10.00	1000.000	0.00
1:MET_18:HN	1:GLU-_17:HN	1.800	5.000	5.000	10.00	10.00	1000.000	0.00
1:PHE_26:HN	1:ALA_25:HB*	1.800	6.500	5.000	10.00	10.00	1000.000	0.00
1:PHE_26:HN	1:PHE_26:HB*	1.800	6.000	5.000	10.00	10.00	1000.000	0.00
1:PHE_26:HN	1:PHE_26:HD*	1.800	7.000	5.000	10.00	10.00	1000.000	0.00
1:PHE_26:HN	1:ASP-_27:HN	1.800	5.000	5.000	10.00	10.00	1000.000	0.00
1:PHE_22:HN	1:LEU_79:HD2*	1.800	6.500	5.000	10.00	10.00	1000.000	0.00

1:PHE_22:HN	1:ILE_19:HG2*	1.800	6.500	5.000	10.00	10.00	1000.000	0.00
1:PHE_22:HN	1:GLU-_21:HB1	1.800	5.000	5.000	10.00	10.00	1000.000	0.00
1:PHE_22:HN	1:GLU-_21:HG1	1.800	5.000	5.000	10.00	10.00	1000.000	0.00
1:PHE_22:HN	1:PHE_22:HB*	1.800	6.000	5.000	10.00	10.00	1000.000	0.00
1:PHE_22:HN	1:PHE_22:HE*	1.800	7.000	5.000	10.00	10.00	1000.000	0.00
1:PHE_22:HN	1:PHE_22:HD*	1.800	7.000	5.000	10.00	10.00	1000.000	0.00
1:ILE_19:HN	1:ILE_19:HD1*	1.800	6.500	5.000	10.00	10.00	1000.000	0.00
1:ILE_19:HN	1:ILE_19:HG11	1.800	5.000	5.000	10.00	10.00	1000.000	0.00
1:ILE_19:HN	1:ILE_19:HG2*	1.800	6.500	5.000	10.00	10.00	1000.000	0.00
1:ILE_19:HN	1:MET_18:HB1	1.800	5.000	5.000	10.00	10.00	1000.000	0.00
1:ILE_19:HN	1:MET_18:HB2	1.800	5.000	5.000	10.00	10.00	1000.000	0.00
1:ILE_19:HN	1:ILE_19:HB	1.800	5.000	5.000	10.00	10.00	1000.000	0.00
1:ILE_19:HN	1:GLU-_17:HN	1.800	5.000	5.000	10.00	10.00	1000.000	0.00
1:ARG+_84:HN	1:VAL_83:HG1*	1.800	6.500	5.000	10.00	10.00	1000.000	0.00
1:ARG+_84:HN	1:VAL_83:HG2*	1.800	6.500	5.000	10.00	10.00	1000.000	0.00
1:ARG+_84:HN	1:ARG+_84:HG1	1.800	5.000	5.000	10.00	10.00	1000.000	0.00
1:ARG+_84:HN	1:VAL_83:HB	1.800	5.000	5.000	10.00	10.00	1000.000	0.00
1:ARG+_84:HN	1:ARG+_84:HD*	1.800	6.000	5.000	10.00	10.00	1000.000	0.00
1:ARG+_84:HN	1:VAL_80:HA	1.800	5.000	5.000	10.00	10.00	1000.000	0.00
1:ARG+_84:HN	1:GLN_85:HN	1.800	5.000	5.000	10.00	10.00	1000.000	0.00
1:ARG+_84:HN	1:VAL_83:HN	1.800	5.000	5.000	10.00	10.00	1000.000	0.00
1:GLU-_77:HN	1:GLU-_77:HG1	1.800	5.000	5.000	10.00	10.00	1000.000	0.00
1:GLU-_77:HN	1:GLU-_77:HG2	1.800	5.000	5.000	10.00	10.00	1000.000	0.00
1:GLU-_77:HN	1:GLU-_76:HN	1.800	5.000	5.000	10.00	10.00	1000.000	0.00
1:GLU-_17:HN	1:GLU-_17:HB1	1.800	5.000	5.000	10.00	10.00	1000.000	0.00
1:[illegible]_17:HN	1:GLU-_17:HB2	1.800	5.000	5.000	10.00	10.00	1000.000	0.00
1[illegible]-_17:HN	1:GLU-_17:HG1	1.800	5.000	5.000	10.00	10.00	1000.000	0.00
1.[illegible]-_17:HN	1:GLU-_17:HG2	1.800	5.000	5.000	10.00	10.00	1000.000	0.00
1:GLN_6:HN	1:GLN_6:HG1	1.800	5.000	5.000	10.00	10.00	1000.000	0.00
1:GLN_6:HN	1:VAL_80:HG2*	1.800	6.500	5.000	10.00	10.00	1000.000	0.00
1:GLN_6:HN	1:GLN_6:HB2	1.800	5.000	5.000	10.00	10.00	1000.000	0.00
1:GLN_6:HN	1:GLN_6:HG2	1.800	5.000	5.000	10.00	10.00	1000.000	0.00
1:GLN_6:HN	1:ASP-_5:HB2	1.800	5.000	5.000	10.00	10.00	1000.000	0.00
1:GLN_6:HN	1:GLN_6:HE22	1.800	5.000	5.000	10.00	10.00	1000.000	0.00
1:GLN_6:HN	1:GLN_7:HE22	1.800	5.000	5.000	10.00	10.00	1000.000	0.00
1:GLN_6:HN	1:ASP-_5:HB1	1.800	5.000	5.000	10.00	10.00	1000.000	0.00
1:LYS+_87:HN	1:LYS+_87:HG1	1.800	5.000	5.000	10.00	10.00	1000.000	0.00
1:LYS+_87:HN	1:LYS+_87:HG2	1.800	5.000	5.000	10.00	10.00	1000.000	0.00
1:LYS+_87:HN	1:VAL_83:HG1*	1.800	6.500	5.000	10.00	10.00	1000.000	0.00
1:LYS+_87:HN	1:LYS+_87:HB1	1.800	5.000	5.000	10.00	10.00	1000.000	0.00
1:LYS+_87:HN	1:LYS+_87:HB2	1.800	5.000	5.000	10.00	10.00	1000.000	0.00
1:LYS+_87:HN	1:MET_86:HB2	1.800	5.000	5.000	10.00	10.00	1000.000	0.00
1:LYS+_87:HN	1:MET_86:HB1	1.800	5.000	5.000	10.00	10.00	1000.000	0.00
1:LYS+_87:HN	1:VAL_83:HA	1.800	5.000	5.000	10.00	10.00	1000.000	0.00
1:LYS+_87:HN	1:ASP-_89:HN	1.800	5.000	5.000	10.00	10.00	1000.000	0.00
1:VAL_80:HN	1:VAL_80:HG1*	1.800	6.500	5.000	10.00	10.00	1000.000	0.00
1:VAL_80:HN	1:VAL_80:HG2*	1.800	6.500	5.000	10.00	10.00	1000.000	0.00
1:VAL_80:HN	1:ALA_10:HB*	1.800	6.500	5.000	10.00	10.00	1000.000	0.00
1:VAL_80:HN	1:VAL_80:HB	1.800	5.000	5.000	10.00	10.00	1000.000	0.00
1:VAL_80:HN	1:LEU_79:HN	1.800	5.000	5.000	10.00	10.00	1000.000	0.00
1:ARG+_47:HN	1:LEU_49:HD1*	1.800	6.500	5.000	10.00	10.00	1000.000	0.00
1:ARG+_47:HN	1:LEU_58:HD1*	1.800	6.500	5.000	10.00	10.00	1000.000	0.00
1:ARG+_47:HN	1:THR_44:HG2*	1.800	6.500	5.000	10.00	10.00	1000.000	0.00
1:ARG+_47:HN	1:ARG+_47:HD*	1.800	6.000	5.000	10.00	10.00	1000.000	0.00
1:ARG+_47:HN	1:GLY_43:HA1	1.800	5.000	5.000	10.00	10.00	1000.000	0.00
1:ARG+_47:HN	1:MET_46:HN	1.800	5.000	5.000	10.00	10.00	1000.000	0.00
1:MET_28:HN	1:MET_28:HE*	1.800	6.500	5.000	10.00	10.00	1000.000	0.00
1:MET_28:HN	1:MET_28:HB1	1.800	5.000	5.000	10.00	10.00	1000.000	0.00
1:MET_28:HN	1:MET_28:HB2	1.800	5.000	5.000	10.00	10.00	1000.000	0.00
1:MET_28:HN	1:MET_28:HG1	1.800	5.000	5.000	10.00	10.00	1000.000	0.00
1:MET_28:HN	1:MET_28:HG2	1.800	5.000	5.000	10.00	10.00	1000.000	0.00
1:MET_28:HN	1:PHE_29:HN	1.800	5.000	5.000	10.00	10.00	1000.000	0.00
1:MET_28:HN	1:ASP-_27:HN	1.800	5.000	5.000	10.00	10.00	1000.000	0.00
1:ALA_12:HN	1:ALA_12:HB*	1.800	6.500	5.000	10.00	10.00	1000.000	0.00
1:ALA_12:HN	1:ARG+_11:HB*	1.800	6.000	5.000	10.00	10.00	1000.000	0.00
1:ALA_12:HN	1:LEU_14:HN	1.800	5.000	5.000	10.00	10.00	1000.000	0.00
1:ALA_12:HN	1:ARG+_11:HN	1.800	5.000	5.000	10.00	10.00	1000.000	0.00
1:GLU-_9:HN	1:GLU-_9:HB*	1.800	6.000	5.000	10.00	10.00	1000.000	0.00
1:GLU-_9:HN	1:GLU-_9:HG1	1.800	5.000	5.000	10.00	10.00	1000.000	0.00
1:GLU-_9:HN	1:GLU-_9:HG2	1.800	5.000	5.000	10.00	10.00	1000.000	0.00
1:GLU-_9:HN	1:GLN_7:HA	1.800	5.000	5.000	10.00	10.00	1000.000	0.00
1:MET_86:HN	1:VAL_83:HG1*	1.800	6.500	5.000	10.00	10.00	1000.000	0.00
1:MET_86:HN	1:VAL_83:HG2*	1.800	6.500	5.000	10.00	10.00	1000.000	0.00
1:MET_86:HN	1:MET_82:HB2	1.800	5.000	5.000	10.00	10.00	1000.000	0.00
1:MET_86:HN	1:LYS+_87:HB1	1.800	5.000	5.000	10.00	10.00	1000.000	0.00
1:MET_86:HN	1:MET_86:HB2	1.800	5.000	5.000	10.00	10.00	1000.000	0.00
1:MET_86:HN	1:MET_86:HG1	1.800	5.000	5.000	10.00	10.00	1000.000	0.00
1:MET_86:HN	1:MET_86:HG2	1.800	5.000	5.000	10.00	10.00	1000.000	0.00

1:MET_86:HN	1:ARG+_84:HA	1.800	5.000	5.000	10.00	10.00	1000.000	0.00
1:MET_86:HN	1:GLN_85:HN	1.800	5.000	5.000	10.00	10.00	1000.000	0.00
1:ASP-_59:HN	1:ASP-_59:HB2	1.800	5.000	5.000	10.00	10.00	1000.000	0.00
1:ASP-_59:HN	1:ASP-_59:HB1	1.800	5.000	5.000	10.00	10.00	1000.000	0.00
1:ASP-_59:HN	1:LYS+_55:HA	1.800	5.000	5.000	10.00	10.00	1000.000	0.00
1:LEU_79:HN	1:LEU_79:HD1*	1.800	6.500	5.000	10.00	10.00	1000.000	0.00
1:LEU_79:HN	1:LEU_79:HD2*	1.800	6.500	5.000	10.00	10.00	1000.000	0.00
1:LEU_79:HN	1:LEU_79:HG	1.800	5.000	5.000	10.00	10.00	1000.000	0.00
1:LEU_79:HN	1:PHE_75:HA	1.800	5.000	5.000	10.00	10.00	1000.000	0.00
1:LEU_79:HN	1:MET_81:HN	1.800	5.000	5.000	10.00	10.00	1000.000	0.00
1:LEU_79:HN	1:GLU-_77:HN	1.800	5.000	5.000	10.00	10.00	1000.000	0.00
1:PHE_75:HN	1:PHE_75:HB1	1.800	5.000	5.000	10.00	10.00	1000.000	0.00
1:PHE_75:HN	1:PHE_75:HB2	1.800	5.000	5.000	10.00	10.00	1000.000	0.00
1:PHE_75:HN	1:ASP-_74:HB1	1.800	5.000	5.000	10.00	10.00	1000.000	0.00
1:PHE_75:HN	1:GLU-_76:HN	1.800	5.000	5.000	10.00	10.00	1000.000	0.00
1:PHE_75:HN	1:ILE_37:HN	1.800	5.000	5.000	10.00	10.00	1000.000	0.00
1:THR_44:HN	1:THR_44:HG2*	1.800	6.500	5.000	10.00	10.00	1000.000	0.00
1:THR_44:HN	1:THR_44:HB	1.800	5.000	5.000	10.00	10.00	1000.000	0.00
1:THR_44:HN	1:GLY_43:HN	1.800	5.000	5.000	10.00	10.00	1000.000	0.00
1:ASP-_30:HN	1:PHE_29:HB1	1.800	5.000	5.000	10.00	10.00	1000.000	0.00
1:ASP-_30:HN	1:MET_28:HN	1.800	5.000	5.000	10.00	10.00	1000.000	0.00
1:ASP-_30:HN	1:ILE_37:HD1*	1.800	6.500	5.000	10.00	10.00	1000.000	0.00
1:ASP-_30:HN	1:ILE_37:HG2*	1.800	6.500	5.000	10.00	10.00	1000.000	0.00
1:ASP-_30:HN	1:ASP-_30:HB1	1.800	5.000	5.000	10.00	10.00	1000.000	0.00
1:ASP-_30:HN	1:ASP-_30:HB2	1.800	5.000	5.000	10.00	10.00	1000.000	0.00
1:ASP-_30:HN	1:PHE_29:HB2	1.800	5.000	5.000	10.00	10.00	1000.000	0.00
1:ASP-_30:HN	1:PHE_29:HN	1.800	5.000	5.000	10.00	10.00	1000.000	0.00
1:ILE_62:HN	1:LEU_58:HA	1.800	5.000	5.000	10.00	10.00	1000.000	0.00
1:ILE_62:HN	1:ILE_62:HG11	1.800	5.000	5.000	10.00	10.00	1000.000	0.00
1:ILE_62:HN	1:ILE_62:HG12	1.800	5.000	5.000	10.00	10.00	1000.000	0.00
1:ILE_62:HN	1:ILE_62:HG2*	1.800	6.500	5.000	10.00	10.00	1000.000	0.00
1:ILE_62:HN	1:ALA_60:HB*	1.800	6.500	5.000	10.00	10.00	1000.000	0.00
1:ILE_62:HN	1:GLU-_63:HN	1.800	5.000	5.000	10.00	10.00	1000.000	0.00
1:GLN_51:HN	1:GLN_51:HB1	1.800	5.000	5.000	10.00	10.00	1000.000	0.00
1:GLN_51:HN	1:ASN_52:HN	1.800	5.000	5.000	10.00	10.00	1000.000	0.00
1:GLN_51:HN	1:GLY_50:HN	1.800	5.000	5.000	10.00	10.00	1000.000	0.00
1:PHE_29:HN	1:ILE_37:HD1*	1.800	6.500	5.000	10.00	10.00	1000.000	0.00
1:PHE_29:HN	1:ASP-_30:HB1	1.800	5.000	5.000	10.00	10.00	1000.000	0.00
1:PHE_29:HN	1:MET_28:HB1	1.800	5.000	5.000	10.00	10.00	1000.000	0.00
1:PHE_29:HN	1:MET_28:HB2	1.800	5.000	5.000	10.00	10.00	1000.000	0.00
1:PHE_29:HN	1:MET_28:HG1	1.800	5.000	5.000	10.00	10.00	1000.000	0.00
1:PHE_29:HN	1:PHE_29:HB1	1.800	5.000	5.000	10.00	10.00	1000.000	0.00
1:PHE_29:HN	1:PHE_29:HB2	1.800	5.000	5.000	10.00	10.00	1000.000	0.00
1:PHE_29:HN	1:PHE_29:HD*	1.800	7.000	5.000	10.00	10.00	1000.000	0.00
1:LEU_14:HN	1:LEU_14:HD1*	1.800	6.500	5.000	10.00	10.00	1000.000	0.00
1:LEU_14:HN	1:LEU_14:HD2*	1.800	6.500	5.000	10.00	10.00	1000.000	0.00
1:LEU_14:HN	1:LEU_14:HB1	1.800	5.000	5.000	10.00	10.00	1000.000	0.00
1:LEU_14:HN	1:LEU_14:HB2	1.800	5.000	5.000	10.00	10.00	1000.000	0.00
1:LEU_14:HN	1:LEU_14:HG	1.800	5.000	5.000	10.00	10.00	1000.000	0.00
1:LEU_14:HN	1:ALA_12:HA	1.800	5.000	5.000	10.00	10.00	1000.000	0.00
1:PHE_13:HN	1:PHE_13:HB	1.800	5.000	5.000	10.00	10.00	1000.000	0.00
1:PHE_13:HN	1:PHE_13:HB1	1.800	5.000	5.000	10.00	10.00	1000.000	0.00
1:PHE_13:HN	1:LEU_14:HD1*	1.800	6.500	5.000	10.00	10.00	1000.000	0.00
1:PHE_13:HN	1:LEU_14:HB2	1.800	5.000	5.000	10.00	10.00	1000.000	0.00
1:PHE_13:HN	1:ARG+_11:HA	1.800	5.000	5.000	10.00	10.00	1000.000	0.00
1:PHE_13:HN	1:PHE_13:HD*	1.800	7.000	5.000	10.00	10.00	1000.000	0.00
1:PHE_13:HN	1:LEU_14:HN	1.800	5.000	5.000	10.00	10.00	1000.000	0.00
1:PHE_13:HN	1:ARG+_11:HN	1.800	5.000	5.000	10.00	10.00	1000.000	0.00
1:GLU-_63:HN	1:ILE_62:HG2*	1.800	6.500	5.000	10.00	10.00	1000.000	0.00
1:GLU-_63:HN	1:GLU-_63:HB1	1.800	5.000	5.000	10.00	10.00	1000.000	0.00
1:GLU-_63:HN	1:GLU-_63:HB2	1.800	5.000	5.000	10.00	10.00	1000.000	0.00
1:GLU-_63:HN	1:GLU-_64:HN	1.800	5.000	5.000	10.00	10.00	1000.000	0.00
1:ASP-_27:HN	1:LYS+_23:HA	1.800	5.000	5.000	10.00	10.00	1000.000	0.00
1:MET_82:HN	1:MET_82:HB1	1.800	5.000	5.000	10.00	10.00	1000.000	0.00
1:MET_82:HN	1:MET_82:HG1	1.800	5.000	5.000	10.00	10.00	1000.000	0.00
1:MET_82:HN	1:MET_82:HB2	1.800	5.000	5.000	10.00	10.00	1000.000	0.00
1:MET_82:HN	1:MET_82:HG2	1.800	5.000	5.000	10.00	10.00	1000.000	0.00
1:MET_82:HN	1:VAL_83:HG2*	1.800	6.500	5.000	10.00	10.00	1000.000	0.00
1:MET_82:HN	1:VAL_83:HN	1.800	5.000	5.000	10.00	10.00	1000.000	0.00
1:ASP-_27:HN	1:LYS+_23:HG*	1.800	6.000	5.000	10.00	10.00	1000.000	0.00
1:ASP-_27:HN	1:ALA_25:HB*	1.800	6.500	5.000	10.00	10.00	1000.000	0.00
1:ASP-_27:HN	1:ASP-_27:HB2	1.800	5.000	5.000	10.00	10.00	1000.000	0.00
1:ASP-_27:HN	1:ASP-_27:HB1	1.800	5.000	5.000	10.00	10.00	1000.000	0.00
1:SER_70:HN	1:GLY_71:HA1	1.800	5.000	5.000	10.00	10.00	1000.000	0.00
1:SER_70:HN	1:SER_70:HB1	1.800	5.000	5.000	10.00	10.00	1000.000	0.00
1:SER_70:HN	1:ASP-_68:HN	1.800	5.000	5.000	10.00	10.00	1000.000	0.00
1:SER_70:HN	1:GLY_69:HN	1.800	5.000	5.000	10.00	10.00	1000.000	0.00
1:SER_70:HN	1:GLY_71:HN	1.800	5.000	5.000	10.00	10.00	1000.000	0.00

1:GLU-_56:HN	1:THR_54:HG2*	1.800	6.500	5.000	10.00	10.00	1000.000	0.00
1:GLU-_56:HN	1:LYS+_55:HD1	1.800	5.000	5.000	10.00	10.00	1000.000	0.00
1:GLU-_56:HN	1:GLU-_56:HB2	1.800	5.000	5.000	10.00	10.00	1000.000	0.00
1:GLU-_56:HN	1:GLU-_56:HG1	1.800	5.000	5.000	10.00	10.00	1000.000	0.00
1:GLU-_56:HN	1:GLU-_56:HG2	1.800	5.000	5.000	10.00	10.00	1000.000	0.00
1:ASN_52:HN	1:GLN_51:HB1	1.800	5.000	5.000	10.00	10.00	1000.000	0.00
1:ASN_52:HN	1:ASN_52:HB1	1.800	5.000	5.000	10.00	10.00	1000.000	0.00
1:ASN_52:HN	1:ASN_52:HB2	1.800	5.000	5.000	10.00	10.00	1000.000	0.00
1:ASN_52:HN	1:PRO_53:HD1	1.800	5.000	5.000	10.00	10.00	1000.000	0.00
1:ASN_52:HN	1:PRO_53:HD2	1.800	5.000	5.000	10.00	10.00	1000.000	0.00
1:MET_46:HN	1:MET_46:HB1	1.800	5.000	5.000	10.00	10.00	1000.000	0.00
1:MET_46:HN	1:MET_46:HG1	1.800	5.000	5.000	10.00	10.00	1000.000	0.00
1:MET_46:HN	1:MET_46:HG2	1.800	5.000	5.000	10.00	10.00	1000.000	0.00
1:GLN_85:HN	1:GLN_85:HB2	1.800	5.000	5.000	10.00	10.00	1000.000	0.00
1:GLN_85:HN	1:GLN_85:HG1	1.800	5.000	5.000	10.00	10.00	1000.000	0.00
1:GLN_85:HN	1:GLN_85:HG2	1.800	5.000	5.000	10.00	10.00	1000.000	0.00
1:GLU-_76:HN	1:GLU-_76:HB1	1.800	5.000	5.000	10.00	10.00	1000.000	0.00
1:GLU-_76:HN	1:GLU-_76:HB2	1.800	5.000	5.000	10.00	10.00	1000.000	0.00
1:GLU-_76:HN	1:GLU-_76:HG*	1.800	6.000	5.000	10.00	10.00	1000.000	0.00
1:SER_15:HN	1:LEU_14:HD1*	1.800	6.500	5.000	10.00	10.00	1000.000	0.00
1:SER_15:HN	1:LEU_14:HB1	1.800	5.000	5.000	10.00	10.00	1000.000	0.00
1:SER_15:HN	1:MET_18:HB1	1.800	5.000	5.000	10.00	10.00	1000.000	0.00
1:SER_15:HN	1:SER_15:HB1	1.800	5.000	5.000	10.00	10.00	1000.000	0.00
1:ARG+_11:HN	1:LEU_79:HD1*	1.800	6.500	5.000	10.00	10.00	1000.000	0.00
1:ARG+_11:HN	1:LEU_14:HD1*	1.800	6.500	5.000	10.00	10.00	1000.000	0.00
1:ARG+_11:HN	1:VAL_80:HG2*	1.800	6.500	5.000	10.00	10.00	1000.000	0.00
1:ARG+_11:HN	1:ALA_10:HB*	1.800	6.500	5.000	10.00	10.00	1000.000	0.00
1:ARG+_11:HN	1:ARG+_11:HB*	1.800	6.000	5.000	10.00	10.00	1000.000	0.00
1:GLU-_64:HN	1:ALA_60:HA	1.800	5.000	5.000	10.00	10.00	1000.000	0.00
1:ASP-_68:HN	1:ASP-_68:HB1	1.800	5.000	5.000	10.00	10.00	1000.000	0.00
1:ASP-_68:HN	1:ASP-_68:HB2	1.800	5.000	5.000	10.00	10.00	1000.000	0.00
1:ASP-_68:HN	1:GLY_69:HN	1.800	5.000	5.000	10.00	10.00	1000.000	0.00
1:GLU-_64:HN	1:ILE_62:HG2*	1.800	6.500	5.000	10.00	10.00	1000.000	0.00
1:GLU-_64:HN	1:ALA_60:HB*	1.800	6.500	5.000	10.00	10.00	1000.000	0.00
1:GLU-_64:HN	1:GLU-_64:HB1	1.800	5.000	5.000	10.00	10.00	1000.000	0.00
1:GLU-_64:HN	1:GLU-_64:HB2	1.800	5.000	5.000	10.00	10.00	1000.000	0.00
1:GLU-_64:HN	1:GLU-_64:HG1	1.800	5.000	5.000	10.00	10.00	1000.000	0.00
1:GLU-_64:HN	1:GLU-_64:HG2	1.800	5.000	5.000	10.00	10.00	1000.000	0.00
1:GLU-_64:HN	1:ILE_62:HA	1.800	5.000	5.000	10.00	10.00	1000.000	0.00
1:ASP-_36:HN	1:ASP-_36:HB1	1.800	5.000	5.000	10.00	10.00	1000.000	0.00
1:ASP-_36:HN	1:GLY_35:HN	1.800	5.000	5.000	10.00	10.00	1000.000	0.00
1:THR_4:HN	1:THR_4:HG2*	1.800	6.500	5.000	10.00	10.00	1000.000	0.00
1:THR_4:HN	1:ASP-_5:HN	1.800	5.000	5.000	10.00	10.00	1000.000	0.00
1:THR_39:HN	1:THR_39:HG2*	1.800	6.500	5.000	10.00	10.00	1000.000	0.00
1:THR_39:HN	1:THR_39:HB	1.800	5.000	5.000	10.00	10.00	1000.000	0.00
1:THR_54:HN	1:THR_54:HG2*	1.800	6.500	5.000	10.00	10.00	1000.000	0.00
1:ASP-_32:HN	1:ALA_31:HB*	1.800	6.500	5.000	10.00	10.00	1000.000	0.00
1:ASP-_32:HN	1:ASP-_32:HB1	1.800	5.000	5.000	10.00	10.00	1000.000	0.00
1:ASP-_32:HN	1:ASP-_32:HB2	1.800	5.000	5.000	10.00	10.00	1000.000	0.00
1:ASP-_32:HN	1:GLY_33:HA*	1.800	6.000	5.000	10.00	10.00	1000.000	0.00
1:ASP-_32:HN	1:ALA_31:HN	1.800	5.000	5.000	10.00	10.00	1000.000	0.00
1:ASP-_32:HN	1:GLY_33:HN	1.800	5.000	5.000	10.00	10.00	1000.000	0.00
1:ASN_52:HD22	1:ASN_52:HB1	1.800	5.000	5.000	10.00	10.00	1000.000	0.00
1:ASN_52:HD22	1:ASN_52:HB2	1.800	5.000	5.000	10.00	10.00	1000.000	0.00
1:ASN_52:HD21	1:ASN_52:HB1	1.800	5.000	5.000	10.00	10.00	1000.000	0.00
1:ASN_52:HD21	1:ASN_52:HB2	1.800	5.000	5.000	10.00	10.00	1000.000	0.00
1:ASN_52:HD22	1:ASN_52:HD21	1.800	5.000	5.000	10.00	10.00	1000.000	0.00
1:GLN_51:HE22	1:GLN_51:HE21	1.800	5.000	5.000	10.00	10.00	1000.000	0.00
1:GLN_7:HE21	1:GLN_7:HG*	1.800	6.000	5.000	10.00	10.00	1000.000	0.00
1:GLN_7:HE22	1:GLN_7:HE21	1.800	5.000	5.000	10.00	10.00	1000.000	0.00
1:GLN_6:HE22	1:GLN_6:HB2	1.800	5.000	5.000	10.00	10.00	1000.000	0.00
1:GLN_6:HE22	1:GLN_6:HG1	1.800	5.000	5.000	10.00	10.00	1000.000	0.00
1:GLN_6:HE22	1:GLN_6:HG2	1.800	5.000	5.000	10.00	10.00	1000.000	0.00
1:GLN_6:HE21	1:GLN_6:HG1	1.800	5.000	5.000	10.00	10.00	1000.000	0.00
1:GLN_6:HE21	1:GLN_6:HG2	1.800	5.000	5.000	10.00	10.00	1000.000	0.00
1:GLN_6:HE22	1:GLN_6:HE21	1.800	5.000	5.000	10.00	10.00	1000.000	0.00
1:GLN_7:HE21	1:THR_4:HG2*	1.800	6.500	5.000	10.00	10.00	1000.000	0.00
1:GLN_7:HE22	1:THR_4:HG2*	1.800	6.500	5.000	10.00	10.00	1000.000	0.00
1:GLN_7:HE22	1:ASP-_5:HB1	1.800	5.000	5.000	10.00	10.00	1000.000	0.00
1:GLN_7:HE22	1:GLN_7:HG*	1.800	6.000	5.000	10.00	10.00	1000.000	0.00
1:GLN_85:HE22	1:GLN_85:HG1	1.800	5.000	5.000	10.00	10.00	1000.000	0.00
1:GLN_85:HE22	1:GLN_85:HG2	1.800	5.000	5.000	10.00	10.00	1000.000	0.00
1:GLN_85:HE22	1:GLN_85:HE21	1.800	5.000	5.000	10.00	10.00	1000.000	0.00
1:GLY_33:HN	1:ALA_31:HB*	1.800	6.500	5.000	10.00	10.00	1000.000	0.00
1:GLY_33:HN	1:ALA_31:HA	1.800	5.000	5.000	10.00	10.00	1000.000	0.00
1:GLY_69:HN	1:ASP-_66:HB1	1.800	5.000	5.000	10.00	10.00	1000.000	0.00
1:GLY_69:HN	1:ASP-_68:HB2	1.800	5.000	5.000	10.00	10.00	1000.000	0.00
1:GLY_69:HN	1:GLY_71:HN	1.800	5.000	5.000	10.00	10.00	1000.000	0.00

1:GLY_34:HN	1:ASP-_30:HB1	1.800	5.000	5.000	10.00	10.00	1000.000	0.00
1:GLY_34:HN	1:ASP-_32:HB2	1.800	5.000	5.000	10.00	10.00	1000.000	0.00
1:GLY_34:HN	1:GLY_33:HN	1.800	5.000	5.000	10.00	10.00	1000.000	0.00
1:GLY_34:HN	1:GLY_35:HN	1.800	5.000	5.000	10.00	10.00	1000.000	0.00
1:THR_72:HN	1:ILE_62:HG2*	1.800	6.500	5.000	10.00	10.00	1000.000	0.00
1:THR_72:HN	1:THR_72:HG2*	1.800	6.500	5.000	10.00	10.00	1000.000	0.00
1:THR_72:HN	1:GLY_71:HN	1.800	5.000	5.000	10.00	10.00	1000.000	0.00
1:ARG+_84:HE	1:VAL_80:HG1*	1.800	6.500	5.000	10.00	10.00	1000.000	0.00
1:ARG+_84:HE	1:ARG+_84:HG1	1.800	5.000	5.000	10.00	10.00	1000.000	0.00
1:ARG+_84:HE	1:ARG+_84:HG2	1.800	5.000	5.000	10.00	10.00	1000.000	0.00
1:ARG+_84:HE	1:ARG+_84:HD*	1.800	6.000	5.000	10.00	10.00	1000.000	0.00
1:ASP-_74:HN	1:ILE_73:HG2*	1.800	6.500	5.000	10.00	10.00	1000.000	0.00
1:ASP-_74:HN	1:ASP-_74:HB1	1.800	5.000	5.000	10.00	10.00	1000.000	0.00
1:VAL_65:HN	1:VAL_65:HG1*	1.800	6.500	5.000	10.00	10.00	1000.000	0.00
1:VAL_65:HN	1:VAL_65:HB	1.800	5.000	5.000	10.00	10.00	1000.000	0.00
1:ALAC_90:HN	1:ASP-_89:HB2	1.800	5.000	5.000	10.00	10.00	1000.000	0.00
1:ALAC_90:HN	1:ASP-_89:HB1	1.800	5.000	5.000	10.00	10.00	1000.000	0.00
1:ALAC_90:HN	1:ALAC_90:HB*	1.800	6.500	5.000	10.00	10.00	1000.000	0.00
1:ALA_31:HN	1:ASP-_30:HB2	1.800	5.000	5.000	10.00	10.00	1000.000	0.00
1:ALA_31:HN	1:ALA_31:HB*	1.800	6.500	5.000	10.00	10.00	1000.000	0.00
1:GLY_43:HN	1:THR_39:HA	1.800	5.000	5.000	10.00	10.00	1000.000	0.00
1:GLY_50:HN	1:LEU_49:HN	1.800	5.000	5.000	10.00	10.00	1000.000	0.00
1:GLU-_67:HN	1:GLU-_67:HB1	1.800	5.000	5.000	10.00	10.00	1000.000	0.00
1:GLU-_67:HN	1:GLU-_67:HG2	1.800	5.000	5.000	10.00	10.00	1000.000	0.00
1:GLU-_67:HN	1:ASP-_68:HN	1.800	5.000	5.000	10.00	10.00	1000.000	0.00
1:THR_4:HN	1:THR_4:HA	1.800	5.000	5.000	10.00	10.00	1000.000	0.00
1:ASP-_5:HN	1:ASP-_5:HA	1.800	5.000	5.000	10.00	10.00	1000.000	0.00
1:GLN_6:HN	1:GLN_6:HA	2.600	3.100	3.100	10.00	10.00	1000.000	0.00
1:GLN_6:HN	1:ASP-_5:HA	3.100	3.600	3.600	10.00	10.00	1000.000	0.00
1:GLN_7:HN	1:GLN_7:HA	2.600	3.100	3.100	10.00	10.00	1000.000	0.00
1:GLN_7:HN	1:GLN_6:HA	2.300	3.600	3.600	10.00	10.00	1000.000	0.00
1:ALA_8:HN	1:ALA_8:HA	2.600	3.100	3.100	10.00	10.00	1000.000	0.00
1:ALA_8:HN	1:GLN_7:HA	3.100	3.600	3.600	10.00	10.00	1000.000	0.00
1:ALA_8:HN	1:ASP-_5:HA	2.800	5.000	5.000	10.00	10.00	1000.000	0.00
1:GLU-_9:HN	1:GLU-_9:HA	2.600	3.100	3.100	10.00	10.00	1000.000	0.00
1:GLU-_9:HN	1:ALA_8:HA	3.100	3.600	3.600	10.00	10.00	1000.000	0.00
1:GLU-_9:HN	1:GLN_6:HA	2.200	3.600	3.600	10.00	10.00	1000.000	0.00
1:ALA_10:HN	1:ALA_10:HA	2.600	3.100	3.100	10.00	10.00	1000.000	0.00
1:ALA_10:HN	1:GLU-_9:HA	2.300	3.600	3.600	10.00	10.00	1000.000	0.00
1:ALA_10:HN	1:GLN_7:HA	2.800	5.000	5.000	10.00	10.00	1000.000	0.00
1:ARG+_11:HN	1:ARG+_11:HA	2.600	3.100	3.100	10.00	10.00	1000.000	0.00
1:ARG+_11:HN	1:ALA_10:HA	3.100	3.600	3.600	10.00	10.00	1000.000	0.00
1:ARG+_11:HN	1:ALA_8:HA	2.800	4.300	4.300	10.00	10.00	1000.000	0.00
1:ALA_12:HN	1:ALA_12:HA	2.600	3.100	3.100	10.00	10.00	1000.000	0.00
1:ALA_12:HN	1:ARG+_11:HA	3.100	3.600	3.600	10.00	10.00	1000.000	0.00
1:ALA_12:HN	1:GLU-_9:HA	2.800	3.600	3.600	10.00	10.00	1000.000	0.00
1:PHE_13:HN	1:PHE_13:HA	2.600	3.100	3.100	10.00	10.00	1000.000	0.00
1:PHE_13:HN	1:ALA_12:HA	3.100	3.600	3.600	10.00	10.00	1000.000	0.00
1:PHE_13:HN	1:ALA_10:HA	2.800	4.300	4.300	10.00	10.00	1000.000	0.00
1:LEU_14:HN	1:LEU_14:HA	2.700	3.100	3.100	10.00	10.00	1000.000	0.00
1:LEU_14:HN	1:PHE_13:HA	2.100	2.700	2.700	10.00	10.00	1000.000	0.00
1:LEU_14:HN	1:ARG+_11:HA	1.800	3.100	3.100	10.00	10.00	1000.000	0.00
1:SER_15:HN	1:LEU_14:HA	1.800	5.000	5.000	10.00	10.00	1000.000	0.00
1:GLU-_16:HN	1:GLU-_16:HA	2.600	3.100	3.100	10.00	10.00	1000.000	0.00
1:GLU-_16:HN	1:SER_15:HA	3.100	3.600	3.600	10.00	10.00	1000.000	0.00
1:GLU-_17:HN	1:GLU-_17:HA	2.600	3.100	3.100	10.00	10.00	1000.000	0.00
1:GLU-_17:HN	1:GLU-_16:HA	3.100	3.600	3.600	10.00	10.00	1000.000	0.00
1:MET_18:HN	1:MET_18:HA	2.600	3.100	3.100	10.00	10.00	1000.000	0.00
1:MET_18:HN	1:GLU-_17:HA	2.900	3.600	3.600	10.00	10.00	1000.000	0.00
1:ILE_19:HN	1:ILE_19:HA	2.600	3.100	3.100	10.00	10.00	1000.000	0.00
1:ILE_19:HN	1:MET_18:HA	2.900	3.600	3.600	10.00	10.00	1000.000	0.00
1:ILE_19:HN	1:GLU-_16:HA	2.800	4.300	4.300	10.00	10.00	1000.000	0.00
1:ALA_20:HN	1:ALA_20:HA	2.600	3.100	3.100	10.00	10.00	1000.000	0.00
1:ALA_20:HN	1:ILE_19:HA	3.100	3.600	3.600	10.00	10.00	1000.000	0.00
1:ALA_20:HN	1:GLU-_17:HA	2.800	3.600	3.600	10.00	10.00	1000.000	0.00
1:GLU-_21:HN	1:GLU-_21:HA	2.600	3.100	3.100	10.00	10.00	1000.000	0.00
1:GLU-_21:HN	1:ALA_20:HA	3.100	3.600	3.600	10.00	10.00	1000.000	0.00
1:GLU-_21:HN	1:MET_18:HA	2.800	3.600	3.600	10.00	10.00	1000.000	0.00
1:PHE_22:HN	1:PHE_22:HA	2.600	3.100	3.100	10.00	10.00	1000.000	0.00
1:PHE_22:HN	1:GLU-_21:HA	2.300	3.600	3.600	10.00	10.00	1000.000	0.00
1:PHE_22:HN	1:ILE_19:HA	2.200	4.300	4.300	10.00	10.00	1000.000	0.00
1:LYS+_23:HN	1:LYS+_23:HA	2.600	3.100	3.100	10.00	10.00	1000.000	0.00
1:LYS+_23:HN	1:PHE_22:HA	3.100	3.600	3.600	10.00	10.00	1000.000	0.00
1:LYS+_23:HN	1:ALA_20:HA	2.200	3.600	3.600	10.00	10.00	1000.000	0.00
1:ALA_24:HN	1:ALA_24:HA	2.600	3.100	3.100	10.00	10.00	1000.000	0.00
1:ALA_24:HN	1:LYS+_23:HA	3.100	3.600	3.600	10.00	10.00	1000.000	0.00
1:ALA_24:HN	1:GLU-_21:HA	2.800	3.600	3.600	10.00	10.00	1000.000	0.00
1:ALA_25:HN	1:ALA_25:HA	2.600	3.100	3.100	10.00	10.00	1000.000	0.00

1:ALA_25:HN	1:ALA_24:HA	3.100	3.600	3.600	10.00	10.00	1000.000	0.00
1:ALA_25:HN	1:PHE_22:HA	2.800	5.000	5.000	10.00	10.00	1000.000	0.00
1:PHE_26:HN	1:PHE_26:HA	2.600	3.100	3.100	10.00	10.00	1000.000	0.00
1:PHE_26:HN	1:ALA_25:HA	3.100	3.600	3.600	10.00	10.00	1000.000	0.00
1:PHE_26:HN	1:LYS+_23:HA	2.800	4.300	4.300	10.00	10.00	1000.000	0.00
1:ASP-_27:HN	1:ASP-_27:HA	2.600	3.100	3.100	10.00	10.00	1000.000	0.00
1:ASP-_27:HN	1:PHE_26:HA	2.300	3.600	3.600	10.00	10.00	1000.000	0.00
1:MET_28:HN	1:MET_28:HA	2.600	3.100	3.100	10.00	10.00	1000.000	0.00
1:MET_28:HN	1:ASP-_27:HA	3.100	3.600	3.600	10.00	10.00	1000.000	0.00
1:MET_28:HN	1:ALA_25:HA	2.800	5.000	5.000	10.00	10.00	1000.000	0.00
1:PHE_29:HN	1:PHE_29:HA	2.600	3.100	3.100	10.00	10.00	1000.000	0.00
1:PHE_29:HN	1:MET_28:HA	3.100	3.600	3.600	10.00	10.00	1000.000	0.00
1:PHE_29:HN	1:PHE_26:HA	2.800	5.000	5.000	10.00	10.00	1000.000	0.00
1:ASP-_30:HN	1:ASP-_30:HA	2.700	3.100	3.100	10.00	10.00	1000.000	0.00
1:ASP-_30:HN	1:PHE_29:HA	2.100	2.900	2.900	10.00	10.00	1000.000	0.00
1:ASP-_30:HN	1:ASP-_27:HA	1.800	3.100	3.100	10.00	10.00	1000.000	0.00
1:ALA_31:HN	1:ALA_31:HA	2.600	3.100	3.100	10.00	10.00	1000.000	0.00
1:ALA_31:HN	1:ASP-_30:HA	3.100	3.600	3.600	10.00	10.00	1000.000	0.00
1:ASP-_32:HN	1:ALA_31:HA	1.800	5.000	5.000	10.00	10.00	1000.000	0.00
1:ASP-_36:HN	1:ASP-_36:HA	1.800	5.000	5.000	10.00	10.00	1000.000	0.00
1:ILE_37:HN	1:ASP-_36:HA	1.800	5.000	5.000	10.00	10.00	1000.000	0.00
1:SER_38:HN	1:ILE_37:HA	1.800	5.000	5.000	10.00	10.00	1000.000	0.00
1:THR_39:HN	1:THR_39:HA	2.600	3.100	3.100	10.00	10.00	1000.000	0.00
1:THR_39:HN	1:SER_38:HA	3.100	3.600	3.600	10.00	10.00	1000.000	0.00
1:LYS+_40:HN	1:LYS+_40:HA	2.600	3.100	3.100	10.00	10.00	1000.000	0.00
1:LYS+_40:HN	1:THR_39:HA	3.100	3.600	3.600	10.00	10.00	1000.000	0.00
1:GLU-_41:HN	1:GLU-_41:HA	1.800	5.000	5.000	10.00	10.00	1000.000	0.00
1:LEU_42:HN	1:LEU_42:HA	2.600	3.100	3.100	10.00	10.00	1000.000	0.00
1:LEU_42:HN	1:GLU-_41:HA	3.100	3.600	3.600	10.00	10.00	1000.000	0.00
1:LEU_42:HN	1:THR_39:HA	2.800	3.600	3.600	10.00	10.00	1000.000	0.00
1:THR_44:HN	1:THR_44:HA	1.800	5.000	5.000	10.00	10.00	1000.000	0.00
1:THR_44:HN	1:GLU-_41:HA	2.800	5.000	5.000	10.00	10.00	1000.000	0.00
1:VAL_45:HN	1:VAL_45:HA	2.600	3.100	3.100	10.00	10.00	1000.000	0.00
1:VAL_45:HN	1:THR_44:HA	2.300	3.600	3.600	10.00	10.00	1000.000	0.00
1:VAL_45:HN	1:LEU_42:HA	2.200	4.300	4.300	10.00	10.00	1000.000	0.00
1:MET_46:HN	1:MET_46:HA	2.600	3.100	3.100	10.00	10.00	1000.000	0.00
1:MET_46:HN	1:VAL_45:HA	3.100	3.600	3.600	10.00	10.00	1000.000	0.00
1:MET_48:HN	1:MET_48:HA	1.800	5.000	5.000	10.00	10.00	1000.000	0.00
1:MET_48:HN	1:VAL_45:HA	2.800	5.000	5.000	10.00	10.00	1000.000	0.00
1:GLN_51:HN	1:GLN_51:HA	1.800	5.000	5.000	10.00	10.00	1000.000	0.00
1:ASN_52:HN	1:ASN_52:HA	2.700	3.100	3.100	10.00	10.00	1000.000	0.00
1:ASN_52:HN	1:GLN_51:HA	2.100	2.700	2.700	10.00	10.00	1000.000	0.00
1:THR_54:HN	1:THR_54:HA	1.800	5.000	5.000	10.00	10.00	1000.000	0.00
1:LYS+_55:HN	1:LYS+_55:HA	2.600	3.100	3.100	10.00	10.00	1000.000	0.00
1:LYS+_55:HN	1:THR_54:HA	2.900	3.600	3.600	10.00	10.00	1000.000	0.00
1:GLU-_56:HN	1:GLU-_56:HA	2.600	3.100	3.100	10.00	10.00	1000.000	0.00
1:GLU-_56:HN	1:LYS+_55:HA	3.100	3.600	3.600	10.00	10.00	1000.000	0.00
1:GLU-_57:HN	1:GLU-_57:HA	2.600	3.100	3.100	10.00	10.00	1000.000	0.00
1:GLU-_57:HN	1:GLU-_56:HA	3.100	3.600	3.600	10.00	10.00	1000.000	0.00
1:LEU_58:HN	1:LYS+_55:HA	1.800	5.000	5.000	10.00	10.00	1000.000	0.00
1:ASP-_59:HN	1:ASP-_59:HA	2.600	3.100	3.100	10.00	10.00	1000.000	0.00
1:ASP-_59:HN	1:LEU_58:HA	3.100	3.600	3.600	10.00	10.00	1000.000	0.00
1:ASP-_59:HN	1:GLU-_56:HA	2.800	4.300	4.300	10.00	10.00	1000.000	0.00
1:ALA_60:HN	1:ALA_60:HA	2.600	3.100	3.100	10.00	10.00	1000.000	0.00
1:ALA_60:HN	1:ASP-_59:HA	3.100	3.600	3.600	10.00	10.00	1000.000	0.00
1:ALA_60:HN	1:GLU-_57:HA	2.800	3.600	3.600	10.00	10.00	1000.000	0.00
1:ILE_61:HN	1:ILE_61:HA	2.600	3.100	3.100	10.00	10.00	1000.000	0.00
1:ILE_61:HN	1:ALA_60:HA	3.100	3.600	3.600	10.00	10.00	1000.000	0.00
1:ILE_61:HN	1:LEU_58:HA	2.800	5.000	5.000	10.00	10.00	1000.000	0.00
1:ILE_62:HN	1:ILE_62:HA	2.600	3.100	3.100	10.00	10.00	1000.000	0.00
1:ILE_62:HN	1:ILE_61:HA	3.100	3.600	3.600	10.00	10.00	1000.000	0.00
1:ILE_62:HN	1:ASP-_59:HA	2.800	5.000	5.000	10.00	10.00	1000.000	0.00
1:GLU-_63:HN	1:GLU-_63:HA	2.600	3.100	3.100	10.00	10.00	1000.000	0.00
1:GLU-_63:HN	1:ILE_62:HA	3.100	3.600	3.600	10.00	10.00	1000.000	0.00
1:GLU-_63:HN	1:ALA_60:HA	2.800	3.600	3.600	10.00	10.00	1000.000	0.00
1:GLU-_64:HN	1:GLU-_64:HA	2.600	3.100	3.100	10.00	10.00	1000.000	0.00
1:GLU-_64:HN	1:GLU-_63:HA	2.900	3.600	3.600	10.00	10.00	1000.000	0.00
1:GLU-_64:HN	1:ILE_61:HA	2.800	5.000	5.000	10.00	10.00	1000.000	0.00
1:VAL_65:HN	1:VAL_65:HA	2.700	3.100	3.100	10.00	10.00	1000.000	0.00
1:VAL_65:HN	1:GLU-_64:HA	2.100	2.700	2.700	10.00	10.00	1000.000	0.00
1:GLU-_67:HN	1:GLU-_67:HA	1.800	5.000	5.000	10.00	10.00	1000.000	0.00
1:THR_72:HN	1:THR_72:HA	1.800	5.000	5.000	10.00	10.00	1000.000	0.00
1:ILE_73:HN	1:ILE_73:HA	2.700	3.100	3.100	10.00	10.00	1000.000	0.00
1:ILE_73:HN	1:THR_72:HA	2.100	2.700	2.700	10.00	10.00	1000.000	0.00
1:ASP-_74:HN	1:ASP-_74:HA	2.700	3.100	3.100	10.00	10.00	1000.000	0.00
1:ASP-_74:HN	1:ILE_73:HA	2.100	2.700	2.700	10.00	10.00	1000.000	0.00
1:PHE_75:HN	1:PHE_75:HA	2.600	3.100	3.100	10.00	10.00	1000.000	0.00
1:PHE_75:HN	1:ASP-_74:HA	2.300	3.600	3.600	10.00	10.00	1000.000	0.00

```
1:GLU-_76:HN        1:GLU-_76:HA        1.800  5.000  5.000 10.00 10.00 1000.000  0.00
1:GLU-_77:HN        1:GLU-_77:HA        2.600  3.100  3.100 10.00 10.00 1000.000  0.00
1:GLU-_77:HN        1:GLU-_76:HA        3.100  3.600  3.600 10.00 10.00 1000.000  0.00
1:PHE_78:HN         1:PHE_78:HA         2.600  3.100  3.100 10.00 10.00 1000.000  0.00
1:PHE_78:HN         1:GLU-_77:HA        3.100  3.600  3.600 10.00 10.00 1000.000  0.00
1:PHE_78:HN         1:PHE_75:HA         2.800  3.600  3.600 10.00 10.00 1000.000  0.00
1:LEU_79:HN         1:PHE_78:HA         1.800  5.000  5.000 10.00 10.00 1000.000  0.00
1:LEU_79:HN         1:GLU-_76:HA        1.800  3.600  3.600 10.00 10.00 1000.000  0.00
1:VAL_80:HN         1:VAL_80:HA         2.600  3.100  3.100 10.00 10.00 1000.000  0.00
1:VAL_80:HN         1:LEU_79:HA         3.100  3.600  3.600 10.00 10.00 1000.000  0.00
1:VAL_80:HN         1:GLU-_77:HA        2.800  3.600  3.600 10.00 10.00 1000.000  0.00
1:MET_81:HN         1:MET_81:HA         2.600  3.100  3.100 10.00 10.00 1000.000  0.00
1:MET_81:HN         1:VAL_80:HA         3.100  3.600  3.600 10.00 10.00 1000.000  0.00
1:MET_81:HN         1:PHE_78:HA         2.800  4.300  4.300 10.00 10.00 1000.000  0.00
1:MET_82:HN         1:MET_82:HA         2.600  3.100  3.100 10.00 10.00 1000.000  0.00
1:MET_82:HN         1:MET_81:HA         3.100  3.600  3.600 10.00 10.00 1000.000  0.00
1:MET_82:HN         1:LEU_79:HA         2.800  4.300  4.300 10.00 10.00 1000.000  0.00
1:VAL_83:HN         1:VAL_83:HA         2.600  3.100  3.100 10.00 10.00 1000.000  0.00
1:VAL_83:HN         1:MET_82:HA         3.100  3.600  3.600 10.00 10.00 1000.000  0.00
1:VAL_83:HN         1:VAL_80:HA         2.800  3.600  3.600 10.00 10.00 1000.000  0.00
1:ARG+_84:HN        1:ARG+_84:HA        2.600  3.100  3.100 10.00 10.00 1000.000  0.00
1:ARG+_84:HN        1:VAL_83:HA         3.100  3.600  3.600 10.00 10.00 1000.000  0.00
1:ARG+_84:HN        1:MET_81:HA         2.800  5.000  5.000 10.00 10.00 1000.000  0.00
1:GLN_85:HN         1:GLN_85:HA         2.600  3.100  3.100 10.00 10.00 1000.000  0.00
1:GLN_85:HN         1:ARG+_84:HA        3.100  3.600  3.600 10.00 10.00 1000.000  0.00
1:GLN_85:HN         1:MET_82:HA         2.800  5.000  5.000 10.00 10.00 1000.000  0.00
1:MET_86:HN         1:MET_86:HA         2.600  3.100  3.100 10.00 10.00 1000.000  0.00
1:MET_86:HN         1:GLN_85:HA         3.100  3.600  3.600 10.00 10.00 1000.000  0.00
1:MET_86:HN         1:VAL_83:HA         2.800  4.300  4.300 10.00 10.00 1000.000  0.00
1:LYS+_87:HN        1:LYS+_87:HA        2.600  3.100  3.100 10.00 10.00 1000.000  0.00
1:LYS+_87:HN        1:MET_86:HA         3.100  3.600  3.600 10.00 10.00 1000.000  0.00
1:LYS+_87:HN        1:ARG+_84:HA        2.800  5.000  5.000 10.00 10.00 1000.000  0.00
1:ALAC_90:HN        1:ALAC_90:HA        1.800  5.000  5.000 10.00 10.00 1000.000  0.00
1:GLY_33:HN         1:GLY_33:HA*        1.800  6.000  5.000 10.00 10.00 1000.000  0.00
1:GLY_34:HN         1:GLY_33:HA*        1.800  6.000  5.000 10.00 10.00 1000.000  0.00
1:GLY_34:HN         1:GLY_34:HA1        1.800  5.000  5.000 10.00 10.00 1000.000  0.00
1:GLY_34:HN         1:GLY_34:HA2        1.800  5.000  5.000 10.00 10.00 1000.000  0.00
1:ASP-_36:HN        1:GLY_35:HA1        1.800  5.000  5.000 10.00 10.00 1000.000  0.00
1:GLY_43:HN         1:GLY_43:HA1        1.800  5.000  5.000 10.00 10.00 1000.000  0.00
1:GLY_43:HN         1:GLY_43:HA2        1.800  5.000  5.000 10.00 10.00 1000.000  0.00
1:THR_44:HN         1:GLY_43:HA1        1.800  5.000  5.000 10.00 10.00 1000.000  0.00
1:MET_46:HN         1:GLY_43:HA1        1.800  5.000  5.000 10.00 10.00 1000.000  0.00
1:GLY_50:HN         1:LEU_49:HA         3.100  5.000  5.000 10.00 10.00 1000.000  0.00
1:GLY_50:HN         1:GLY_50:HA1        1.800  5.000  5.000 10.00 10.00 1000.000  0.00
1:GLY_50:HN         1:GLY_50:HA2        1.800  5.000  5.000 10.00 10.00 1000.000  0.00
1:GLN_51:HN         1:GLY_50:HA1        1.800  5.000  5.000 10.00 10.00 1000.000  0.00
1:GLN_51:HN         1:GLY_50:HA2        1.800  5.000  5.000 10.00 10.00 1000.000  0.00
1:GLY_69:HN         1:GLY_69:HA1        1.800  5.000  5.000 10.00 10.00 1000.000  0.00
1:GLY_69:HN         1:GLY_69:HA2        1.800  5.000  5.000 10.00 10.00 1000.000  0.00
1:SER_70:HN         1:GLY_69:HA1        1.800  5.000  5.000 10.00 10.00 1000.000  0.00
1:SER_70:HN         1:GLY_69:HA2        1.800  5.000  5.000 10.00 10.00 1000.000  0.00
1:THR_72:HN         1:GLY_71:HA1        1.800  5.000  5.000 10.00 10.00 1000.000  0.00
1:THR_72:HN         1:GLY_71:HA2        1.800  5.000  5.000 10.00 10.00 1000.000  0.00
!
#NMR_dihedral
1:ALAN_1:CA     1:ALAN_1:C     1:SER_2:N      1:SER_2:CA      175.000 -175.000 10.00 10.00 1000.000
1:SER_2:CA      1:SER_2:C      1:MET_3:N      1:MET_3:CA      175.000 -175.000 10.00 10.00 1000.000
1:MET_3:CA      1:MET_3:C      1:THR_4:N      1:THR_4:CA      175.000 -175.000 10.00 10.00 1000.000
1:THR_4:CA      1:THR_4:C      1:ASP-_5:N     1:ASP-_5:CA     175.000 -175.000 10.00 10.00 1000.000
1:ASP-_5:CA     1:ASP-_5:C     1:GLN_6:N      1:GLN_6:CA      175.000 -175.000 10.00 10.00 1000.000
1:GLN_6:CA      1:GLN_6:C      1:GLN_7:N      1:GLN_7:CA      175.000 -175.000 10.00 10.00 1000.000
1:GLN_7:CA      1:GLN_7:C      1:ALA_8:N      1:ALA_8:CA      175.000 -175.000 10.00 10.00 1000.000
1:ALA_8:CA      1:ALA_8:C      1:GLU-_9:N     1:GLU-_9:CA     175.000 -175.000 10.00 10.00 1000.000
1:GLU-_9:CA     1:GLU-_9:C     1:ALA_10:N     1:ALA_10:CA     175.000 -175.000 10.00 10.00 1000.000
1:ALA_10:CA     1:ALA_10:C     1:ARG+_11:N    1:ARG+_11:CA    175.000 -175.000 10.00 10.00 1000.000
1:ARG+_11:CA    1:ARG+_11:C    1:ALA_12:N     1:ALA_12:CA     175.000 -175.000 10.00 10.00 1000.000
1:ALA_12:CA     1:ALA_12:C     1:PHE_13:N     1:PHE_13:CA     175.000 -175.000 10.00 10.00 1000.000
1:PHE_13:CA     1:PHE_13:C     1:LEU_14:N     1:LEU_14:CA     175.000 -175.000 10.00 10.00 1000.000
1:LEU_14:CA     1:LEU_14:C     1:SER_15:N     1:SER_15:CA     175.000 -175.000 10.00 10.00 1000.000
1:SER_15:CA     1:SER_15:C     1:GLU-_16:N    1:GLU-_16:CA    175.000 -175.000 10.00 10.00 1000.000
1:GLU-_16:CA    1:GLU-_16:C    1:GLU-_17:N    1:GLU-_17:CA    175.000 -175.000 10.00 10.00 1000.000
1:GLU-_17:CA    1:GLU-_17:C    1:MET_18:N     1:MET_18:CA     175.000 -175.000 10.00 10.00 1000.000
1:MET_18:CA     1:MET_18:C     1:ILE_19:N     1:ILE_19:CA     175.000 -175.000 10.00 10.00 1000.000
1:ILE_19:CA     1:ILE_19:C     1:ALA_20:N     1:ALA_20:CA     175.000 -175.000 10.00 10.00 1000.000
1:ALA_20:CA     1:ALA_20:C     1:GLU-_21:N    1:GLU-_21:CA    175.000 -175.000 10.00 10.00 1000.000
1:GLU-_21:CA    1:GLU-_21:C    1:PHE_22:N     1:PHE_22:CA     175.000 -175.000 10.00 10.00 1000.000
1:PHE_22:CA     1:PHE_22:C     1:LYS+_23:N    1:LYS+_23:CA    175.000 -175.000 10.00 10.00 1000.000
1:LYS+_23:CA    1:LYS+_23:C    1:ALA_24:N     1:ALA_24:CA     175.000 -175.000 10.00 10.00 1000.000
1:ALA_24:CA     1:ALA_24:C     1:ALA_25:N     1:ALA_25:CA     175.000 -175.000 10.00 10.00 1000.000
1:ALA_25:CA     1:ALA_25:C     1:PHE_26:N     1:PHE_26:CA     175.000 -175.000 10.00 10.00 1000.000
1:PHE_26:CA     1:PHE_26:C     1:ASP-_27:N    1:ASP-_27:CA    175.000 -175.000 10.00 10.00 1000.000
```

```
1:ASP-_27:CA   1:ASP-_27:C   1:MET_28:N   1:MET_28:CA   175.000 -175.000 10.00 10.00 1000.000
1:MET_28:CA    1:MET_28:C    1:PHE_29:N   1:PHE_29:CA   175.000 -175.000 10.00 10.00 1000.000
1:PHE_29:CA    1:PHE_29:C    1:ASP-_30:N  1:ASP-_30:CA  175.000 -175.000 10.00 10.00 1000.000
1:ASP-_30:CA   1:ASP-_30:C   1:ALA_31:N   1:ALA_31:CA   175.000 -175.000 10.00 10.00 1000.000
1:ALA_31:CA    1:ALA_31:C    1:ASP-_32:N  1:ASP-_32:CA  175.000 -175.000 10.00 10.00 1000.000
1:ASP-_32:CA   1:ASP-_32:C   1:GLY_33:N   1:GLY_33:CA   175.000 -175.000 10.00 10.00 1000.000
1:GLY_33:CA    1:GLY_33:C    1:GLY_34:N   1:GLY_34:CA   175.000 -175.000 10.00 10.00 1000.000
1:GLY_34:CA    1:GLY_34:C    1:GLY_35:N   1:GLY_35:CA   175.000 -175.000 10.00 10.00 1000.000
1:GLY_35:CA    1:GLY_35:C    1:ASP-_36:N  1:ASP-_36:CA  175.000 -175.000 10.00 10.00 1000.000
1:ASP-_36:CA   1:ASP-_36:C   1:ILE_37:N   1:ILE_37:CA   175.000 -175.000 10.00 10.00 1000.000
1:ILE_37:CA    1:ILE_37:C    1:SER_38:N   1:SER_38:CA   175.000 -175.000 10.00 10.00 1000.000
1:SER_38:CA    1:SER_38:C    1:THR_39:N   1:THR_39:CA   175.000 -175.000 10.00 10.00 1000.000
1:THR_39:CA    1:THR_39:C    1:LYS+_40:N  1:LYS+_40:CA  175.000 -175.000 10.00 10.00 1000.000
1:LYS+_40:CA   1:LYS+_40:C   1:GLU-_41:N  1:GLU-_41:CA  175.000 -175.000 10.00 10.00 1000.000
1:GLU-_41:CA   1:GLU-_41:C   1:LEU_42:N   1:LEU_42:CA   175.000 -175.000 10.00 10.00 1000.000
1:LEU_42:CA    1:LEU_42:C    1:GLY_43:N   1:GLY_43:CA   175.000 -175.000 10.00 10.00 1000.000
1:GLY_43:CA    1:GLY_43:C    1:THR_44:N   1:THR_44:CA   175.000 -175.000 10.00 10.00 1000.000
1:THR_44:CA    1:THR_44:C    1:VAL_45:N   1:VAL_45:CA   175.000 -175.000 10.00 10.00 1000.000
1:VAL_45:CA    1:VAL_45:C    1:MET_46:N   1:MET_46:CA   175.000 -175.000 10.00 10.00 1000.000
1:MET_46:CA    1:MET_46:C    1:ARG+_47:N  1:ARG+_47:CA  175.000 -175.000 10.00 10.00 1000.000
1:ARG+_47:CA   1:ARG+_47:C   1:MET_48:N   1:MET_48:CA   175.000 -175.000 10.00 10.00 1000.000
1:MET_48:CA    1:MET_48:C    1:LEU_49:N   1:LEU_49:CA   175.000 -175.000 10.00 10.00 1000.000
1:LEU_49:CA    1:LEU_49:C    1:GLY_50:N   1:GLY_50:CA   175.000 -175.000 10.00 10.00 1000.000
1:GLY_50:CA    1:GLY_50:C    1:GLN_51:N   1:GLN_51:CA   175.000 -175.000 10.00 10.00 1000.000
1:GLN_51:CA    1:GLN_51:C    1:ASN_52:N   1:ASN_52:CA   175.000 -175.000 10.00 10.00 1000.000
1:ASN_52:CA    1:ASN_52:C    1:PRO_53:N   1:PRO_53:CA   175.000 -175.000 10.00 10.00 1000.000
1:PRO_53:CA    1:PRO_53:C    1:THR_54:N   1:THR_54:CA   175.000 -175.000 10.00 10.00 1000.000
1:THR_54:CA    1:THR_54:C    1:LYS+_55:N  1:LYS+_55:CA  175.000 -175.000 10.00 10.00 1000.000
1:LYS+_55:CA   1:LYS+_55:C   1:GLU-_56:N  1:GLU-_56:CA  175.000 -175.000 10.00 10.00 1000.000
1:GLU-_56:CA   1:GLU-_56:C   1:GLU-_57:N  1:GLU-_57:CA  175.000 -175.000 10.00 10.00 1000.000
1:GLU-_57:CA   1:GLU-_57:C   1:LEU_58:N   1:LEU_58:CA   175.000 -175.000 10.00 10.00 1000.000
1:LEU_58:CA    1:LEU_58:C    1:ASP-_59:N  1:ASP-_59:CA  175.000 -175.000 10.00 10.00 1000.000
1:ASP-_59:CA   1:ASP-_59:C   1:ALA_60:N   1:ALA_60:CA   175.000 -175.000 10.00 10.00 1000.000
1:ALA_60:CA    1:ALA_60:C    1:ILE_61:N   1:ILE_61:CA   175.000 -175.000 10.00 10.00 1000.000
1:ILE_61:CA    1:ILE_61:C    1:ILE_62:N   1:ILE_62:CA   175.000 -175.000 10.00 10.00 1000.000
1:ILE_62:CA    1:ILE_62:C    1:GLU-_63:N  1:GLU-_63:CA  175.000 -175.000 10.00 10.00 1000.000
1:GLU-_63:CA   1:GLU-_63:C   1:GLU-_64:N  1:GLU-_64:CA  175.000 -175.000 10.00 10.00 1000.000
1:GLU-_64:CA   1:GLU-_64:C   1:VAL_65:N   1:VAL_65:CA   175.000 -175.000 10.00 10.00 1000.000
1:VAL_65:CA    1:VAL_65:C    1:ASP-_66:N  1:ASP-_66:CA  175.000 -175.000 10.00 10.00 1000.000
1:ASP-_66:CA   1:ASP-_66:C   1:GLU-_67:N  1:GLU-_67:CA  175.000 -175.000 10.00 10.00 1000.000
1:GLU-_67:CA   1:GLU-_67:C   1:ASP-_68:N  1:ASP-_68:CA  175.000 -175.000 10.00 10.00 1000.000
1:ASP-_68:CA   1:ASP-_68:C   1:GLY_69:N   1:GLY_69:CA   175.000 -175.000 10.00 10.00 1000.000
1:GLY_69:CA    1:GLY_69:C    1:SER_70:N   1:SER_70:CA   175.000 -175.000 10.00 10.00 1000.000
1:SER_70:CA    1:SER_70:C    1:GLY_71:N   1:GLY_71:CA   175.000 -175.000 10.00 10.00 1000.000
1:GLY_71:CA    1:GLY_71:C    1:THR_72:N   1:THR_72:CA   175.000 -175.000 10.00 10.00 1000.000
1:THR_72:CA    1:THR_72:C    1:ILE_73:N   1:ILE_73:CA   175.000 -175.000 10.00 10.00 1000.000
1:ILE_73:CA    1:ILE_73:C    1:ASP-_74:N  1:ASP-_74:CA  175.000 -175.000 10.00 10.00 1000.000
1:ASP-_74:CA   1:ASP-_74:C   1:PHE_75:N   1:PHE_75:CA   175.000 -175.000 10.00 10.00 1000.000
1:PHE_75:CA    1:PHE_75:C    1:GLU-_76:N  1:GLU-_76:CA  175.000 -175.000 10.00 10.00 1000.000
1:GLU-_76:CA   1:GLU-_76:C   1:GLU-_77:N  1:GLU-_77:CA  175.000 -175.000 10.00 10.00 1000.000
1:GLU-_77:CA   1:GLU-_77:C   1:PHE_78:N   1:PHE_78:CA   175.000 -175.000 10.00 10.00 1000.000
1:PHE_78:CA    1:PHE_78:C    1:LEU_79:N   1:LEU_79:CA   175.000 -175.000 10.00 10.00 1000.000
1:LEU_79:CA    1:LEU_79:C    1:VAL_80:N   1:VAL_80:CA   175.000 -175.000 10.00 10.00 1000.000
1:VAL_80:CA    1:VAL_80:C    1:MET_81:N   1:MET_81:CA   175.000 -175.000 10.00 10.00 1000.000
1:MET_81:CA    1:MET_81:C    1:MET_82:N   1:MET_82:CA   175.000 -175.000 10.00 10.00 1000.000
1:MET_82:CA    1:MET_82:C    1:VAL_83:N   1:VAL_83:CA   175.000 -175.000 10.00 10.00 1000.000
1:VAL_83:CA    1:VAL_83:C    1:ARG+_84:N  1:ARG+_84:CA  175.000 -175.000 10.00 10.00 1000.000
1:ARG+_84:CA   1:ARG+_84:C   1:GLN_85:N   1:GLN_85:CA   175.000 -175.000 10.00 10.00 1000.000
1:GLN_85:CA    1:GLN_85:C    1:MET_86:N   1:MET_86:CA   175.000 -175.000 10.00 10.00 1000.000
1:MET_86:CA    1:MET_86:C    1:LYS+_87:N  1:LYS+_87:CA  175.000 -175.000 10.00 10.00 1000.000
1:LYS+_87:CA   1:LYS+_87:C   1:GLU-_88:N  1:GLU-_88:CA  175.000 -175.000 10.00 10.00 1000.000
1:GLU-_88:CA   1:GLU-_88:C   1:ASP-_89:N  1:ASP-_89:CA  175.000 -175.000 10.00 10.00 1000.000
1:ASP-_89:CA   1:ASP-_89:C   1:ALAC_90:N  1:ALAC_90:CA  175.000 -175.000 10.00 10.00 1000.000
```

Calculation parameters

This is the parameter file used by the Biosym DGII program to generate the 64 structures.

```
NAME_0='BIOSYM DGII NMR_project=ntnc_5 mol=NTNC_5  Wed Jan  5 11:53:44 1994'
                    export NAME_0 # <= 80 char description of system
BASE_0=ntnc_5;          export BASE_0     # base name for all associated files
NSTR_0=40;              export NSTR_0     # number of structures to try to make
ARCH_0=iris;            export ARCH_0     # architecture of computer to use
NICE_0=19;              export NICE_0     # niceness of calculations
LOGF_0=mail;            export LOGF_0     # log file (mail ==> mailed to user)
TRAN_1=step1;           export TRAN_1     # base of transcript file for step1
VERB_1=silent;          export VERB_1     # verbosity of step1 transcript
RLIB_1=stereo.lib;      export RLIB_1     # residue library in DISGEO format
LLIB_1=aalink.lib;      export LLIB_1     # link library in DISGEO format
ALIB_1=nradii.lib;      export ALIB_1     # atom radii library in DISGEO format
OMEG_1=10;                                # omega wobble in degrees
TRAN_2=step2;           export TRAN_2     # base of transcript file for step2
VERB_2=report;          export VERB_2     # verbosity of step2 transcript
PREC_2=0.0001;          export PREC_2     # precision of input bounds for step2
TOLN_2=0.1;             export TOLN_2     # tolerance for violations for step2
TRI1_2=yes;             export TRI1_2     # control for triangle smoothing
PLAN_2=group;           export PLAN_2     # strategy for tetrangle smoothing
CRIT_2=0.1;             export CRIT_2     # convergence criterion for tetrangle
PASS_2=1;               export PASS_2     # maximum number of passes in tetrangle
TRAN_3=step3;           export TRAN_3     # base of transcript for step3
VERB_3=report;          export VERB_3     # verbosity of step3 calculations
METH_3=prospective;     export METH_3     # method to use for selection of distances
ALPH_3=uniform;         export ALPH_3     # probability distribution for selection
EDIM_3=4;               export EDIM_3     # dimension in which to embed coordinates
PRES_3=no;              export PRES_3     # preserve the radius of gyration
IMAX_3=200;             export IMAX_3     # iteration limit for eigencalculation
ECVG_3=0.0001;          export ECVG_3     # convergence criteria for eigencalculation
CRIT_3=0.001;           export CRIT_3     # criterion of inverse calculation
GTSV_3=20;                                # saved value of Guttman transformations
GUTT_3=20;              export GUTT_3     # number of Guttman transformations
LCGI_3=100;             export LCGI_3     # no. iterations for linear conjugate
gradient
LCGK_3=0.001;           export LCGK_3     # conv. criteria for linear conjugate
gradient
LSWF_3=range_inv;       export LSWF_3     # type of weights for least-squares fit
CMPI_3=yes;             export CMPI_3     # Calculate MP Inverse? during R & A
majorize
RMDM_3=yes;             export RMDM_3     # remove old distance matrix files
TRAN_4=step4;           export TRAN_4     # base of transcript for step4
WCHI_4=0.1;             export WCHI_4     # weight to give chirality error
WDIM_4=0.2;             export WDIM_4     # weight to give dimensionality error
PROJ_4=0.3;             export PROJ_4     # factor by which to project start
UPWT_4=1;               export UPWT_4     # upper weight limit for cook and cool
KCSV_4=2800;                              # saved initial energy in kcal / mole
KCAL_4=2800;            export KCAL_4     # initial energy in kcal / mole
XRAD_4=1;               export XRAD_4     # extra radius (-x opt for cook and cool)
TMAX_4=200;             export TMAX_4     # maximum temperature in degrees K
TINI_4=1;               export TINI_4     # initial  temperature in degrees K
HEAT_4=2;               export HEAT_4     # max. fractional temp. incr. per step
STEP_4=2e-13;           export STEP_4     # step size for simulation in sec.
MASS_4=1000;            export MASS_4     # mass of all atoms in Daltons
FAIL_4=0.01;            export FAIL_4     # annealing a failure if error exceeds
KLIM_4=20000;           export KLIM_4     # maximum number of simulation steps
KOSV_4=100;                               # Saved value of KOUT
KOUT_4=100;             export KOUT_4     # one line of output every KOUT steps
LLIM_4=250;             export LLIM_4     # minimization iteration limit
LOUT_4=10;              export LOUT_4     # one line of output every LOUT iter's
GRAD_4=0.0001;          export GRAD_4     # min. quits if RMS gradient deceeds
PRSV_4=200;                               # saved value of preview SA
PREV_4=0;               export PREV_4     # preview SA for this number steps
LBWT_4=10;              export LBWT_4     # lower bound weight
CTWT_4=1;               export CTWT_4     # contact weight
EFXF_4=sparse;          export EFXF_4     # error function form
```